INFLAMMATORY AND PROLIFERATIVE CHARACTERISTICS OF LATE ARTERIOVENOUS FISTULA STENOSIS: THERAPEUTIC POTENTIAL OF DICLOFENAC

A thesis presented by

Mark MacAskill BSc Hons

In fulfilment of the requirement for the degree of
Doctor of Philosophy

2014

Strathclyde Institute of Pharmacy and Biomedical Sciences

University of Strathclyde

This thesis is the result of the author's original research. It has been composed by the author and has not been previously submitted for examination which has led to the award of a degree.

Signed:

Date:

ACKNOWLEDGEMENTS

First and foremost I would like to thank my supervisors Dr. Paul Coats, Dr. Susan Currie and Prof. Roger Wadsworth for all their contributions, guidance and support. I would especially like to thank Paul for giving me the opportunity to work on this project, for giving me the freedom to take my ideas further and for providing honest useful criticism. I would also like to thank Susan for helping me with the cell biology aspect of this project, and her encouragement throughout the final year of my PhD. Roger's contribution to this project was immeasurable, and it is with great sadness that he is no longer with us. I learned so much from having Roger as a mentor, and his influence will stay with me for the rest of my career.

I would like to thank our clinical collaborators Mr David Kingsmore and Dr. Emma Aitken, as well as all surgical staff at the Glasgow Western Infirmary and Gartnavel General Hospital, for their clinical input and organisation of tissue donations. I am grateful to David for his help developing the *in vivo* model, and Emma for her guidance in ultrasonography and clinical interpretation of rabbit biochemistry/haematology profiling. My thanks and appreciation is extended to all the staff in the biological procedures unit. I would especially like to thank Graeme Mackenzie for the significant contribution he made to this study by providing technical assistance during surgery, ultrasound, AMPK staining of rabbit tissue and immunoblotting for p38. I thank Dr. Marie-Ann Ewart for her guidance on AMPK, her kind gift of antibody and agonist/antagonist aliquots and providing $AMPK^{-/-}$ mouse aorta for the explantation of VSM cells. I would also like to thank Prof. Bob Jones for his kind support and advice.

Throughout my PhD I have made many friends within the cardiovascular and cell biology groups, as well as the wider SIPBS community. I have had a lot of fun socialising with these people over the past three years, with "Friday lunch" always being the highlight of my week. I would specifically like to thank Emma Torrance, Zuhair Al Sulti and Graeme Mackenzie for their friendship and making my time in the laboratory enjoyable.

I would not be at this stage in my life if it wasn't for the love and support of my family, fiancée Leanne and best friend Daniel. I would especially like to thank my parents who inspired me to work hard and achieve everything I have today. Sadly, during the course of this study I lost both my Granny Kelly and Aunt Adele. I know that they would be proud of me, especially my Gran who would have loved to tell everyone her grandson was a doctor! Most of all I would like to thank my fiancée Leanne for all her love and support, and putting up with me through all the stressful times.

I dedicate this thesis to you all!

Nihil Sine Labore

PUBLICATIONS

MacAskill, M., Wadsworth, R.M., Aitken, E., Kingsmore, D., Coats, P., 2014. TLR-4 activation in arteriovenous fistula failure and generation of a pro-inflammatory hyper-proliferative vascular smooth muscle cell response. *Nephrol. Dial. Transplant.* (In preparation)

MacAskill, M., Wadsworth, R.M., Ewart, M-A., Mackenzie, G., Aitken, E., Kingsmore, D., Currie, S., Coats, P., 2014. Injury driven arteriovenous fistula stenosis is inhibited by diclofenac mediated AMPK activation. *Arterioscler. Thromb. Vasc. Biol.* (In preparation)

MacAskill, M., Wadsworth, R.M., Kingsmore, D., Coats, P., 2013. Rabbit arteriovenous fistula model and identification of a therapeutic agent to increase fistula patency. Arterioscler. Thromb. Vasc. Biol. 33:A554.

MacAskill, M., Wadsworth, R.M., Kingsmore, D., Coats, P., 2012. Arteriovenous fistula stenosis: vascular remodelling, inflammation and the development of a rabbit model. Proc. Physiol. Soc. 27, C85.

MacAskill, M., Wu, J., Wadsworth, R.M., Kingsmore, D., Coats, P., 2011. Arteriovenous fistula failure: vascular smooth muscle cell proliferation and the role of inflammation. Proc. Physiol. Soc. 25, C13 & PC13.

POSTER COMMUNICATIONS

Arteriosclerosis, Thrombosis and Vascular Biology Scientific Sessions, 1-3rd May 2013. MacAskill, M., Wadsworth, R.M., Kingsmore, D., Coats, P., Rabbit arteriovenous fistula model and identification of a therapeutic agent to increase fistula patency. Appendix I

Scottish Cardiovascular Forum, 2nd February 2013. MacAskill, M., Wadsworth, R.M., Kingsmore, D., Coats, P., Development of a rabbit model of arteriovenous fistula remodelling. Appendix II

University of Strathclyde Research Day, 7th June 2012. MacAskill, M., Wadsworth, R.M., Kingsmore, D., Coats, P., Vascular access failure in haemodialysis patients. Appendix III

Physiological Society: Vascular Smooth Muscle Physiology Meeting, 6-8th December 2011. MacAskill, M., Wu, J., Wadsworth, R.M., Kingsmore, D., Coats, P., Arteriovenous fistula failure: vascular smooth muscle cell proliferation and the role of inflammation. Appendix IV

ORAL COMMUNICATIONS

Physiological Society Main Meeting, 2-5th July 2012. MacAskill, M., Wadsworth, R.M., Kingsmore, D., Coats, P., Arteriovenous fistula stenosis: vascular remodelling, inflammation and the development of a rabbit model.

Physiological Society: Vascular Smooth Muscle Physiology Meeting, 6-8th December 2011. MacAskill, M., Wu, J., Wadsworth, R.M., Kingsmore, D., Coats, P., Arteriovenous fistula failure: vascular smooth muscle cell proliferation and the role of inflammation.

TABLE OF CONTENTS **PAGE**

LIST OF FIGURES

CHAPTER 1.

CHAPTER 3.

CHAPTER 4.

CHAPTER 5.

CHAPTER 6.

LIST OF TABLES

LIST OF ABBREVIATIONS

ACC	Acetyl-Coa Carboxylase
ADP	Adenosine Diphosphate
AICAR	5-Aminoimidazole-4-Carboxamide Ribonucleotide
ALT	Alanine Aminotransferase
AMPK	5' Adenosine Monophosphate-Activated Protein Kinase
ANOVA	Analysis of Variance
AOPP	Advanced Oxidation Protein Products
AP-1	Activator Protein 1
APES	3-Aminopropyltriethoxysilane
ApoE3	Apolipoprotein E
AST	Aspartate Aminotransferase
ATM	Ataxia Telangiectasia Mutated
ATP	Adenosine Triphosphate
AVF	Arteriovenous Fistula
BP	Blood Pressure
BSA	Bovine Serum Albumin
CaMKK	Calcium/Calmodulin-Dependent Protein Kinase Kinase
cAMP	Cyclic Adenosine Monophosphate
CD14	Cluster of Differentiation 14
CDK	Cyclin-Dependent Kinase
cGMP	Cyclic Guanosine Monophosphate
CINC-1	Cytokine-Induced Neutrophil Chemoattractant 1
Cip/Kip	CDK Interacting Protein/Kinase Inhibitory Protein
CKD	Chronic Kidney Disease
CKI	Cyclin-Dependent Kinase Inhibitor
COX	Cyclooxygenase
CRP	C-Reactive Protein
CY3	Cyanine 3
DAB	3,3'-Diaminobenzidine
DAMPS	Damage Associated Molecular Patterns

DAPI	4',6-Diamidino-2-Phenylindole
DGKC	German Society for Clinical Chemistry
DMSO	Dimethyl Sulfoxide
DNA	Deoxyribonucleic Acid
DOPPS	Dialysis Outcomes and Practice Patterns Study
DPI	Diphenylene Iodonium
EC_{50}	Half Maximal Effective Concentration
EDTA	Ethylenediaminetetraacetic Acid
ELISA	Enzyme-Linked Immunosorbent Assay
EMLA	Eutectic Mixture of Local Anaesthetics
ERK	Extracellular Signal-Regulated Kinase
ESRF	End Stage Renal Failure
EVA	Ethylene Vinyl Acetate
FACS	Fluorescence-Activated Cell Sorting
FCS	Foetal Calf Serum
FPT III	Farnesyl Protein Transferase Inhibitor III
GAPDH	Glyceraldehyde 3-Phosphate Dehydrogenase
GBM	Glomerular Basement Membrane
G-CSF	Granulocyte-Colony Stimulating Factor
GGT	Gamma-Glutamyl Transpeptidase γ
GM-CSF	Granulocyte Macrophage Colony-Stimulating Factor
H&E	Haematoxylin and Eosin
Hb	Haemoglobin
HCT	Haematocrit
HD	Haemodialysis
HEK	Human Embryonic Kidney
Hr	Hour
HRP	Horseradish Peroxidase
HSP	Heat Shock Protein
ICAM-1	Intercellular Adhesion Molecule 1
IFCC	International Federation of Clinical Chemistry
IgA	Immunoglobulin A

IgG	Immunoglobulin G
IκB	I Kappa B
IKK	IκB Kinase
IL	Interleukin
IP-10	Interferon Gamma-Induced Protein 10
IRAK	Interleukin-1 Receptor-Associated Kinase
ISE	Ion-Specific Electrode
I-TAC	Interferon–Inducible T Cell Alpha Chemoattractant
JAK2	Janus Kinase 2
JNK	c-Jun N-terminal Kinases
KDOQI	Kidney Disease Outcomes Quality Initiative
LKB-1	Liver Kinase B1
L-name	N (G)-Nitro-L- Arginine Methyl Ester
LPS	Lipopolysaccharide
MAPK	Mitogen-Activated Protein Kinase
MCH	Mean Corpuscular Haemoglobin
MCHC	Mean Corpuscular Haemoglobin Concentration
MCP-1	Monocyte Chemotactic Protein-1
MCV	Mean Corpuscular Volume
MD-2	Lymphocyte Antigen 96
Min	Minute
MIP-1β	Macrophage Inflammatory Protein-1β
MKK	Mitogen-Activated Protein Kinase Kinase
mRNA	Messenger Ribonucleic Acid
mTOR	Mammalian Target Of Rapamycin
MTT	Dimethyl Thiazolyl Diphenyl Tetrazolium Salt
MyD88	Myeloid Differentiation Primary Response 88
NADP	Nicotinamide Adenine Dinucleotide Phosphate
NF-κB	Nuclear Factor Kappa-Light-Chain-Enhancer of Activated B Cells
NOS	Nitric Oxide Synthase
NSAID	Non-Steroidal Anti-Inflammatory Drugs
PAMPS	Pathogen-Associated Molecular Patterns

PBS	Phosphate Buffered Saline
PCNA	Proliferating Cell Nuclear Antigen
PDGF	Platelet-Derived Growth Factor
PMA	Phorbol 12-Myristate 13-Acetate
PTFE	Polytetrafluoroethylene
Rac-1	Ras-Related C3 Botulinum Toxin Substrate 1
RBC	Red Blood Cell
RDW	Red Cell Distribution Width
RRT	Renal Replacement Therapy
SAPK	Stress-Activated Protein Kinase
SDS	Sodium Dodecyl Sulfate
Sec	Second
SEM	Standard Error of the Mean
siRNA	Small Interfering Ribonucleic Acid
SMA	Smooth Muscle Actin
STAT3	Signal Transducer and Activator of Transcription 3
TAB1/2	Mitogen-Activated Protein Kinase Kinase Kinase 7-Interacting Protein 1/2
TAK1	Mitogen-Activated Protein Kinase Kinase Kinase 7
TBARS	Thiobarbituric Acid Reactive Substances
TGF-β	Transforming Growth Factor B
TLR	Toll-Like Receptor
TNF-α	Tumor Necrosis Factor α
TRAF6	TNF Receptor Associated Factor 6
TSC	Tuberous Sclerosis Protein
TTBS	Tris-Buffered Saline Containing Tween 20
URR	Urea Reduction Ratio
VCAM-1	Vascular Cell Adhesion Protein 1
VSM	Vascular Smooth Muscle
WBC	White Blood Cell

ABSTRACT

An arteriovenous fistula (AVF) is a vein graft which is created to permit vascular access allowing haemodialysis to be performed. AVFs are associated with failure rates as high as 50% at 6 months. Failure is principally due to vascular smooth muscle cell proliferation, leading to the development of neointima causing stenosis and impaired blood flow. The aims of this study were to; 1) explore the inflammatory and proliferative characteristics of AVF stenosis and the role of TLR-4, 2) assess the ability of anti-inflammatory diclofenac to inhibit VSM cell proliferation, 3) develop a novel model of AVF in the rabbit to assess the impact of cannulation injury and the effect of topical diclofenac and 4) investigate the mechanisms responsible for diclofenac mediated activity.

Human stenotic AVF segments and cell explants taken from haemodialysis patients vs. healthy long saphenous vein controls were shown to have significantly higher TLR-4 expression and activation of the downstream kinase IRAK-4. Also associated with AVF stenosis was an increased expression of pro-inflammatory cytokines including MCP-1. VSM cell explants derived from stenosed AVF had a significantly increased capacity to proliferative vs. healthy controls, which was inhibited by diclofenac treatment. Using a novel rabbit AVF model, cannulation injury was shown for the first time to drive stenosis. Topical diclofenac significantly inhibited this injury response, reducing mean vein wall width from 46.8±5.7μM to 15.8±1.8μM, comparable to 16.7±1.6μM in the non-injured AVF. In addition to previously well defined COX inhibition, evidence was generated in this study to implicate AMPK in the anti-proliferative activity of diclofenac.

Therefore, activation of TLR-4 in AVF stenosis appears to play a significant role in the generation of an inflammatory and proliferative VSM cell response. Cannulation injury, which undoubtedly causes a pro-inflammatory response, significantly contributes to AVF stenosis which is inhibited by prophylactic topical diclofenac via the activation of AMPK.

Chapter 1

Introduction

1.1 General introduction

Kidney failure is a significant problem in the UK, with over 50,965 patients receiving renal replacement therapies (RRT) in 2010, according to the 2011 UK renal registry annual report (Ansell *et al.*, 2010). The creation of an arteriovenous fistula (AVF) for vascular access is the first choice for patients receiving haemodialysis (Rayner *et al.*, 2004). One of the most common sites for fistula creation is the forearm between the radial artery and cephalic vein (K. Konner, 2003), such as the radiocephalic AVF shown in Fig. 1.1. Using a successfully matured AVF is associated with less complications and has longer patency compared to alternatives such as artificial grafts (Beathard and First, 2003). In fact, AVFs are associated with a six fold reduction in the risk of systemic sepsis (Thomson *et al.*, 2007).

The arteriovenous fistula was first developed in 1965 by Kenneth Appell at the Bronx Veterans Administration Hospital (Brescia *et al.*, 1966). Radial-cephalic AVF were created in 12 patients to support haemodialysis treatment. Later, AVF revolutionised the treatment of kidney failure patients and was widely implemented in Europe and the USA Before AVF and artificial grafts, external venous shunts were used to provide long term access (Quinton *et al.*, 2004). Cannulas would be placed in the artery and vein via a subcutaneous tunnel which formed a tight fitting puncture. An external fitting was then used to connect the arterial and venous blood flow which was left in place until dialysis, where it was substituted for the haemodialyser. This type of access was uncomfortable for the patient, had a high incidence of thrombosis and infection, and could potentially disconnect causing severe haemorrhage (Burger *et al.*, 1995). Presently, in patients where a functional fistula is not available, an artificial polytetrafluoroethylene (PTFE) graft may be used to gain vascular access. Synthetic PTFE grafts allow access when the patient's blood vessels are not suitable (Senkaya *et al.*, 2003). Using the Dialysis Outcomes and Practice Patterns Study (DOPPS), a study published in 2002 analysed the use of PTFE grafts and other methods used for vascular access in 133 units across the USA. It was found that the failure rate of synthetic grafts was higher compared to AVF (Young *et al.*, 2002). Another alternative to AVF is the use of a catheter inserted into a central vein. However, as detailed by the Kidney Disease Outcomes Quality

Initiative (KDOQI) this is widely discouraged (Rayner *et al.*, 2004). The KDOQI aims to establish AVF as the most efficient method for vascular access, and highlight the dangers of using methods such as catheters, which are 5 times more likely to result in infection.

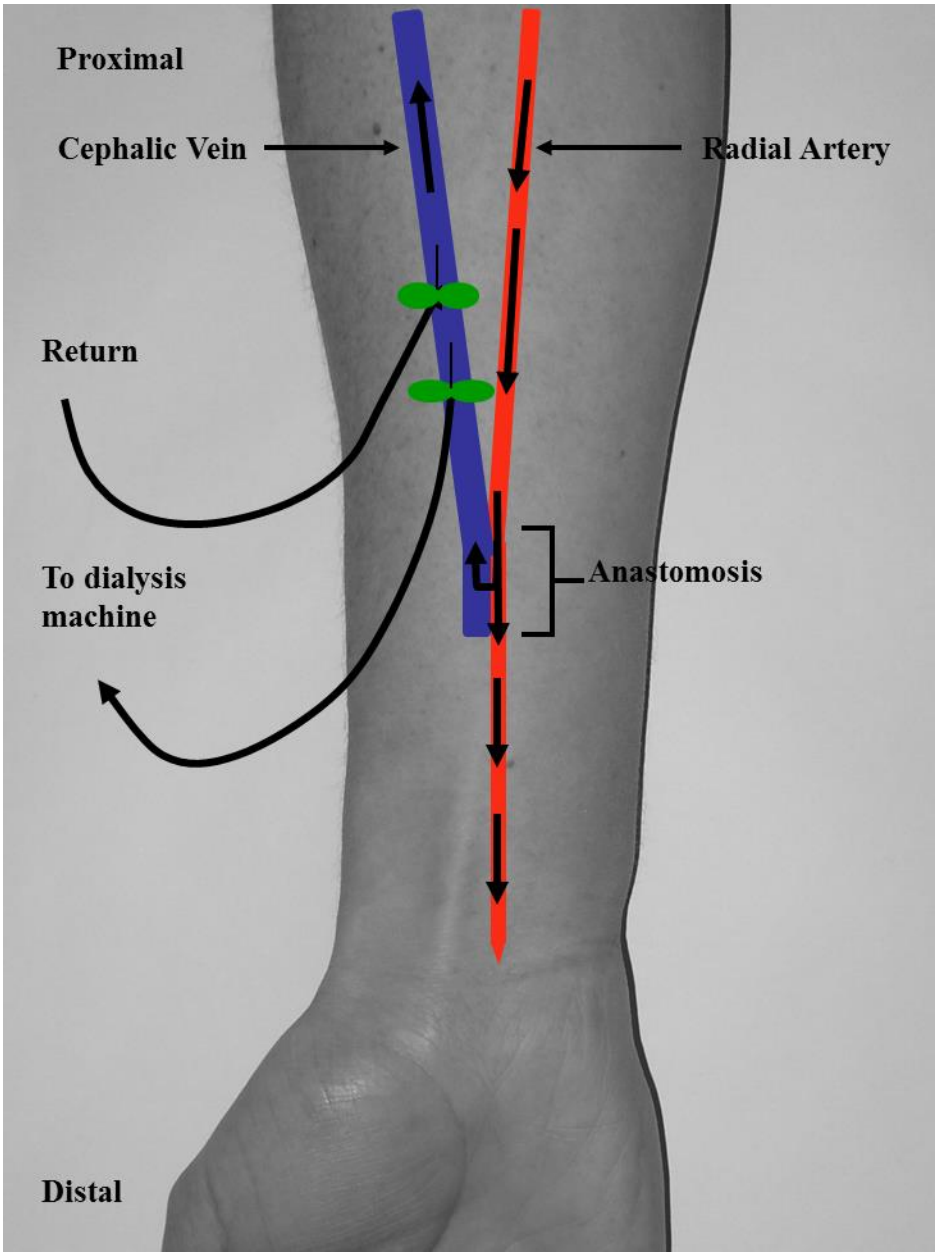

Figure 1.1. Radiocephalic arteriovenous fistula. *This figure illustrates the direction of blood flow which would occur in an end to side radiocephalic AVF. The distal cephalic vein is ligated, with the proximal end anastomosed onto the radial artery. The high pressure arterial flow now entering the venous circulation will cause the cephalic vein to mature, making it a suitable access point for cannulation in haemodialysis (K. Konner, 2003).*

Despite AVFs being the first choice for vascular access, they are also associated with frequent complications. One study investigated the primary patency rates of AVF created at the wrist (289 patients) and elbow (79 patients) over 6, 12 and 24 months (Field *et al.*, 2008). The patency rates of these grafts were 49, 41 and 32% respectively for wrist AVF, and 57, 51 and 38% for elbow grafts. While some patients have grafts which remain usable for several years, there are clearly a large proportion of patients, 51% according to Field *et al.*, in which the fistula fails within 6 months. The main cause of failure is intimal hyperplasia due to vascular smooth muscle (VSM) cell proliferation, and thrombus formation, leading to occlusion of the vein (Roy-Chaudhury *et al.* 2007, Lee & Roy-Chaudhury 2009). This occlusion limits blood flow through the AVF to the extent where it is no longer enough to support the haemodialysis procedure. Primary revision and creation of new fistulae due to complete failure has a significant impact on patient life quality. The reduction in life quality is even greater when clinicians are forced to use central line catheters when a functional fistula is not possible. Also associated with this is the significant financial strain which is placed on the NHS. In the year 2000 the number of patients receiving RRT was 30,000 at a total cost of £600 million (Roderick *et al.*, 2005). Later, in 2005 the cost of treating the 41,776 patients on RRT was 1-2% of the total NHS budget, even though RRT patients only represented 0.05% of the general population (Baboolal *et al.*, 2008). The latest figures show that 53,207 patients were on RRT in 2011 (Shaw *et al.*, 2013). Therefore, if the trend of increasing RRT continues, the financial implications for the future will be significant. Currently, there is no clear understanding of the specific mechanisms which are associated with vascular occlusion in the renal patient, and no prophylactic intervention therapies available to offset AVF stenosis. Therefore, a greater understanding of the triggers and mechanisms of fistula failure are needed in order to increase the patency of AVF and improve access for patients on haemodialysis.

Blood vessels

Blood vessels are dynamic conduits which transport blood around the body. An artery is a blood vessel which carries oxygenated blood away from the heart at high pressure towards the rest of the body. As depicted in Fig. 1.2, arteries consist of three layers, the tunica adventitia, tunica media and tunica intima. The adventitia contains flexible fibrous tissue containing large amounts of elastin and collagen, giving structure to the vessel and preventing tearing during movement. This elastic tissue allows continuous flow of blood along the periphery during cardiac relaxation, and therefore acts as a pressure reservoir (Sherwood, 2003). The main cellular components of the adventitia are fibroblasts and immune cells. The second layer, tunica media, is made up of smooth muscle cells with an elastic connective tissue portion at either side. In arteries, the layer of smooth muscle cells is considerably large, in order to maintain the high pressure of arterial flow. These cells can contract and relax to control vessel diameter; vital to maintain cardiovascular regulation. Finally the intima, the innermost layer around the lumen, is made up of endothelial cells which act as an interface between the circulation and vessel tissue, aiding the transport of oxygen, nutrients and immune cells. Endothelial cells reduce the turbulence of blood flow by providing a smooth surface, as well as secretion of paracrine agents such as nitric oxide which can act on adjacent smooth muscle cells to cause vasodilation (Widmaier *et al.*, 2007). Veins are also made up of three layers, the adventitia, media and intima (Fig. 1.2). The adventitia provides structure to the vein, in a function similar to arteries. However, it contains considerably less elastin and more collagen, allowing greater distension of the vessel. The media of veins also consists of smooth muscle cells; however this layer is considerably thinner than in arteries. The smooth muscle layer of veins also have little inherent myogenic tone, allowing greater distension and stretch to accommodate greater quantities of blood. Veins are therefore considered volume reservoirs, maintaining peripheral venous pressure and return volume to the heart. The large luminal diameter in veins allows the transport of blood at low pressure back to the heart by providing low resistance (Thibodeau and Patton, 2003).

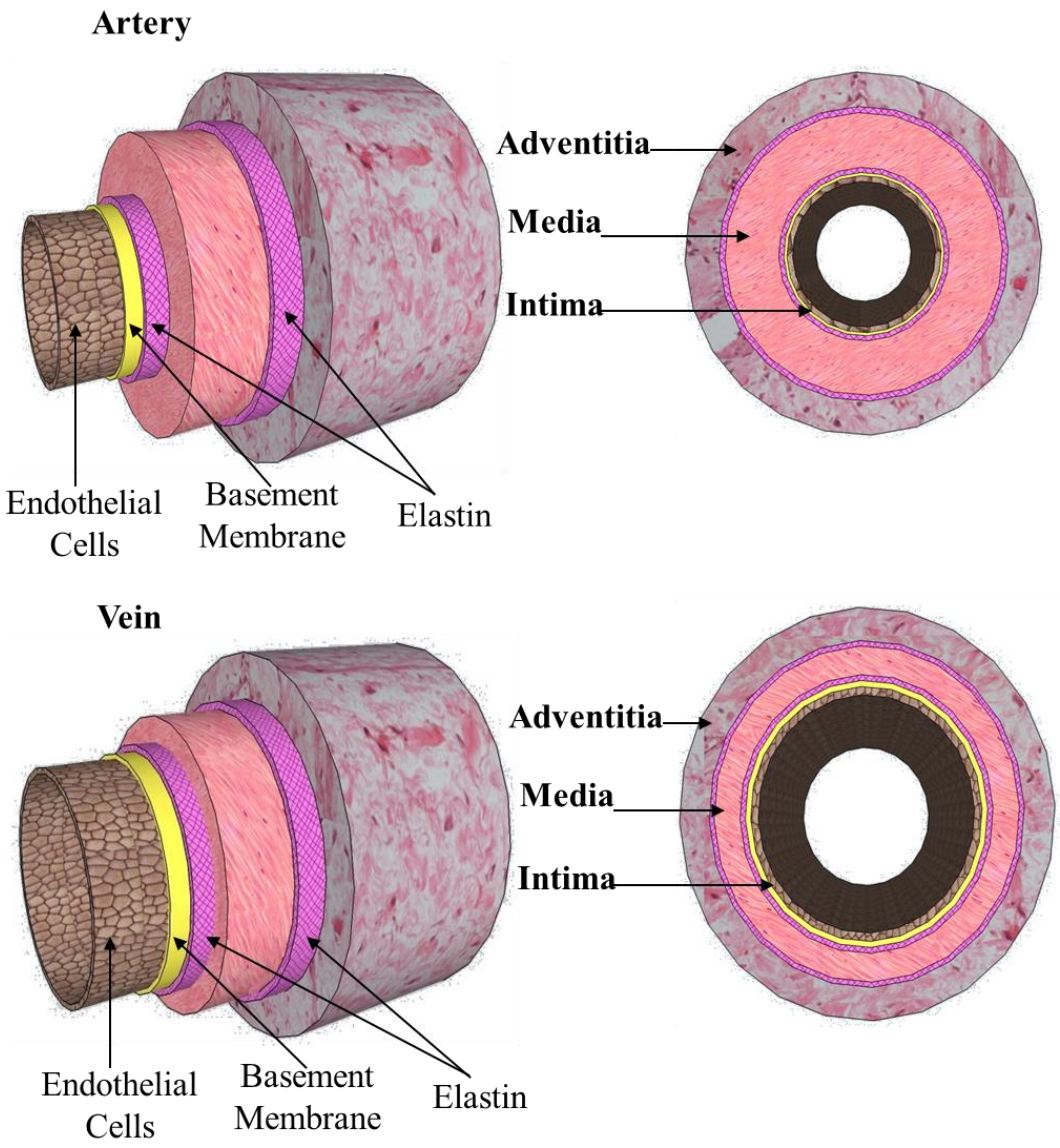

Figure 1.2. Illustration of blood vessel structure. *The tunica intima consists of endothelial cells and a basement membrane (yellow), the tunica media contains smooth muscle cells with a layer of elastin (purple) at either side, and the adventitia consists of loose connective tissue. One of the major differences between arteries and veins is the size of the medial layer, which is considerably thicker in arteries due to the transport of high pressure blood. However, the lumen of veins is larger than that of arteries, providing little vascular resistance to allow the transport of low pressure blood back to the heart.*

Maturation of arteriovenous fistulae

Following the creation of an AVF, careful monitoring of vein wall thickness and blood flow using Doppler ultrasound is undertaken until sufficient maturation has occurred. This process can take as little as 4-6 weeks, but in some cases it can take several months. Maturation of the venous branch is initiated by an increase in hoop wall stress (Hayashi and Naiki, 2009) and shear stress (Asif *et al.*, 2006). Shear stress rate is an indicator of the difference in blood velocity between the centre of the vessel and the boundary layer. Following anastomosis, blood flow, shear stress and hoop wall stress are increased within the vein. Mechanically, vessels try to maintain their original level of wall and shear stress. In the AVF, vasodilation of the vein occurs, eventually leading to an increase in VSM cells of the medial layer and maturation of the AVF (Konner 2003, Monos 1980). A larger vessel diameter means a lower shear and wall stress. This response was demonstrated in 6 male patients undergoing AVF creation and maturation (Corpataux *et al.*, 2002). Within the first week following AVF creation, the flow rate within the vein had increased to 539 ml/min. This caused shear stress to increase from a normal range of 5-10 dyn/cm^2 to 24.5 dyn/cm^2, and subsequently vessel diameter to increase from 2.4mm to 4.4mm. Blood flow and pressure within the vein was constant for the remainder of the study. At week 12, the diameter of the vessel increased to 6.6mm, bringing the shear stress rate down to 10.4 dyn/cm^2, back to within a normal range. This was accompanied by an increase in the wall cross sectional area, from 4.4mm^2 to 6.9mm^2. In other words, vascular remodelling of the venous arm and maturation of the fistula.

Vascular remodelling is vital to the success of an AVF, as without it the vein would not be able to support haemodialysis. Unfortunately, maturation of AVF is highly variable depending on the patient and their clinical history. One study has shown that failure to mature is associated with increased age, Caucasian race and previous peripheral and coronary vascular events (Lok *et al.*, 2006). The distensibility of veins prior to AVF creation has also been show to correlate with failure to mature. However, patient clinical characteristics and history are not the only factors. The level of a surgeon's skill has been shown to contribute to failure to mature, with factors such as vessel handling, kinking and endothelial injury thought to play a role

(He *et al.*, 2002; Klaus Konner, 2003). AVF failure to mature should not be confused with the later failure of AVF. In this thesis, failure to mature will not be investigated as this process can be vastly improved by surgical skill and careful attention to known risk factors. Instead, this study will investigate the late failure of AVF which are used for dialysis and subsequently developed stenosis.

1.2 Inflammation and arteriovenous fistula failure

Inflammatory profile in arteriovenous fistula stenosis

Currently, the specific mechanisms which are associated with peripheral vascular occlusion in the renal patient are poorly defined. However, it is thought that an inflammatory response is central to the pathology seen in these patients. The role of TNF-α and IL-1β in the development of neointima in vein grafts used for bypass procedures has long been known (Faries *et al.*, 1996). This group used a rat model of venous bypass intimal hyperplasia to measure the expression of several cytokines by immunohistochemistry. The grafted veins were studied at 6 hours, 2 days, 1 week, 2 weeks and 4 weeks post-surgery. After 2 weeks, the venous intimal hyperplasia reached its maximum. IL-1β and TNF-α were shown to be significantly increased compare to controls, with maximum expression of IL-1β occurring at 2 days and TNF-α occurring at 1 week. Dialysis patients have been shown to have increased systemic expression of pro-inflammatory cytokines compared to healthy individuals (Papayianni *et al.*, 2002). In another study looking at the involvement of TNF-α, serum was collected from haemodialysis patients and healthy individuals and analysed using a MultiAnalyte Profiling Base Kit (Lobo *et al.*, 2013). In this, Lobo and colleagues demonstrated significantly increased levels of TNF-α, IL-1, CRP, VCAM-1 and ICAM-1 compared to controls. The expression of these inflammatory proteins had a positive correlation with uric acid concentration. This suggests that hyperuremia in these patients is likely to cause an increase in basal activation of inflammatory pathways.

Patients undergoing haemodialysis are also widely accepted to exhibit high levels of oxidative stress (Nguyen-Khoa *et al.*, 2001). Nguyen-Khoa *et al.*, analysed lipid and protein markers of oxidative stress in dialysis patients. Levels of lipid oxidation were quantified by thiobarbituric acid reactive substances (TBARS) and protein oxidation by advanced oxidation protein products (AOPP). Lipid oxidation was markedly increased compared to healthy individuals. Also, the importance of superoxide production following arterial balloon injury in a rabbit intimal hyperplasia model has been demonstrated (Azevedo *et al.*, 2000). This group found

that immediately following insult, there was a significant rise in superoxide which had fallen dramatically by day 7, the height of intimal hyperplasia.

Specifically in relation to AVF, IL-6 has been highlighted as a key protein in the development of AVF stenosis (Marrone *et al.*, 2007). Venous fragments and peripheral-blood mononuclear cells were collected at AVF creation and subsequent failure. Immunofluorescence was used to assess the expression of gp180 and phosphorylation of JAK2/STAT3, part of the IL-6 signalling pathway. Both proteins were significantly upregulated in stenotic AVF tissue vs. control. Peripheral-blood mononuclear cells taken following the development of AVF stenosis had significantly higher IL-6 mRNA expression. The evidence presented in this section establishes that haemodialysis patients are in a heightened state of inflammation. However, more experiments are needed focussing on comparisons between the inflammatory cytokine/chemokine response in patients with functional AVF vs. AVF stenosis, rather than comparisons to healthy individuals.

Toll-like receptor activation and vascular proliferative disease

The activation of Toll-Like Receptors (TLR) could provide a link between the pro-inflammatory and hyper-proliferative responses seen in AVF stenosis. TLRs are a family of transmembrane receptors preserved throughout evolution (Hughes and Piontkivska, 2008). They recognize a number of microbial components, as well as endogenous molecules which are released during tissue injury (Asea *et al.*, 2002). As part of the innate immune system, activation of these receptors is vital for the generation of a response, as well as the promotion of wound healing and other healthy processes (Montero Vega and de Andrés Martín, 2009). Since TLRs play a role in cell proliferation during injury, it is plausible that they also play a role in the development of intimal hyperplasia There are two possible mechanisms through which activation of TLR may occur in the AVF; the endogenous release of damage associated molecular patterns (DAMPs) such as heat shock proteins (HSP) in response to haemodynamic change and needle injury (Hochleitner *et al.*, 2000), and

the presence of a sub-clinical infection or commensal bacteria releasing pathogen associated molecular patterns (PAMPs) (Ott *et al.*, 2006).

Damage associated molecular patterns (DAMPs)

HSP are found in all cells and are responsible for chaperoning proteins within the cell to mediate their correct folding. However, HSP do not take part in the final assembly of new structures (Xu, 2002). When cells are exposed to stress, these proteins can be released into the circulation where they alert the immune system via TLR. The altered haemodynamic conditions that are created in the vein of an AVF can cause the release of HSP from vascular cells (Hochleitner *et al.*, 2000). Also, as part of dialysis treatment, the AVF is subjected to multiple cannulations weekly, causing tissue damage and potentially the release of HSP. The importance of HSP-60 on TLR mediated vascular smooth muscle cell proliferation has been demonstrated (De Graaf *et al.*, 2006). Double immunostaining for HSP-60 and TLR-2/TLR-4 revealed a co-localisation in failed human AVF. Expression of these proteins was not found in control saphenous veins. Ki67, a nuclear protein which is associated with cell proliferation, was investigated in a vascular smooth muscle cell line to assess the ability of HSP-60 to stimulate proliferation. De Graaf reported a significant dose dependent increase in cell proliferation, which was attenuated in another experiment by the addition of anti TLR-2/4 antibodies. Finally, this group studied HSP-60 stimulated human embryonic kidney (HEK) cells transfected with either TLR-2 or TLR-4/MD-2. The presence of either of these proteins caused a significant increase in cell proliferation. Later, a study published in 2011 used an interpositional vein graft in ApoE3 leiden mice to demonstrate increased TLR-4 expression within the graft (Karper *et al.*, 2011). TLR-4 expression peaked at 1 day post procedure and remained significantly increased over the following 28 days. HSP60 was detected locally in the intimal lesions along with TLR-4. The vein graft procedure was then repeated in TLR-4 deficient mice, resulting in 48% less vessel thickening compared to wild type controls. Similar results were obtained in the APOE mice when TLR-4 was silenced locally by lentivirus. These studies suggest

that the release of HSP-60 in patients could significantly contribute to VSM cell proliferation via activation of TLR-2/4.

Pathogen associated molecular patterns (PAMPs)

The presence of diverse bacterial signatures in atherosclerotic lesions of patients with coronary heart disease could lead to TLR activation, suggesting that PAMPs may contribute to this vascular proliferative disease (Ott *et al.*, 2006). In AVF stenosis, PAMPS may originate from infectious bacteria, but also the wide array of commensal bacteria found in the body. In haemodialysis patients, the potential for infection at the AVF cannulation site is considerable. PAMPs have been shown to considerably contribute to VSM cell proliferation (Lin *et al.*, 2006). In this study, the effect of lipopolysaccharide (LPS) upon human aortic VSM cells was assessed. LPS is a molecular marker found only on gram negative bacteria, which is recognised by a TLR-4/MD-2 complex as part of the innate immune system. Its presence is believed to be a risk factor for cardiovascular disease (Kiechl *et al.*, 2001). As expected, the addition of LPS caused an increase in TLR-4 messenger ribonucleic acid (mRNA) expression, as well as MAPK pathways (p38, ERK1/2 and SAPK/JNK). This response was blocked by Rac-1 inhibition, which is responsible for reactive oxygen species and MAPK stimulation. It was also blocked by a non-specific NADP oxidase inhibitor, diphenylene iodonium (DPI). Finally, the addition of LPS in a rabbit aorta balloon injury model resulted in a significantly increased neointimal hyperplastic response. The effect of LPS on VSM cells was also assessed in another study (Yang *et al.*, 2005). LPS stimulation of coronary artery smooth muscle cells resulted in an increased expression of ERK 1/2, MCP-1, IL-6 and IL-12. Addition of exogenous CD14, a cell surface marker essential in TLR-4 activation, enhanced the stimulation of these proteins. In contrast, expression of a dominant negative form of TLR-4 inhibited the LPS induced effect. Therefore, VSM cells activated by TLR-4 are likely to play a role in generating a proliferative phenotype through the production of inflammatory cytokines. Since only small levels of PAMPs are needed in order to activate a response, and sub-clinical infections are extremely hard to diagnose, an anti-bacterial agent may not be effective under

clinical conditions. Instead, targeting the activation of TLRs or the resulting downstream pathways may be a better therapeutic strategy.

NF-κB and vascular proliferative disease

The main inflammatory pathway downstream of TLR-4 activation is nuclear factor kappa-light-chain-enhancer of activated B cells (NF-κB), as shown in Fig. 1.3. The pathway regulates gene expression for pro-inflammatory proteins which activate a cascade of subsequent pathways (Ghosh *et al.*, 1998). NF-κB is activated in the TLR-4 pathway via TRAF6 signalling to TAK1, which activates the IκB-kinase complex to phosphorylate the IκB proteins (Sato *et al.*, 2005). Subsequent ubiquitination and proteasomal degradation of IκB leads to the release of NF-κB into the nucleus, resulting in the transcription of inflammatory cytokines and adhesion molecules (Karin and Ben-Neriah, 2000). The importance of NF-κB in vascular proliferative disease has long been known (Bourcier, 1997; Brand *et al.*, 1996). Also, NF-κB is responsible for the generation of pro-inflammatory cytokines and chemokines such as TNF-α and MCP-1 which are associated with AVF stenosis. Experimentally, it has been shown that inhibition of NF-κB in rabbit interpositional vein graft using NF-κB decoy oligodeoxynucleotides significantly inhibits the development of intimal hyperplasia (Miyake *et al.*, 2006). Also, using a rat AVF model it has been shown that NF-κB activity measured by a chemiluminescence-based assay kit is significantly increased 1 week post AVF creation (Juncos *et al.*, 2011). Therefore NF-κB is another pathway downstream of TLR-4 activation which may be important in AVF stenosis.

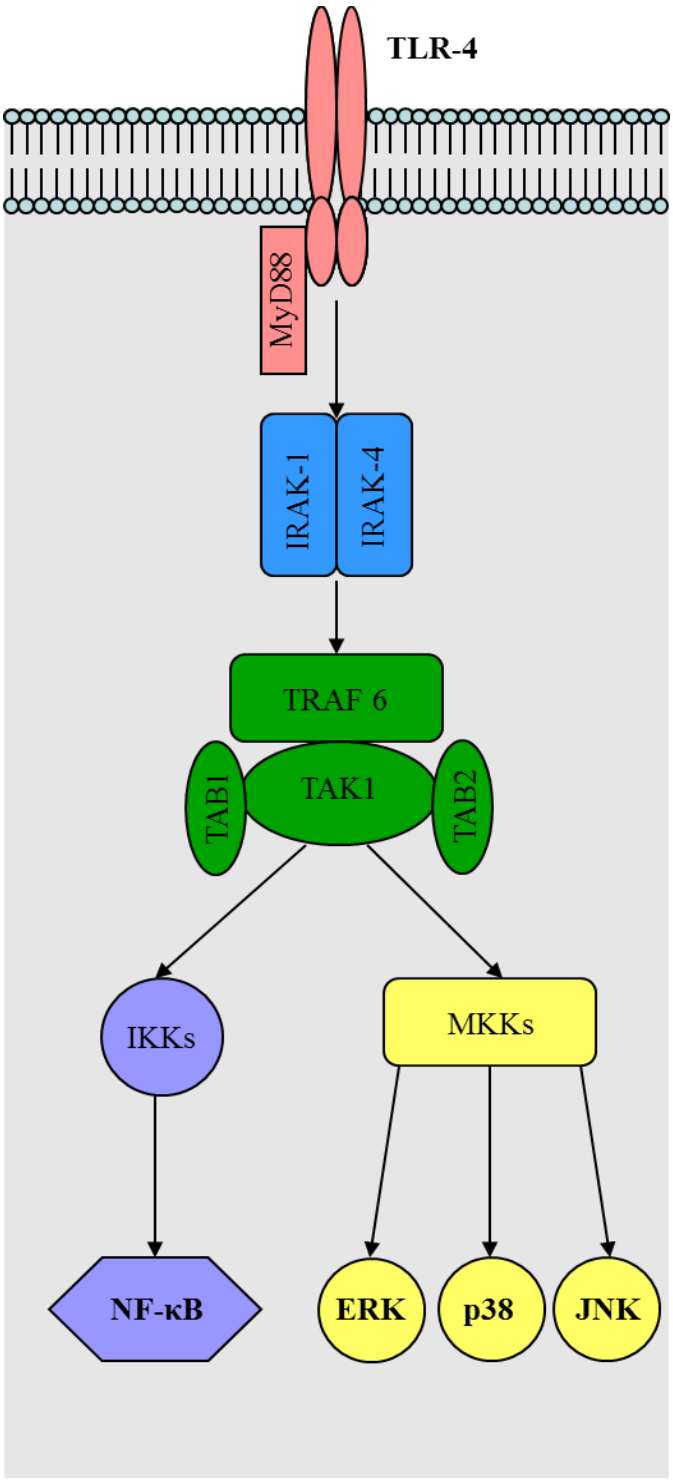

Figure 1.3. TLR-4 activation leading to cell proliferation and inflammation. *Activation of TLR causes a cascade which leads to the activation of MAPK and NF-κB pathways. This pathway results in an inflammatory/proliferative response in VSM cells (Han et al., 1994; Boyer and Lemichez, 2004; Han, 2006; Landström, 2010).*

1.3 Vascular smooth muscle cell proliferation

Cell proliferation of VSM cells plays an important role in the maturation of an AVF. Thereafter, in certain patients a hyper-proliferative response can occur leading to the development of intimal hyperplasia and stenosis. The activation of inappropriate proliferation leading to occlusion in AVF is poorly defined. While there are parallels between this condition and atherosclerosis, intimal hyperplasia of AVF remains very different. For example, atherosclerosis can develop over years (Ross, 1993), in contrast with the matter of months it takes for AVF stenosis to occur. This suggests that the events which trigger these two vascular pathologies differ greatly.

VSM cells are normally in a quiescent G0 phenotype, and have a low rate of proliferation (Gordon *et al.*, 1990). However, when exposed to a mitogenic stimulus, they move into G1 of interphase and start to proliferate. There are numerous activators of VSM cell proliferation; platelet derived growth factor (PDGF) produced by thrombosis (Englesbe *et al.*, 2004) and inflammatory cytokines such as TNF-α and IL-1 (Charron *et al.*, 2006) are just two examples. These proliferative processes are driven by the activation of the mitogen-activated protein kinase (MAPK) pathways (Jacob *et al.*, 2005). There are three well defined sub pathways of MAPK; extracellular signal-regulated kinases 1/2 (ERK1/2), c-Jun amino-terminal kinases (JNKs) and the p38 MAPKs (Chang and Karin, 2001). Stimulation of the aforementioned pathways occurs continuously, and begins with a stimulus, such as a cytokine or growth factor, leading to a cascade of kinase phosphorylation and activation of transcription factors controlling cellular events such as proliferation or apoptosis (Johnson and Lapadat, 2002).

Cross talk of pathways controlling inflammation and proliferation

Activation of VSM cell proliferation can occur upon stimulation by an inflammatory signal such as the cytokine IL-6 (Y. Son *et al.*, 2008) or activation of TLR-4 (Lin *et al.*, 2007). The majority of research in this field has been carried out in immune cells. Within this program of work, the activation of TLR-4 in proliferation of non-immune cells (VSM) will be investigated. As shown in Fig. 1.3, the activation of

TLR-4 with a ligand such as LPS activates a cascade leading to both inflammatory and proliferative pathways. Signalling through the MyD88 pathway causes the recruitment and auto-phosphorylation of IRAK-4/IRAK-1. The phosphorylated complex can then bind to TRAF6 and activate MAPK kinase kinase (MAPKKK) signalling pathways, leading to the activation of NF-κB and MAPK (Kopp and Medzhitov, 1999). Activation of the MAPK pathway ultimately leads to the translocation of transcription factors such as AP-1 into the nucleus, leading to the transcription of proliferation associated proteins (Karin, 1995). MAPK is discussed in more detail within section 1.3.1.

1.3.1 The mitogen-activated protein kinase pathway and vascular proliferative disease

ERK pathway

ERK is a member of the MAPK signalling pathway which consists of two subunits, ERK1 and ERK2 (Boulton and Cobb, 1991). Phosphorylation of ERK is mainly associated with a proliferative response to a mitogenic stimulus (Lewis *et al.*, 1998). Classically ERK is activated by the stimulation of a tyrosine kinase receptor, leading to the activation of Ras. This proto-oncogene then activates a signalling cascade including MKK 1/2, leading to ERK1/2 phosphorylation (Marshall, 1995). Mutations which activate Ras have been linked to a wide range of tumours (Lawrence *et al.*, 2008). Previously, research within the cardiovascular group at the University of Strathclyde has shown the importance of the Ras activated MAPK pathway in cell proliferation leading to vascular pathology (Coats *et al.*, 2008). Ras membrane localisation was reduced in human VSM cells using a Ras farnesyl transferase inhibitor (FPT III). This lead to inhibition of foetal calf serum (FCS) stimulated cell proliferation and inhibition of platelet derived growth factor (PDGF) stimulated ERK1/2 activation. Using a rabbit stent insertion model, FPT III significantly reduced in-stent restenosis.

In addition to classical activation of ERK by growth hormones, it has been widely demonstrated that ERK can become phosphorylated during TLR-4 stimulation by LPS (Hong *et al.*, 2009; Lin *et al.*, 2007, 2006; Son *et al.*, 2008; Yang *et al.*, 2005). The role of MAPK signalling in LPS stimulated IL-6 production by human aortic VSM cells has been demonstrated (Son *et al.*, 2008). Three dominant negative genes were applied to different groups of cells prior to stimulation; a MKK1 (ERK1/2), MKK3 (p38) and MKK4 (JNK) negative. These MAPK kinases form part of the cascade which leads to activation of each MAPK. Only the attenuation of ERK1/2 and p38 pathways inhibited IL-6 promotion. A similar result was shown when MAPK inhibitors U0126 (ERK1/2) and SB202190 (p38) were added prior to stimulation. In another study the role of ERK and NF-κB in the generation of the pro-inflammatory cytokine IL-8 was investigated (Hong *et al.*, 2009). Human aortic

VSM cells stimulated by LPS underwent significantly increased activation of ERK and NF-κB resulting in IL-8 production. When ERK was attenuated by a dominant negative of MKK1, LPS stimulated IL-8 production was reduced. These studies clearly show that activation of the ERK1/2 pathway is a downstream consequence of TLR activation which can contribute to VSM cell proliferation and inflammatory cytokine production, as shown in Fig. 1.3.

p38 pathway

The p38 MAPK pathway is activated more so by environmental stresses than mitogens, and was first identified in response to LPS stimulation of mammalian cells (Han *et al.*, 1994) through the mechanisms shown in Fig. 1.3. p38 MAPK can become activated by ultraviolet irradiation, hypoxia, ischemia, heat shock, oxidative stress, activation of TLRs and inflammatory cytokines IL-1 and TNF-α (Obata *et al.*, 2000). Therefore, due to the nature of its activation, p38 MAPK is thought to play an important role in the pathogenesis of cardiovascular disease.

p38, as well as ERK and JNK activation have been studied in response to vein graft arterialisation (Saunders *et al.*, 2004). A canine carotid-jugular vein graft model was used, with tissues harvested at a number of time points up to 28 days, by which time significant intimal hyperplasia had developed. Vein to vein graft was used as a control which developed no intimal hyperplasia Phosphorylation of p38 and ERK, but not JNK, were found to be significantly upregulated compared to the vein to vein grafts up to 4 days after arterial grafting, analysed by immunoblotting. In another study, the role of p38 activation in LPS induced IL-6 production by rat VSM cells was investigated (Chu *et al.*, 2010). Like the effect of attenuating ERK which was discussed in the previous section, the attenuation of p38 by pharmacological inhibition (SB203580) greatly reduced the level of IL-6 production. Therefore, the p38 pathway has been shown to play an important role in the generation of an inflammatory and proliferative phenotype and may be involved in AVF stenosis.

JNK pathway

JNK activation is one of the main signalling events activated in response to stressful stimuli, such as TLR-4 activation by LPS (Davis, 2000; Factor *et al.*, 1998). As shown in Fig. 1.3, activation of the TLR complex stimulates TRAF6, which in the presence of TAB1/2 activates the protein kinase TAK1 (Landström, 2010). TAK1 activation can lead to phosphorylation of MKK4 or MKK7, activating JNK to promote expression of transcription factor c-Jun (Sato *et al.*, 2005). c-Jun, which is also stimulated by the ERK pathway, is essential for the expression of AP-1 to promote cell proliferation; therefore it is likely to play a role in AVF stenosis (Weston and Davis, 2007). The role of c-Jun in the development of intimal hyperplasia has been investigated in sections of human saphenous vein obtained during bypass surgeries (Ni *et al.*, 2010). The vessels were segmented and cultured in RPMI (20% FCS). At random, a group of veins were treated with Dz13, a c-Jun DNAzyme, for 14 days. Dz13 treatment significantly reduced intimal hyperplasia compared to controls. Then, using a rabbit jugular-carotid vein graft model, the effect of blocking c-Jun *in vivo* was assessed. Prior to the procedure, veins were incubated with either vehicle or Dz13 containing solution. Intimal hyperplasia was significantly lower in Dz13 treated group compared to controls. This study highlights the role of JNK in vascular proliferation; however JNK activation is associated with cell apoptosis which can potentiate an inflammatory and proliferative response (Onai, 1998).

The role of JNK and p38 mediated apoptosis and proliferation was assessed using a mouse femoral artery wire injury model (Zou *et al.*, 2007). In this study JNK and p38 activation peaked at 10 min post arterial injury, measured by zymography. This was immediately followed by an increase in cell apoptosis within the vessel peaking at day 1, and cell proliferation peaking at day 7; resulting in a significant intimal hyperplastic response. Pharmacological inhibition of JNK and p38 independently reduced intimal hyperplasia. Therefore, it appears that JNK induced apoptosis at day 1 stimulates cell proliferation at day 7, most likely in an indirect manner through release of intracellular components following cell death. JNK may therefore play an important role in AVF stenosis via activation of apoptosis and proliferation.

1.3.2 The cell cycle and vascular proliferation

Downstream of the MAPK proliferative cascade, VSM cells must pass through a number of checkpoints which allow cell cycle progression and ultimately cell division. VSM cell division involves two processes; interphase in which the cell prepares and undergoes deoxyribonucleic acid (DNA) synthesis, and mitosis which is the process of cell division. The four phases of interphase, also known as the cell cycle, are shown in Fig. 1.4. Normally VSM cells are quiescent, and in the G0 phase of the cell cycle (Gordon *et al.*, 1990). When cells are stimulated by a mitogen, activation of MAPK occurs, in turn resulting in the production of the proto-oncogenes c-fos, c-myc, and ras amongst others (Hunter, 1997). c-fos and c-myc lead to increased expression of cyclins D and E, which are essential for progression through G1 phase (Phuchareon and Tokuhisa, 1995). The activation of cyclin-dependent kinases (CDK) is also essential for cyclin function. CDK4/6 are required for cyclin D activity during G1, CDK2 is required by cyclins E and A during S phase and CDK1 is essential for cyclin B during G2 and M (Nurse, 1994; Sherr, 1994). At the end of G1 the cell reaches the restriction point (R), and it is then committed to DNA synthesis. The S phase is the stage at which DNA replication occurs, and G2 is the stage at which proteins essential to division are synthesised. The cell can now enter into mitosis (M) and begin to divide (Charron *et al.*, 2006).

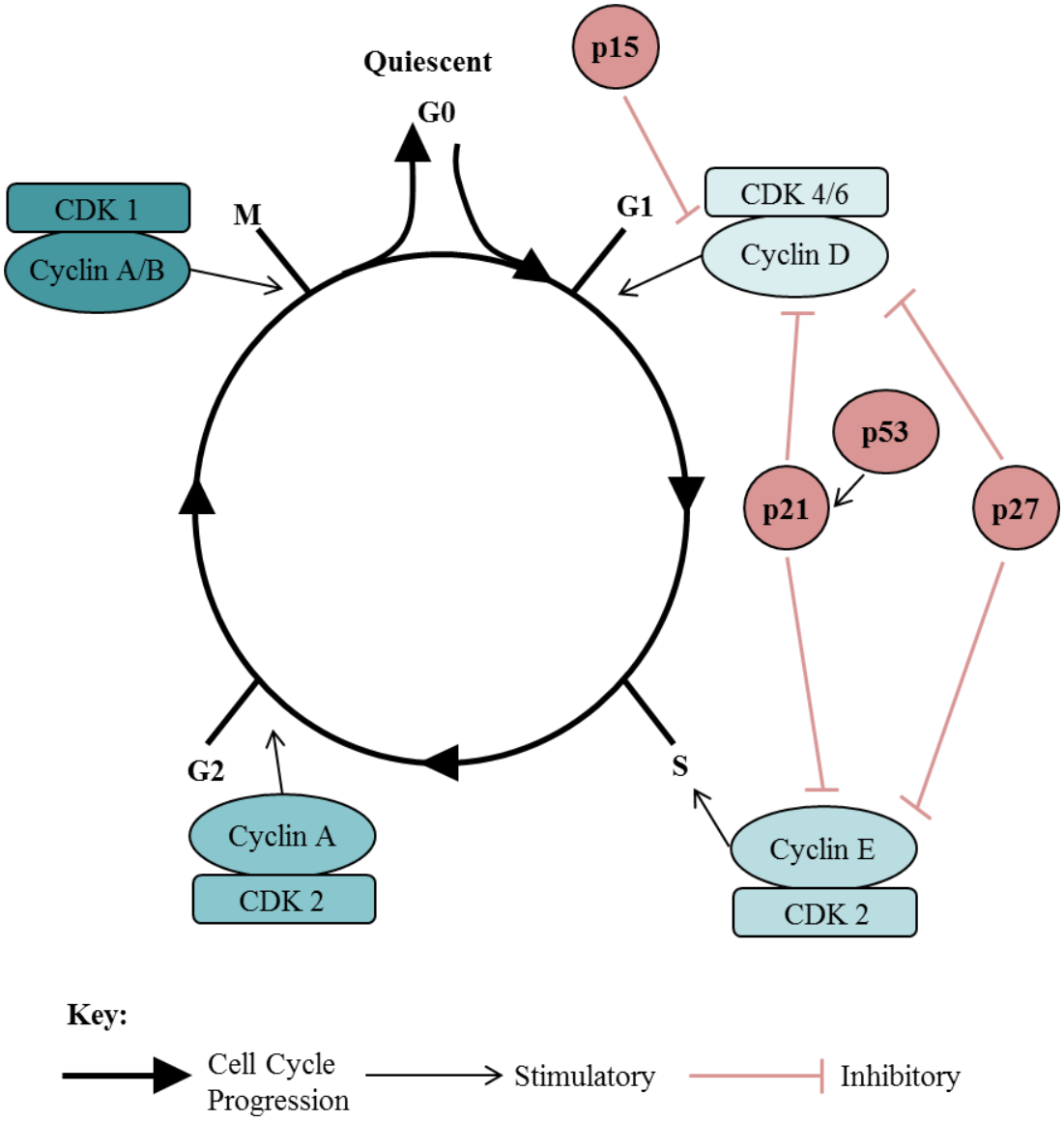

Figure 1.4. Vascular smooth muscle cell cycle. *This figure demonstrates the different stages of the cell cycle which occur during proliferation activated by mitogenic stimulation. In blue are the cyclins and CDKs which are essential for each phase of cell cycle progression. In red are the cell cycle inhibitory proteins which act upon specific cyclins to halt cell cycle progression (Charron et al., 2006).*

Mediators of cell cycle

Cell cycle progression is directly controlled through the regulation of CDKs by cell cycle inhibitory proteins (CKI). These can be split into two groups; inhibitors of CDK4 (INK4) and the CDK interacting protein/kinase inhibitory protein (Cip/Kip). The first group, INK4, is made up of p15, p16, p18 and p19. These CKIs can directly inactivate CDKs 4/6, causing inhibition of cyclin D activity (Sherr and Roberts, 1995). p15, shown in Fig. 1.4, can be stimulated by transforming growth factor-β (TGF-β) to form a complex with CDK4 or CDK6 and inhibit their binding to cyclin D (Hannon and Beach, 1994). The Cip/Kip family of direct inhibitors include p21, p27 and p57. These CKI regulators bind directly with the CDK/cyclin complex. For example, both p21 and p27 (Fig. 1.4) can bind with either cyclin D-CDK4 or cyclin E-CDK2 and stop G1 progression (Harper *et al.*, 1993; Polyak *et al.*, 1994).

There are various upstream activators of CKIs which utilise their inhibitory actions to halt cell cycle progression. TGF-β can not only activate p15 but also p27 to halt progression in the G1 phase. TGF-β is part of a large family of proteins which exhibit regulatory actions on cell growth, differentiation and matrix deposition (Massagué, 2000). TGF-β acts by causing heteromeric interaction of two receptors, TGF-β type I and II. This then initiates an intracellular signalling cascade of SMAD proteins which relay the signal to the nucleus and direct transcriptional responses (Derynck *et al.*, 1998). As a result, there is an increase in the expression of p15 mRNA, as well as an increase in binding of p15 to CDK4/6, as shown in Fig. 1.4 (Hannon and Beach, 1994; Reynisdottir *et al.*, 1995). This p15 binding event triggers the release of p27 and p21 (independent of p53 activation), which then associates with the cyclin E/CDK2 complex to halt cell cycle progression. Normally, in healthy VSM cells which are in the G0 phase the expression of p27 is high. Following cell stimulation, the resulting oncogenes c-myc and ras inhibit expression of p27 to allow cell cycle progression (Leone *et al.*, 1997).

Activation of VSM cell proliferation can occur when there is an imbalance between the level of stimulation and expression of CKIs. The expression of p21, p27, CDK2 and proliferating cell nuclear antigen (PCNA) was studied in failed AVF vs. healthy

vein and arteries (De Graaf *et al.*, 2003). p21 was found to be significantly decreased in failed AVF vs. healthy controls; with no significant difference in p27 expression. In addition, CDK2 and PCNA were significantly increased vs. healthy controls. This thereby indicates that AVF failure could be due to a disruption in p21 induced cell cycle regulation of VSM cells, allowing an increased rate of proliferation. Other studies have also shown that p21 is an important regulator of VSM cell proliferation *in vitro* and *in vivo* (Tanner *et al.*, 2000; Yang *et al.*, 1996). Therefore, targeting of key CKI regulators may be a useful strategy in the development of new vascular proliferative disease therapies.

AMP-activated protein kinase mediated control of cell cycle

AMP-activated protein kinase (AMPK) is a highly conserved serine/threonine protein kinase involved in homoeostasis of cellular metabolism (Hardie and Carling, 1997). AMPK exists as a heterotrimeric complex containing three subunits; α, β and γ. The α subunit, consisting of α1 and α2, is the main catalytically active component (Crute, 1998). AMPK is activated during a reduction in the AMP: ATP ratio, due to a decrease in nutrient supply or increase in cellular demand. This then activates catabolic processes and inhibits energy consuming anabolic pathways such as cell proliferation (Hardie *et al.*, 1998). Fig. 1.5 shows the mechanisms though which AMPK activation inhibits proliferation via cell cycle arrest. This process was investigated in human aortic VSM cells (Igata *et al.*, 2005). The AMPK agonist 5-Aminoimidazole- 4-carboxamide ribonucleoside (AICAR) was used to induce AMPK phosphorylation. It is believed AICAR activates the ataxia telangiectasia mutated (ATM) kinase which can then directly phosphorylate AMPK (Sun *et al.*, 2007). Igata and colleagues demonstrated an AICAR mediated concentration dependent increase in AMPK phosphorylation and subsequently a decrease in cell proliferation stimulated by both FCS and platelet derived growth factor-BB (PDGF-BB). AICAR induced an increase in total and phosphorylated levels of p53, as well as an increase in p21 mRNA. AICAR treatment resulted in an increased population of G0/G1 phase cells measured by flow cytometry. All of the AICAR induced effects on cell cycle were reversed by insertion of a dominant negative AMPK by

adenovirus. AMPK stimulated G1 arrest though p53/p21 has also been confirmed in other cell types such as mouse embryonic fibroblasts (Jones *et al.*, 2005) and melanoma cells (Petti *et al.*, 2012). Therefore, AMPK may be a valid therapeutic target which could regulate VSM cell hyper-proliferation via cell cycle arrest.

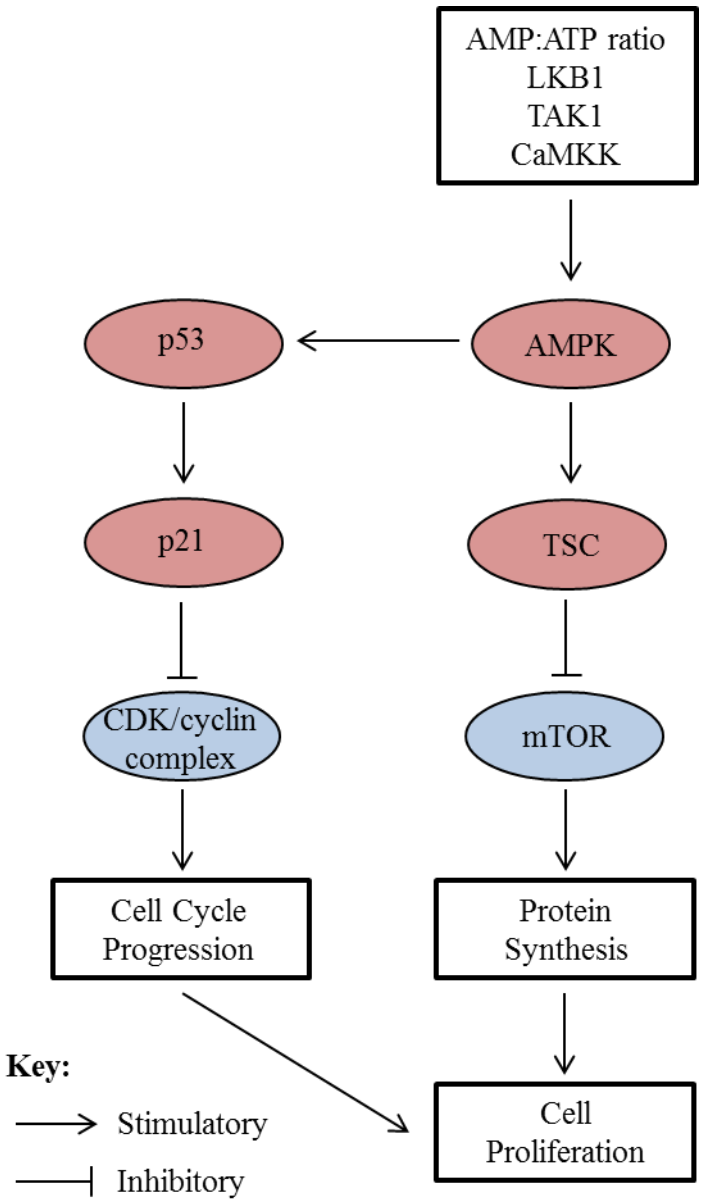

Figure 1.5. AMPK as an indirect regulator of cell cycle progression and proliferation. *The phosphorylation of AMPK leads to inhibition of cell cycle progression via activation of p53 and p21. Protein synthesis, also essential for cell proliferation, is down-regulated by activation of AMPK via tuberous sclerosis complex (TSC) inhibition of mammalian target of rapamycin (mTOR) (Motoshima et al., 2006).*

1.4 *In vivo* AVF models

A translational *in vivo* model of AVF remodelling is an important tool in the study of AVF failure. Such a model would give greater insight into the events which take place in AVF failure at different time points, and not just at the end as studied in human tissues. Also, an *in vivo* model would allow interventional studies to be undertaken. This would allow the efficacy of various drugs and inhibitors to be demonstrated in an intact system with a fully functioning immune system.

Rodent AVF models

There are a number of vein graft models in use for the study of bypass failure. However, the haemodynamic stresses which arise from interpositional vein grafts are different to those which are present at the anastomosis of an AVF. Therefore, general vein graft models are of limited use in the study of AVF remodelling. Both mice and rats have been used previously for AVF creation (Juncos *et al.*, 2011). An end to side anastomosis between the common carotid artery and jugular vein of a mouse was used to study the role of monocyte chemoattractant protein-1 (MCP-1) in remodelling. The advantage of this type of model is that genetically deficient mice can be used to show a causative role. It was found that creation of an AVF within MCP-1 knockout mice were significantly protected from adverse remodelling. Also, a rat AVF model has been used to investigate the role of N^G-nitro-L-arginine methyl ester (L-name), a nitric oxide synthase (NOS) inhibitor, in remodelling (Croatt *et al.*, 2010). An end to side anastomosis was created between the femoral artery and femoral vein. The administration of L-name was associated with a significant increase in venous neo-intima formation, as well as an increase in pro-inflammatory MCP-1 and cytokine-induced neutrophil chemoattractant-1 (CINC-1). An end to side femoral rat AVF model has also been used in another study (Langer *et al.*, 2010). In this study, animals were split into a control group and a group which received an adenine rich diet to induce chronic kidney disease (CKD). Ultrasound was used to demonstrate a significantly increased level of neointimal thickening in the CKD group over time. This was accompanied by an increase in peak systolic velocity at the anastomosis, a sign of stenosis. Histological analysis confirmed the

significant increase in neo-intima within the CKD group, as well as shrinkage in the medial layer. CKD disease was also associated with a significant increase in calcification of the AVF. Using these *in vivo* rodent models, a number of important proteins and mechanisms have been demonstrated. However, the size of AVF which can be achieved in these animals limits the studies which can be undertaken. For example, these models would not allow the incorporation of cannulation injury, which is as yet unexplored.

Rabbit AVF models

One of the first studies to use a rabbit AVF experimental model was published in 1987 (Greenhill and Stehbens, 1987). The aim of this was to investigate the chronic effects of altered haemodynamics on arteries feeding the AVF. The fistula was created by anastomosing the right femoral artery and femoral vein in a side to side fashion for a distance of 8mm. This type of graft allows arterial blood flow to the lower limb, as well as the draining of blood back through the femoral vein. A similar side to side fistula can be created in humans for vascular access, although an end to side anastomosis is preferred (Klaus Konner, 2003). Greenhill and Stehbens used scanning electron microscopy to analyse the artery which feeds the AVF. It was found that the diameter increased by 1.5 times, with the remaining artery distal to the anastomosis showing no alteration. Over the course of the study (285 days), transverse and longitudinal tears in the internal elastic lamina were observed along the entire afferent artery back to the abdominal aortic bifurcation, but not in the unoperated left side. This study demonstrated the effects of altered haemodynamics on arteries feeding the AVF; however it did not study the effect of this change on the venous branch. In 1995, this group published a subsequent paper which aimed to use this method to establish a model for atherosclerosis (Jones & Stehbens 1995). Animals were investigated up to 895 days post AVF creation for the development of fibro-fatty lesions in arteries proximal to the anastomosis. As before, they identified micro-fractures in the internal elastic lamina, as well as considerable intimal proliferation. Other ultra-structural changes included a dystrophic basement membrane, necrosis of smooth muscle cells and accumulation of foam cells. These

results suggest that augmented haemodynamic stresses associated with the formation of a femoral AVF may induce changes in the feeding arteries similar to that which occur in human atherosclerosis (Williams and Tabas, 1995).

A rabbit femoral side to side AVF has also been created experimentally by different groups in two other studies (Ricard *et al.*, 1992; Sun *et al.*, 2005). The aim of Ricard *et al.* was to establish an original model for heart volume overload. They found that femoral-femoral AVF caused a 50% increase in mean cardiac output, which was evaluated up to 11 weeks post procedure; demonstrated by dimensional echocardiogram and Doppler flow measurement at the aortic ring. The aim of Sun *et al.* was to evaluate colour Doppler flow imaging in the diagnosis of peripheral vascular diseases. Again, these studies did not evaluate the remodelling which is undergone in the venous branch of the AVF. However, these papers provide assurance that with appropriate surgical techniques and after care the establishment of a side to side fistula in rabbit femoral vessels is feasible.

An alternative method to establish an AVF is an end to end anastomosis, where the distal artery and vein are ligated. This technique was applied to a bone tissue engineering model (Dong *et al.*, 2010). An end to end, femoral arteriovenous loop was created which could then be placed in a coral bone construct. The increase in wall sheer stress within the vein triggered angiogenesis within the coral construct, which is normally a major obstacle in bone tissue engineering. According to the study, no major surgical complications or thrombosis occurred from this AVF creation method. Therefore, an end to end anastomosis is another technique which may be employed in creation of a rabbit femoral AVF, and may allow greater control over the position due to the creation of a loop. The unilateral blood flow that this technique allows is only limited by the flow of the arterial blood. However, with this type of anastomosis there is an increased risk of severe peripheral ischemia.

This study aims to develop, where possible, a clinically relevant rabbit model of AVF remodelling. The previous rabbit studies reviewed in this section have focussed on either arterial remodelling or the cardiac effects of AVF creation. The

model which is presented in this thesis will focus on the changes which occur in the venous branch of the fistula, and for the first time evaluate the effect of needle injury. In addition to this, the model will be used as part of an interventional study using a drug which is clinically available for use in renal failure patients.

1.5 Therapies in AVF failure

Current treatment strategies

There are two parameters which are used to determine a hemodynamically relevant stenosis; a greater than 50% reduction in lumen diameter measured by angiography or ultrasound and the presence of a physiological abnormality such as elevated venous pressure or decreased blood flow (Besarab and Work, 2006). Current treatment strategies consist of either surgical repair or endovascular techniques carried out in an outpatient setting. Surgical repair includes among others; creation of a more proximal anastomosis, vein patching and PTFE graft interposition. Also, surgical thrombectomy can be used to rescue thrombosed fistulae (Lipari *et al.*, 2007). However, surgical procedures have a significant patient burden. Therefore, endovascular techniques such as percutaneous transluminal angioplasty are an attractive option. Prophylactic percutaneous transluminal angioplasty of stenosis in functioning forearm AVF has been shown to significantly improve access survival and decrease access-related morbidity (Tessitore, 2003). However, the disadvantage of these procedures are that they require frequent revision as the 12 month patency rate can be as low as 26% (Clark *et al.*, 2002).

The potential of clinically available therapeutics

A prophylactic pharmacological intervention to increase AVF patency is the ideal solution to a significant problem. However, the best stage at which to intervene is not clear. The lack of kidney function in these patients must also be taken into consideration. It is obvious that this will have an impact on renally excreted drugs, but there is also evidence that agents which are extensively metabolised in the liver and intestine may also be impaired (Sun *et al.*, 2006). This is thought to be caused by the build-up of ureamic toxins which inhibit the action of cell transporters such as; organic anion/cation transporters, intestinal efflux transporters, and hepatic metabolising enzymes. These points must be taken into consideration when selecting possible therapeutics. The advantage of using agents which are already available for other conditions is that they will be clinically well defined and extensively studied.

Two main approaches have been taken in the trial of clinically available drugs to treat AVF stenosis; anti-platelet and anti-proliferative.

Anti-platelet therapy in AVF failure

Non-steroidal anti-inflammatory drugs (NSAIDs) are an extensively studied family of compounds which inhibit the enzyme cyclooxygenase (COX) to produce analgesic, anti-pyretic and anti-inflammatory effects. Aspirin, part of the NSAID family, is widely prescribed to patients at risk of cardiovascular disease for its anti-platelet properties (Antithrombotic Trialists' Collaboration 2002). This is achieved by irreversible inhibition of COX in platelets, leading to inhibition of thromboxane A2 production, a potent inducer of platelet aggregation. Cyclooxygenase dependent production of the anti-thrombotic agent prostacyclin by cells within the vessel wall is quickly recovered following aspirin treatment; thus, causing overall anti-thrombotic activity (Weksler et al., 1983). It has been proposed that aspirin may be beneficial in prolonging the survival of AVF grafts. This was investigated using the DOPPS database (Hasegawa *et al.*, 2008). This study used the details of 2815 patients consistently receiving aspirin collected between 1996-2004. Continued use of aspirin at one year significantly lowered the risk of final AVF failure, with no association with increased gastrointestinal bleeding among the subjects.

The efficacy of other anti-platelet drugs have also been studied in patients requiring vascular access (Dixon *et al.*, 2009)**.** The effect of dipyridamole plus aspirin therapy on primary graft patency rates was investigated in a double blind, placebo controlled trial. The study took place over 13 centres in the US, and involved 649 patients over 4.5 years. The average primary patency rate at year 1 on the placebo group was 23%, which was significantly increased to 28% in the dipyridamole plus aspirin group. No increased incidences of adverse events at the AVF site, or gastrointestinal bleeding were found in this study. These studies suggest that anti-platelet therapy, particularly via inhibition of COX, may increase AVF patency rates. However, the risk of adverse bleeding is still of concern as a previous randomised clinical trial of clopidogrel plus aspirin had to be halted for this reason (Kaufman *et al.*, 2003).

Anti-proliferative therapy in AVF failure

The main issue for current and future therapies to address in AVF failure is the formation of neointimal hyperplasia within the vein caused by VSM cell proliferation (Roy-Chaudhury *et al.*, 2007; Lee and Roy-Chaudhury, 2009). The majority of therapies which have been trialled in the past have been anti-platelet drugs, with only some small anecdotal studies focussed on anti-proliferative agents. Indeed, some of the therapeutic benefit of anti-platelet drugs may arise from other anti-proliferative activity. Dipyridamole, detailed in the previous section for its anti-platelet activity, has been shown to inhibit vascular proliferation (Singh *et al.*, 1994). Singh *et al.* demonstrated in the nineties that dipyridamole inhibited VSM cell proliferation in a dose dependent manner. Using a rabbit carotid balloon injury model, dipyridamole was shown to significantly reduce the amount of intimal thickening which developed. Similar effects were not seen in dipyridamole analogues SH-869 and mopamidol, suggesting that cell growth inhibition was independent of the anti-platelet activity. More recently, the mechanisms responsible for dipyridamole's activity have been investigated using human arterial and venous VSM cells (Zhuplatov *et al.*, 2006). Dipyridamole caused a concentration and time dependent increase in cyclic adenosine monophosphate (cAMP) and cyclic guanosine monophosphate (cGMP) in both arterial and venous cells. Specific competitive inhibitors of protein kinases A and G attenuated the anti-proliferative effects of dipyridamole, with inhibition of protein kinase G having a more pronounced effect on venous cells. Cell cycle analysis of dipyridamole treated cells reveal an increased population of cells in G0/G1, and a subsequent reduction in the S phase. This study suggests a dipyridamole induced increase in cAMP and cGMP can activate downstream pathways which cause cell cycle arrest.

Like dipyridamole, some of aspirin's therapeutic benefit may also be mediated by anti-proliferative activity. The frequency of aspirin use and the incidence of fatal cancer was investigated previously (Thun *et al.* in 1993). With an increased frequency of aspirin use there was a significant decrease in recorded fatalities in cancers of the oesophagus, stomach, colon, and rectum. Then in 1995, a direct inhibitory effect of aspirin on rat glioma cancer cell proliferation was demonstrated

(Aas *et al.,* 1995). This effect was also demonstrated with salicylic acid treatment, but not with indomethacin or piroxicam (also NSAID), indicating that the activity was independent of prostaglandin inhibition. The main mechanistic insight shown in this paper was a marked 35% reduction in ATP synthesis compared to non-treated cells. In the same study, aspirin was also shown to inhibit tumour formation induced by the same rat glioma cells in an *in vivo* rat model. Further mechanistic insight into aspirin and other NSAID anti-proliferative activity has been demonstrated (Brooks *et al.,* 2003). Salicylate based NSAIDs caused a post G1/S block via the hyper-phosphorylation of p107 resulting in increased levels of cyclin A; whereas non-salicylate NSAIDs caused an accumulation of cells in G0/G1. All NSAIDs were shown to induce expression of cell cycle regulators p21 and p27.

Recently, inhibition of AMPK was implicated in aspirin's anti-proliferative activity (Sung and Choi, 2011). The therapeutic benefit was examined on VSM cells explanted from healthy and spontaneously hypertensive rats. Aspirin significantly increased the phosphorylation of AMPK and acetyl-CoA carboxylase (downstream protein activated by AMPK) in a time and concentration dependent manner. These effects were more pronounced in VSM cells from the hypertensive rats; as basal phosphorylation of AMPK was lower vs. healthy controls. This correlated with a concentration dependent decrease in proliferation of cells derived from hypertensive rats. Also in hypertensive VSM cells, aspirin increased expression of p53 and p21, leading to a decrease in phosphorylation of cyclin D and cyclin E. These aspirin induced changes in cell cycle proteins and overall proliferation were blocked by the addition of AMPK inhibitor compound C; as well as AMPK knock-down by siRNA More recently it was demonstrated that aspirin directly binds to AMPK via the β1 subunit (Hawley *et al.,* 2012). This was shown *in vitro* and *in vivo* by mutating AMPKβ1 which subsequently inhibited aspirin induced AMPK activation. This mechanism of activation was the same as a commercially available AMPK agonist A-769662.

The extent to which aspirin mediated AMPK activation contributes to aspirin's reported therapeutic benefits is not clear. The cardio-protective dose of aspirin

(81mg) prescribed for its anti-platelet activity in all of the trials may be too low to activate the AMPK pathway. Most studies have indicated that aspirin is needed in the micromolar range in order to inhibit proliferation (Aas *et al.*, 1995; Brooks *et al.*, 2003; Hawley *et al.*, 2012). Such concentrations are achieved in high dose aspirin (325mg) used for its anti-inflammatory activity (Day *et al.*, 1989). However, adverse bleeding events which have ended clinical trials in the past are still a major limitation in its oral use (Kaufman *et al.*, 2003). The role of AMPK in the anti-proliferative activity of other more potent, non-salicylate based, NSAIDs is yet to be assessed.

Application of therapies in AVF failure

The therapies and trials discussed in previous sections have all involved oral delivery of a pharmacological agent. However, a high systemic concentration of agent is more likely to cause side effects such as adverse bleeding in the case of NSAIDs. Therefore, targeted local delivery should result in a higher concentration of agent at the site of action, while maintaining or reducing the original dosage. Perivascular delivery is an example of such an approach; where an agent is placed around or near the fistula/graft to release an agent over time. A system for this type of delivery was developed in a pig model of arteriovenous grafts (Kelly *et al.*, 2006). Kelly *et al.* used an ethylene vinyl acetate (EVA) polymeric matrix containing polyethylene glycol to control the release of the anti-proliferative drug paclitaxel. Paclitaxel is an anti-proliferative chemotherapeutic agent that causes polymerisation of microtubules in the cell during G2/M phase of the cycle, leading to cell arrest (Wang *et al.* 2000). Previously, paclitaxel has been shown to be effective against malignant tumours (Rowinsky, 1997). As with most anti-cancer drugs, adverse effects have ruled out their systemic application in vulnerable end stage renal failure patients. However through local delivery, high concentrations of the agent can be achieved which would be toxic if they were present systemically. Previous studies have demonstrated that this type of delivery system allows paclitaxel to diffuse throughout the whole vessel into the intima (Melhem *et al.*, 2006). Kelly *et al.* used a porcine model in which a PTFE graft was placed between the femoral artery and vein to create an arteriovenous graft. A paclitaxel eluting or control wrap was then applied around the

graft-vein anastomosis. The animals were sacrificed at early (10–11 days), middle (23–24 days) and late (32–38 days) time points. By the mid time point, the control wrap grafts had developed a 20.6% luminal stenosis, which increase to 49.5% by the later time point. The paclitaxel eluting wrap grafts showed no signs of luminal stenosis up to the end of the study. There was no local toxicity associated with the drug eluting wrap, assessed histologically at the time of sacrifice. Also, paclitaxel was not detected in the systemic circulation, even during the maximal release point. Blood parameters of the animals remained normal. Clearly, this type of treatment has the potential to limit juxta-anastomosis neointimal development. A limitation of this study was that the effect of this treatment on maturation of the graft was not studied, which could be assessed by ultrasound. Also, the long term effectiveness of the therapy to control the development of stenosis is yet to be evaluated. A large, multi-centre clinical trial using this approach was halted in 2009 due to an increased incidence of infection in patients (ClinicalTrials.gov Identifier: NCT00448708). In another randomized clinical trial, the efficacy of paclitaxel-coated balloon vs. non-coated balloon angioplasty in failing vascular access grafts was assessed (Katsanos and Karnabatidis, 2012). According to the 6 month interim results, cumulative target lesion primary patency for paclitaxel coated balloon angioplasty was 70% vs. 25% in non-coated balloon angioplasty. Again, no major or minor complications were present in either group within the study.

Topical administration is another form of application which could prove to be efficacious. The advantage of this route is that it could be applied at any time without the need for a surgical or endovascular outpatient procedure. Currently, research into topical application of therapeutic agents to improve arteriovenous fistula patency is limited. The main topical treatment currently in use is a lidocaine/prilocaine cream (EMLA) used for its analgesic properties during fistula venepuncture (Çelik *et al.*, 2011). However, the combined effect of topical heparin spray and traditional anti-platelet therapy has been assessed in a small number of patients using the results of a retrospective registry in Italy (Stuard *et al.*, 2010). Topical heparin use in combination with anti-platelet therapy for 6 months increased the amount of AVF still suitable for dialysis by 22.2%. Again, this is another

potential treatment which may prevent early failure of AVF; but the effect on long term patency is unknown.

1.6 Summary

Failure of AVF through adverse vascular remodelling is a complex, multifactorial process. However, it is clear that early and late failures of AVF are driven by different events. Early AVF failure tends to be due to the formation of neointima at the venous anastomosis or the formation of thrombus. Both of these events result in a reduction in flow through the vein, hindering the maturation response. There is significant evidence to suggest that this type of failure is largely due to surgical technique, vessel selection and patient background. However, less is known about the late failure of AVFs which have been used successfully to dialyse before developing stenotic lesions at different points along the vein. Again, stenosis in these grafts causes blood flow to decrease to a level which is no longer adequate for the haemodialysis to occur. There is anecdotal evidence to suggest that these lesions form in areas of the fistula which receive cannulation injury. However, to date the research into the contribution of needle injury in AVF stenosis is limited. What is clear is that both inflammatory and proliferative mechanisms play a significant role in late AVF failure. The role that inflammation plays in the hyper-proliferative response is unclear. However, previous research suggests the TLR-4 pathway may be involved in the pathological response by stimulation of both inflammation and proliferation. Identification of a pathway which is upregulated during AVF stenosis could be an important discovery for the development of future therapeutics. In the short term, these insights could justify the use of an already available pharmacological strategy which targets both of these pathological mechanisms downstream of TLR-4 activation, such as NSAID.

In order to validate observations made from *in vitro* experimentation, a clinically relevant *in vivo* model is vital. Currently, a number of animal models exist in both rodents and rabbits. The advantage of mouse models is the large variety of genetically deficient strains which could be used to validate the role of a specific protein or pathway. However, the size of rodent vessels makes good anastomosis difficult to achieve. Also, cannulation of the fistula in these rodent models would not be possible, therefore limiting their clinical relevance to late AVF failure. Studies which have utilised rabbit AVF models in the past have done so for reasons other

than AVF stenosis, i.e. cardiac overload, arterial remodelling, tissue engineering. Therefore a need exists for a clinically relevant rabbit model which can be used to investigate events and mechanisms in AVF stenosis and validate potential therapies.

1.7 Hypothesis and aims

The hypothesis being investigated in this thesis is that cannulation injury is a major event in late stenosis of AVF. Through this injury, TLR-4 can become activated in VSM cells and lead to a phenotypic switch resulting in hyper-proliferation within the vessel wall. A prophylactic therapeutic approach which targets either TLR-4, or the downstream inflammatory and proliferative pathways will prolong AVF patency.

The aims of this PhD study are to:

1. Use tissue and blood samples from human failed AVF vs. healthy controls to investigate inflammatory and proliferative characteristics present during AVF failure and the role of TLR-4.

2. Use explanted human VSM cells to investigate a currently available therapy which targets both inflammation and proliferation downstream of TLR-4.

3. Develop a novel and clinically relevant *in vivo* model of AVF remodelling which can be used to investigate the contribution of cannulation injury to the proliferative response.

4. Use this *in vivo* model as part of an interventional study using the therapeutic agent identified in aim 2.

5. Investigate the mechanisms responsible for any successful agents identified from the interventional study in aim 4.

Chapter 2

General Methods

2.1 Materials

Amersham (UK)

^{3}H thymidine solution

Corning Incorporated (USA)

T25 tissue culture flasks

DakoCytomation (Denmark)

DAB chromagen and substrate

Gibco (UK)

Ham's F12 medium

Penicillin streptomycin

Tryple Express

Waymouth's medium

National Diagnostics (USA)

Histoclear II

Histomount

Nunc (Denmark)

6 well plate

PerkinElmer (USA)

Emulsifier-safe scintillation fluid

Sigma-Aldrich (UK)

3-aminopropyltriethoxysilane

Acetic acid

Acetone

Bovine serum albumin

Disodium phosphate

Dithiothreitol

EDTA

Eosin

Ethanol

Foetal calf serum

Glycerol

H_2O_2

Hematoxylin Gill's III

Monopotassium phosphate

Paraformaldehyde

Potassium chloride

Sodium chloride

Sodium citrate

Sodium diphosphate

Sodium hydroxide

Sodium lauryl sulphate

Trichloroacetic acid

Triton X 100

Trizma base

Tween 20

TPP (Switzerland)

24 well plate

96 well plate

WVR (USA)

Glass coverslips

Microscope slides

Paraffin wax

2.2 Ethical approval

Ethical approval for the use of human tissues was obtained from the West of Scotland Ethics Committee and Strathclyde University Ethics Committee. Written informed consent was obtained from each subject to utilise excess tissue for research. Ethical approval for the use of animals in this study was obtained from the Home Office, as well as Strathclyde University Ethics Committee. All *in vivo* work was carried out according to the Animals (Scientific Procedures) Act 1986.

2.3 Histological sectioning and staining of vascular tissues

2.3.1 Fixation, wax embedding and cutting of tissues

Vessel segments were fixed in 10% paraformaldehyde for a minimum of 24 hr prior to processing. Tissues were then processed in a Citadel 1000 (Thermo Shandon, UK) processor overnight in the following conditions:

- 70% ethanol: 3 hr
- 90% ethanol: 3.5 hr
- 100% ethanol: 2 hr
- 100% ethanol: 1 hr
- 1:1 (v/v) of ethanol: histo-clear: 1 hr
- 100% histoclear: 1 hr
- 100% histoclear: 1 hr
- paraffin wax: 2 hr
- paraffin wax: 2 hr

Thereafter tissues were embedded in paraffin wax using a Leica EG1140H (Leica Microsystems, UK) embedder and 5μm sections cut using a Leica RM2125RTF (Leica Microsystems, UK) microtome. Tissue sections were floated onto silanated slides using a water bath at 60°C. Slides were silanated using the following protocol:

- acetone wash: 10 min
- submersed in 3-aminopropyltriethoxysilane (APES) solution (0.1% APES in acetone): 10 min

- running tap water: 10 min
- covered and air dried for 48 hr

Wax embedded sections were mounted on salinated slides and placed in an oven set between 60-65°C for 30 minutes. On their day of use, the slides were placed again in an oven at 60-65°C for 15 minutes.

2.3.2 Rehydration and dehydration of tissue slides

Prior to histological staining or immunohistochemistry, tissue sections were rehydrated using a Varistain 24-4 auto strainer (Thermo Shandon, UK) in the following solutions:

- histoclear: 10 min
- histoclear: 10 min
- histoclear: 10 min
- 100% ethanol: 5 min
- 100% ethanol: 5 min
- 100% dH_2O: 5 min

At the end of staining, the slides were dehydrated using the following protocol:

- 100% ethanol: 10 min
- 100% ethanol: 10 min
- 100% ethanol: 10 min
- histoclear: 5 min
- histoclear: 5 min
- histoclear: 5 min

2.3.3 Haematoxylin and eosin

The tissue slides were rehydrated as stated in section 2.3.2, and placed into metal racks for staining by haematoxylin and eosin (H&E) using the following procedure:

- Haematoxylin: 6 min
- dH_2O: 1 min

- Acid alcohol (1%): 3 sec
- dH_2O: 1 min
- Scots tap water substitute: 2 min
- dH_2O: 1 min
- Eosin: 1 min
- dH_2O: 1 min

Thereafter slides were dehydrated and mounted using histomount and 24x50mm coverslips. Slides were left to dry overnight before analysis.

2.3.4 Immunostaining

Rehydrated slides underwent antigen retrieval to break the formalin bonds which form in fixed tissue. This was performed using either Tris-EDTA buffer (10mM Tris base, 1mM EDTA, 0.05% Tween 20, pH 9.0) or Sodium Citrate buffer (10mM Sodium Citrate, 0.05% Tween 20, pH 6.0), which was preheated in a pressure cooker. The slides were placed in the cooker and heated in a 900watt microwave for 7 min. After depressurisation and cooling, slides were washed in phosphate buffered saline (PBS) (137mM NaCl, 2.7mM KCl, 10mM Na2HPO4, 2mM KH2PO4, pH 7.4).

Thereafter endogenous peroxidase activity was blocked using buffered 1.5% H_2O_2 for 10 min, followed by a PBS wash. To block non-specific binding, 10% serum (from a source compatible with the antibodies) was added to the sections for 1 hr at room temperature. Serum was then replaced with 10% serum containing the primary antibody at an appropriate concentration for 1-3 hr at room temperature, or overnight at 4°C. The slides were then washed in three changes of PBS before adding an appropriate concentration of the secondary antibody at room temperature for 1 hr. Slides were then washed as before, and DAB added for 5-15 min to visualise the staining. The slides were counter stained with haematoxylin, dehydrated and mounted.

2.3.5 Computer analysis of histological/immunohistochemical sections

A digital image of each section was captured under identical conditions using Adobe Photoshop v5 on a Leica DM LB2 microscope using a Leica DFC320 camera (Leica Microsystems, UK). Image J was used to quantify; the size of a structure within a vessel, the percentage of positive stained nuclei within a field of view, the staining intensity of a particular protein/component or the percentage staining within the vessel. The staining intensity/percentage staining was quantified by adjusting the colour thresholds to isolate the colour of interest. The intensity of the signal or percentage positive pixels was then quantified relative to the area of the vessel. Statistical significance between control and stenosed groups was calculated using an unpaired T-test on Minitab v15 and the graphs were plotted using Microsoft Excel 2010. A p value of <0.05 was considered significant.

2.4 *In vitro* vascular smooth muscle cell studies

2.4.1 Vascular smooth muscle cell explantation and culture

Within a Class 2 culture hood human/rabbit/mouse vascular tissues were cleaned from adherent material, cut into 3mm segments and either placed into T25 tissue culture flasks or a six well plate containing 1:1 Waymouths: Ham's F12 with 15% FCS, 1% penicillin streptomycin. The flasks/plates were placed in a tissue culture incubator (37°C, 5% CO_2, 100% humidity) where the medium was changed every 72 hr. Spontaneous explantation of vascular smooth muscle (VSM) cells occurred after approximately one week, and reached 70% confluency by four weeks. Thereafter cells were sub-cultured for assay or stored at -80°C. All experiments were conducted with cells between passages 1-4.

2.4.2 Characterisation of vascular smooth muscle cells

VSM cell explants were characterised by their growth morphology analysed by brightfield microscopy and expression of α-smooth muscle actin (SMA) analysed by immunofluorescence. Cells were grown to 50% confluency on 13x13mm glass

coverslips. The coverslips were then fixed in 4% paraformaldehyde, washed in PBS, and permeablised using 0.1% Triton X-100. To block non-specific binding, 10% goat serum was added to the cover slips for 30 min at room temperature. This was removed and replaced with a mouse monoclonal anti-α-SMA IgG used at 1:400 dilution (Sigma, UK) overnight at 4°C. Thereafter slides were washed in three changes of PBS before adding a fluorescein conjugated anti-mouse secondary IgG used at 1:1000 dilution (Vector Laboratories, UK) at room temperature for 45 min. Coverslips were mounted using hard set vector-shield containing the nuclear dye DAPI (Vector Laboratories, UK) and visualised under a Nikon Eclipse E600 epifluorescent microscope (Nikon, UK).

2.4.3 ^{3}H-thymidine incorporation assay

Cell proliferation was determined using serum-induced [^{3}H]-thymidine incorporation as described previously (Coats *et al.*, 2008). VSM cells were seeded at 20,000 cells/well into a 24 well plate in the presence of culture medium containing either 10 or 15% FCS. Cells were then quiesced for either 24 or 48 hr in media containing 0.1% (v/v) FCS. The quiesced cells were stimulated with 10% FCS for 24 hr, with the addition of 1μCi/well of ^{3}H thymidine (Amersham, UK) for the final 6 hr. The cells were then washed with ice cold PBS and four changes of 10% trichloroacetic acid; after which the contents of each well were solubilised with 250μl lauryl sulphate (10%) plus sodium hydroxide (0.2M). The contents of each well were then transferred to a scintillant tube containing 2ml scintillation fluid and radioactivity was quantified by liquid scintillation in DPM^{-1}.

2.4.4 Immunoblotting of VSM cell lysates

Treated/stimulated VSM cells were washed with ice cold PBS and lysed by addition of boiling sample buffer (0.125M Tris–HCl (pH 6.7), 0.5mM Na4P2O7, 1.25mM EDTA, 1.25% (v/v) glycerol, 0.5% (w/v) SDS, 25mM dithiothreitol and 0.02% (w/v) bromophenol blue). Samples were loaded on to a 10% SDS page gel (minimum of 20μg total protein per well), and following electrophoresis, proteins were transferred

to a nitrocellulose membrane. Membranes were blocked for 1 hr at room temperature in 3% BSA and incubated overnight in primary antibody. The following day the membranes were washed for 4x15 min in TTBS (50mM Tris-Cl, pH 7.6; 150mM NaCl) and a HRP-conjugated secondary antibody was added for 1 hr at room temperature. The blots were then washed for 2x10 min in TTBS and developed using an enhanced chemiluminescence kit (Thermo Scientific Peirce, USA).

Chapter 3

Investigation of the inflammatory and proliferative characteristics of human AVF failure and the role of TLR-4

3.1 Introduction

The surgical creation of an AVF is vital to the treatment of patients with chronic renal failure, providing a vascular access point for haemodialysis. However, AVFs are unfortunately associated with relatively low patency rates, and often require further surgery to repair or resection the vessel (Field *et al.*, 2008). Failure is mediated by the development of intimal hyperplasia and thrombus, leading to occlusion of the AVF (Roy-Chaudhury *et al.* 2007, Lee & Roy-Chaudhury 2009). This reduces the amount of blood which can flow thought the vein, and is therefore no longer suitable for haemodialysis. Intimal hyperplasia involves VSM cells undergoing proliferation and migrating into the lumen. Currently, the specific mechanisms which are associated with peripheral vascular occlusion in the renal patient are poorly defined. An inflammatory response is known to contribute to neointimal development in these patients, with certain inflammatory mediators such as TNF-α, IL-1β, IL-6, IL-8 and MCP-1 shown to have a crucial role (Schepers *et al.*, 2006; Tedgui and Mallat, 2001). Specifically, dialysis patients have significantly higher levels of ICAM-1, VCAM-1 and MCP-1 in their serum compared to healthy individuals (Papayianni *et al.*, 2002). IL-6 has also been implicated in AVF stenosis, demonstrated by an increase in IL-6 RNA within peripheral blood mononuclear cells assessed during AVF stenosis vs. AVF creation (Marrone *et al.*, 2007).

Fistulae are subjected to regular venepuncture which provides an opportunity for infection. Also diverse bacterial signatures are known to be present in atherosclerotic lesions of patients with coronary heart disease. Therefore, a possible mechanism for activation of immune pathways in vascular proliferative disease could be via activation of toll-like receptors (TLR) (Ott *et al.*, 2006). It has been widely reported that when VSM cells are challenged with LPS (a TLR-4 agonist), there is a significant increase in the phosphorylation of the ERK MAPK pathway, which is central to cell proliferation (Hong *et al.*, 2009; Lin *et al.*, 2007, 2006; Son *et al.*, 2008; Yang *et al.*, 2005). The release of endogenous damage associated molecular patterns (DAMPs) which activate TLR, such as HSP, can occur in response to haemodynamic change and needle injury during AVF stenosis (Hochleitner *et al.*,

2000). This was demonstrated by showing co-localisation of HSP-60 and TLR-2/TLR-4 in human failed AVF (De Graaf *et al.*, 2006).

Within a healthy vessel, VSM cells have a low cell turnover rate and are therefore mostly in a quiescent G_0 phenotype (Gordon *et al.*, 1990). When stimulated by a mitogenic stimulus the cell can enter the cell cycle leading to proliferation. There are a number of key signalling pathways which drive this process, including activation of MAPK (Lawrence *et al.*, 2008). Downstream of MAPK, there are a number of other pathways and check points which ultimately control cell proliferation (Charron *et al.*, 2006). However, the triggers which lead to the activation of VSM cell hyper-proliferation are not known, but inflammatory events (such as TLR activation) are likely to contribute. Despite all the molecular and in vivo evidence, there remains only one study which has demonstrated that activation of TLR-4 can lead to increased proliferation of VSM cells in vitro (Lin *et al.*, 2007). This study was performed using human aortic smooth muscle cells. In response to LPS stimulation these cells exhibited increased TLR-4 expression, increased phosphorylation of MAPK's ERK and JNK, and increased proliferation measured by BrdU uptake. TLR-4 mediated proliferation was confirmed by attenuation of proliferation using a TLR-4 neutralising antibody.

Given the potential importance of both inflammatory and proliferative pathways in driving vascular remodelling, a therapeutic agent which has both anti-inflammatory and anti-proliferative activity may be beneficial. NSAIDs are a family of clinically well defined agents with established anti-inflammatory actions, as well as less well studied anti-proliferative properties in VSM cells (Brooks *et al.*, 2003). Despite these activities, this class of agents have not yet been used successfully in dialysis patients, with some concerns over adverse bleeding events associated with systemic application (Kaufman *et al.*, 2003).

In this chapter, the differences between human long saphenous vein (referred to as Control) and stenotic cephalic vein taken from failed AVF (referred to as Stenosed) will be compared. Using these tissues, the aims of this chapter are to:

1. Assess the morphological changes undergone during AVF stenosis
2. Investigate the inflammatory profile of AVF stenosis
3. Explore a potential role for TLR 4 in AVF stenosis by examining quantitative changes in expression
4. Determine the proliferative characteristics of vascular smooth muscle cells derived from stenotic AVF
5. Assess the ability of diclofenac, an NSAID, to reduce VSM cell proliferation.

3.2 Materials and methods

3.2.1 Materials

Sigma-Aldrich (UK)

Acid fuchsin

Alcian blue

Aniline blue

Biebrich scarlet

Bromophenol blue

Diclofenac sodium

Fast red

Lipopolysaccharides from Escherichia coli 0111:B4

MTT

Phosphomolybdic acid

Phosphotungstic acid

Propidium iodide

RNase

Sirius red

Toluidine blue

Thermo Scientific (UK)

Hoechst 33342

3.2.2 Tissue collection

Long saphenous vein was obtained with prior consent from patients undergoing elective surgery for varicose veins. Stenosed and non-stenosed cephalic vein was obtained with prior consent from patients undergoing arteriovenous fistula creation or revision. Immediately after the tissues were isolated they were placed in sterile medium (1:1 Waymouths: Hams F12) and transported on ice to the laboratory according to guidelines stipulated by the University's statutory advisory committee

on safety and occupational health. For experimentation, long saphenous vein was used as a healthy control in comparison to the stenosed cephalic vein, which formed the experimental group.

3.2.3 Patient data

The demographic details of patients providing tissue samples are summarised in Table 3.1. Samples of long saphenous vein were obtained from healthy patients (n=16) undergoing elective surgery for varicose veins. The mean age of these patients was 56.3±14.1 years. Mean serum creatinine in this control group was 80.4±13.5µmol/dl. All patients in this group were normotensive and non-diabetic.

Failed fistula samples (n=16) were obtained from stenotic arterialised veins of patients with established AVF. These patients required surgical revision for venous outflow stenosis. All of the patients with failed fistulae had end stage renal failure (ESRF) (Table 3.2). All but two of the patients with failed fistula were on haemodialysis (HD), with the remaining failed fistula donated from patients with failing renal transplants. The mean duration on HD at the time of obtaining the tissue was 4.7±3.6 years. Mean urea reduction ratio (URR) was 69.3±7.6. 43.75% of patients with failed fistula had a previously failed AVF. Two fistulae were brachiobasilic, 11 brachiocephalic and 3 radiocephalic AVF.

	Control (n=16)	**Failed Fistula (n=16)**	**p-value**
Age (years)	56.3± 14.1	61± 13.8	0.42
Gender (percentage male)	62.5%	58.8%	0.87
Systolic BP (mmHg)	131.6± 19.5	136.9± 10.9	0.33
Diastolic BP (mmHg)	79.6± 9.2	78.3± 7.6	0.67
Diabetes	0.0%	35.3%	0.009**
Hypertension	25.0%	64.7%	0.013*
Haemoglobin	133.7± 13.6	113.6± 16.2	<0.001**
White Blood Cell	7.6± 2.5	7.5± 1.9	0.82
Platelets	307.9± 101.1	223.1± 67.0	0.007*
Sodium	139.1± 3.9	137.8± 2.7	0.29
Calcium (adj)	2.4± 0.2	2.4± 0.2	0.7
Albumin	38.9± 2.5	29.7± 6.8	0.002**
C-Reactive Protein	2.2± 2.0	34.1± 40.3	0.008**

Table 3.1 Demographic details of patients providing tissue samples. Results are presented as mean ±S.D., n=32. A chi-squared test (or Fisher's exact test where n<5) has been used to compare categorical data.

Cause of Renal Failure	Number of Patients
Diabetic nephropathy	n=5 (31.3%)
Glomerulonephritis	n=3 (18.8%)
Drug induced (cyclosporin/ NSAID) 2 (14.3%)	n=2 (12.5%)
IgA nephropathy 2 (14.3%)	n=2 (12.5%)
Hypertensive nephropathy	n=1 (6.3%)
Anti-GBM disease 1 (5.9%)	n=1 (6.3%)
APCKD 1 (5.9%)	n=1 (6.3%)
Reflux nephropathy 1 (5.9%)	n=1 (6.3%)

Table 3.2 Cause of renal failure in patients with failed fistula.

3.2.4 Alcian blue

To highlight extracellular matrix proteoglycans, rehydrated tissue slides were placed in alcian blue staining solution for 20 min, followed by a 1 min wash in distilled water. Slides were counter stained with nuclear fast red for 1 min and washed as before. Finally the slides were dehydrated, mounted and left to dry overnight before analysis. Quantitative analysis was performed on one section per human sample.

3.2.5 Picrosirius red

To highlight collagen deposition, rehydrated slides were placed in picrosirius red staining solution for 1 hr, followed by two changes of acidified water. The slides were then dehydrated, mounted and left to dry overnight before analysis. The stained tissues were visualised by brightfield microscopy, and crossed polarised filter microscopy on a Leica DM LB2 microscope using a Leica DFC320 camera (Leica Microsystems, UK). Quantitative analysis was performed on one section per human sample.

3.2.6 Masson's trichrome

To highlight collagen deposition and visualise smooth muscle the tissues were stained in the following solutions:

- weigert's iron haematoxylin: 10 min
- running warm tap water: 10 min
- dH_2O: 1 min
- biebrich scarlet-acid fuchsin: 15 min
- dH_2O: 1 min
- phosphomolybdic-phosphotungstic acid: 15 min
- aniline blue: 10 min
- dH_2O: 1 min
- acetic acid (1%): 5 min
- dH_2O: 1 min
- 95% ethanol: 3 sec

- 100% ethanol: 3 sec

The slides were then dehydrated, mounted and left to dry overnight before analysis. Quantitative analysis was performed on one section per human sample.

3.2.7 Toluidine blue

To highlight mast cells present within the vessel, tissue slides were placed in toluidine blue staining solution for 3 min, followed by a wash for 1 min in distilled water. Slides were counter stained with nuclear fast red for 1 min and washed as before. Finally the slides were dehydrated, mounted and left to dry overnight before analysis. Quantitative analysis was performed on one section per human sample.

3.2.8 Immunohistochemistry for α-smooth muscle actin (α-SMA)

Immunohistochemistry was performed as detailed in chapter 2, section 2.3.4. Specifically, a sodium citrate buffer was used in the antigen retrieval step. Tissue sections were blocked using 10% goat serum. A mouse monoclonal anti-α-SMA IgG (Sigma, UK) was used at 1:400 dilution for 3 hr at room temperature. An anti-mouse HRP linked IgG antibody (New England Biolabs, UK) was used at 1:1000 dilution for 1 hr at room temperature to detect the primary, which was visualised by DAB substrate.

3.2.9 Immunohistochemistry for proliferating cell nuclear antigen (PCNA)

Immunohistochemistry was performed as detailed in chapter 2, section 2.3.4. Specifically, a TRIS EDTA buffer was used in the antigen retrieval step. The tissue was then blocked using 10% goat serum. A rabbit polyclonal anti-PCNA IgG (Abcam, UK) was used at 1:200 dilution overnight at 4°C. An anti-rabbit HRP linked IgG antibody (New England Biolabs, UK) was used at 1:200 dilution for 1 hr at room temperature to detect the primary, which was visualised by DAB substrate. The sections were measured by randomising the slides and selecting five fields of view within each vessel. From this, the percentage of positively stained nuclei

(brown) to negatively stained nuclei (dark blue) was calculated. Quantitative analysis was performed on one section per human sample.

3.2.10 Immunofluorescence for TLR-4

Immunohistochemistry was performed as detailed in chapter 2, section 2.3.4. Specifically, a sodium citrate buffer was used in the antigen retrieval step. The tissue was then blocked using 10% goat serum. A mouse monoclonal anti-TLR-4 IgG (Abcam, UK) was used at 1:100 dilution overnight at 4°C. A Texas Red conjugated anti-mouse IgG (Vector Laboratories, UK) was used at 1:250 dilution to detect the primary. The slides were then mounted using hard-set vectashield with DAPI (Vector Laboratories, UK) as a counterstain and viewed under a Leica TCS SP5 confocal microscope, based on a DM6000B upright microscope. The optimal spectral range of 610-610nm was identified for the Texas Red antibody, at the same time minimising inherent autofluorescence. Three fields of view were selected in each vessel and the percentage pixel staining was quantified. This process was also carried out in negative controls, which didn't receive the primary antibody, the results of which were subtracted from the experimental slides. Quantitative analysis was performed on one section per human sample.

3.2.11 Proteome array of patient blood samples

In this experiment, blood samples were compared between patients who were receiving haemodialysis via a non-stenosed AVF vs. AVF with stenosis. The clinical details of these patients are shown in Table 3.3. Blood samples were collected using serum collection tubes (Greiner Bio One, Germany) from patients just prior to their dialysis session. The samples where centrifuged at 2000g to collect the serum and stored at -80°C. A human cytokine array (Cat. No. ARY005, R&D Systems, USA) was carried out by incubating the serum samples with nitrocellulose arrays containing 36 immobilised antibodies against different human inflammatory proteins. These were then detected using a secondary HRP conjugated antibody which was part of the kit, followed by visualisation using an enhanced chemiluminescence kit (Thermo Scientific Peirce, USA).

	Non-Stenosed AVF (n=2)	Stenosed AVF (n=4)
Age (years)	65± 1.4	67.75± 2.5
Gender (% male)	100	100
Systolic BP (mmHg)	140± 7.1	137.5± 6.5
Diastolic BP (mmHg)	75± 7.1	83± 10.1
Diabetes	No	No
Hypertension	Controlled	Controlled
Haemoglobin	106.5± 13.4	110.3± 18.0
White Blood Cell	6.6± 1.4	7.6± 1.5
Platelets	210± 68.6	240.5± 58.5
Sodium	136± 2.8	139.8± 1.9
Calcium (adj)	2.34± 0.1	2.5± 0.0
Albumin	32± 9.9	29.8± 3.8
C-Reactive Protein	23± 19.8	41.8± 35.7

Table 3.3. Demographic details of patients used for systemic proteome analysis. Results are shown as the mean ±S.D.

3.2.12 MCP-1 ELISA

The patents shown in Table 3.3 were also used for MCP-1 quantification. An ELISA was then carried out according to the manufacturer's instructions (Cat. No. 438804, Biolegend, San Diego, USA) by first of all coating the wells of a 96 well plate with capture antibody, followed by a blocking step. In between each step the wells were washed 3 times with PBS. 100µl of serum sample/standard was added to each coated well and incubated for 2 hr at room temperature. The wells were then washed and incubated with a detection antibody for 1 hr at room temperature. This was followed by a 30 min incubation at room temperature with Avidin-HRP. MCP-1 levels were then detected by 3,3',5,5'-Tetramethylbenzidine (TMB) substrate solution, followed by the addition of 1M H_2SO_4. Absorbance was quantified on a Spectramax M5 plate reader at 450nm (Molecular Devices, USA).

3.2.13 Stimulation of human cell explants

The VSM cells were quiesced for 48 hr in 0.1% (v/v) FCS, during which time they were incubated with or without; diclofenac sodium (43.75µM- 175µM) for 24 hr, OxPAPC (Invivogen, USA) for 20 min. Cells were then stimulated for 24 hr with either FCS (0.1-10%) or LPS (100ng/ml) + FCS (1%). Proliferation was measured by a ^{3}H-thymidine incorporation assay as described in section 2.4.3. Experiments were carried out in triplicate wells.

3.2.14 FACS cell cycle analysis of cell explants

Cell cycle analysis was carried out using propidium iodide to stain for intracellular DNA content. Cells were seeded at 100,000 cells per well of a 6 well plate. Once the cells were adherent, fresh medium was added and the cells were returned to the incubator for 48 hr. Cells were then lifted with tryple express, centrifuged at 300g, re-suspended in cold PBS, and fixed by adding 70% cold ethanol for a minimum of 1 hr. The cells were washed with PBS and centrifuged at 300g for 10 min, after which 50µl/ml of RNase A was added and incubated at 37°C for 1 hr. The samples were then stained with propidium iodide (50µl/ml). Cell cycle parameters were set to

10,000 gated events and analysed using fluorescence-activated cell sorting (FACS) on a FACScan flow cytometer (Becton Dickinson, UK) running FACS Diva software (Becton Dickinson, UK).

3.2.15 IRAK-4 expression in vascular smooth muscle cell lysates

Western blotting was carried out as described in section 2.4.4. Quiesced VSM cells were stimulated with LPS (100ng/ml) for 15 min. A mouse polyclonal anti-phosphorylated IRAK-4 or anti-total IRAK-4 (Abcam, UK) was used at 1:1000 dilution overnight at 4°C. For detection of the primary antibody a HRP-conjugated anti-mouse secondary at 1:7500 dilution (Cell Signalling Technology, USA) was used for 1 hr at room temperature.

3.2.16 Viability of cells following treatment using inclusion/exclusion of dyes

Cell membrane disruption was used as a marker of cell death in explants treated with a working concentration of pharmacological agent. Cells were grown to 50% confluency on 13x13mm glass coverslips, and exposed to the test agents for 24 hr. The coverslips were incubated with a 1:1 mixture of Hoechst 33342 (only retained within the nucleus of live cells) and propidium iodide (only permeable when the cell membrane has become compromised), followed by three washes of PBS. The coverslips were mounted using hard set vector-shield without DAPI and visualised under x200 magnification on a Nikon Eclipse E600 epifluorescent microscope (Nikon, UK).

3.2.17 Viability of cells following treatment by MTT assay

Mitochondrial activity of cells treated with pharmacological agents was also used to assess the viability of cells. Cells were quantified on a haemocytometer using trypan blue (0.4%) and seeded at 5,000 cells/well in a 96 well plate. Once all cells had adhered overnight, the medium was removed and replaced with medium containing the test agent. After 24 and 48 hr the MTT assay (Sigma, UK) was performed

according to the manufacturer's instructions by incubating the cells with 10% MTT reagent solution, followed by dilution of formazan product by DMSO. The absorbance was then measured at 590 nm with a reference filter of 620 nm on a Spectramax M5 plate reader (Molecular Devices, USA).

3.3 Results

3.3.1 Morphology of arteriovenous fistula failure

The pathophysiology of failed human arteriovenous fistulae vs. healthy long saphenous vein controls was investigated using a number of histological techniques. Haematoxylin and eosin was primarily used to visualise the structure of the vessels (Fig. 3.1). Fig. 3.1.A shows three examples of healthy long saphenous vein controls. These vessels have a relatively thin medial layer and a wide patent lumen allowing the flow of blood. Fig. 3.1.B shows three examples of stenosed cephalic vein taken from failed AVF. These examples show inward hypertrophic remodelling which has caused stenosis in the vessel. This is quantified as a vessel wall: lumen ratio in Fig. 3.1.C. Thrombus formation also plays a role in the failure of AVF, which can be seen in the second and third images of Fig. 3.1.B.

A

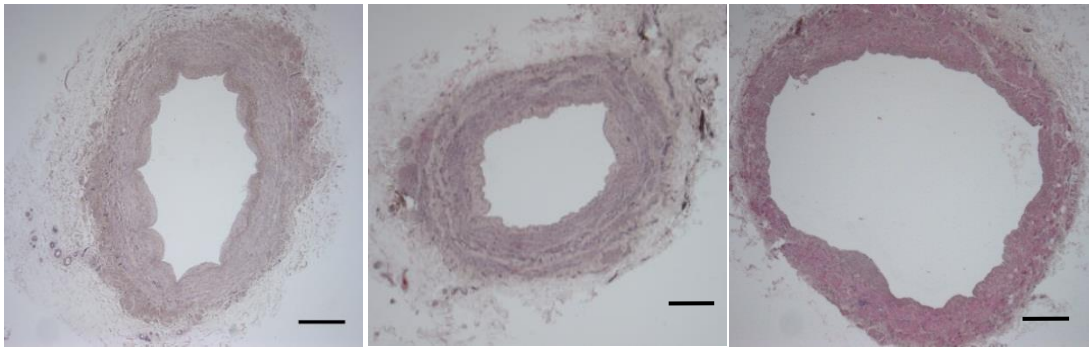

B

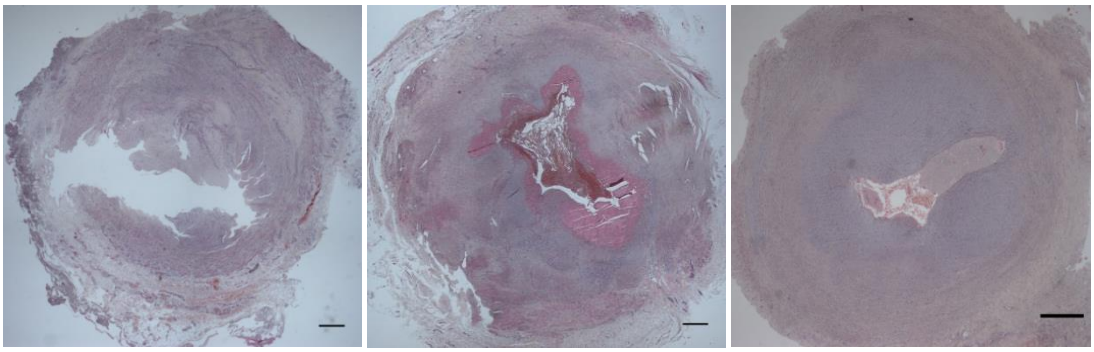

C

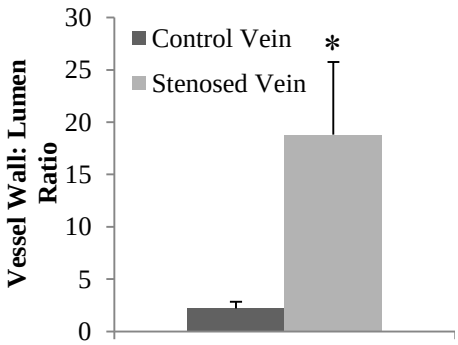

Figure 3.1. Haematoxylin and eosin stain showing the changes undergone in AVF stenosis. ***A)*** *Examples of healthy long saphenous vein (Control).* ***B)*** *Examples of stenotic AVF vein segments (Stenosed).* ***C)*** *Quantification of the vessel wall: lumen ratio with a significant increase in failed AVF vein segments. Results are shown as the mean ±S.E.M., n=7 & 8 for control & stenosed respectively, *p<0.05 (unpaired T-test), all scale bars= 500µm.*

The extent of α-smooth muscle actin (α-SMA) positive cells present within the neointima was examined by immunohistochemistry (Fig. 3.2). In the healthy control vein and original medial layer of the stenotic vessels it is evident that the VSM cells are uniformly distributed around the vessel (Fig. 3.2.A-C). VSM cells within the neointima were also positive for α-SMA, but had a chaotic distribution. The accumulation of these cells suggested that there would be a change in the levels of proliferation undergone within the vein. Therefore, the vessels were also probed for proliferating cell nuclear antigen (PCNA), shown in Fig. 3.3. The percentage of cells undergoing proliferation significantly increased from 3.5±1.5% in control veins to 33.6±4.9% within the stenosed.

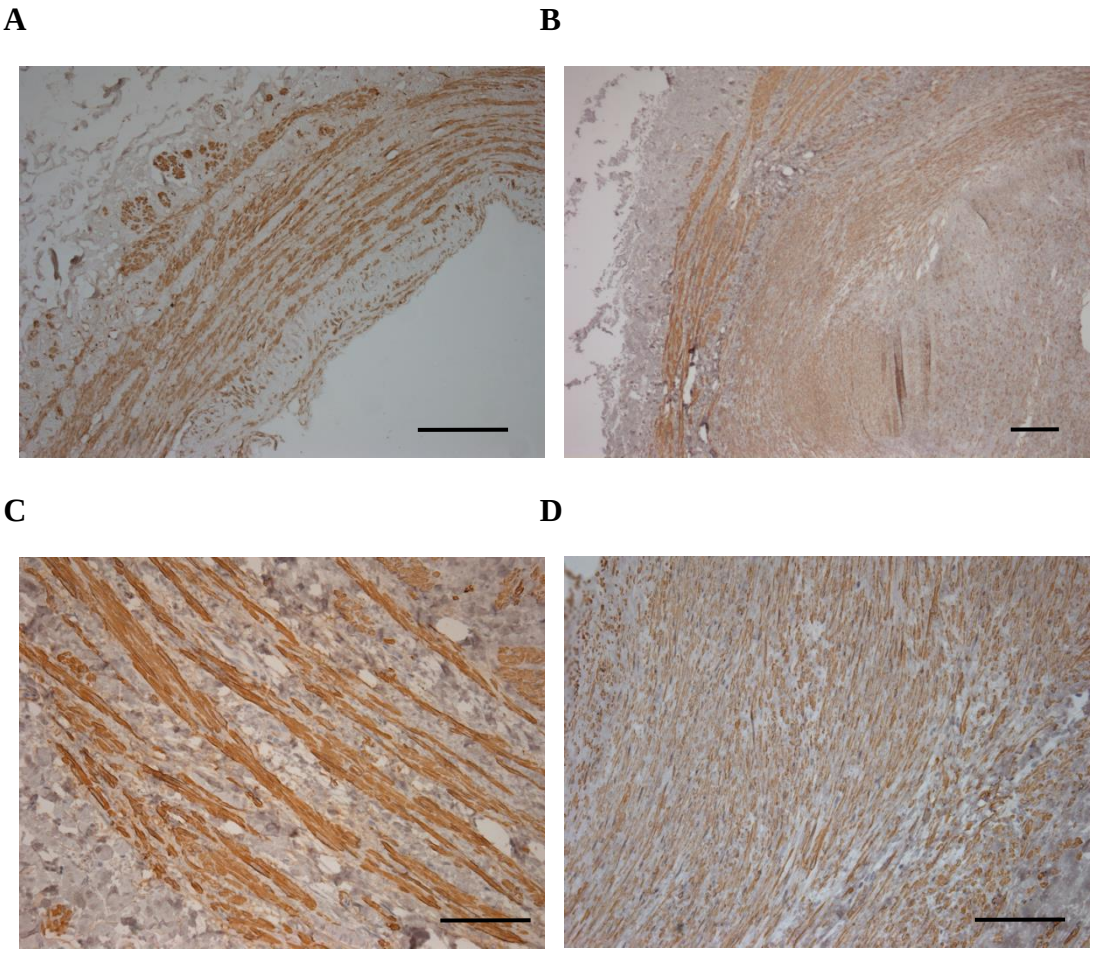

Figure 3.2. Immunohistochemistry for α-smooth muscle actin (α-SMA) visualised by DAB staining (Brown). ***A)*** *Expression of α-SMA within the medial layer of a healthy control long saphenous vein, scale bar= 200µm.* ***B)*** *Expression of α-SMA within a stenotic AVF vein, scale bar= 200µm.* ***C)*** *Distribution of α-SMA positive cells within the original medial layer of a stenotic AVF vein, scale bar= 100µm.* ***D)*** *Distribution of α-SMA positive cells within the neointima of a stenotic AVF vein, scale bar= 100µm.*

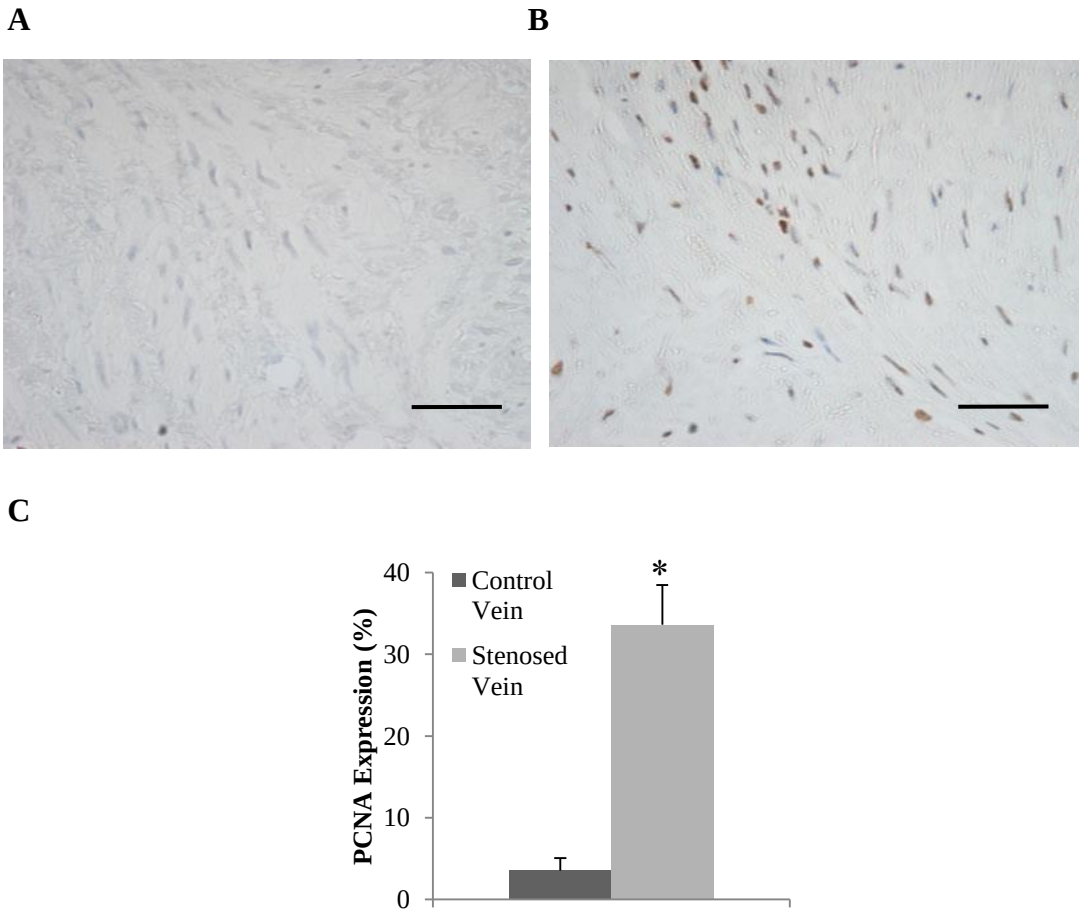

Figure 3.3. Immunohistochemistry for PCNA visualised by DAB staining. ***A)*** *An example of PCNA expression (Brown) within a control vein.* ***B)*** *An example of PCNA expression within a stenosed vein.* ***C)*** *Comparison of the percentage PCNA positive cells within control vs. stenosed. Results are shown as the mean ±S.E.M., n=5 & 8 for control & stenosed respectively, *p<0.05 (unpaired T-test), all scale bars= 100µm.*

Associated with VSM cell proliferation and vascular remodelling is the deposition of extracellular matrix. Proteoglycans are a component of extracellular matrix which were analysed using alcian blue staining (Fig. 3.4). Fig. 3.4.A shows the basal level of proteoglycans expressed at the media/intima interface. Fig. 3.4.B shows up-regulation of proteoglycans at the leading edge of proliferation. Medial layer proteoglycan staining intensity was significantly upregulated by three fold for stenosed vs. control. In addition to proteoglycans, total collagen was measured using the picrosirius red stain analysed by brightfield (Fig. 3.5.A) and crossed polarised light microscopy (Fig. 3.5.B). In brightfield, collagen was widely expressed in both groups of tissue, with no significant differences. The polarised light, which has a higher specificity for collagen (Puchtler *et al.*, 1973), also showed no significant differences for control vs. stenosed (Fig. 3.5.B) Since collagen deposition was expected to increase along with vascular remodelling similar to proteoglycans, massons trichrome was also used to measure collagen (Fig. 3.6). Masson's trichrome allows the differentiation of collagen and muscle within the vessel. As before there was no significant difference in total collagen composition (Fig. 3.6.C).

A **B**

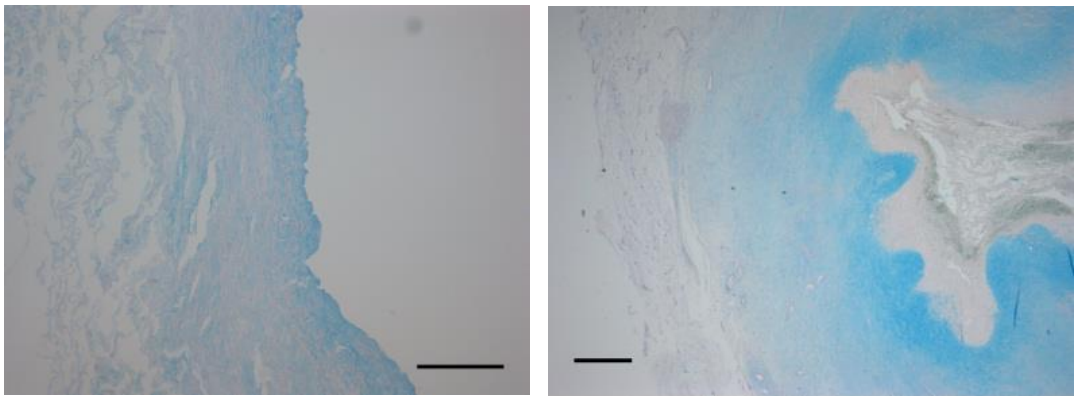

C

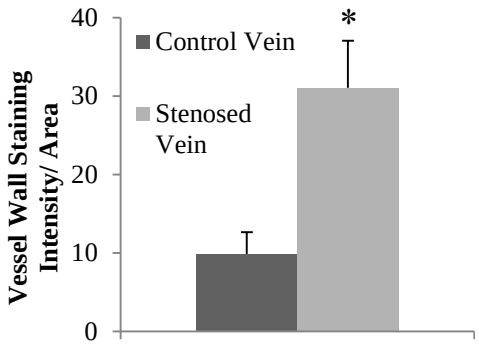

Figure 3.4. Alcian blue staining of extracellular matrix proteoglycans (blue). ***A)*** *Proteoglycan deposition within a control vein.* ***B)*** *Proteoglycan deposition within a stenosed vein.* ***C)*** *Proteoglycan staining intensity within the medial area. Results are shown as the mean ±S.E.M., n=7, *p<0.05 (unpaired T-test), all scale bars= 500µm.*

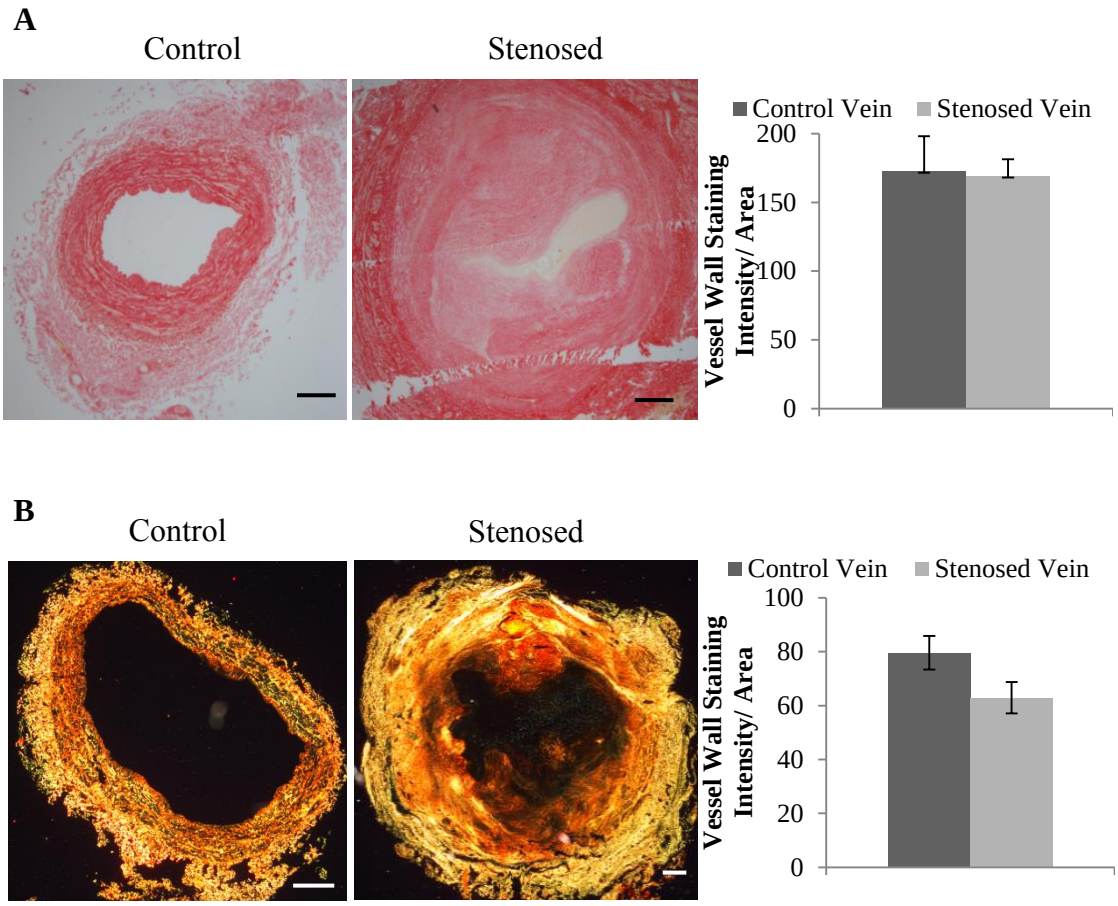

Figure 3.5. Picrosirius red stain for total collagen. ***A)*** *Initial trial of brightfield analysis of total collagen showing no significant difference in expression (Red) between control and stenosed vein. Results are shown as the mean ±S.E.M., n=3.* ***B)*** *Total collagen visualised by crossed polarised light, with no significant difference in collagen expression. Results are shown as the mean ±S.E.M., n=6, all scale bars=500µm.*

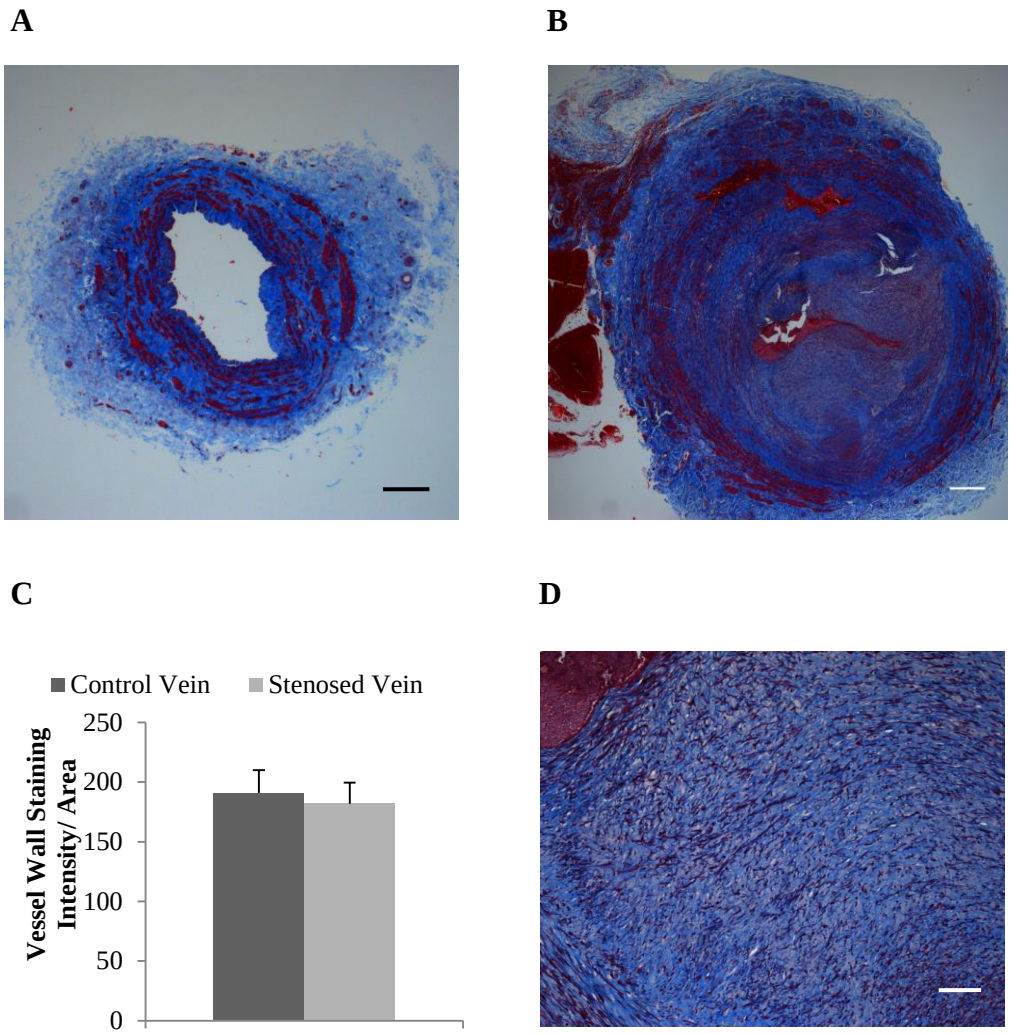

Figure 3.6. Masson's trichrome staining of total collagen (Blue) and muscle (Red). ***A)*** *Collagen and smooth muscle distribution within a control vein, scale bar= 500µm.* ***B)*** *Collagen and smooth muscle distribution within a stenosed vein, scale bar= 500µm.* ***C)*** *Collagen staining intensity within the medial area showing no significant difference in control vs. stenosed. Results are shown as the mean ±S.E.M., n=7 & 8 for control & stenosed respectively.* ***D)*** *Expression of collagen within the neointima of a stenotic vein, scale bar= 50µm.*

3.3.2 The inflammatory characteristics of arteriovenous fistula failure

A large cellular component of vascular access graft neointimal lesions are immune cells (Roy-Chaudhury *et al.*, 2009). As shown in Fig. 3.7, infiltration of what could be leukocytes (Fig. 3.7.A) and lymphocytes (Fig. 3.7.B) were observed within stenotic veins. Identification of these cell infiltrates was based on their distinctive cell morphology when stained with H & E. In addition to this, staining for specific markers could also be carried out. Toluidine blue, which stains cells with a high metachromatic content, was used to identify mast cells within the vessels. In Fig. 3.7.C-E, the amount of mast cells/mm^2 was quantified. Mast cell expression was five times higher in stenosed vs. control vein. No other immune cell types were quantified.

Inflammatory cell infiltration has been shown to be an important part of the pathogenesis, thus the inflammatory profiles of patients with AVF stenosis vs. functional AVF was measured. Serum was collected from control and stenotic patients, (male subjects, non-diabetic and age matched). The control group had undergone dialysis through a functional arteriovenous fistula for a minimum of 2.9 years, with patency confirmed at time of blood collection by ultrasonography. The stenotic patients met the same criteria apart from the presence of vascular stenosis within their arteriovenous fistula. The inflammatory profiles were investigated by proteome array. This assay consists of 36 antibodies raised against a range of cytokines, chemokines and acute phase proteins that are immobilised on a nitrocellulose membrane. Fig. 3.8.A and 3.8.B show example blots for the control and stenotic groups respectively. As shown in these figures, the top corners and the bottom left corner of the blot are positive controls, and the bottom right is a negative control. Densitometry was carried out on these duplicate blots, which were then expressed as a fold change relative to the positive control. Proteins which had a greater than 2 fold change are summarised in Fig. 3.8.C. There appeared to be an increase in a number of pro-inflammatory proteins within the stenotic group, particularly MCP-1 which was increased by 7.1 fold vs. control. In Fig. 3.8.D, MCP-1 expression from the same samples was measured by ELISA. There appears to be a

small increase in MCP-1 associated with stenosis, however this change was not as large as the one seen in the array experiment.

The TLR-4 pathway could play a significant role in AVF stenosis as it has the ability to active both inflammatory and proliferative signalling as discussed in chapter 1 (pages 11-14). Whole vessel expression of total TLR-4 was quantified by immunofluorescence in Fig. 3.9. Optimisation to reduce autofluorescence resulted in a large amount of the positive signal being lost. However, correcting for remaining autofluorescence, a significantly higher expression of TLR-4 in stenotic tissue was demonstrated (6.6 ± 2.1 vs. 16.4 ± 3.3, $^{*}p<0.05$ using an unpaired T-test).

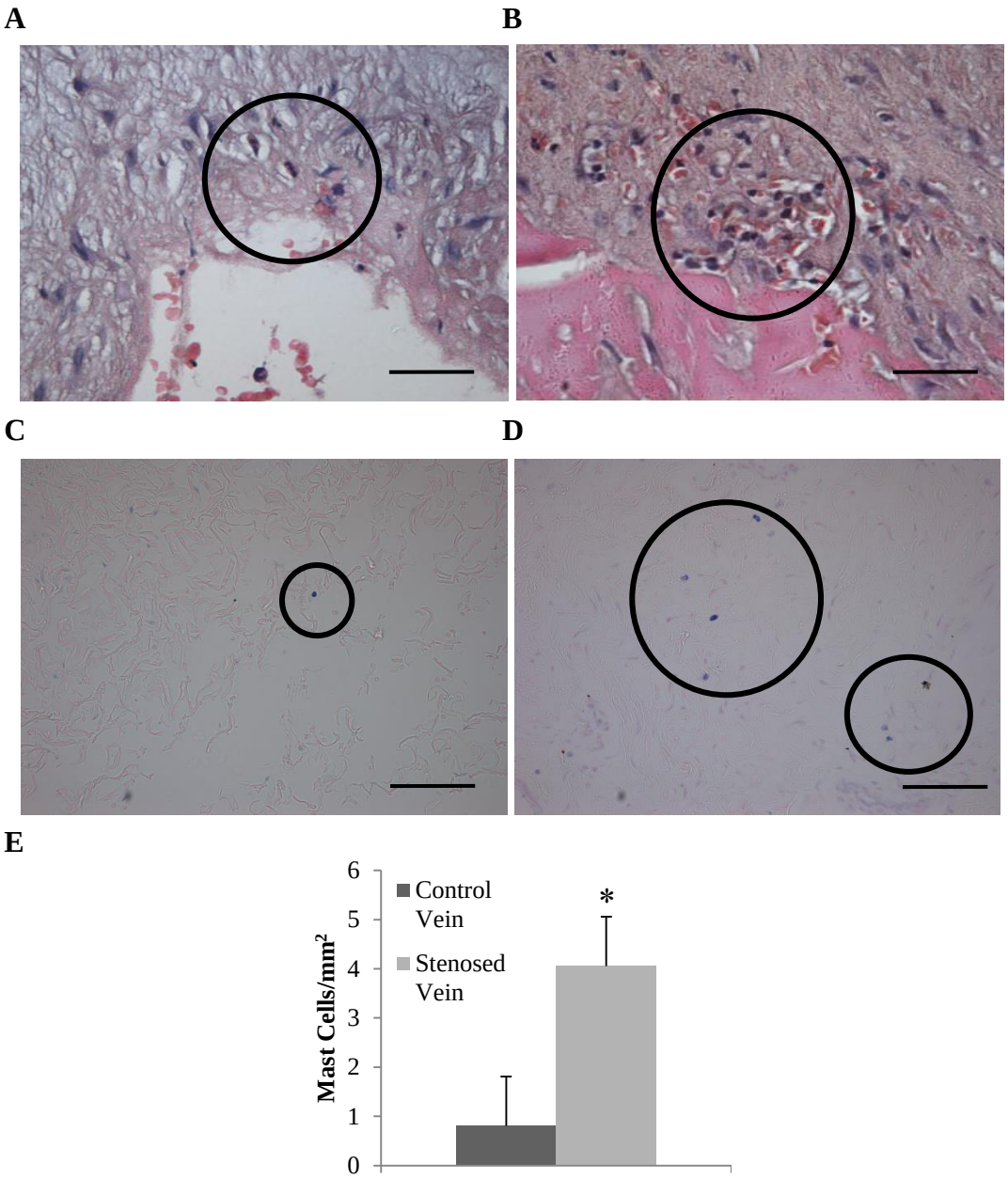

Figure 3.7. Infiltration of inflammatory cells in stenotic AVF. *Evident in H&E stained stenotic vessels is an infiltration of what could be leukocytes (**A**, circled) and lymphocytes (**B**, circled) into stenotic tissue from the lumen.* ***C)*** *An example image of toluidine blue staining for mast cells (purple, circled) in control vein and* ***D)*** *stenosed vein.* ***E)*** *Quantification of the number of mast cells per mm^2 within control vs. stenosed. Results are shown as the mean ±S.E.M., n=8 & 7 for control & stenosed respectively, *p<0.05 (unpaired T-test), all scale bars= 100µm.*

A

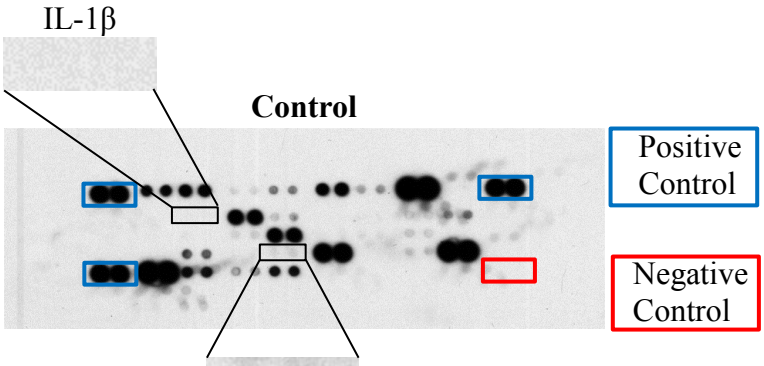

B

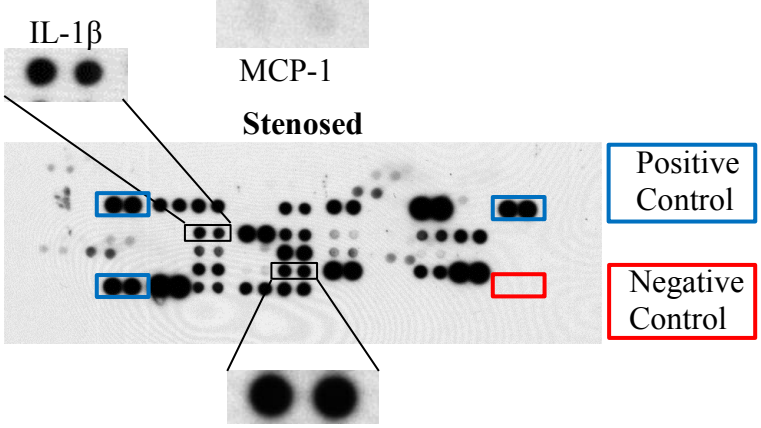

C

> 2 fold change		
Protein	**Change**	**Fold**
IL-1β	Stenosed Only	N/A
IL-4	Stenosed Only	N/A
MCP-1	↑	7.1
G-CSF	↑	4.6
MIP-1β	↑	4.1
IL-2	↑	3.7
GM-CSF	↑	2.0
IL-5	Control Only	N/A
I-TAC	↓	12.4
IP-10	↓	3.0
IL-23	↓	2.2

D

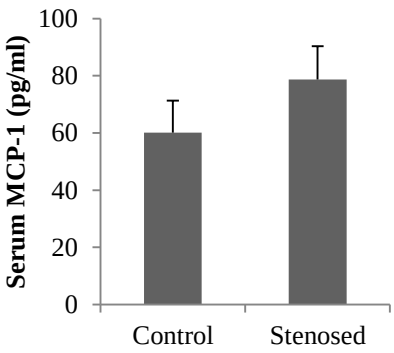

Figure 3.8. Proteome array analysis of serum samples from patients with stenosed AVF vs. patients with functional AVF. ***A)*** *An example array taken from control patients with functional AVF and* ***B)*** *from stenotic AVF patients.* ***C)*** *Densitometry was carried out on the arrays, and proteins which had a greater than 2 fold change are shown. Results are shown as the mean ± S.E.M, n=2 & 4 for the control and stenotic patients respectively.* ***D)*** *Serum MCP-1 concentration in the same patient samples measured by ELISA. Results are shown as the mean ± S.E.M, n=2 & 4 for the control and stenotic patients respectively.*

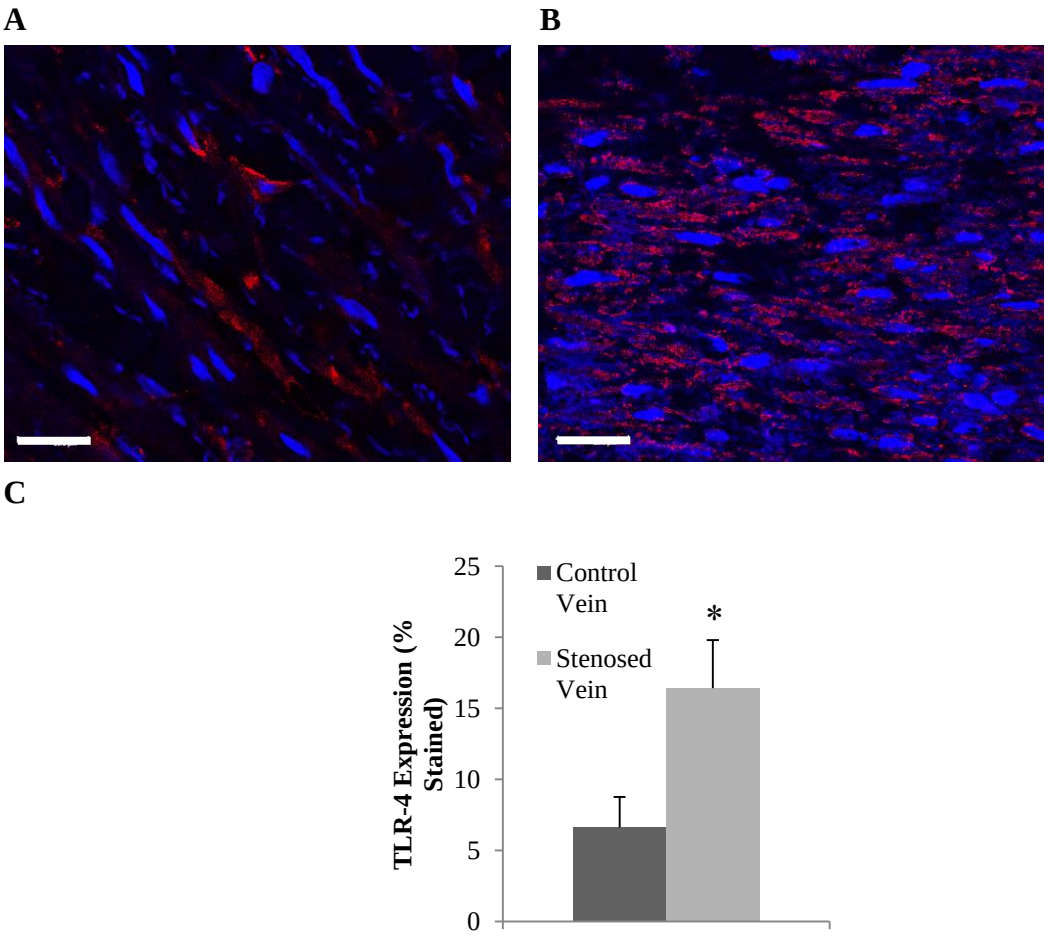

Figure 3.9. TLR-4 expression and activation in stenotic vs. healthy vein. ***A)*** *TLR-4 immunofluorescence in control veins.* ***B)*** *TLR-4 immunofluorescence in stenotic veins.* ***C)*** *Comparison of total TLR-4 expression, quantified by removing background autofluorescence and measuring the ratio of positive pixels/total pixels. Results are shown as the mean ±S.E.M., n=8 & 7 for control & stenosed respectively, *p<0.05 (unpaired T-test), all scale bars= 200µm.*

3.3.3 Stenotic arteriovenous fistula cell explant studies

VSM cells were explanted from either healthy long saphenous vein (control) or stenosed AVF. Characterisation was based on their growth patterns, as well as their expression of α-SMA. Fig. 3.10.A shows the growth pattern of a confluent patch of cells, which displays the characteristic hill and valley morphology associated with this type of cell. Fig. 3.10.B shows that all cells were positive for α-SMA.

The cell proliferative capacity of these populations was compared using ^{3}H thymidine incorporation. This assay is based on the incorporation of ^{3}H labelled thymidine into the DNA of cells which have entered the S phase of the cell cycle. Therefore, it is a measure of DNA synthesis in preparation for proliferation. After a 48 hr quiescence period in 0.1% FCS, cells were stimulated with FCS (0.1%-10%). As is shown in Fig. 3.11, there was a concentration dependent increase in incorporation of ^{3}H thymidine. The results are expressed as a fold increase compared to non-stimulated cells. When the proliferation of both cell populations are compared, explants derived from stenosed vein had a significantly higher capacity to proliferate ($p<0.005$ general linear ANOVA). At 10% stimulation, cells derived from stenosed AVF had a 1.7 fold greater proliferative capacity vs. control cells. Cell cycle analysis was carried out in the same populations of cells (Fig. 3.12). Propidium iodide was used to intercalate with DNA in individual cells, giving an indication of the cell cycle stage. When both sets of cells are compared, the stenotic explants appear to have a higher population of cells in the G2/M stages of the cycle (28.1 ± 4.5 vs. 21.7 ± 5.1); however these results failed to achieve statistical significance ($p=0.44$, unpaired T-test).

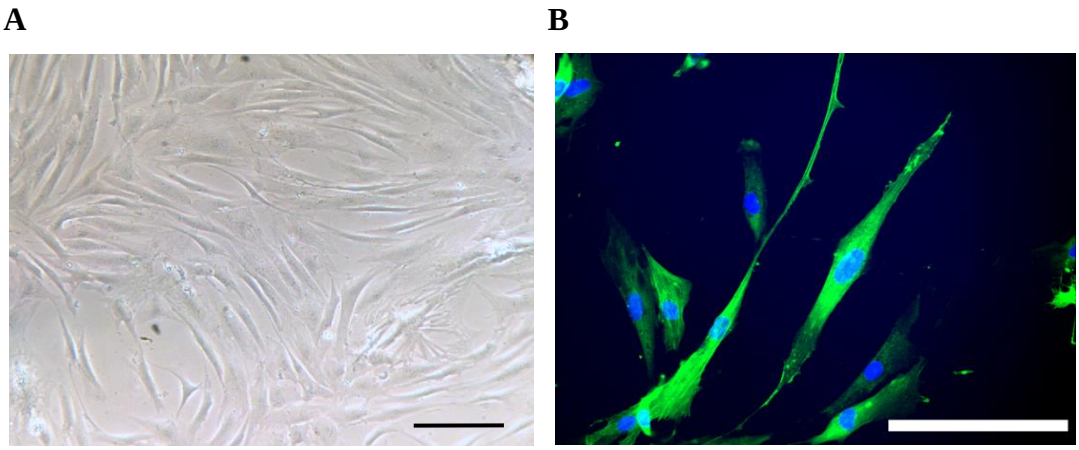

Figure 3.10. Human vascular smooth muscle cell explant characterisation. ***A)*** *Growth morphology of VSM cell explants, scale bar= 200µm.* ***B)*** *Immunocytochemistry of cell explants for α-SMA expression visualised by immunofluorescence (Green), scale bar= 50µm.*

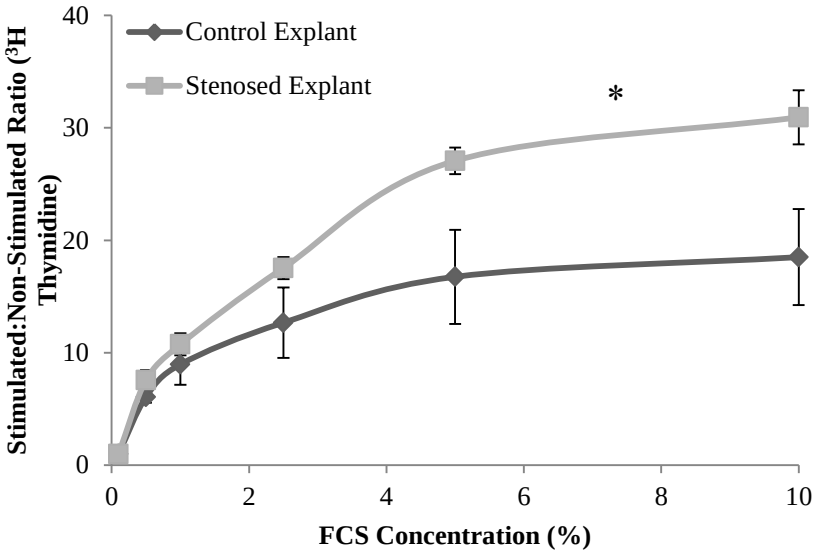

Figure 3.11. The proliferative capacity of stenosed vs. control explants. *^{3}H thymidine incorporation was used to analyse DNA synthesis, a measure of proliferation. After 48 hr in low serum media (0.1%), the cells were stimulated with various concentrations of FCS. Results are shown as the mean fold increase vs. non-stimulated cells, ± S.E.M., n=6, *=p<0.005 (general linear ANOVA).*

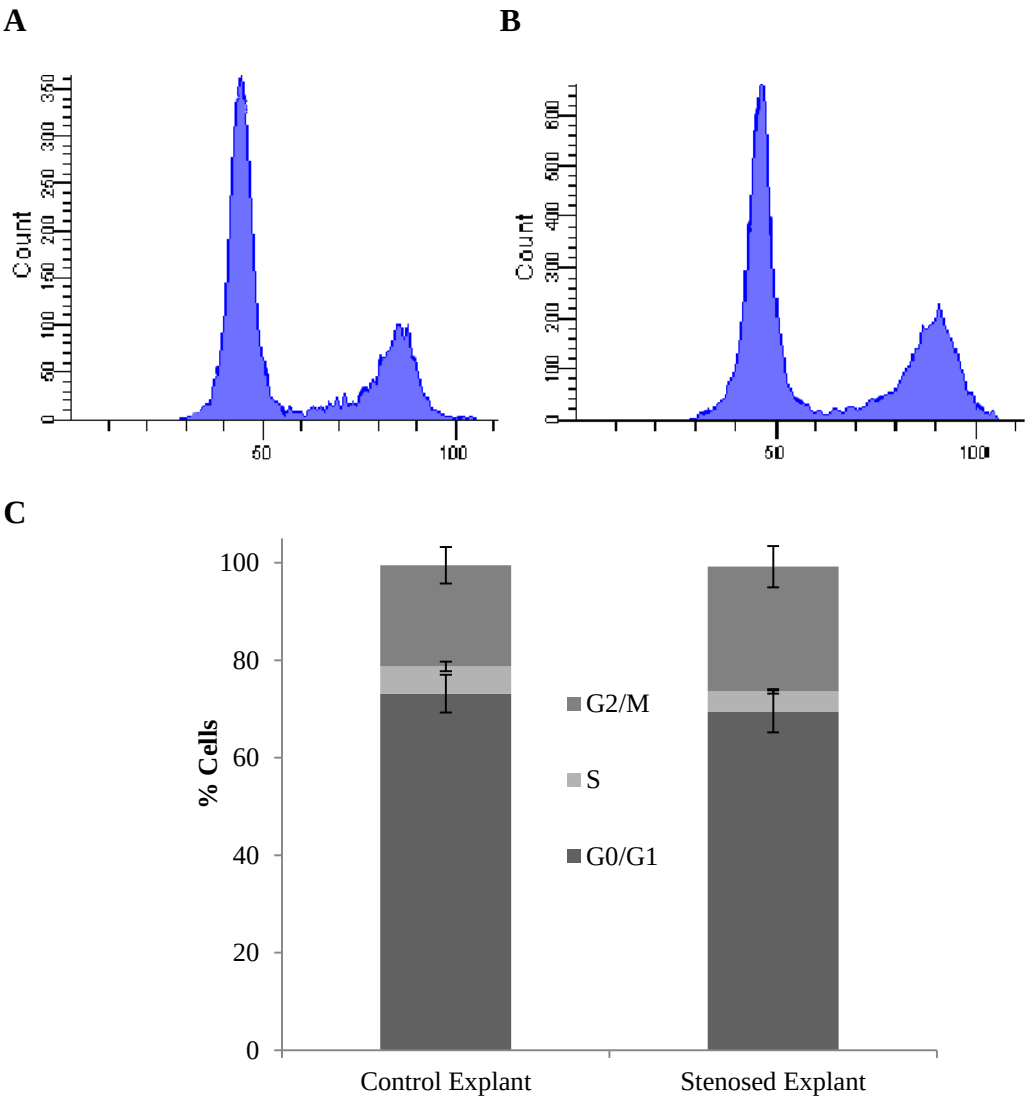

Figure 3.12. FACS analysis of stenosed vs. control explants. *Cells were stimulated with 15% FCS for 48 hr before fixation and analysis.* ***A)*** *Example plot from the control explant group.* ***B)*** *Example plot from the stenosed explant group.* ***C)*** *The mean of cell cycle phases for both groups of explants. Results are shown as the mean ± S.E.M, n=4 & 5 for control & stenosed respectively.*

3.3.4 Activation of TLR-4 during vascular smooth muscle cell proliferation

LPS, a potent TLR-4 agonist (Yang, Coriolan, Murthy, *et al.*, 2005), was used to investigate the activation of TLR-4 in VSM cell proliferation. Fig. 3.13.A shows that stimulation of TLR-4 by LPS in VSM cells directly causes a significant 28% increase in proliferation. Activation of the TLR-4 pathway was also investigated in these cells. IRAK-4 is a serine-threonine kinase which acts downstream of activated TLR-4, but is also involved in IL-1 signalling (Picard *et al.*, 2011). Fig. 3.13.B shows that upon LPS stimulation, IRAK-4 phosphorylation increases. More importantly, the basal phosphorylation of IRAK-4 is significantly higher in stenotic cells vs. controls.

To confirm that activation of TLR-4 was responsible for the increased proliferation, cells were pre-incubated with the TLR-4 antagonist OxPAPC (30µg/ml) 20 min prior to stimulation. Cell proliferation in the presence of OxPAPC decrease to baseline levels equal to quiesced cells (Fig. 3.14.A). Therefore, OxPAPC inhibited the 28% increase in proliferation caused by LPS, as well as the FCS mediated response. To confirm this, cells were treated with OxPAPC and stimulated with 1% FCS only (Fig. 3.14.B). Again, cell proliferation was reduced to baseline levels. An MTT assay was used to confirm that OxPAPC at 30µg/ml was having no effect on the viability of the cells (Fig. 3.14.C).

A

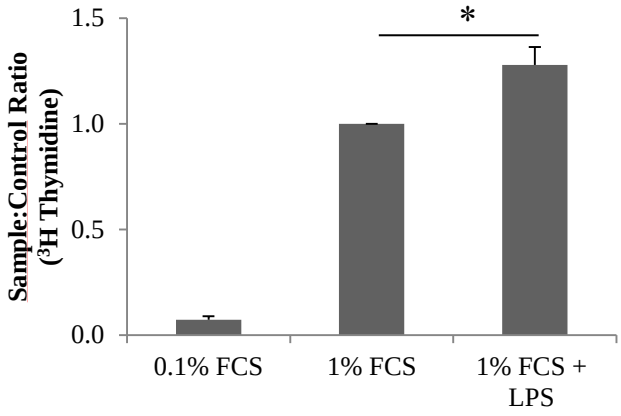

B

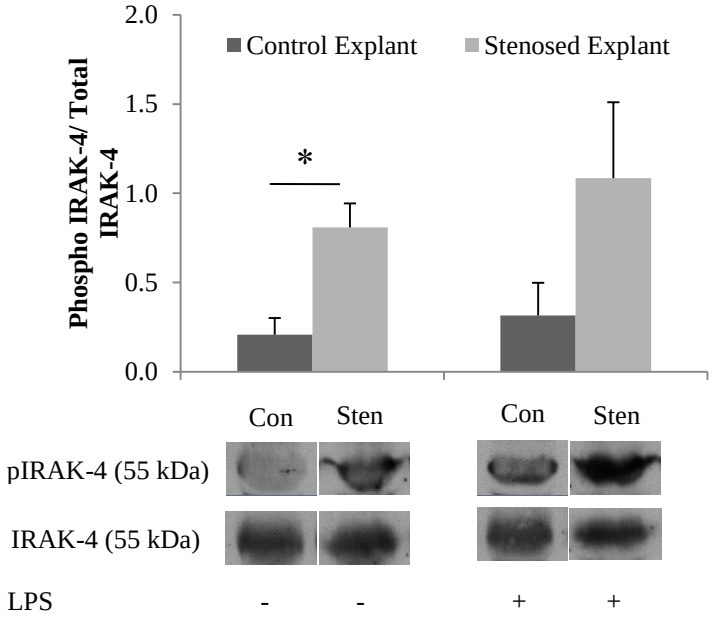

Figure 3.13. LPS-dependent stimulation of TLR-4 in proliferating vascular smooth muscle cells. ***A)*** *The proliferation of quiescent VSM cells stimulated with TLR-4 agonist LPS (100ng/ml) in the presence of 1% FCS, measured by* ^{3}H *thymidine incorporation. Results are shown as the mean ±S.E.M., n=6, *=p<0.05 (paired T-test).* ***B)*** *Basal and stimulated (LPS 100ng/ml) expression of activated IRAK-4 showing increased basal activation within stenotic (Sten) vs. control (Con) explants. Results are shown as the mean ±S.E.M., n=3, *=p<0.05 (unpaired T-test).*

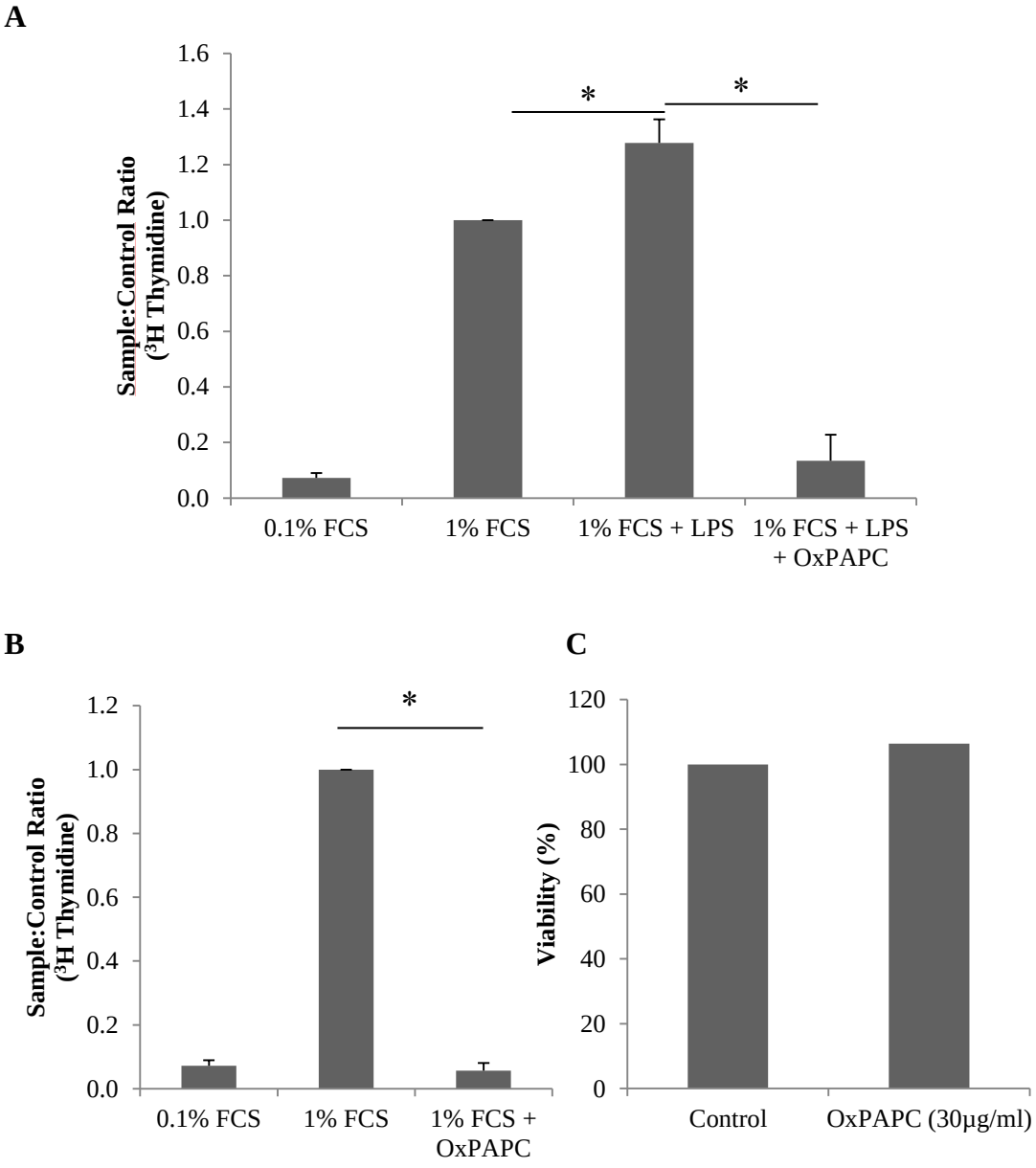

Figure 3.14. The effect of OxPAPC (TLR-4 antagonist) on the proliferation of vascular smooth muscle cells. ***A)*** *Cells stimulated with 1% FCS + LPS (100ng/ml) in the presence of OxPAPC (30ug/ml), n=6.* ***B)*** *Cells stimulated with 1% FCS in the presence of OxPAPC, n=6.* ***C)*** *The viability of VSM cells treated with 30ug/ml of OxPAPC for 24 hr, measured by MTT assay, n=2. All results are shown as the mean ±S.E.M., *=p<0.05 (paired T-test).*

3.3.5 The effect of diclofenac on human vascular smooth muscle cell proliferation

The ability of diclofenac to inhibit VSM cell proliferation was investigated. The maximum concentration used in these experiments was 175µM, based on the concentrations used in a previous study (Brooks *et al.*, 2003). Quiescent VSM cells were treated with diclofenac for 24 hr prior to stimulation with 10% FCS; proliferation was measured by ^{3}H thymidine incorporation (Fig. 3.15.A). Diclofenac caused a significant concentration dependent decrease in proliferation when compared to non-treated VSM cells. There was no difference in the level of diclofenac-dependent inhibition in VSM cells derived from control or stenosed tissues. The ability of diclofenac to inhibit LPS stimulated proliferation was measured in Fig. 3.15.B. With diclofenac pre-treatment (175µM), the LPS + FCS mediated proliferative response was reduced to baseline levels. The viability of diclofenac treated cells was assessed by inclusion/exclusion of fluorescent dyes and MTT assay to rule out cytotoxicity (Fig. 3.16). Diclofenac had no effect on cell viability.

A

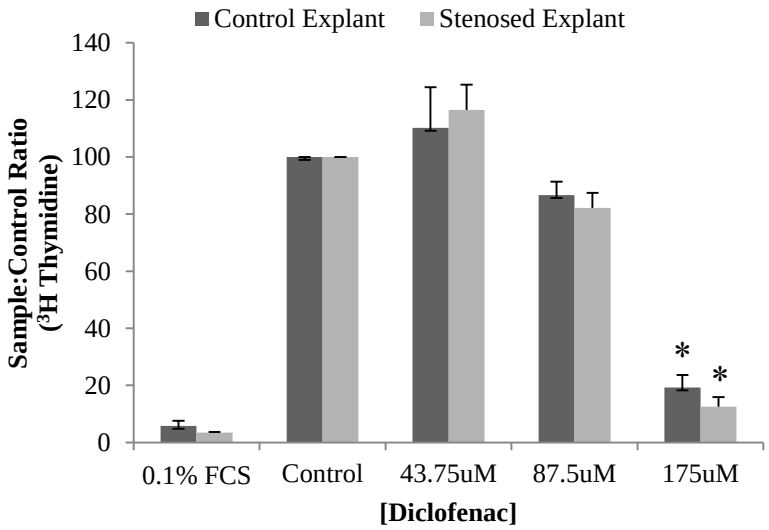

B

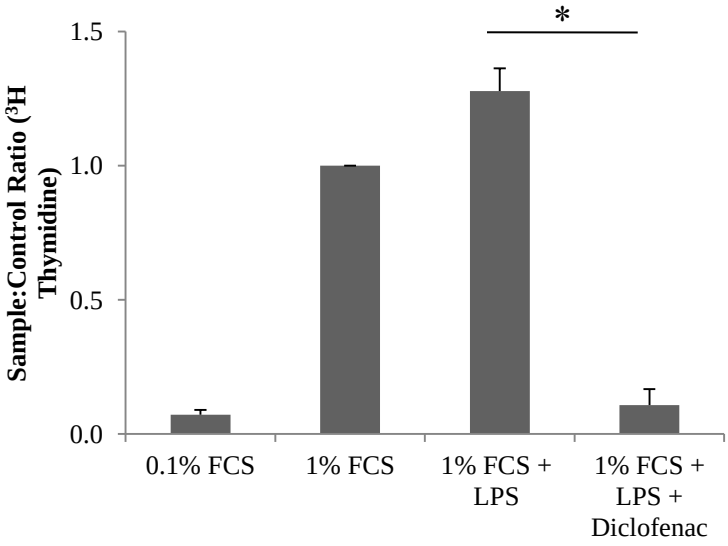

Figure 3.15. The effect of diclofenac on the proliferation of vascular smooth muscle cells. ***A)*** *Inhibition of FCS stimulated VSM cells by diclofenac. Quiesced cells were treated with diclofenac for 24 hr, before being stimulated with 10% FCS and quantified by ^{3}H thymidine incorporation. Results are shown as the mean ± S.E.M., n=6, general linear ANOVA p<0.05, *=post-hoc Dunnett's vs. control p<0.05.* ***B)*** *Inhibition of LPS (100ng/ml) stimulated VSM cells by diclofenac. Results are shown as the mean ±S.E.M., n=6, *=p<0.05 (unpaired T-Test).*

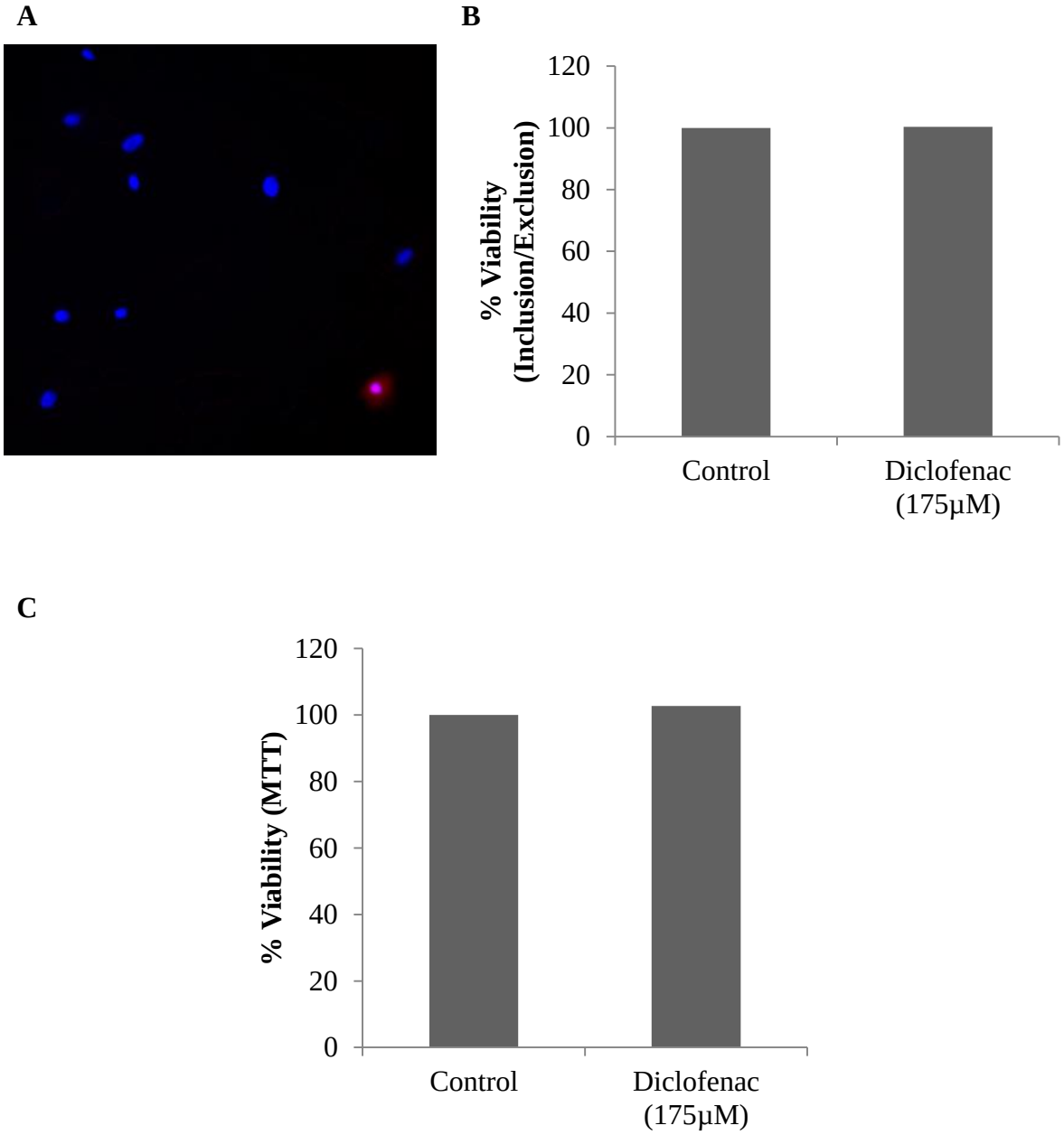

Figure 3.16. The viability of cells treated with diclofenac. ***A)*** *An example image from the inclusion/exclusion of dyes in treated cells. Hoechst 33342 selectively stains live cells blue, and propidium iodide stains dead cells red.* ***B)*** *Quantification of inclusion/exclusion dyes on cells treated with diclofenac for up to 48 hr. Results are shown as the mean of one experiment, carried out in triplicate.* ***C)*** *% viability of cells treated with diclofenac over 24 hr, measured by MTT assay. Results are shown as the mean of two experiments, carried out in triplicate.*

3.4 Discussion

3.4.1 Morphology of arteriovenous fistula stenosis

Histological analysis of failed AVFs using haematoxylin and eosin demonstrated that significant inward hypertrophic remodelling occurred (Fig. 3.1). This, combined with thrombus formation within the lumen of the fistula would likely render the AVF inadequate to accommodate the necessary perfusion pressure and flow required for haemodialysis. This observation is widely accepted (Roy-Chaudhury *et al.* 2007, Lee & Roy-Chaudhury 2009 & Van Tricht *et al.* 2005). To characterise the cells present within the neointima of stenotic veins, the VSM cell marker α-SMA was used (Fig. 3.2). All of the cells were positive for this marker. These neointimal cells lacked the organisation seen in the original medial layer. α-SMA is the most widely used marker to identify VSM cells (Fatigati and Murphy, 1984; Gabbiani *et al.*, 1981; Owens and Thompson, 1986); however this marker is also expressed by other cells types including myofibroblasts (Skalli *et al.*, 1989). Without the use of another marker such as desmin, there is a possibility that the cells could also be myofibroblasts. The problem with these markers is that they can be expressed at various levels depending on the cell phenotype (Rensen *et al.*, 2007). Expression of α-SMA and desmin can become reduced when the cell phenotype switches from contractile to synthetic, making standardisation of markers difficult. Also, a previous study has reported that the majority of cells within venous neointima were α-SMA and vimentin positive, suggesting a major myofibroblast component (Roy-Chaudhury *et al.*, 2009). They also reported a low expression of α-SMA and desmin positive cells, which they classed as VSM cells. However, the lack of classical VSM cells reported within AVF neointima could be explained by an increase in a contractile phenotype. Overall, this study does not rule out the possibility that the cells within the neointima are a mixture of myofibroblasts and synthetic VSM cells.

Whether the accumulation of cells within the neointima occurs due to proliferation of cells within the vessel wall, or migration from other sources, has not been clearly established. What is clear is that regardless of their origin or phenotype, the hallmark of this type of remodelling is hyper-proliferation. Within stenosed AVF,

the number of cells undergoing proliferation was almost 10 fold greater in AVF vs. non-stenosed controls (Fig. 3.3). As VSM cells are generally in a quiescent phenotype (Gordon *et al.*, 1990), the data presented in this study demonstrates a phenotypic switch of the cells to a synthetic, hyper-proliferative phenotype. The observation of an increased rate of cell proliferation within failed AVF has been shown previously using similar methods (Rekhter *et al.*, 1993). The proliferative characteristics of these synthetic phenotype cells warrant further study, which was performed later in section 3.3.3 of this chapter. As for the mechanism driving cell accumulation in the neointima, there is likely a mixture of both proliferation and migration. Previously, a pig vein graft model has been used to demonstrate the migration of adventitial fibroblasts through the media into the neointima, where they took on a myofibroblast phenotype (Shi *et al.*, 1997). Circulating bone marrow derived cells could also be a source of migratory cells. Evidence generated from a rat AVF model demonstrated the presence of bone marrow derived endothelial and smooth muscle cells in the neointima of the venous branch (Caplice *et al.*, 2007). However, this study was later contradicted in 2011 by demonstrating that the origin of cells within neointima are of a local origin, and not derived from the feeding artery or bone marrow (Skartsis *et al.*, 2011). Therefore, the origin of cells within the neointima of stenosed AVF is not clear. What is known is that their presence is the main contributing factor to this pathology, and as such they are a target for future therapeutic strategies.

Key to remodelling is deposition of extracellular matrix, which allows cells to migrate into the lumen (Madri *et al.*, 1991). Extracellular matrix is a major component of intimal lesions within vein grafts; in particular collagen and proteoglycans (Mitra *et al.*, 2006). In this study there is clear evidence of extracellular matrix deposition within the stenotic veins (Fig. 3.4). Proteoglycan deposition was significantly increased at the leading edge of proliferation. Collagen, another vital component of the extracellular matrix was also assessed by several different methods. Picrosirius red revealed no significant differences in collagen expression between control and stenosed veins when measured by brightfield and polarised light microscopy (Fig. 3.5). Likewise massons trichrome staining was also

used to visualise collagen, which again showed no significant differences in overall expression between the groups (Fig. 3.6). However, massons trichrome highlighted the differences in the arrangement of the VSM cells and collagen. In the healthy controls and original media layers of stenotic veins, the cells are uniformly distributed around the vessel lumen with thin layers of collagen between the cells (Fig. 3.6.A and Fig. 3.6.B). In Fig. 3.6.D, it was evident that within the neointima there was a higher expression of collagen and less cellular material, which results in stiffening of the vessel. A number of studies have demonstrated that collagen deposition during vascular remodelling stimulates the migration of cells into the neointima, which is particularly evident following injury (Madri *et al.*, 1991). The conclusions which can be drawn from our data may be limited by the fact that only total collagen expression was analysed. As there are many different collagen types, immunohistochemistry for specific collagens may reveal differences in expression between groups. As far as possible, the cross sections used have been taken from similar sites along the failed venous branch. However, due to variances in the size of vessels and the availability of samples, there was considerable heterogeneity. This makes the acquisition of statistically significant data difficult. Nonetheless, the study of human tissues allows the elucidation of the important characteristics of AVF failure which would not be possible with other methods alone (i.e. animal studies, *in vitro* culture).

3.4.2 Inflammation and arteriovenous fistula stenosis

As discussed in the introduction (Section 1.2), inflammation may be a possible trigger which could lead to the activation and proliferation of VSM cells during remodelling. From the biochemistry profiles of the patients involved in this study (Table 3.1), the stenotic patient group have significantly increased levels of the inflammatory marker C-reactive protein (CRP). This finding is supported by another study (Milburn *et al.*, 2013). A heightened inflammatory state in these patients could be due to hyperuremia (Kanellis & Kang 2005), as well as the process of haemodialysis (Schouten *et al.* 2000). The data in this present study demonstrates an increased presence of inflammatory cell infiltrates within stenotic AVFs (Fig. 3.7).

One component of this infiltrate is mast cells, shown by toluidine blue staining to be five times higher in human stenotic AVF compared to controls (Fig. 3.7.C). The infiltration of mast cells in vein grafts has been known for a long time (Cross *et al.*, 1998). Also, chymase expressing mast cell infiltration has been shown to take place following AVF placement in a canine model (Jin *et al.*, 2005). In patients with impaired kidney function, venous neointimal lesions have significantly higher expression of mast cell chymase compared to healthy vessel segments (Wasse *et al.*, 2011). Therefore, mast cells appear to be an important cellular component within the neointima of stenosed AVF. This study is limited as the presence of other immune cells within the neointima, such monocytes/macrophages, were not analysed. As it has been shown that macrophages make up a considerable cellular component in stenotic lesions (Roy-Chaudhury et al., 2009), the presence of these cells should be assed in the future by immunohistochemistry for CD14.

The production of pro-inflammatory/chemotactic proteins by both immune and non-immune cells is surely a factor in the process of immune cell infiltration during AVF failure. The inflammatory profiles of patients with stenosis were investigated using a proteome array panel (Fig. 3.8.A-C). Serum samples were collected from sex and age matched individuals with or without a functional fistula for comparison. The largest difference seen between these groups was an increase in MCP-1. However, this increase within the stenotic samples was not confirmed by ELISA as the number of patients available for this experiment was not enough to demonstrate statistical significance. This data is the first report that MCP-1 is not only increased in haemodialysis patients (Papayianni *et al.*, 2002), but may be specifically during stenosis. The importance of MCP-1 in AVF failure has been demonstrated using two rodent models (Juncos *et al.*, 2011). In this study, following AVF creation, MCP-1 mRNA and protein were significantly increased which was accompanied by an increased in NF-κB and AP-1 activity. In an MCP-$1^{-/-}$ strain, the development of venous stenosis was significantly reduced. In a rat model of AVF, Juncos and co-workers demonstrated that MCP-1 was co-localised with proliferating VSM cells, the endothelium and infiltrating lymphocytes. These findings, along with data presented in this current study, suggest that MCP-1 may play a role in the pathogenesis of AVF

stenosis. The overall profile of the stenotic patients from the cytokine array suggests that they are undergoing a pro-inflammatory immune response, indicated by the presence of MCP-1, IL-1β, IL-2, MIP-1β. This finding is supported by many studies which have studied the roles of these types of cytokines in vascular stenosis (Brody *et al.*, 1992; Croatt *et al.*, 2010; Faries *et al.*, 1996; Liu *et al.*, 2008; Marrone *et al.*, 2007; Yang *et al.*, 2005). Also, previous unpublished work carried out by the cardiovascular research group at Strathclyde University has found that when VSM cells derived from stenotic AVF are challenged by phorbol 12-myristate 13-acetate (PMA), they produced significantly greater amounts of MCP-1 and IL-6. The high throughput of a technique such as a proteome array makes it ideal for generating an inflammatory prolife. However, the main limitation of techniques such as this is that they do not give a quantifiable concentration of a protein, and they usually have low statistical power. The fact that expression of a particular protein may be elevated two fold does not necessarily mean that this increase would be clinically significant. Therefore, a quantifiable method such as an ELISA must always be used along with high throughput screening methods, and preferably with a higher number of participants.

Inflammatory and proliferative responses are central to AVF failure, and identification of a common pathway of activation could lead to a powerful treatment strategy in the future. In this study, we investigated whether TLR-4 plays a role in AVF failure, and whether activation of this pathway could lead to a proliferative response. Previously, the expression of TLR-2 and TLR-4 with or without co-localisation of TLR ligand HSP60 in stenotic AVF vs. controls was investigated by immunohistochemistry (De Graaf *et al.*, 2006). This qualitative study found that TLRs were only expressed in stenotic lesions, and were absent from controls. In this study, the expression of TLR-4 was quantified using immunofluorescence. TLR-4 was present in both stenotic and healthy long saphenous vein controls (Fig. 3.9.A-B). More importantly, the expression of TLR-4 was significantly increased within stenotic AVF vs. healthy controls (Fig. 3.9.C). Other studies published since De Graaf *et al.* have also reported expression of TLR-4 in freshly isolated human long saphenous vein (Karper *et al.*, 2011). Therefore it is likely that TLR-4 staining in the

control group is genuine, and the failure to show this by De Graaf *et al.* could be due to the sensitivity of their detection technique. Immunofluorescence was used in our study to allow direct quantification of TLR-4 expression within the vessels; revealing a significant increase within stenotic vessels. The main limitation of this experiment was endogenous autofluorescence within the vessel. Therefore, negative controls (without primary antibody) were also quantified and subtracted from experimental readings to increase the accuracy of TLR-4 staining. However, an isotype control antibody was not used and therefore the possibility of secondary non-specific signal cannot be ruled out. Also, due to variation in length of tissue specimen and size of stenotic lesion, choosing consistent regions for staining between samples was difficult. Therefore, the region were the stenosis was most severe was chosen for quantification. As a result, this region may not be a true representation of the whole sample.

3.4.3 The link between inflammation and hyper-proliferation

The role of TLR-4 activation in the proliferation of vascular smooth muscle cells in vitro was investigated using LPS simulated VSM cells harvested from control long saphenous vein and stenotic AVF. Stimulation of cells with LPS causes a significant increase in their proliferative response (Fig. 3.13.A). However, this response only occurs in the presence of 1% FCS, as no effect is generated in serum starved cells. A concentration of 1% FCS was chosen to evoke a proliferative response below the EC_{50}, leaving capacity for further proliferation by LPS. The lack of response with low serum media suggests that LPS alone is not enough to cause proliferation, but in the presence of another stimulus it can prime the cells towards proliferation. LPS, and other TLR agonists such as HSP60, act as 'danger molecules' to alert and activate nearly all cells in the body to a threat (Asea *et al.*, 2002). Therefore, TLR-4 stimulation of cells causes activation and increases their response to stimuli (Montero Vega and de Andrés Martín, 2009). Also, in the body TLR activation leads to the production of cytokines and growth factors from other cells which are not present in these in vitro studies (Heo *et al.*, 2008). Therefore, if LPS in the absence of other

immune factors can lead to proliferation in vitro, then it is reasonable to assume that this response would be even greater *in vivo*.

The phospholipid OxPAPC was used to validate the role of TLR-4 in LPS mediated proliferation. OxPAPC has been reported to antagonise TLR-4 activation at the cell membrane (Erridge *et al.*, 2008). Specifically, it acts by competitive interaction with the accessory proteins CD14 and LPS-binding protein. Therefore, in this study it was hypothesised that there would be a reduction in the proliferation caused by LPS with OxPAPC pre-treatment. However, both FCS and LPS mediated proliferation were inhibited (Fig. 3.14). There are three possible explanations for this; 1) OxPAPC was having an effect on the viability of the cells, 2) the culture medium was contaminated by LPS or 3) OxPAPC was acting though another mechanism to inhibit FCS-dependent proliferation. OxPAPC was shown in this study to have no effect on the viability of cells at the working concentration, and therefore the first option is unlikely. The medium and tips used for these experiments are certified by the manufacturers to be endotoxin free. However, it is possible they could have become contaminated during the course of the experiment and therefore in the future these components could be tested using a straight forward endotoxin assay. The third explanation is the most likely; that OxPAPC does not solely antagonise TLR-4. Oxidised phospholipids are known to have a wide range of biological effects, both pro and anti-inflammatory, and therefore OxPAPC is likely to act on many pathways (Greig *et al.*, 2012). To confirm that TLR-4 activation is mediating the increased proliferation, another method of antagonising the pathway such as a neutralising antibody (Lin *et al.*, 2007) could be used in any future experiments.

As well as expression of TLR-4 and LPS mediated proliferation, activation of the TLR-4 pathway was also investigated in the healthy control vs. stenotic cells. Two pathways exist for the activation of the TLR-4 pathway: the myeloid differentiation factor 88 (MyD88)–dependent and MyD88–independent pathways. The MyD88-dependent pathway signals through the IRAK-4 kinase to cause a cascade which will lead to the activation of NF-κB and MAPK as described in chapter 1 (Fig. 1.3) (Akira and Takeda, 2004). This pathway is common to most TLR signalling,

although much of the previous work has focussed on immune cells. Upon LPS stimulation, IRAK-4 phosphorylation increased to a similar extent in both sets of cells (Fig. 3.13.B). More importantly however, basal phosphorylation of IRAK-4 was significantly increased within the stenotic explants. Therefore, for the first time we have demonstrated that TLR-4 activation primes VSM cells to proliferate, and cells derived from stenotic AVF have higher basal activation of the TLR-4 pathway. This could be in part responsible for the increased proliferation which is seen within the vein wall.

The proliferative characteristics of cells derived from stenotic AVF and healthy controls were analysed further. ^{3}H thymidine incorporation revealed significant differences in the proliferative capacities of cells derived from stenotic AVF vs. healthy controls (Fig. 3.11). Upon FCS stimulation, the cells derived from stenotic AVF had 1.7 times ($p<0.005$) greater proliferative capacity when stimulated with the maximum concentration of FCS compared to controls. The implication of this is that the cells have retained their hyper-proliferative phenotype, even after being placed in an artificial culture environment. Cell cycle analysis was carried out by staining cells with propidium iodide and analysing by FACs (Fig. 3.12). There were no statistical differences between control and stenotic VSM cells. However, in the stenosed cells there was a trend towards an increase in the G2/M stages of the cell cycle, suggesting a greater level of proliferation. The time point used in this experiment was 48 hr post stimulation. As this type of analyses shows a snapshot of the cell cycle at the time the cells were fixed, a different time point may give more insight.

Like all primary cell explantation and culture, there exists a possibility that the explants are heterogeneous in nature. What can be ruled out is the presence of endothelial cells as the medium used was not conducive to their growth. All of the cells explanted were α-SMA expressing-smooth muscle type cells. There is a possibility that the explants could contain myofibroblasts. However this has more physiological relevance as it is known that within neointima of stenotic veins there

are multiple smooth muscle related cells and phenotypes (Roy-Chaudhury *et al.*, 2009).

The mounting evidence for the role of TLR-4 in AVF stenosis presented in this chapter highlights this pathway as a potential future target for therapeutic intervention. However, targeting of TLR-4 systemically could have a wide range of side effects as TLR-4 is expressed in all tissues (Zarember and Godowski, 2002). Therefore, localised targeting is essential. In AVF stenosis, the point at which it would be best to inhibit TLR-4 is not clear. As activation of this pathway primes cells and triggers a response, one strategy would be to apply the therapy at fistula creation. However, as it has been shown that TLR-4 is activated by HSP released by haemodynamic forces during maturation (De Graaf *et al.*, 2006; Hochleitner *et al.*, 2000a; Karper *et al.*, 2011), this process may contribute to beneficial remodelling and form an essential part of the maturation response. These issues need to be addressed for the successful use of TLR therapies in the prevention of AVF stenosis. Currently, there are no clinically available inhibitors of TLR activation. However Idera Pharmaceuticals are developing an antagonist of TLR-7 and TLR-9 (IMO-3100) predominantly for use in autoimmune diseases. IMO-3100 has been shown to supress TLR-7/9 inflammatory responses in treated human peripheral blood mononuclear cells (Jiang *et al.*, 2009). Safety of this lead agent was assessed in phase I trials, and in phase II it was shown to have a significant therapeutic benefit in the autoimmune disorder psoriasis. Therefore, it is likely that pharmacological inhibition of select TLRs may be clinically available in the near future. However, as there are no TLR-4 therapies currently being trialled, targeting inflammation and proliferation of VSM cells downstream of TLR-4 is the best option.

3.4.4 The anti-proliferative potential of a classically anti-inflammatory drug

The therapeutic potential of diclofenac was investigated in this chapter. As well as its clinically well-defined anti-inflammatory activity, diclofenac has also been shown to inhibit proliferation of VSM cells (Brooks *et al.*, 2003). In this study, diclofenac was shown to have anti-proliferative properties on FCS and LPS stimulated VSM

cell proliferation (Fig. 3.15). The level of inhibition seen was equal in both control and stenotic explants. More importantly, this agent had no effect on the viability of cells at the active concentration (Fig. 3.16). The mechanism through which diclofenac inhibits VSM cell proliferation are as yet not known. However many NSAIDs have anti-proliferative actions independent of their anti-inflammatory cyclooxygenase activity (Tegeder *et al.*, 2001). Proposed mechanisms for NSAID anti-proliferative activity include the inhibition of transcriptional activity of NF-κB (Kopp and Ghosh, 1994; Marra and Liao, 2001), as well as Ca^2 dependent inactivation of calcium release activated calcium channels (Muñoz *et al.*, 2011). A third mechanism of action is the activation of AMPK, which was discussed in chapter 1 (section 1.3.2 & figure 1.5) in relation to aspirin's anti-proliferative activity (Sung and Choi, 2011). This could potentially link with the mechanism proposed by Muñoz *et al.*, as an upstream kinase of AMPK is calmodulin-dependent protein kinase (CaMKK). To the best of our knowledge there have been no studies to date which have investigated the role of AMPK in diclofenac mediated inhibition of proliferation. Therefore, this pathway was investigated in chapters 4 and 5 of this thesis.

3.5 Conclusion

In summary, the data presented in this chapter shows that inward hypertrophic remodelling is due to the proliferation of VSM cells, extracellular matrix deposition and inflammatory cell infiltration. For the first time, pro-inflammatory cytokines have been shown to be specifically increased during stenosis, and not just generally increased in dialysis patients; although further experiments with larger populations of patients are needed. An increase in TLR-4 expression and basal activation in stenotic patients may prime their VSM cells towards hyper-proliferation. Interestingly, this hyper-proliferative phenotype is even retained by the cells following cell culture. Finally, diclofenac has the potential to be used prophylactically to increase AVF patency due to its anti-proliferative activity in stenotic VSM cell explants. The novel nature of this observation merits further study.

Chapter 4

Development and characterisation of an AVF model in the rabbit; effects of topical diclofenac treatment

4.1 Introduction

The response to vascular injury which develops into adverse remodelling likely evolved as a reparative mechanism. Mechanical trauma from clamping, suturing and changes in haemodynamic stresses are unavoidable consequences of vascular surgery which stimulate an inflammatory response (Konner, 2003). Endothelial cell disruption is one event which occurs in such injuries, and has been found to stimulate VSM cell proliferation even in absence of medial injury via reduction of nitric oxide and stimulation of inflammation (Fingerle et al., 1990; Tarry and Makhoul, 1994; Topper et al., 1996). In AVF stenosis, haemodynamic injury has been highlighted as a main upstream event (Fillinger *et al.*, 1990). As discussed in chapter 1 (page 11), increased haemodynamic forces can cause an increase in expression of HSP which generate an inflammatory and proliferative response in VSM cells via the activation of TLR-4 (Hochleitner *et al.*, 2000).

Another mechanical stress which is likely to contribute to AVF stenosis by generating an inflammatory response is cannulation injury. However, to date the majority of studies investigating AVF stenosis and cannulation have focussed on the development of aneurysm and haematoma, rather than the development of vascular stenosis. There are three main types of cannulation technique which can be used in vascular access. Rope ladder puncture uses a different cannulation site along the length of the vein, area puncture always uses the same area for cannulation and buttonhole puncture uses the exact same site each time (Krönung, 1984). During each cannulation, vessel wall tissue is displaced leading to the formation of a thrombus. This slightly increases tissue mass and leads to the deposition of scar tissue, a consequence of an immune response. When area and rope ladder puncture are used, scar tissue forms along the length of the vein which leads to an increased chance of aneurysm and haematoma (K. Konner, 2003). Recent findings have suggested that the buttonhole technique allows easier cannulation of AVF due to the support of surrounding scar tissue (Verhallen et al., 2007). Also, buttonhole cannulation causes displacement of the thrombus resulting from a previous cannulation, and is therefore associated with lower complication rates (van Loon *et al.*, 2010). To date, only one study has examined AVF neointimal development

during repeated cannulation (Hsiao *et al.*, 2010). In this, 104 patients receiving buttonhole cannulation for maintenance haemodialysis were studied for 1 year. Intimal lesions were found in 40% of the venous puncture sites. However none of these lesions resulted in a clinically significant luminal stenosis. Significant stenosis was found in 36.5% of the patients at non-puncture sites, 22.1% of which were juxta-anastomosis and 14.4% of which were between the outflow and inflow button hole cannulation sites (sites shown in Fig. 1.1). This small study highlights the potential for remodelling which occurs at the anastomosis and in/near the cannulation sites. Clearly, more research is needed to determine the extent that cannulation injury contributes to vascular remodelling. Therefore, the aims of this chapter are to:

1. Develop a rabbit model of AVF remodelling which incorporates cannulation injury of a type and frequency similar to that of haemodialysis.

2. Use this model as part of an interventional study to assess the therapeutic potential of topical diclofenac, which has previously been shown to inhibit VSM cell proliferation in chapter 1.

4.2 Materials and methods

4.2.1 Study design

AVFs were created in White New Zealand rabbits. The study was designed with two phases post AVF creation; a maturation period between days 0-28 and an experimental period between days 28-56. During the maturation period, the AVF was monitored by ultrasound. In the second phase, animals were split into three groups; a control group which received no injury or intervention, an injury group which received area cannulation injury three times a week and an intervention group which received injury as well as topical diclofenac.

4.2.2 Induction and maintenance of anaesthesia

The animals were given a pre-medication of hypnorm (0.3ml/kg, VetaPharma Ltd., UK) intramuscularly 15 min prior to surgery. During surgery the rabbit's body temperature, respiration and heart beat were observed and recorded. Based on respiration and heart rate, the concentration of isoflurane was adjusted between 1-1.5% (Oxygen $1lmin^{-1}$, Nitrous Oxide $1lmin^{-1}$). Subcutaneous Rimadyl (4mg/kg, Pfizer, UK) was also given at the time of surgery.

4.2.3 Creation of the femoral arteriovenous fistula

A site proximal to the right knee was chosen to create the AVF due to the superficial nature of the vessels. Following a 5cm skin incision on the inside right thigh, the sartorius muscle was carefully parted. The femoral artery and vein were then isolated as shown in Fig. 4.1. Heparin (1000I.U.) was given intravenously just prior to proximal and distal clamping of the vessels. A longitudinal 5mm incision was made in the wall of both the femoral artery and vein. Thereafter, the artery and vein were sutured together to create a side to side anastomosis using 10-0 polyamide suture (Ethicon, USA). The distal vein was then tied off using a 4-0 suture (Ethicon, USA) to ensure unidirectional blood flow through the vein, effectively creating an end to side anastomosis. Blood flow was restored to the fistula by removing all of

the clamps. Following this, the wound was closed using a combination of subcuticular and interrupted suturing. The animals were then recovered on a heat mat under supervision until they were moving independently. They were then transferred back to their cage and periodically checked for the remainder of the day.

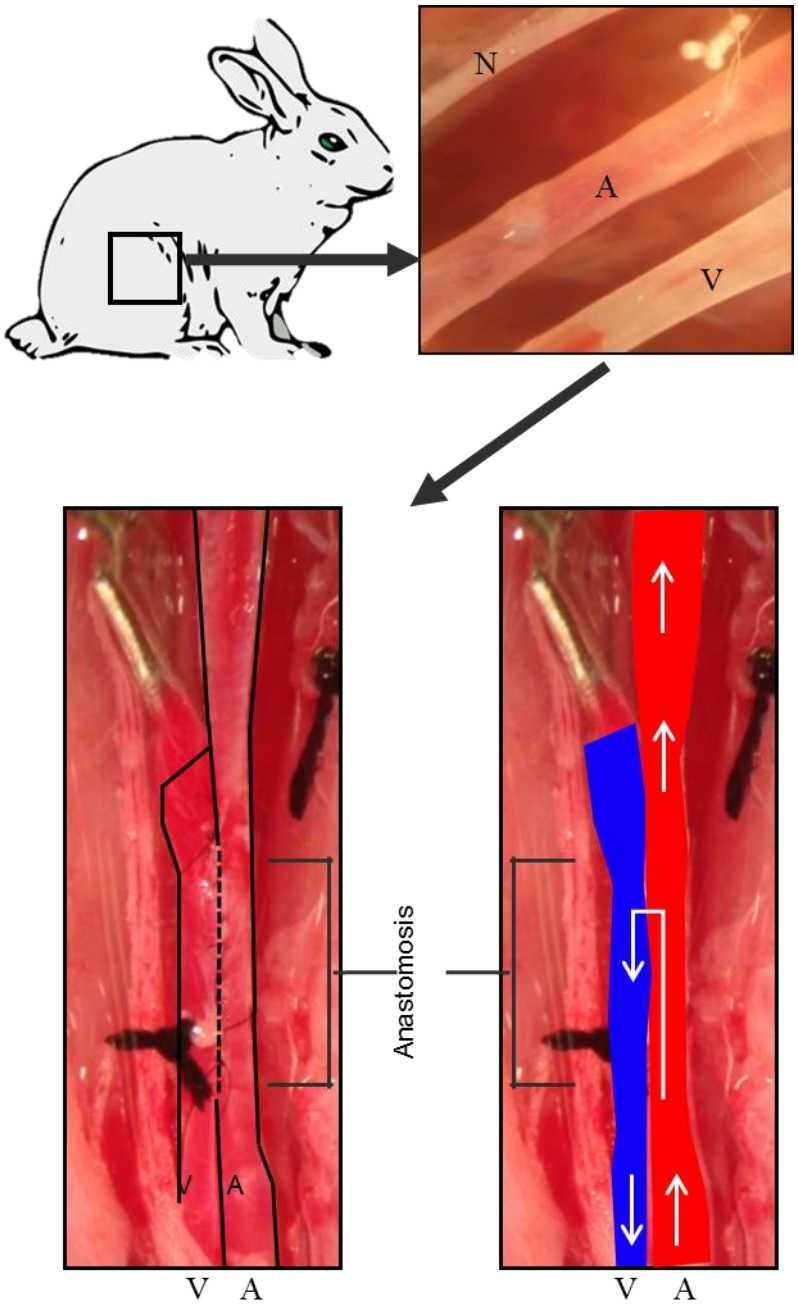

Figure 4.1. Femoral AVF creation. *The hind limb of the rabbit was chosen for the creation of an AVF. The neurovascular bundle was separated into femoral artery (A), vein (V) and nerve (N). A side to side anastomosis was created using 10-0 polyamide suture (red= artery, blue=vein) followed by ligation of the distal vein.*

4.2.4 Ultrasonography of arteriovenous fistula

Ultrasound measurements were performed using a Philips Sono 5500 and a linear array probe (6-15mHz) 10 days following arteriovenous creation. This 10 day period allowed sufficient time for the wound to heal. Prior to ultrasonography the animals were pre-medicated with hypnorm (0.2ml/kg) intramuscularly. Animals were placed supine in a sterile area and fur was removed from the surgical site using electric clippers. The probe was placed perpendicular to the vessels and Brightness mode (B-mode) ultrasound was used to visualise the patency of vessels and to measure vessel diameter. Colour Doppler mode was used to visualise the direction of blood flow within the AVF and Pulsed Wave Doppler mode was used to measure the velocity of blood passing though the AVF. At least two measurements were recorded for velocity and diameter in the venous branch proximal to the anastomosis. The blood flow (ml/min) was calculated using the following formula:

$$\text{Blood Flow (ml/min)} = \text{Velocity (cm/s)} \times \text{Vessel Area (cm}^2\text{)} \times 60$$

4.2.5 Blood biochemistry and haematological profiles

Blood samples were taken from the marginal ear vein; pre-surgery, immediately following recovery from anaesthesia, at the end of the maturation period (Day 28) and then at the end of the experimental period (Day 56) for each group. Analysis was carried out by Veterinary Diagnostic Services based at the University of Glasgow. For biochemistry analysis, blood samples were collected in EDTA coated vials and analysed on an Olympus AU 640 clinical chemistry analyser using IFCC/DGKC approved methods. Blood electrolytes were analysed on the same system by Indirect ISE. For haematological analysis, blood samples were collected in heparin coated vials and analysed on a Siemens Advia 2120 haematology system, with an additional 5 part differential carried out manually.

4.2.6 Cannulation injury

Cannulation injury to the venous branch of the AVF was performed three times a week during days 28-56 of the experiment using a 23 gauge needle (BD Microlance, USA). As the vessels were not immediately visible under the skin, cannulation was carried out under the guidance of ultrasound to visualise the position of the needle in the vein and ensure it hadn't penetrated through the back wall of the vessel. Prior to the procedure animals were pre-medicated with hypnorm (0.3ml/kg) intramuscularly and placed supine. Fur was removed as before from the surgical site and the fistula located by its pulse. The surface of the skin was sterilised before a saline (Dechra, UK) charged needle was placed into the venous branch of the AVF which sits on top of the feeding artery. Successful injury to the vein was confirmed by the presence of blood in the head of the needle, as well as visualisation of the needle tip in the vein by B-mode ultrasound. The needle was then removed after being in place for approximately 30 sec. Pressure was applied to the cannulation site for several minutes to avoid haematoma The site was then monitored for a further 5 min to ensure the injury site had clotted. Animals were also monitored later in the day to ensure the puncture site had healed.

4.2.7 Application of topical diclofenac

Diclofenac diethylammonium gel (1.16%, Novartis, UK) was given topically to the appropriate group of animals during days 28-56. Animals received 750mg of gel over a 9cm^2 area (equivalent to 1mg/cm^2 dose of diclofenac) twice a day, Monday-Friday. On a day in which injury was to be performed, the first dose of diclofenac was given 3 hr prior to cannulation which allowed absorption of the gel and a period of time for the drug to take effect. The second dose was given immediately after injury. In the days between the injury procedure, animals were given topical diclofenac in the morning and afternoon. All animals receiving topical diclofenac had an Elizabethan collar in place at all times to avoid any oral dosing of the drug while grooming.

4.2.8 In situ paraformaldehyde fixation of the arteriovenous fistula

Following euthanasia by intravenous injection of sodium pentobarbital (1ml/kg), the animal's abdominal cavity was opened and the thoracic aorta and vena cava were exposed. A cannula was then positioned in the aorta distal to the renal artery and proximal to the iliac bifurcation. Using a reservoir placed above the animal, a litre of saline was passed through the lower body and out via an incision made in the vena cava. Once the fluid leaving the animal was clear, 4% paraformaldehyde was flushed through the lower body before the vena cava was clamped. The pressure of the solution entering the artery was then set to 100mmHg by placing the reservoir 1.3m above the perfusing animal, and left for 2 hr in a fume hood. The AVF and contralateral control vessels were removed with some of the surrounding muscle still attached and placed in fresh 4% paraformaldehyde solution. These were stored at 4^{o}C until use.

4.2.9 Immunohistochemistry for AMPK

Immunohistochemistry was performed as detailed in chapter 2, section 2.3.4. Specifically, a sodium citrate buffer was used in the antigen retrieval step. The tissue was then blocked using 10% goat serum. A polyclonal rabbit anti-AMPK IgG (Cell Signalling Technology, USA) was used at 1:200 dilution overnight at 4°C. AMPK expression was visualised using a Vectastain Elite ABC Kit according to the manufacturer's instructions by incubation with a biotinynlated anti-rabbit IgG for 1 hr at room temperature, incubation with the VECTASTAIN® ABC Reagent for 30 min at room temperature (Vector Laboratories, UK) followed by visualisation with DAB substrate.

4.3 Results

4.3.1 Monitoring of AVF maturation

The maturation of rabbit femoral AVF was monitored using a number of different ultrasound techniques. As shown in Fig. 4.2.A-B, B-mode was used to visualise the patency of the vessels and measure their lumen diameters. This was carried out when the surgical wound had sufficiently healed; around 10 days post AVF procedure. Confirmation of flow through the fistula was also determined at this point using colour Doppler ultrasound. Using this technique, blood moving away from the heart was automatically coloured in red, and blood towards the body in blue. As shown in the example image (Fig. 4.2.C) and schematic (Fig. 4.2.D), flow could be detected traveling along the artery, which then crossed the anastomosis and back along the vein.

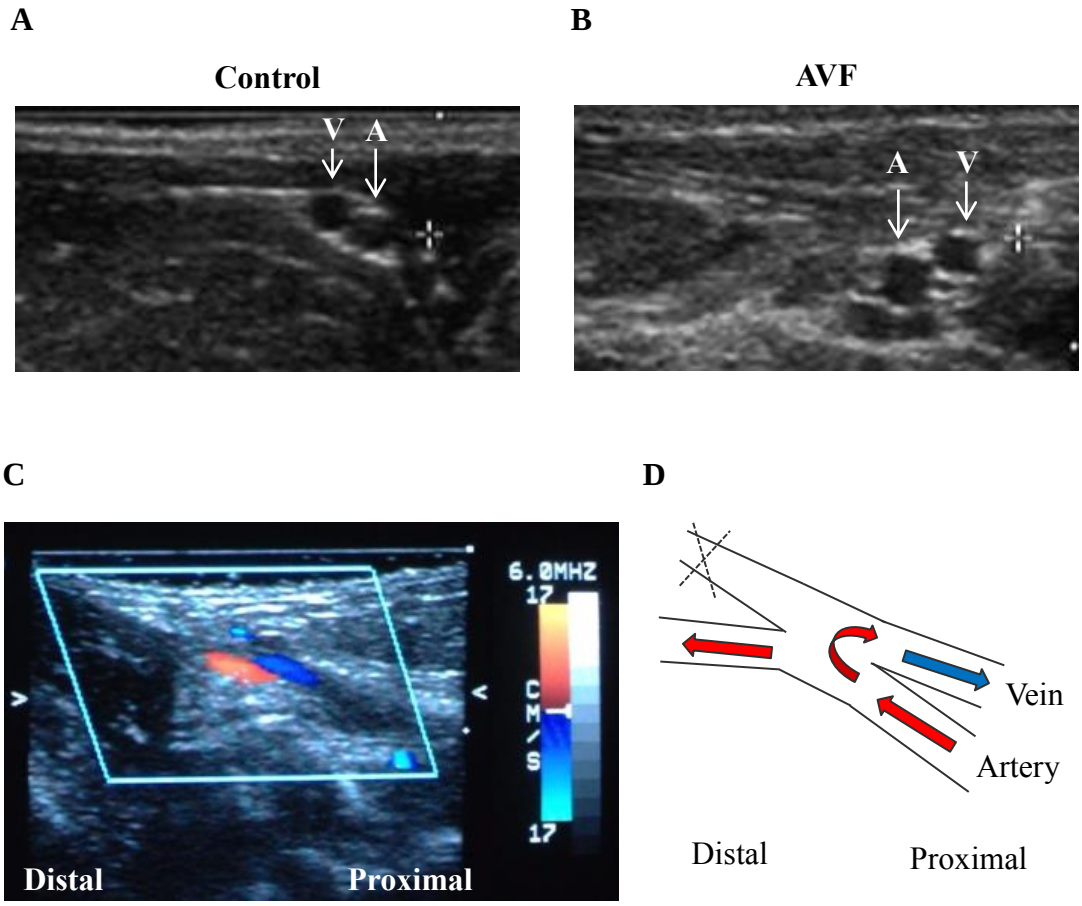

Figure 4.2. B-mode and colour Doppler ultrasound of rabbit femoral AVF. ***A)*** *Cross sectional B-mode ultrasound of contralateral control vessels.* ***B)*** *Cross sectional B-mode ultrasound proximal to the anastomosis of the AVF.* ***C)*** *An example colour Doppler ultrasound image showing the flow through the AVF from the artery (red) to the vein (blue).* ***D)*** *Schematic of AVF blood flow shown in C.*

The velocity of blood and vessel diameter were analysed every five days during maturation using B-mode and Pulsed Wave Doppler. These measurements were used to calculate blood flow through the vein (Fig. 4.3). Fig. 4.3.A shows an example velocity waveform during the early stages of maturation. The presence of a pulsatile waveform in the vein indicates arterial flow. Prior to fistula creation, attempts were made to measure venous velocity. However as the vein sits on top of the artery (as seen in Fig. 4.2.A), and has relatively low velocity, reliable measurements were not possible. At the end of the maturation period, velocity of blood had increased, as shown in Fig. 4.3.B example image. The graph in Fig. 4.3.C shows a summary of this time dependent increase in velocity, which was significantly higher at day 28 vs. day 10. Venous lumen diameter also appeared to increase, although this was not statistically significant (Fig. 4.3.D). Overall, there was a significant time dependent rise in blood flow, increasing from 42.1±5.0ml/min at day 10 to 60.5±7.2ml/min at day 28.

Biochemical and haematological analysis was also undertaken in blood samples collected pre/post-surgery and at the end of maturation. The only significant changes in biochemical parameters were small increases in potassium and creatinine levels, and a decrease in alkaline phosphatase immediately following surgery (Table 4.1). Haematological parameters such as red/white blood cell counts and were not altered by surgery or AVF maturation (Table 4.2).

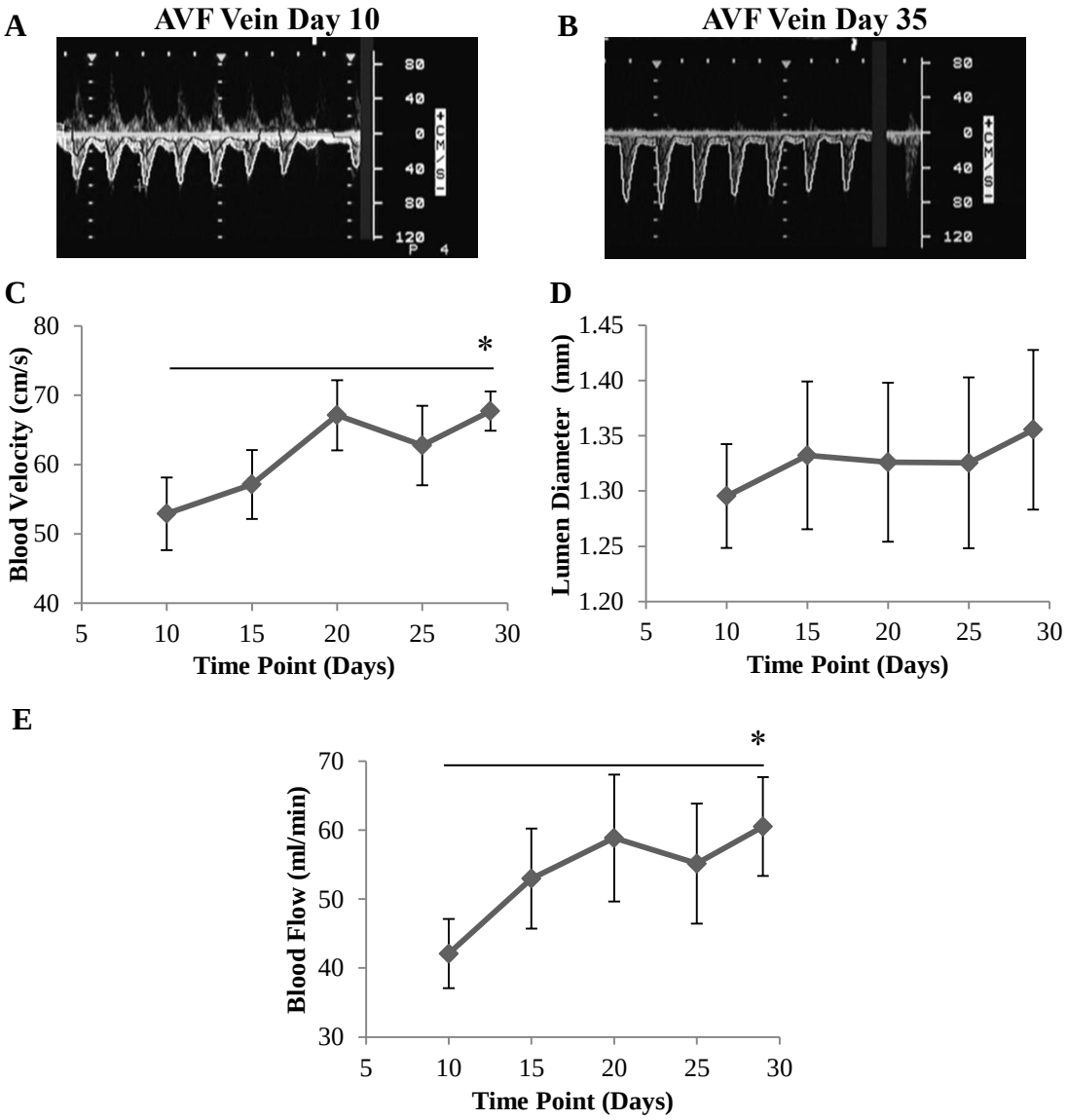

Figure 4.3. AVF maturation associated changes in blood flow and diameter. ***A)*** *An example of blood velocity (cm/s) in the venous branch of AVF during early vessel maturation.* ***B)*** *An example of blood velocity in the venous branch of AVF after vessel maturation.* ***C)*** *Changes in blood velocity measured every five days over the maturation period by Pulsed Wave Doppler.* ***D)*** *Changes in diameter of the venous AVF lumen measured every five days over the maturation period using B-mode.* ***E)*** *Using the data obtained from Pulsed Wave Doppler and B-mode, blood flow through the venous branch was calculated (ml/min). All results are shown as the mean ±S.E.M., n=11, *=p<0.05 paired t-test for day 10 vs. day 30.*

Biochemical Profile	Pre-Surgery		Post-Surgery		Day 28		Units
	Mean	S.E.M.	**Mean**	S.E.M.	**Mean**	S.E.M.	
Sodium	**145.2**	1.1	**148.0**	2.0	**145.9**	0.8	mmol/l
Potassium	**3.3**	0.0	**4.1***	0.3	**4.8**	0.9	mmol/l
Sodium: Potassium Ratio	**44.0**	0.3	**36.7**	3.3	**33.5**	5.5	mmol/l
Chloride	**95.8**	2.5	**94.2**	0.2	**93.4**	0.5	mmol/l
Calcium	**3.2**	0.1	**3.3**	0.1	**3.5**	0.1	mmol/l
Phosphate	**2.4**	0.2	**3.8**	0.3	**4.3**	1.2	mmol/l
Urea	**6.2**	0.5	**10.2**	0.3	**7.3**	0.3	mmol/l
Creatinine	**77.8**	3.0	**122.0***	13.4	**100.0**	7.5	mmol/l
Cholesterol	**0.9**	0.1	**0.7**	0.0	**0.9**	0.2	µmol/l
Triglyceride	**1.1**	0.2	**0.8**	0.1	**0.8**	0.1	mmol/l
Total Bilirubin	**0.8**	0.5	**1.0**	0.4	**0.5**	0.3	mmol/l
ALKPhos	**503.0**	63.1	**395.0***	22.0	**324.8**	24.0	µmol/l
AST	**32.3**	14.6	**78.3**	14.2	**51.5**	11.0	U/l
ALT	**34.5**	4.3	**35.0**	5.0	**46.8**	7.0	U/l
GGT	**3.0**	0.6	**5.0**	2.6	**5.8**	1.0	U/l
Total Protein	**52.7**	2.4	**52.0**	0.7	**58.5**	0.3	g/l
Albumin	**40.3**	1.5	**37.8**	0.9	**42.0**	1.0	g/l
Globulin	**12.3**	1.2	**14.3**	0.3	**16.5**	0.9	g/l
Albumin: Globulin Ratio	**3.3**	0.3	**2.7**	0.1	**2.6**	0.2	g/l

Table 4.1. Blood biochemistry profile during AVF maturation. *Blood samples were taken immediately before surgery, after recovery and then at the end of the maturation period. The following parameters were abbreviated; alkaline phosphatase (ALKPhos), aspartate aminotransferase (AST), alanine aminotransferase (ALT) and γ-glutamyl transferase (GGT). Results are shown as the mean ±S.E.M., n=4, *=p<0.05 for pre vs. post-surgery (paired T-test).*

Haematology Profile	Pre-Surgery		Post-Surgery		Day 28		Units
	Mean	S.E.M.	Mean	S.E.M.	Mean	S.E.M.	
RBC	**5.9**	0.0	**6.1**	0.1	**6.2**	0.2	$x10^{12}/l$
Hb	**12.3**	0.2	**12.9**	0.4	**12.8**	0.4	g/dl
HCT	**38.1**	0.7	**39.6**	0.7	**40.7**	1.3	%
MCV	**64.6**	1.1	**64.8**	0.7	**66.0**	1.8	fl
MCH	**20.8**	0.3	**21.1**	0.5	**20.7**	0.4	pg
MCHC	**32.3**	0.7	**32.6**	0.8	**31.4**	0.3	g/dl
RDW	**13.7**	0.3	**15.1**	0.5	**15.3**	0.3	%
WBC	**3.8**	0.4	**5.0**	0.5	**4.8**	0.4	$x10^{9}/l$
Neutrophils	**0.8**	0.1	**2.8**	0.4	**1.5**	0.0	$x10^{9}/l$
Lymphocytes	**2.2**	0.5	**1.7**	0.1	**2.6**	0.3	$x10^{9}/l$
Monocytes	**0.1**	0.0	**0.1**	0.0	**0.1**	0.1	$x10^{9}/l$
Eosinophils	**0.2**	0.0	**0.1**	0.0	**0.1**	0.1	$x10^{9}/l$
Basophils	**0.5**	0.1	**0.3**	0.1	**0.4**	0.1	$x10^{9}/l$

Table 4.2. Haematological profile during AVF maturation. *Blood samples were taken immediately before surgery, after recovery and then at the end of the maturation period. The following parameters were abbreviated; red blood cell count (RBC), haemoglobin (Hb), haematocrit (HCT), mean corpuscular volume (MCV), mean corpuscular haemoglobin (MCH), mean corpuscular haemoglobin concentration (MCHC), red cell distribution width (RDW), white blood cell count (WBC). Results are shown as the mean ±S.E.M., n=4.*

4.3.2 Monitoring of AVF remodelling during injury and diclofenac intervention

In the second phase of the study, the animals were split into a control group, a group that received cannulation injury and a group that received the same cannulation injury along with diclofenac treatment. The effect of these variables on blood flow was measured by ultrasound (Fig. 4.4). Venous blood velocity appeared to peak at approximately 80cm/s in the diclofenac group at day 45. This did not occur in the other groups until around day 55 (Fig. 4.4.A). Increases in vessel lumen diameter appeared more obvious at earlier stages following AVF surgery in animals receiving cannulation injury, irrespective of diclofenac treatment. Taken together, blood flow appeared to increase earlier in the diclofenac treated group (Fig. 4.4.C). However, none of these trends were statistically significant.

Again, biochemical and haematological parameters were measured during this experimental phase at day 28, and then at day 56 for each group. There were no statistically significant changes in biochemical or haematological parameters between any of the groups.

A

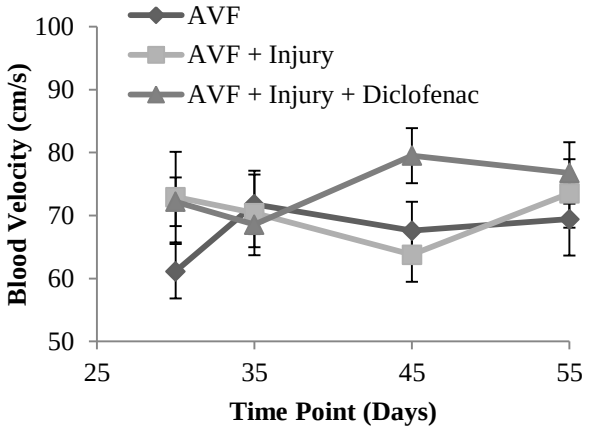

B

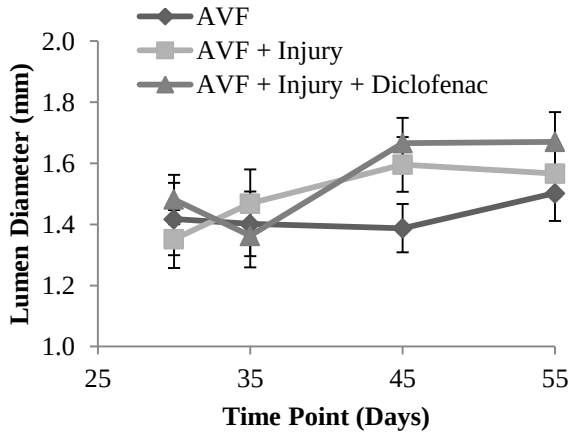

C

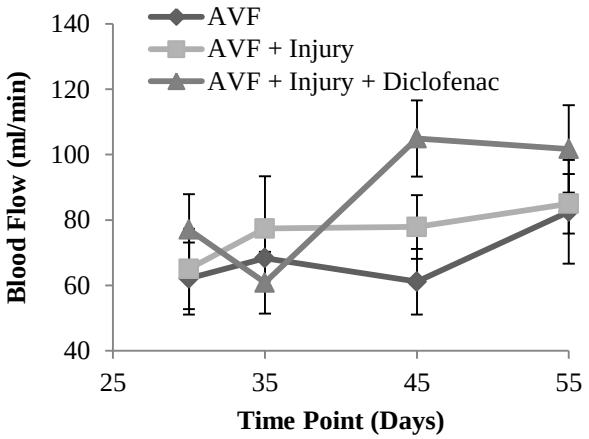

Figure 4.4. The effect of cannulation injury and topical diclofenac intervention on venous AVF diameter and blood flow. ***A)*** *Changes in blood velocity during injury and intervention.* ***B)*** *Changes in venous lumen diameter during injury and intervention.* ***C)*** *Changes in venous blood flow during injury and intervention. All results are shown as the mean ±S.E.M., n=7, 6 and 6 for AVF, AVF + Injury and AVF + Injury + Diclofenac respectively.*

Biochemical Profile	Day 28		Day 56						Units
			Non-Injured		Injured		Injured + Diclofenac		
	Mean	S.E.M.	Mean	S.E.M.	Mean	S.E.M.	Mean	S.E.M.	
Sodium	**145.9**	0.8	**146.1**	1.3	**145.9**	0.9	**144.5**	1.2	mmol/l
Potassium	**4.8**	0.9	**6.4**	2.9	**4.3**	0.8	**4.8**	0.8	mmol/l
Sodium: Potassium Ratio	**33.5**	5.5	**33.5**	7.9	**36.8**	4.9	**32.0**	4.2	mmol/l
Chloride	**93.4**	0.5	**96.9**	1.9	**97.0**	0.7	**100.1**	2.5	mmol/l
Calcium	**3.5**	0.1	**3.5**	0.0	**3.4**	0.1	**3.4**	0.0	mmol/l
Phosphate	**4.3**	1.2	**3.6**	2.0	**3.6**	1.2	**3.2**	1.4	mmol/l
Urea	**7.3**	0.3	**8.1**	1.3	**6.8**	0.4	**9.3**	1.2	mmol/l
Creatinine	**100.0**	7.5	**99.0**	13.6	**98.8**	5.4	**114.0**	7.3	mmol/l
Cholesterol	**0.9**	0.2	**0.8**	0.2	**0.8**	0.2	**0.9**	0.3	µmol/l
Triglyceride	**0.8**	0.1	**1.0**	0.2	**0.8**	0.1	**0.8**	0.1	mmol/l
Total Bilirubin	**0.5**	0.3	**1.3**	1.3	**0.3**	0.3	**1.3**	0.8	mmol/l
ALKPhos	**324.8**	24.0	**280.3**	29.7	**243.5**	39.0	**173.8**	21.1	µmol/l
AST	**51.5**	11.0	**44.5**	7.2	**58.3**	9.8	**43.0**	8.6	U/l
ALT	**46.8**	7.0	**47.8**	6.0	**52.0**	5.3	**44.3**	12.6	U/l
GGT	**5.8**	1.0	**8.3**	1.9	**4.5**	0.5	**2.7**	0.3	U/l
Total Protein	**58.5**	0.3	**58.8**	0.9	**57.3**	1.3	**49.3**	5.6	g/l
Albumin	**42.0**	1.0	**41.8**	0.3	**41.0**	0.9	**37.7**	1.7	g/l
Globulin	**16.5**	0.9	**17.0**	0.7	**16.3**	1.8	**17.0**	0.6	g/l
Albumin: Globulin Ratio	**2.6**	0.2	**2.5**	0.1	**2.7**	0.4	**2.2**	0.1	g/l

Table 4.3. Blood biochemistry following cannulation injury and diclofenac intervention. *Blood samples were collected at the beginning of the experimental period, and at the end for each group. Results are shown as the mean ±S.E.M., n=4.*

Haematology Profile	Day 28		Day 56						Units
			Non-Injured		Injured		Injured + Diclofenac		
	Mean	S.E.M.	Mean	S.E.M.	Mean	S.E.M.	Mean	S.E.M.	
RBC	**6.2**	0.2	**6.3**	0.2	**5.7**	0.2	**5.4**	0.1	$x10^{12}/l$
Hb	**12.8**	0.4	**13.5**	0.4	**12.2**	0.1	**11.7**	0.2	g/dl
HCT	**40.7**	1.3	**41.5**	0.7	**38.3**	1.1	**35.8**	0.7	%
MCV	**66.0**	1.8	**66.4**	2.3	**67.5**	1.5	**67.0**	2.3	fl
MCH	**20.7**	0.4	**21.5**	0.5	**21.5**	0.5	**21.9**	0.2	pg
MCHC	**31.4**	0.3	**32.4**	0.7	**31.9**	0.7	**32.7**	0.7	g/dl
RDW	**15.3**	0.3	**13.5**	0.3	**13.6**	0.2	**14.1**	0.2	%
WBC	**4.8**	0.4	**5.3**	0.4	**5.0**	1.0	**4.0**	0.5	$x10^{9}/l$
Neutrophils	**1.5**	0.0	**1.3**	0.4	**1.4**	0.4	**1.3**	0.2	$x10^{9}/l$
Lymphocytes	**2.6**	0.3	**3.3**	0.5	**3.0**	0.5	**2.3**	0.3	$x10^{9}/l$
Monocytes	**0.1**	0.1	**0.1**	0.0	**0.1**	0.0	**0.1**	0.0	$x10^{9}/l$
Eosinophils	**0.1**	0.1	**0.2**	0.1	**0.1**	0.0	**0.1**	0.0	$x10^{9}/l$
Basophils	**0.4**	0.1	**0.4**	0.1	**0.4**	0.1	**0.3**	0.1	$x10^{9}/l$

Table 4.4. Blood haematology following cannulation injury and diclofenac intervention. *Blood samples were collected at the beginning of the experimental period, and at the end for each group. Results are shown as the mean ±S.E.M., n=4.*

4.3.3 AVF induced vascular remodelling in the artery and at the anastomosis

At the end of the study, vessels were perfusion fixed *in situ*, wax processed and stained using H&E. Fig. 4.5 shows an example of the remodelling which took place at the anastomosis site. Within 5mm of the anastomosis, both vessels were patent and had undergone vascular remodelling (Fig. 4.5.A). Fig. 4.5.B shows healthy integration of the artery and vein at the anastomosis, with both vessels appearing to have intact endothelial barriers. Also, in this image suture material is visible on the outside of the vessels. Great care was taken during surgery to avoid loose suture being trapped within the anastomosis, which as indicated in this image was successful.

The focus of this study is remodelling within the venous branch of the AVF. However, a degree of arterial neointima was also present within the feeding artery. As shown in Fig. 4.6, arterial neointima was present within millimetres of the AVF, along with some degradation of the original media layer (Fig. 4.6.B). This remodelling was not present 1cm proximal to the anastomosis (Fig. 4.6.A).

A

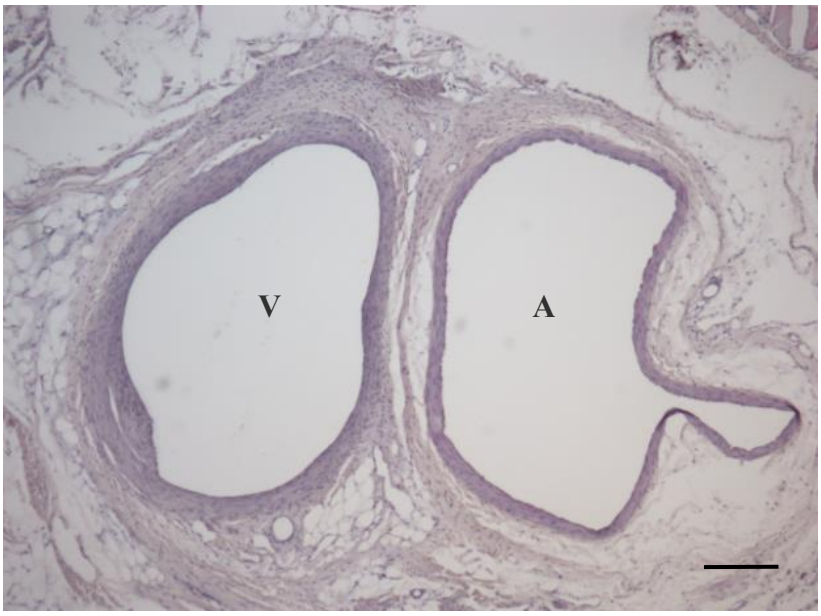

B

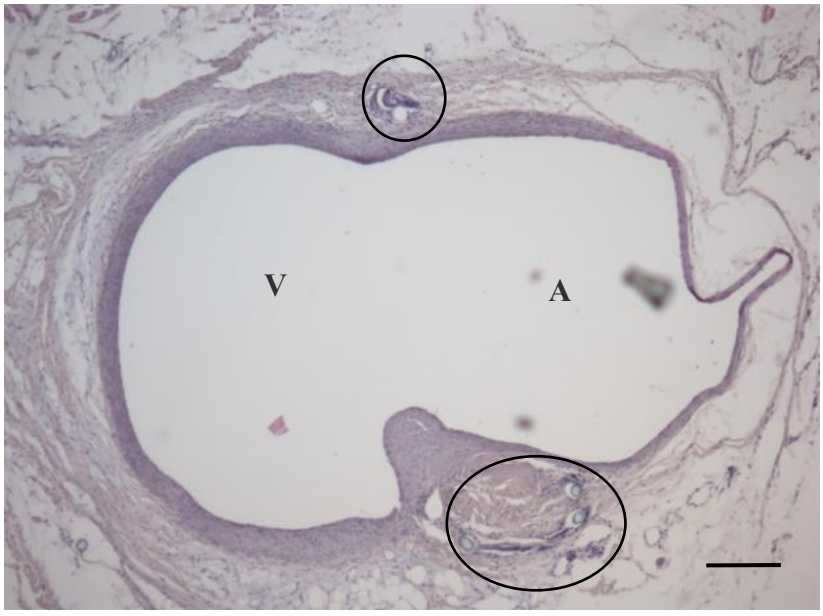

Figure 4.5. Integration of artery and vein at anastomosis. ***A)*** *Shows an example image of the femoral artery (A) and vein (V) of the AVF, approximately 5mm proximal to the anastomosis.* ***B)*** *Shows an example of arterial-venous integration at the anastomosis site. Suture material is circled. All scale bars=200µm.*

A

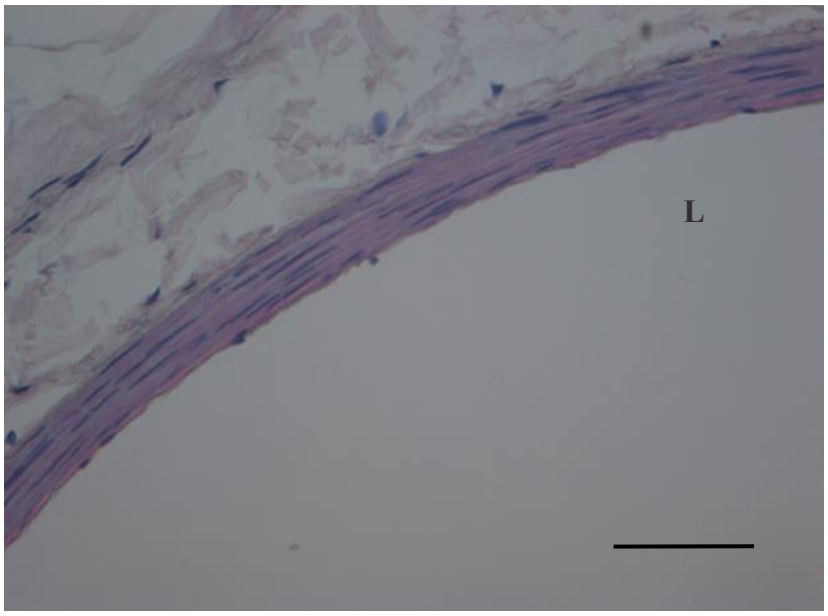

B

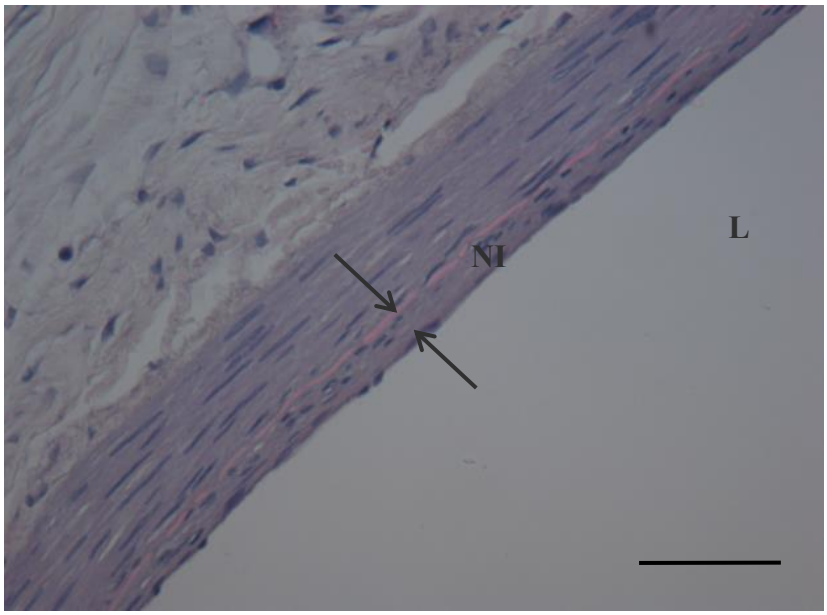

Figure 4.6. Arterial remodelling within the AVF. ***A)*** *Shows an example of the feeding femoral artery approximately 1cm proximal to the anastomosis.* ***B)*** *Shows an example of the same artery, but within 3mm of the anastomosis. The original internal elastic lamina is highlighted between two arrows, L=lumen, NI=neointima All scale bars=50µm.*

4.3.4 Cannulation induced venous remodelling and intervention by diclofenac

The effect of AVF creation, cannulation injury and diclofenac intervention on vascular remodelling within the venous branch of the AVF was assessed by quantifying vein wall width (Fig. 4.7). The creation of an AVF resulted in a significant increase in mean vein wall width from 10.5±0.9μm to16.6±1.6μm (Fig. 4.7.B and 4.7.E). With cannulation injury three times a week, there was a significant 2.8 fold increase in vein wall thickness vs. non-injured AVF (Fig. 4.7.C and E). This remodelling consisted of an increased cellular component, as well as degradation of the original vein wall at the adventitial side of the vessel. Daily topical diclofenac treatment caused a significant 3 fold decrease in vein wall thickness.

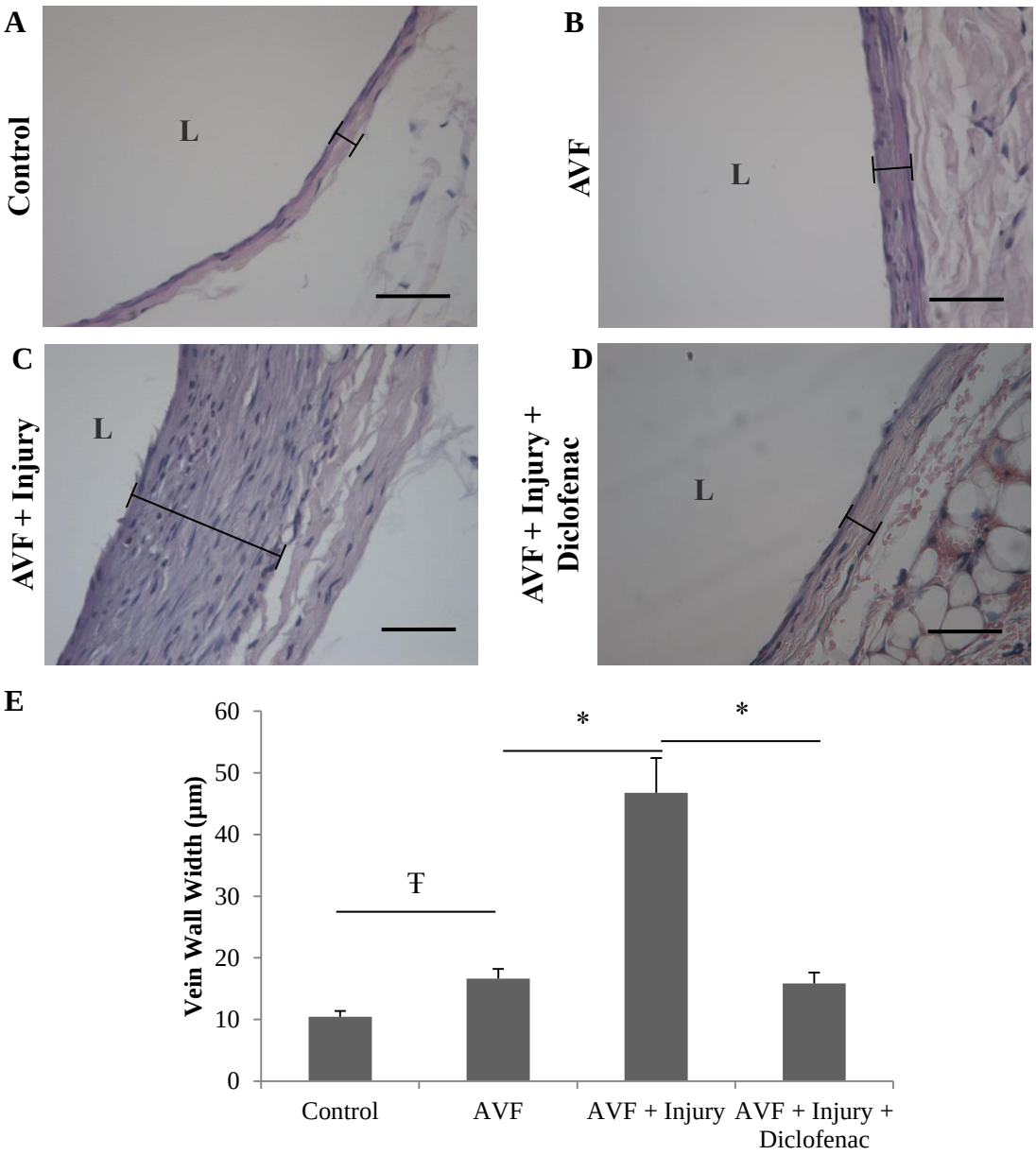

Figure 4.7. Venous remodelling of AVF following injury with/without diclofenac intervention. *Venous architecture was visualised by H&E staining in;* ***A)*** *control unoperated femoral vein,* ***B)*** *AVF,* ***C)*** *AVF with cannulation injury and* ***D)*** *injured AVF with diclofenac. Scale bars=50µm, L=lumen.* ***E)*** *Remodelling was quantified by measuring vein wall width for each group (indicated in the examples). Results are shown as the mean ±S.E.M., n=7, 7, 6 & 6 for control, AVF, AVF + Injury and AVF + Injury + Diclofenac respectively. Ŧ= p<0.05 unpaired t-test for unoperated control vs. AVF, *= p<0.05 one way ANOVA with post hoc bonferroni's correction for AVF vs. AVF + Injury & AVF + Injury vs. AVF + Injury + Diclofenac.*

4.3.5 AMPK expression during diclofenac intervention

The expression of AMPK during fistula injury and diclofenac treatment was assessed by immunohistochemistry (Fig. 4.8). An amplification step was needed to detect AMPK by DAB. This resulted in some staining within the negative controls (same tissue and protocol, minus the primary antibody). Therefore for each section used, counterpart negative controls were also quantified and subtracted from the percentage staining in the experimental tissues. AMPK was expressed in both endothelial and VSM cells (Fig. 4.8.A). There was no change in AMPK expression following creation of an AVF (Fig. 4.8.B and E). However cannulation injury of the vein appears to be associated with a decrease in expression, although this was not statistically significant (Fig. 4.8.C and E). In the animals which received injury + diclofenac treatment, percentage AMPK staining significantly increased from 3.3±1.0 in the injury only animals to 19.5±4.2 (Fig. 4.8.D and E).

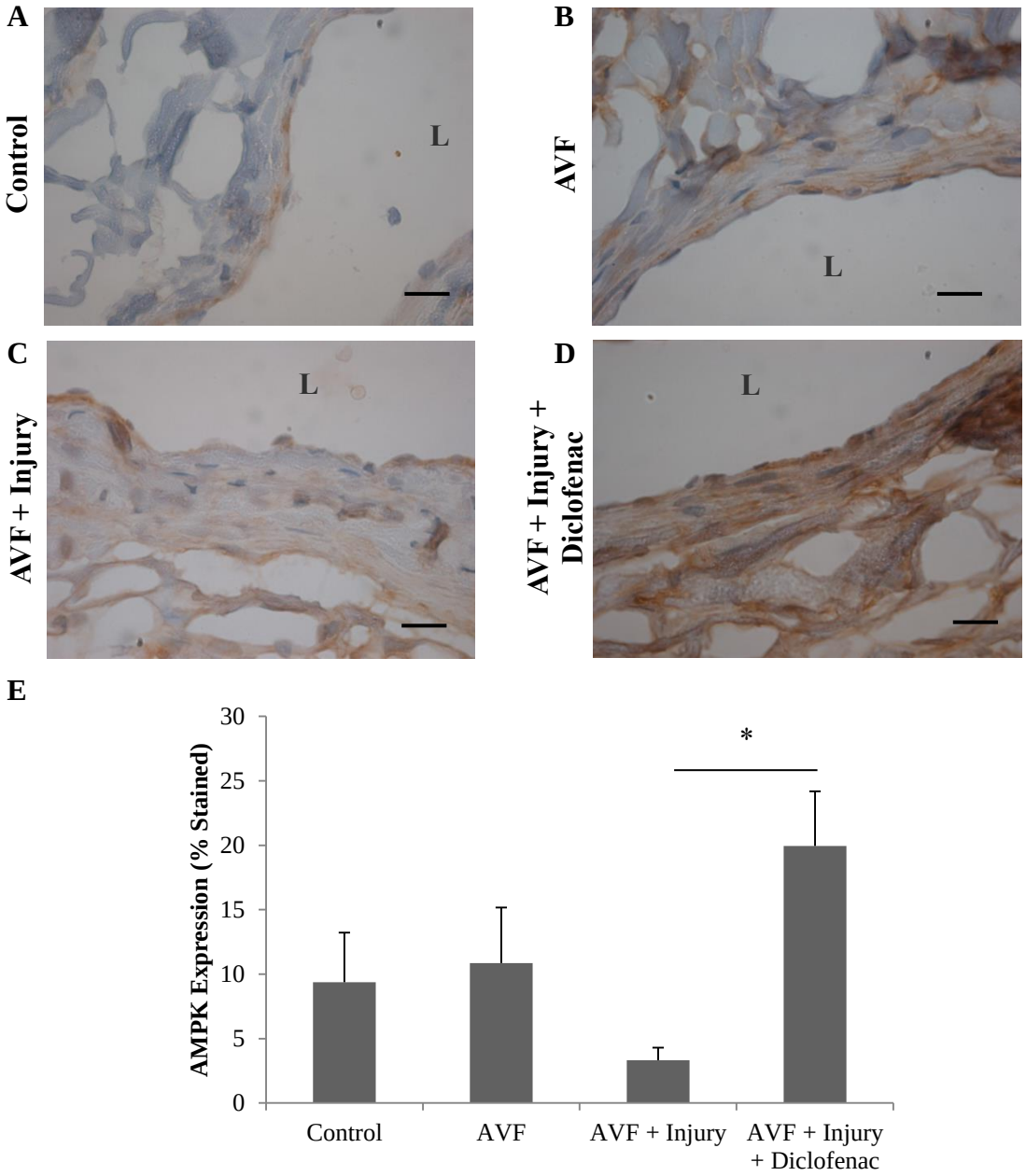

Figure 4.8. AMPK expression in AVF following injury with/without diclofenac intervention. *Immunohistochemistry was used to visualise AMPK in;* ***A)*** *control unoperated femoral vein,* ***B)*** *AVF,* ***C)*** *AVF with cannulation injury and* ***D)*** *injured AVF with diclofenac. Scale bars=10µm, L=lumen.* ***E)*** *AMPK expression was quantified in each group. Results are shown as the mean ±S.E.M., n=4, 5, 6 & 5 for control, AVF, AVF + Injury and AVF + Injury + Diclofenac respectively. *= p<0.05 one way ANOVA with post hoc bonferroni's correction for AVF + Injury vs. AVF + Injury + Diclofenac.*

4.4 Discussion

4.4.1 Rabbit femoral AVF maturation

A number of ultrasound techniques were used in this study to monitor maturation of the AVF. Following creation of the femoral AVF, vessels remained patent and flow was detected moving directly from the artery into the vein using colour Doppler ultrasound. In the cross sectional image taken using B-mode in Fig. 4.2.B, the vein is positioned on top of the artery proximal to the anastomosis. This is the same position that was present in the neurovascular bundle prior to AVF creation, which can be seen in the contralateral control vessels in Fig. 4.2.A Therefore, it appears the surgical technique did not result in vessel torsion, a factor which has been implicated in failure of AVF (Konner 2003).

Using Pulsed Wave Doppler, the presence of a pulsatile flow in the vein was demonstrated. As veins act as pressure reservoirs, their blood velocity tends to be low with a flat waveform. In this study we were unable to reliably measure venous blood velocity in unoperated control vessels due to the vessels proximity to the artery. However, measurement of femoral vein blood velocity is possible and has been successfully measured previously (Qian *et al.*, 2010). In this study the velocity of blood within rabbit femoral veins (also White New Zealand) was 6.5cm/s with a flat waveform. Therefore, a venous blood velocity of 52cm/s which was achieved 10 days post AVF creation in this study indicates a substantial increase compared to normal levels if compared to the Qian study (Fig. 4.3.C). Along with velocity, venous lumen diameter and blood flow increased over the maturation period (Fig. 4.3.C-E). Clinically, an AVF is said to have matured if there has been an increase in venous diameter and blood flow, preferably to >4mm and >500ml/min (Robbin *et al.*, 2002). This response occurs due to outward hypertrophic remodelling which the vein undergoes in order to compensate for the increase in wall and shear stress exerted by the arterial flow (Hayashi & Naiki 2009; Asif *et al.*, 2006). Therefore, the significant increase of venous blood flow seen in this study over the first four weeks indicates the likelihood that outward hypertrophic remodelling has taken place and the fistula has undergone maturation.

Blood parameters were also analysed during the first four weeks of the study. The only statistical differences in the blood biochemistry profiles between pre-surgery and post-surgery were in potassium, ALKPhos and creatinine levels (Table 4.1). The small changes in potassium and ALKPhos due to the surgical procedure are unlikely to be clinically significant. The transient increase in creatinine post-surgery could be due to the anaesthesia and/or a small degree of dehydration. At the end of the maturation period, creatinine levels had resolved. There were no changes seen in the haematological profiles (Table 4.2). This is reassuring as it implies that creation and maturation of a femoral AVF did not affect the overall health of the animal.

4.4.2 The effect of cannulation injury and diclofenac on blood parameters

The ultrasonography results of blood flow during the second phase of this study did not reveal any significant differences and were therefore inconclusive. However, both injury groups appeared to show an earlier change (increase) in venous lumen diameter vs. the non-injured group (Fig. 4.4.B). In humans, it is known that repeated cannulation of a specific area in the AVF leads to dilatation of the lumen (Hsiao *et al.*, 2010; Krönung, 1984). Therefore it is likely that the injury associated increase in venous diameter seen in this model is also due to tissue displacement and remodelling.

Blood parameters were again investigated in the second phase of the study. There were no statistically significant differences in these parameters; implying that cannulation injury to the AVF and diclofenac administration did not affect the overall health of the animal. The lack of significant blood parameter changes in animals which received diclofenac is particularly important as this family of drugs are potentially nephrotoxic (Brater, 2002). In addition to these markers, MCP-1 measurement was also attempted in this study. MCP-1 is a pro-inflammatory chemokine increased in haemodialysis patients and has been associated with stenosis in a murine AVF model (Lobo, *et al.* 2013; Juncos, *et al.* 2011). Due to a lack of commercially available rabbit MCP-1 ELISA/antibodies, a human MCP-1 ELISA kit

(Cat. No. 438804, Biolegend, UK) was used. Human and rabbit MCP-1 share 70% homology; however this kit could not detect rabbit MCP-1.

4.4.3 AVF driven remodelling and the effect of cannulation with/without diclofenac

Previous studies using rabbit AVF models have focussed on the remodelling which takes place within the feeding artery (Greenhill and Stehbens, 1987; Jones and Stehbens, 1995). In these studies it was found that tears formed in the proximal artery, with neointima formed close to the anastomosis site. A similar pattern of remodelling within the feeding artery was found in this study. However, the main aim of the model in the current study was to assess the remodelling which occurs in the vein. Creation of an AVF resulted in a significant increase in vein wall thickness. This change was subtle and displayed no signs of endothelial damage. Therefore this remodelling appears to be healthy, beneficial remodelling associated with maturation of the AVF. This kind of remodelling is stimulated by the adaptation of the vein to changes in haemodynamic forces, rather than a pathological event.

In this study, for the first time we present evidence which suggests that cannulation injury is a central event in adverse AVF remodelling. Previous evidence for the role of cannulation injury in AVF stenosis has been based on limited clinical findings and studies which have analysed the effect of injury on other types of vein graft (Nielsen *et al.*, 2001). In our study, needle puncture in a frequency similar to that which is undergone in dialysis caused a 2.8 fold increase in the amount of remodelling which occurs (Fig. 4.7). Therefore, future treatment strategies which aim to increase the patency of AVF should target cannulation injury. Using this newly developed translational model, an intervention study was conducted using topical diclofenac. The aim was to give this anti-inflammatory and anti-proliferative agent prophylactically after vessel maturation. It was anticipated that this would target injury driven vessel remodelling. As is evident in Fig. 4.7, twice daily topical delivery of diclofenac significantly reduced vein wall thickness induced by cannulation. The resulting level of vein wall thickness was comparable to that of the

non-injured AVF. Therefore, prophylactic diclofenac inhibits cannulation driven adverse remodelling. This suggests diclofenac has the ability to target only injury driven inflammatory and proliferative mechanisms, without affecting hemodynamically induced maturation. The main advantages of this type of therapy are that high concentrations of the drug can be achieved locally, while avoiding possible adverse side effects. Also, topical treatment can be introduced following the initial maturation phase; unlike perivascular therapies which are usually delivered at fistula creation (Melhem *et al.*, 2006).

Patients undergoing dialysis are known to have systemically increased levels of pro-inflammatory proteins due to a number of factors including activation of immune cells in the dialysis circuit (Papayianni *et al.*, 2002). However, the AVF itself can be a major inducer of inflammatory proteins which can then enter the systemic circulation. This highlights the importance of targeting the AVF locally with an agent such as diclofenac. In a study conducted on 26 patients with AVF, blood samples from the AVF and contralateral vein were taken and measurements of high sensitivity CRP (hs-CRP) levels performed (Milburn *et al.*, 2012). Blood sampled at the AVF had double the concentration of hs-CRP vs. blood from the contralateral vein. This suggests that the AVF is a major source of inflammatory proteins which can affect systemic circulation.

Diclofenac was selected for use in this present study as it has been clinically well defined, has potent anti-inflammatory activity, anti-proliferative activity and is available as a topical preparation (diclofenac diethylammonium). However, these properties are shared by other members of the NSAID family such as indomethacin which has a similar anti-proliferative IC_{50} as diclofenac (Piazza et al., 2010). Therefore the therapeutic potential of these other agents should also be studied. Also, higher preparations of topical diclofenac (up to 3%) are available for use in humans. This preparation was not selected for the current study as it is only approved for certain conditions. 3% diclofenac preparation is currently used to treat actinic keratosis, which is a proliferative skin condition that can lead to invasive squamous cell carcinoma (Nelson, 2013). However, the mechanism of action in

treating this condition is not clear (Martin and Stockfleth, 2013), but it is possible that these mechanisms are similar to the mechanism responsible for the diclofenac activity demonstrated in this chapter.

As discussed in chapter 1 (pages 33-35), many of the drugs which belong to the NSAID family have proven anti-proliferative activity (Brooks *et al.*, 2003). These activities have been shown to be mediated by p21 activation, which inhibits cyclin D1 and causes cell cycle arrest (Bock *et al.*, 2007). Aspirin is the most studied member of the NSAIDs, and it has been demonstrated that aspirin causes activation of AMPK, which then signals through the p53-p21 pathway to inhibit cell cycle progression (Sung and Choi, 2011). Therefore, it is possible that diclofenac may also exert its effects via activation of AMPK. Expression of AMPK in the different groups of this study was measured by immunohistochemistry (Fig. 4.8). AMPK expression in the injury + diclofenac group was shown to be significantly higher compared to injury only (Fig. 4.8). Thus, diclofenac-mediated inhibition of adverse AVF remodelling may be via AMPK activation in a manner similar to aspirin. AMPK expression appeared to decrease in the injured vs. non-injured group, however this was not statistically significant ($p=0.09$). As well as demonstrating that aspirin mediates AMPK activation, the study by Sung and Choi also demonstrated that hyper-proliferative VSM cells from spontaneously hypertensive rats had significantly lower AMPK expression. Since activation of AMPK results in inhibition of ATP consuming cell processes such as cell proliferation, a lower basal AMPK expression would allow a higher rate of proliferation, and therefore remodelling. However, further studies using the rabbit model are needed to support this hypothesis in AVF remodelling. A limitation in this experiment was the significant background signal within negative controls (without primary antibody), and that no isotype control was used.

The AVF model developed in this chapter was designed to be as clinically relevant as possible. This included the creation of an AVF using an anastomosis technique which is used clinically, instead of using a more straightforward approach such as arterial end to venous end/side (Castier *et al.*, 2006; Dong *et al.*, 2010). Ultrasonic

monitoring during the maturation period in this model also mimicked the clinical situation. However, it is the addition of regular cannulation injury to the AVF which makes this model translational and original. The main limitation of this study is that it does not take into account the effect of impaired kidney function, which results in increased systemic levels of uric acid (Shahbazian *et al.*, 2009). Clinically it has been shown that increased levels of uric acid in haemodialysis patients has a positive correlation with an increase in inflammatory markers IL-6 and TNF-α; which are known to contribute to vascular remodelling (Lobo *et al.*, 2013). This variable can be studied using subtotal nephrectomy, which has been carried out previously in a rat AVF model (Croatt *et al.*, 2010). In this study it was found that subtotal nephrectomy caused a significant increase in neointimal development in the venous branch of AVF. This procedure has also been carried out in rabbits, although not for the study of AVF (Eddy *et al.*, 2013). Therefore, subtotal nephrectomy could be used in future studies with the model presented in this chapter to further enhance its translational relevance.

4.5 Conclusion

Creation of a rabbit femoral-femoral AVF with ligation of the distal vein results in a patent fistula which has a good exchange of blood from the artery directly into the vein. Over the first four weeks this then stimulates a maturation response which results in an increased lumen diameter and blood flow, as well as an increase in vein wall thickness. Regular cannulation injury to the AVF results in a further significant increase in vein wall thickness, and therefore it is likely to play a major role in adverse AVF remodelling. Finally, in this model prophylactic topical diclofenac treatment causes inhibition of the injury driven response. This effect may be mediated by the activation of AMPK, which merits further investigation.

Chapter 5

The role of AMPK in the mechanisms underlying the anti-proliferative activity of diclofenac

5.1 Introduction

Diclofenac is a member of the NSAID family and has well established anti-inflammatory, anti-pyretic and analgesic actions. In 1971, J.R. Vane published a study which demonstrated that cyclooxygenase (COX) mediated inhibition of prostaglandin synthesis was responsible for the mechanism of aspirin and aspirin-like drugs (Vane, 1971). This discovery was awarded a Nobel Prize in 1982. Subsequently, two isoforms of COX were demonstrated, COX-1 and inducible COX-2 (Kujubu *et al.,* 1991). COX-1 is constitutively expressed in most tissues, whereas COX-2 is expressed at low levels under basal conditions (Kargman *et al.,* 1996). COX-2 is termed inducible as it is upregulated in response to inflammatory stimuli such as LPS (Macrophages *et al.,* 1994). Inhibition of COX-2 is responsible for many of NSAIDs therapeutic activities (Mitchell *et al.,* 1994).

A treatment strategy which targets both inflammation and proliferation in AVF stenosis would be advantageous. Potent inhibition of COX-2 by diclofenac would have an impact on the resulting inflammation. However, the anti-proliferative properties of diclofenac are likely to be independent of this activity. This is based on the significantly different concentrations of diclofenac required for each of these effects. The IC_{50} required for inhibition of COX-2 is 50nM (Brideau *et al.*, 1996), whereas the IC_{50} required for anti-proliferative activity is 170µM (Brooks *et al.,* 2003). Interestingly, the anti-proliferative effect of selective and non-selective COX inhibitors are equal in wild type and cyclooxygenase-null mouse embryo fibroblasts; indicating a COX independent mechanism (Zhang & Morham 1999). Therefore, it is unlikely that diclofenac mediates anti-proliferative activity via inhibition of COX. Instead, another potential target of diclofenac during inhibition of cell proliferation may be AMPK. AMPK is a highly conserved serine/threonine protein kinase which is involved in homoeostasis of cellular metabolism (Hardie and Carling, 1997). Activation of AMPK occurs when ATP levels are low, causing an increase in catabolic pathways and a reduction in ATP consuming activities including cell proliferation (Hardie *et al.*, 1998; Igata *et al.*, 2005). Acetyl-CoA carboxylase (ACC) is a downstream enzyme which is directly phosphorylated by AMPK to regulate the metabolism of fatty acids (Park *et al.*, 2002), and can therefore act as a

marker for AMPK activation. AMPK maybe a potential target of diclofenac as the anti-proliferative activity of aspirin is mediated by this kinase (Sung and Choi, 2011). Diclofenac has been shown to inhibit cell proliferation in a manner similar to aspirin, via up-regulation of p21 which causes cell cycle arrest (Brooks *et al.*, 2003). This involves the down regulation of the G1 associated kinase Cyclin D1. The expression of this cyclin is essential for cell cycle progression. It therefore seems possible that the anti-proliferative action of diclofenac may also be via AMPK. This is a novel hypothesis which to date has not been investigated.

The ability of topical diclofenac to inhibit injury driven adverse vascular remodelling *in vivo* has been demonstrated (Chapter 4, Section 4.3.4). However, mechanistic insight into the anti-proliferative activity of diclofenac is essential. The elucidation of this mechanism will provide further evidence to support the clinical use of topical diclofenac to increase AVF patency, as well as aiding the development of future treatment strategies. Therefore, the aims of this chapter are to:

1. Investigate the effect of diclofenac on early proliferative events (ERK & p38 phosphorylation) and during the later stages of cell proliferation (cell cycle regulation by p21, and expression of G1 associated cyclin D1)

2. Investigate the role of AMPK in the modulation of proliferation by diclofenac

5.2 Materials and methods

5.2.1 Stimulation of rabbit/mouse cell explants

VSM cells were quiesced for 24 hr in 0.1% (v/v) FCS, during which time they were incubated with or without; diclofenac (5µM- 170µM, lower concentrations rounded to the nearest unit of 2.5µM; Sigma-Aldrich, UK) for 24 hr, AMPK agonist A-769662 (30µM; Tocris, UK) for 1 hr or antagonist compound C (10µM; Tocris, UK) for 1 hr. Cells were then stimulated for 24 hr with 10% FCS and proliferation measured by ^{3}H-thymidine incorporation as described in section 2.4.3.

5.2.2 Western blotting of AMPK/proliferative proteins

Western blotting was carried out as described in section 2.4.4. VSM cells were treated as outlined in section 5.2.1. To measure AMPK protein expression cells were lysed before stimulation. For analysis of MAPK proteins, cells were stimulated with 10% FCS for 15 min and lysed. To assess cell cycle proteins, cells were stimulated with 10% FCS for 8 hr and lysed. The following primary antibodies were used:

- anti-phospho/Total AMPK rabbit IgG, 1/100 (Cell Signalling Tech., USA)
- anti-phospho/Total ACC rabbit IgG, 1/1000 (Cell Signalling Tech., USA)
- anti-phospho/Total ERK rabbit IgG, 1/1000 (Cell Signalling Tech., USA)
- anti-phospho/Total p38 rabbit IgG, 1/1000 (Cell Signalling Tech., USA)
- anti-Cyclin D1 rabbit IgG, 1/1000 (Santa Cruz Biotechnology Inc., USA)
- anti-p21 rabbit IgG, 1/1000 (Santa Cruz Biotechnology Inc., USA)
- anti-GAPDH mouse IgG, 1/40000 (Cell Signalling Tech., USA)

For detection of the primary antibody, a HRP-conjugated anti-rabbit IgG at 1/2000 dilution (Cell Signalling Tech., USA) or anti-mouse IgG at 1/10000 dilution (Stratech Scientific Ltd, UK) was used. For the detection of total proteins following analysis of phosphorylated, immunoblots were stripped using mild stripping buffer (25 mM glycine-HCl, pH 2, 1% (w/v) SDS) at room temperature for 1 hour.

5.2.3 Viability of cells following treatment using trypan blue

Treated VSM cells were removed from their wells using Tryple Express before being centrifuged at 200g and resuspended in 100µl of culture medium. The cells were then mixed 1:1 (v/v) with 0.4% trypan blue (Sigma-Aldrich, UK) and viability quantified using a haemocytometer. VSM cells with disrupted membranes appeared blue, while live cells resisted the dye. The percentage of live cells was calculated in an untreated control, and compared to cells which had been incubated with the test agents.

5.2.4 siRNA silencing of AMPKα1/2

To transfect one well, AMPKα1/2 siRNA (Santa Cruz Biotechnology Inc., USA) was diluted in 100µl of Opti-MEM (Gibco, UK) to make a final well concentration of 40pmol. The transfection solution was prepared by diluting 7.5µl/well of Lipofectamine RNAi Max transfection reagent (Life Technologies, UK) in 100µl of Opti-MEM. siRNA transfection solution was then prepared by mixing a 1:1 (V/V) ratio of AMPKα1/2 siRNA solution and Lipofectamine solution. Growth medium was removed from the VSM cells, and replaced with 1.8ml of Opti-MEM for 6 well plates and 450µl for 24 well plates. 200µl of siRNA transfection solution was then added to a well of a 6 well plate, and 50µl to a well of a 24 well plate. The following day, Opti-MEM was removed and replaced with regular growth medium and the cells were left for a further 48 hr before experimentation.

5.2.5 Culture and explantation of mouse aortic AMPKα1$^{-/-}$ VSM cells

Wild type and AMPKα1$^{-/-}$ aortas were obtained from 8 week old sv129 mice. VSM cells were then explanted and cultured from the vessels as described in Chapter 2, Section 2.4.1. Cell proliferation was measured by ^{3}H thymidine incorporation as described in section 2.4.3.

5.3 Results

5.3.1 The effect of diclofenac on rabbit VSM cell proliferative mechanisms

VSM cells were explanted from freshly isolated rabbit femoral vein. Characterisation was based on growth patterns, as well as expression of α-SMA. Fig. 5.1.A shows the growth pattern of a confluent patch of cells, which displays the characteristic hill and valley morphology associated with this type of cell. Fig. 5.1.B shows that all cells were positive for α-SMA To confirm that diclofenac mediated inhibition of VSM cell proliferation was not specific to human VSM cells, diclofenac [5μM-170μM] was assessed in rabbit VSM cells using ^{3}H thymidine incorporation proliferation assay. Fig. 5.2 shows a diclofenac mediated concentration dependent decrease in FCS stimulated VSM cell proliferation.

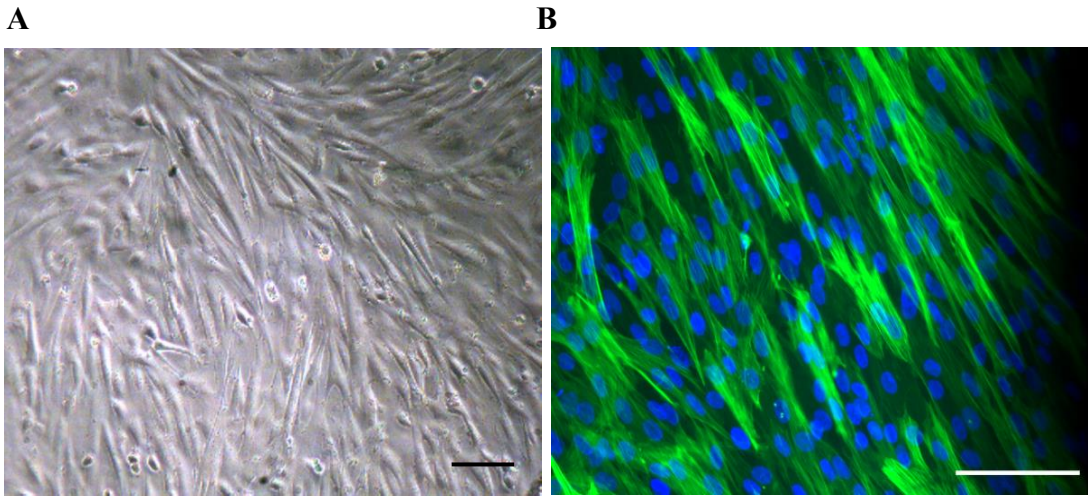

Figure 5.1. Rabbit vascular smooth muscle cell explant characterisation. ***A)*** *Growth morphology of VSM cell explants.* ***B)*** *Immunocytochemistry of cell explants for α-SMA expression visualised by immunofluorescence (Green), all scale bars= 50µm.*

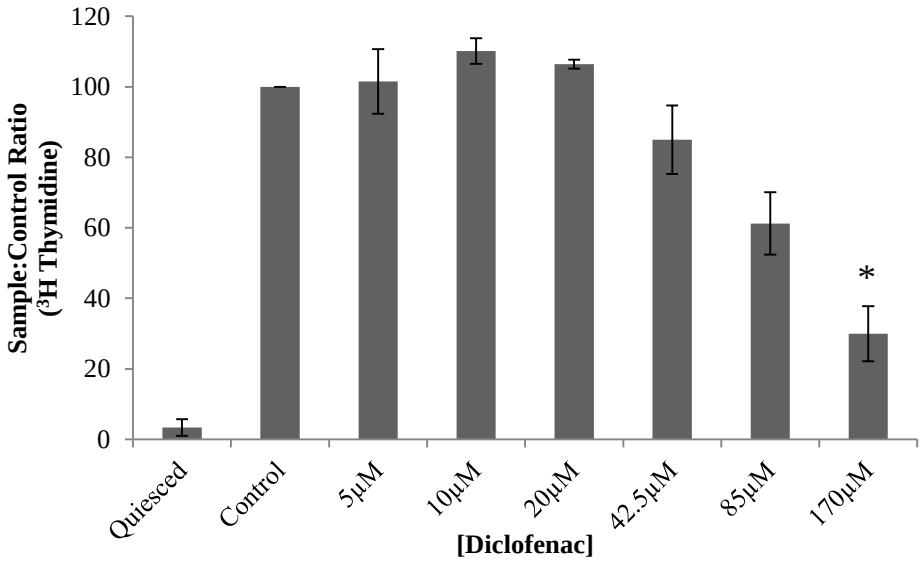

Figure 5.2. The anti-proliferative capacity of diclofenac on rabbit VSM cells. *Quiesced VSM cells were treated with diclofenac and stimulated for 24 hr with 10% FCS. Proliferation was measured by ^{3}H thymidine incorporation. Results are shown as the mean ±S.E.M., n=4, general linear ANOVA $p<0.05$, *=post-hoc Dunnett's vs. control $p<0.05$.*

To assess the effect of diclofenac on the activation of proliferation early in the response, activation of ERK was investigated (Fig 5.3). Under basal conditions phosphorylation of ERK was high, although the cells still had the capacity for further phosphorylation when stimulated by 10% FCS. Diclofenac pre-treatment had no effect on FCS stimulated ERK activation. Another MAPK pathway which is activated early in the proliferative response is p38, which was investigated in Fig. 5.4. Under basal conditions p38 was not expressed. Upon stimulation with 10% FCS there was an increase in both total and phosphorylated p38. Like ERK, p38 was unaffected by diclofenac pre-treatment. Therefore, cell cycle associated proteins p21 and cyclin D1 were investigated in treated cells to assess diclofenac's impact on events late in the proliferative response. The basal and stimulated expression of p21 was inconsistent between different sets of cells (Fig. 5.5). As a result, the diclofenac mediated response was also variable. Cyclin D1 showed a consistent increase in expression upon simulation with FCS; which was inhibited in a dose dependent manner by diclofenac (Fig. 5.6). At the maximum concentration assessed (170μM), cyclin D1 expression was significantly decreased by 60%.

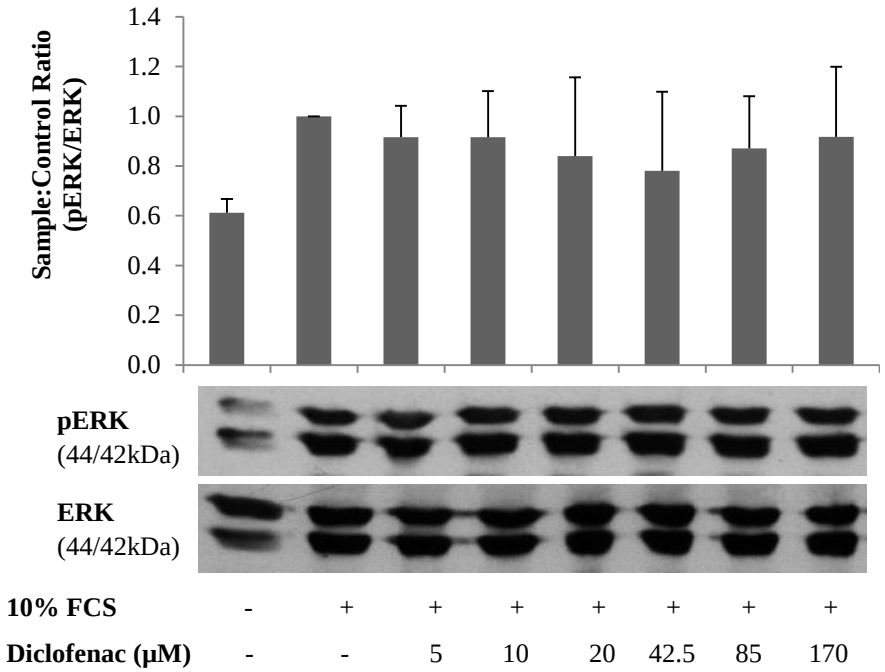

Figure 5.3. FCS stimulated ERK activation with diclofenac pre-treatment. *Quiesced VSM cells were treated with diclofenac and stimulated for 15 min with 10% FCS. Immunoblots were probed for pERK, stripped and reprobed for ERK. Results are shown as the mean ±S.E.M., n=3.*

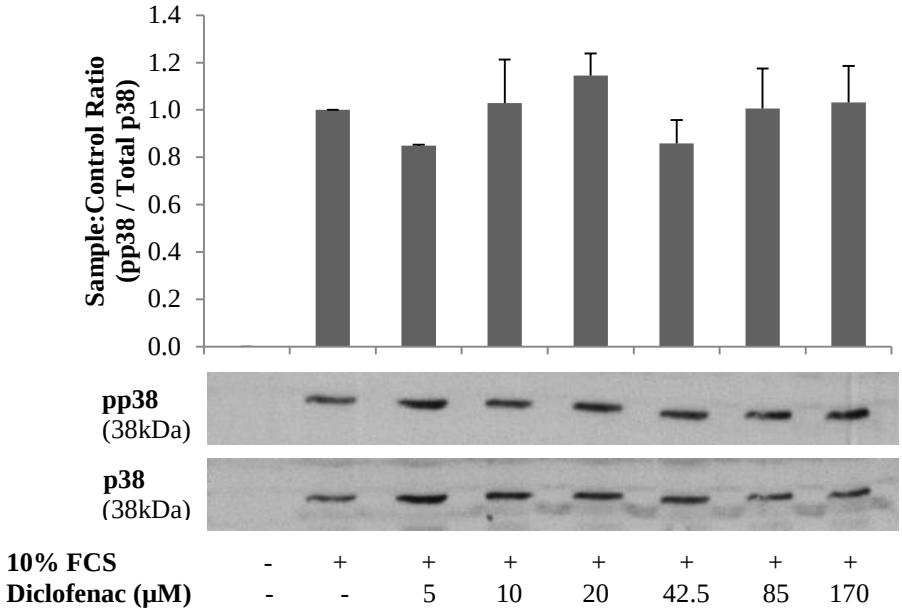

Figure 5.4. FCS stimulated p38 activation with diclofenac pre-treatment. *Quiesced VSM cells were treated with diclofenac and stimulated for 15 min with 10% FCS. Immunoblots were probed for pp38, stripped and reprobed for p38. Results are shown as the mean ±S.E.M., n=3.*

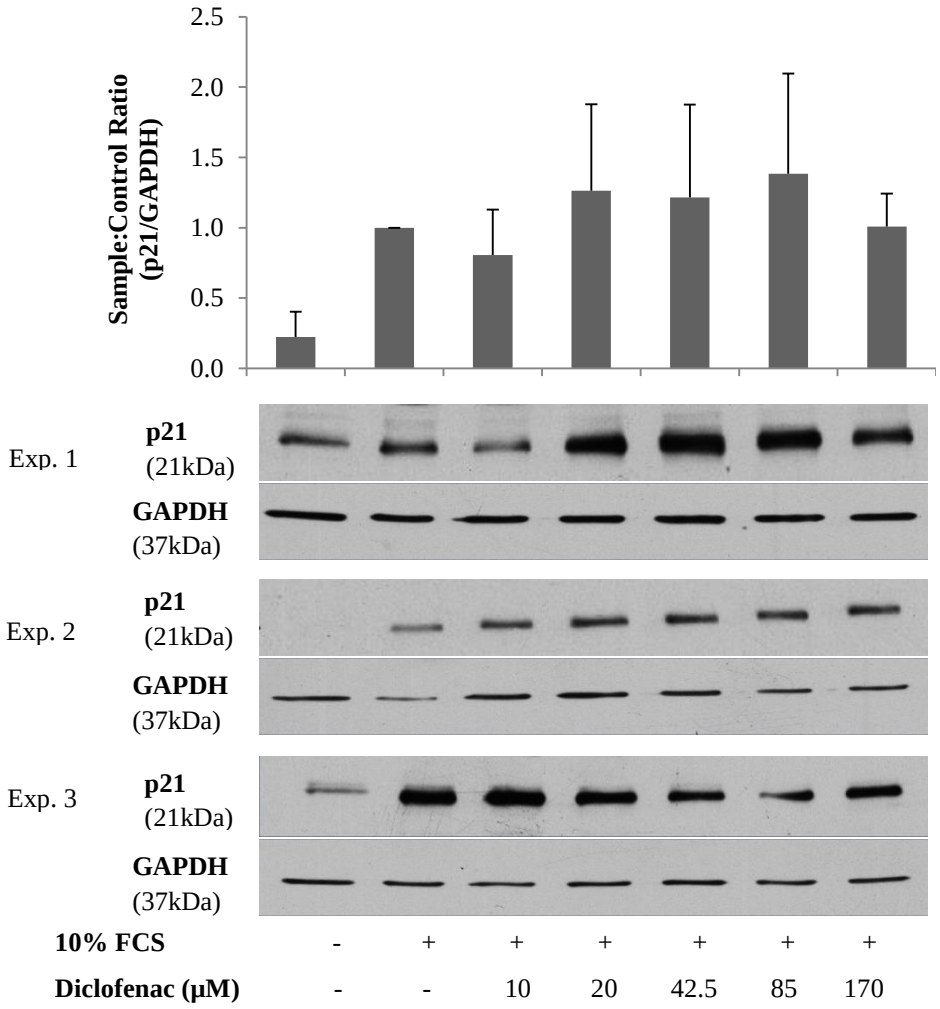

Figure 5.5. Diclofenac mediated change in FCS stimulated p21 expression. *Quiesced VSM cells were treated with diclofenac and stimulated for 8 hr with 10% FCS. Three different experiments for p21 expression in different sets of cells are shown. Results are shown as the mean ±S.E.M., n=3.*

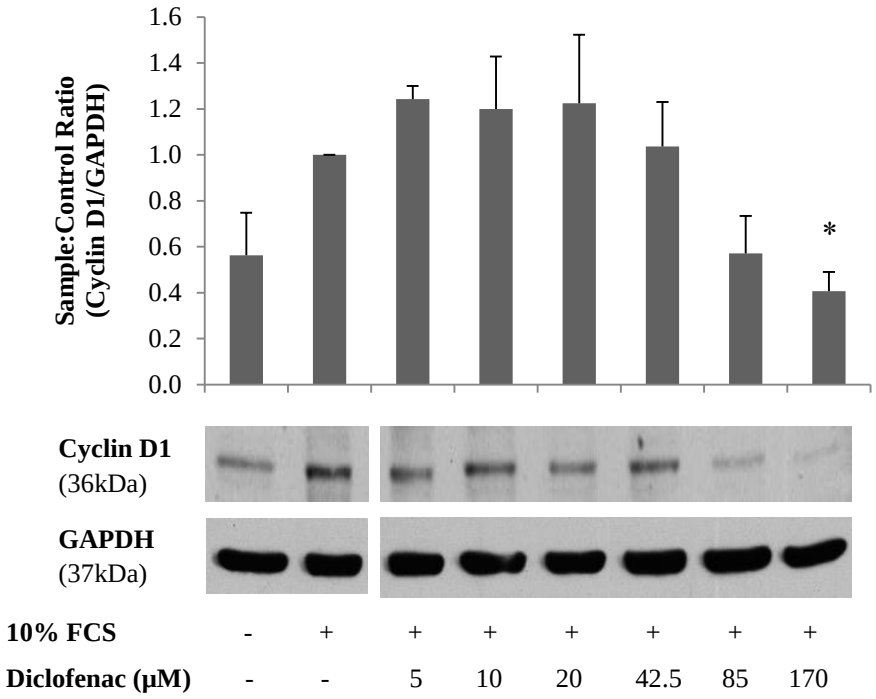

Figure 5.6. Diclofenac mediated reduction in FCS stimulated cyclin D1 expression. *Quiesced VSM cells were treated with diclofenac and stimulated for 8 hr with 10% FCS. Immunoblots were probed for cyclin D1, stripped and reprobed for GAPDH. Results are shown as the mean ±S.E.M., n=6, general linear ANOVA $p<0.05$, *=post-hoc Dunnett's vs. control $p<0.05$.*

5.3.2 Elucidating the role of AMPK in modulation of proliferation by diclofenac using pharmacological inhibition

The effect of diclofenac on AMPK phosphorylation, and activation of downstream ACC was assessed. The panel shown in Fig. 5.7.A shows example blots of VSM cells treated with diclofenac and measured for AMPK and ACC expression. The phosphorylated AMPK antibody detected one band, whereas the total AMPK antibody detected two; one for AMPKα1 and another for AMPKα2. Phosphorylation of AMPK was detected at basal conditions, and phosphorylation significantly increased with diclofenac treatment in a concentration dependent manner. At the maximal diclofenac concentration, AMPK phosphorylation increased by 12.8 fold vs. untreated controls (Fig. 5.7.B). In contrast, with an increasing concentration of diclofenac total AMPK expression appeared to decreased. Immunoblotting for ACC was performed to show progression through the AMPK pathway, examples of which are shown in the lower half of the panel in Fig. 5.7.A Both the phosphorylated and total antibodies detected two bands which represent ACCα and ACCβ. An even greater concentration dependent increase was seen in the phosphorylation of downstream ACC; which was increased by 23.8 fold vs. untreated controls at the maximum diclofenac concentration (Fig. 5.7.C).

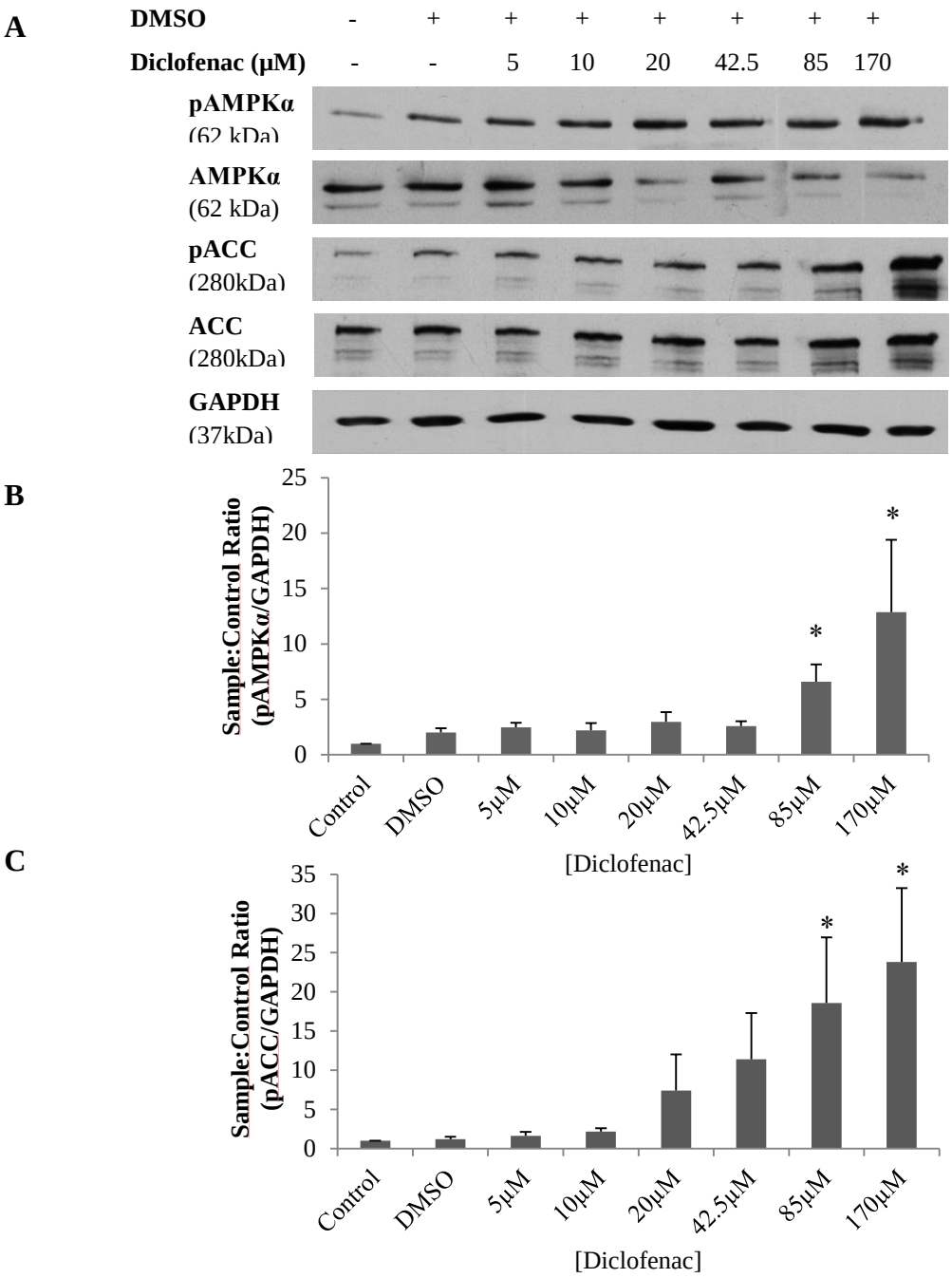

Figure 5.7. Diclofenac induced AMPK phosphorylation and ACC activation. *Quiesced VSM cells were treated for 24 hr with diclofenac.* ***A)*** *Example blots showing the activation (phosphorylation) of AMPK and ACC by diclofenac. Immunoblots were probed for either pAMPK or pACC, stripped and reprobed for AMPK or ACC respectively.* ***B)*** *Quantification of diclofenac induced AMPK phosphorylation.* ***C)*** *Quantification of diclofenac induced ACC phosphorylation. All results are shown as the mean ±S.E.M., n=6, general linear ANOVA $p<0.05$, *=post-hoc Dunnett's vs. control $p<0.05$.*

To confirm the role of AMPK in diclofenac activity, the pharmacological AMPK inhibitor compound C, as well as the activator A-769662, were used. Firstly, the effect of these agents on basal AMPK activation was measured (Fig. 5.8). Compound C treatment for 1 hr significantly reduced basal phosphorylation of AMPK (Fig. 5.8.A). Treatment with the agonist A-769662 appeared to cause a small increase in AMPK phosphorylation; however this was not statistically significant. The AMPK response to the vehicle (0.1% DMSO) was variable as two of the six cells used showed a decrease in phosphorylation. Compound C did not affect ACC phosphorylation as ACC has a low expression under basal conditions (Fig. 5.8.B). However A-769662 caused a significant 11.3 fold increase in ACC phosphorylation vs. untreated controls, indicating activation of AMPK.

Fig. 5.9 shows the effect of these agents on diclofenac mediated AMPK activation and progression. Compound C significantly reduced AMPK phosphorylation by 49% (Fig. 5.9.A). Downstream of this, diclofenac mediated phosphorylation of ACC was reduced by 60% with compound C treatment (Fig. 5.9.B). Unexpectedly, diclofenac in combination with A-769662 caused a statistically significant decrease in AMPK phosphorylation, but had no effect on ACC activation.

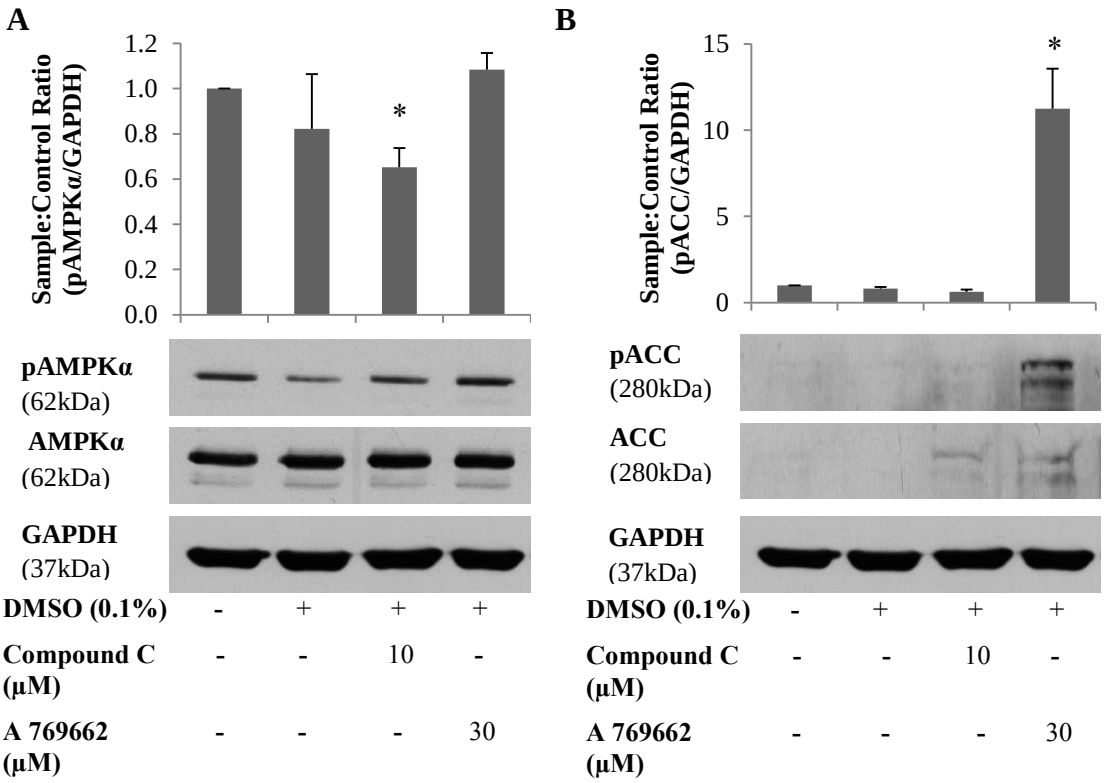

Figure 5.8. The effect of AMPK antagonist (compound C) and agonist (A-769662) on basal AMPK and ACC phosphorylation. *Quiesced VSM cells were treated with the agents for 1 hr. Immunoblots were probed for either pAMPK or pACC, stripped and reprobed for AMPK or ACC respectively.* ***A)*** *Quantification and an example immunoblot showing the effect of these agents on basal AMPK phosphorylation, n=6.* ***B)*** *Quantification and an example immunoblot showing the effect of these agents on basal ACC phosphorylation, n=4. All results are shown as the mean ±S.E.M., *=p<0.05 (paired T-test vs. untreated).*

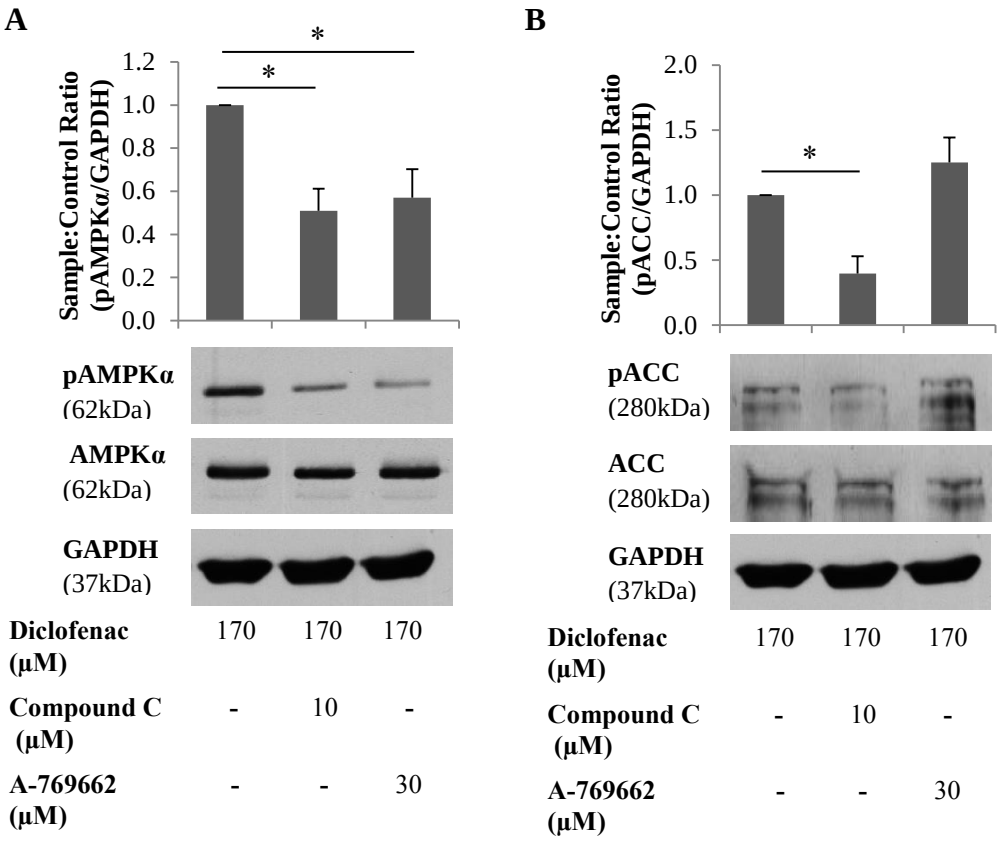

Figure 5.9. The effect of compound C and A-769662 on diclofenac induced AMPK and ACC phosphorylation. *Quiesced VSM cells were treated with diclofenac for 24 hr, and compound C/ A-769662 for 1 hr. Immunoblots were probed for either pAMPK or pACC, stripped and reprobed for AMPK or ACC respectively.* ***A)*** *Quantification and an example immunoblot showing the effect of these agents on diclofenac activated AMPK.* ***B)*** *Quantification and an example immunoblot showing the effect of these agents on diclofenac activated ACC. All results are shown as the mean ±S.E.M., n=4, *=p<0.05 (paired T-test).*

The effect of compound C and A-769662 on the anti-proliferative activity of diclofenac was assessed by ^{3}H thymidine incorporation (Fig. 5.10). It was expected that compound C would reverse some of the diclofenac mediated activity. Instead, contrary to the hypothesis, compound C in combination with diclofenac significantly reduced proliferation to a greater extent than diclofenac alone. This significant inhibition of proliferation also took place when the cells were treated with compound C alone. On its own, A-769662 had no inhibitory effect on cell proliferation, and had no effect on diclofenac's activity. The toxicity of the agents used in these experiments was assessed by the trypan blue. Fig. 5.11.A shows that none of these agents effected cell viability at their active concentrations. Fig. 5.11.B shows that compound C alone caused a significant reduction in FCS stimulated ERK phosphorylation, indicating non-selectivity.

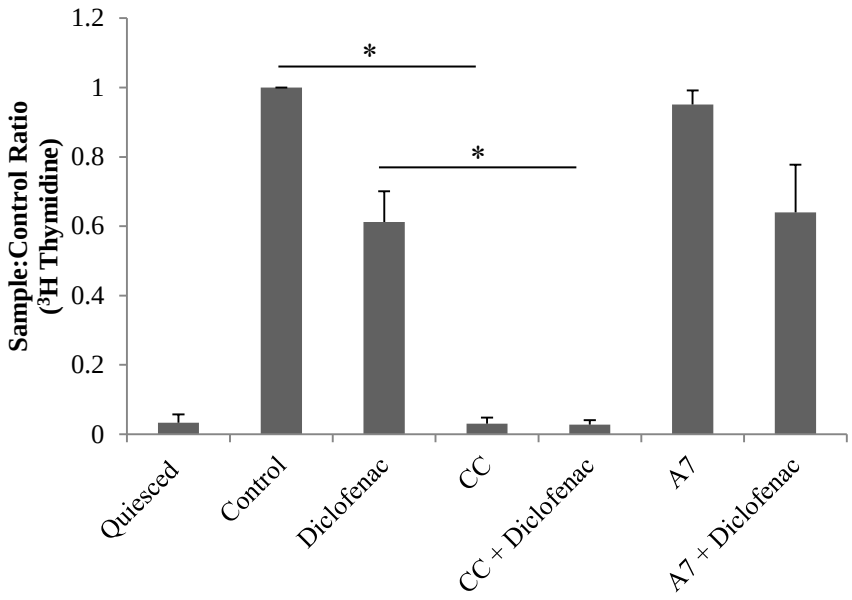

Figure 5.10. The effect of compound C and A-769662 on the anti-proliferative activity of diclofenac. *Quiesced VSM cells were treated with or without diclofenac (85µm) for 24 hr and/or compound C (CC, 10µm) / A-769662 (A7, 30µm) for 1 hr before being stimulated with 10% FCS. Proliferation was measured by ^{3}H thymidine incorporation. Results are shown as the mean ±S.E.M., n=4, *=p<0.05 (paired T-test).*

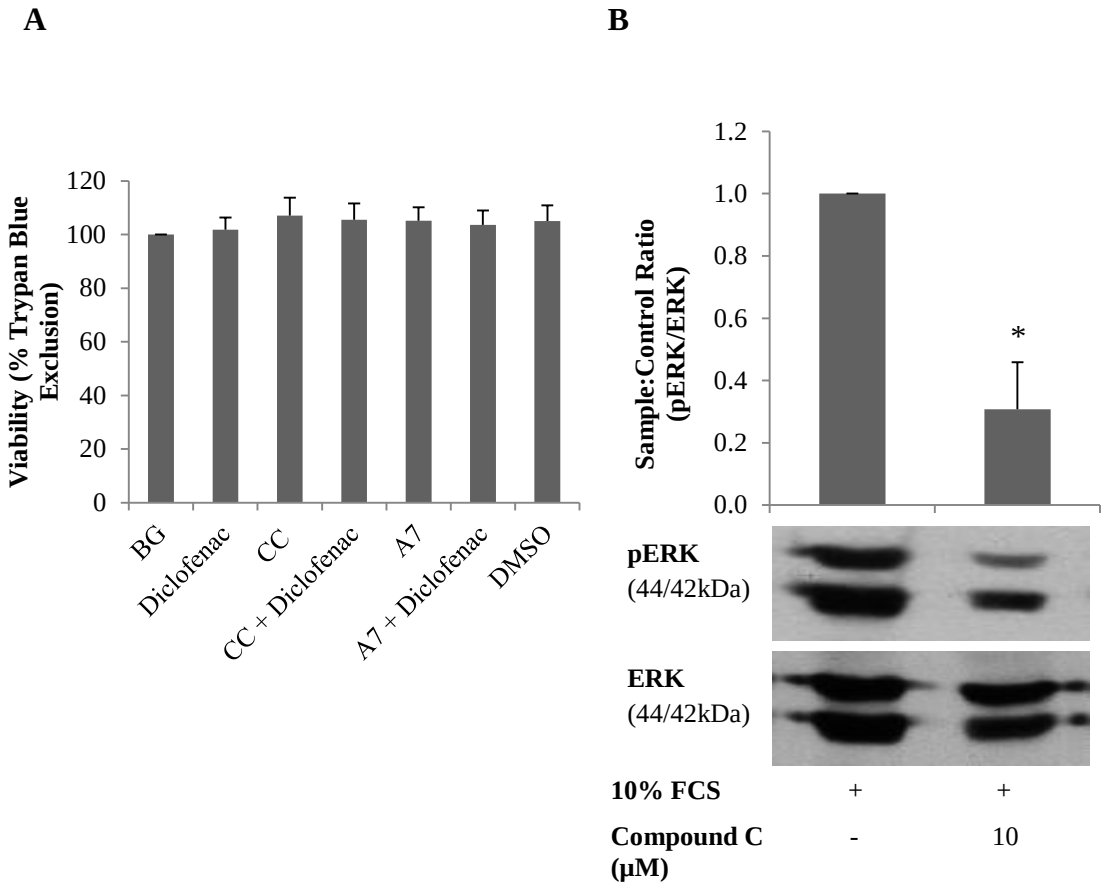

Figure 5.11. The AMPK independent activity of compound C. ***A)*** *Viability of VSM cells treated with or without diclofenac (175µm) for 48 hr and/or compound C (CC, 10µm) / A-769662 (A7, 30µm) for 25 hr, analysed by trypan blue, n=4.* ***B)*** *Quantification and an example immunoblot showing the effect of compound C (10µm, 1 hr) on ERK phosphorylation; n=3, *=p<0.05 (paired T-test). Immunoblots were probed for pERK, stripped and reprobed for ERK. All results are shown as the mean ±S.E.M.*

5.3.3 Elucidating the role of AMPK in modulation of proliferation by diclofenac using siRNA protein repression

The repression of AMPK α1/2 protein expression by siRNA was optimised under different conditions in Fig. 5.12. AMPK was significantly repressed 48 hr post transfection using 20, 40 and 80pmols siRNA (Fig. 5.12.A). At 72 hr post transfection, AMPK expression was reduced further again (Fig. 5.12.B). Using the maximum transfection time and siRNA concentration, AMPK expression was repressed by 95% (Fig. 5.12.C). However, scrambled control siRNA also reduced AMPK expression by 56%. Figure 5.13 shows the level of repression that was achieved in each set of cells used, as well as the effect on diclofenac activity. The level of AMPK repression that was achieved with 40pmol siRNA at 48 hr transfection was inconsistent. Shown in Fig. 5.13.A is an example from VSM cell 1 which had the highest repression at 97.8%, as well as VSM cell 3 which had the lowest repression at 38.9%. The mean level of AMPK repression was 68.4±9.6%, which reduced the mean diclofenac response to 91.3±11.1% compared to control siRNA. Again, the resulting diclofenac response was also inconsistent, with two sets of cells showing enhanced inhibitory activity.

A

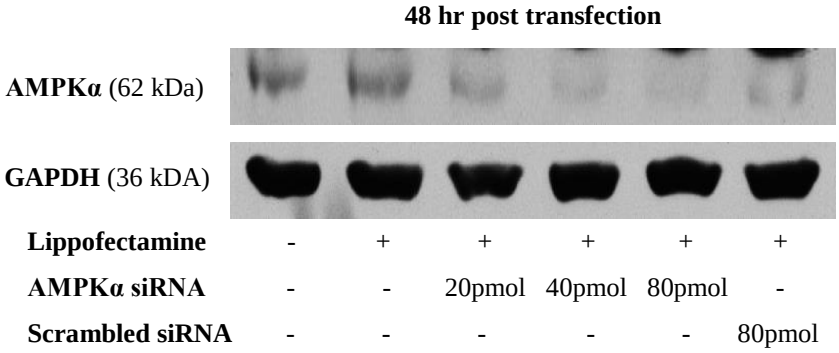

B

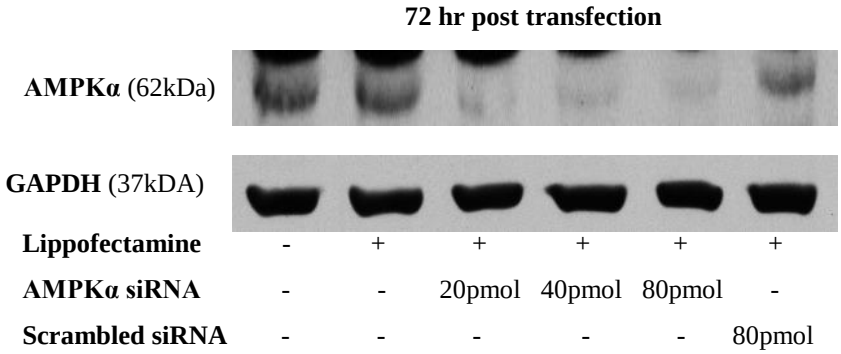

C

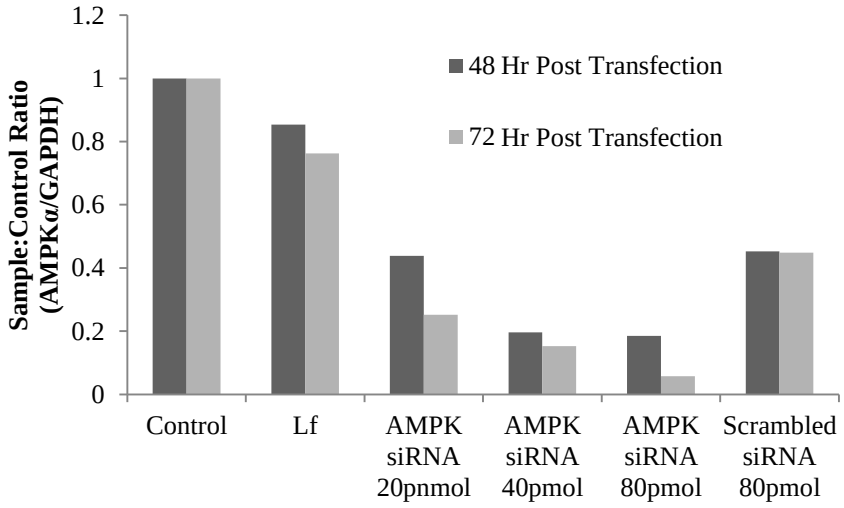

Figure 5.12 AMPKα1/2 siRNA repression optimisation. ***A)*** *Shows an example blot 48 hr post transfection.* ***B)*** *Shows an example blot 72 hr post transfection.* ***C)*** *AMPKα1/2 repression was quantified, demonstrating a time and concentration dependent reduction in expression, Lf= lipofectamine only. Results are shown as the mean, n=2.*

A

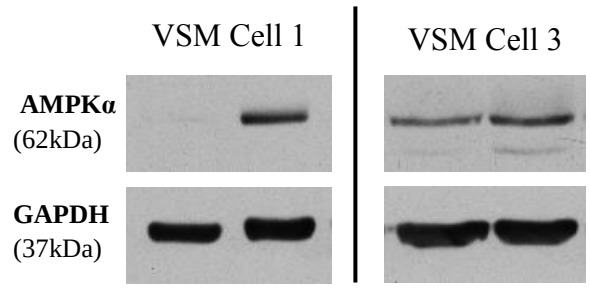

Control siRNA (40pmol)	-	+	-	+
AMPK α siRNA (40pmol)	+	-	+	-

B

	Repression of Expression (%)	**Diclofenac Activity (%)**
VSM Cell 1	97.8	57.2
VSM Cell 2	64.1	86.0
VSM Cell 3	38.9	118.9
VSM Cell 4	77.3	112.1
VSM Cell 5	64.1	82.4
Average	**68.4**	**91.3**
S.E.M.	**9.6**	**11.1**

Figure 5.13. Inconsistent repression of AMPK and diclofenac activity. ***A)*** *Shows examples of the inconsistent repression of AMPK which was achieved using 40pmol of siRNA over 48 hr.* ***B)*** *Shows a summary of AMPK repression in each set of cells, as well as the effect on diclofenac activity (inhibition of proliferation by diclofenac in AMPKα siRNA relative to control siRNA treated cells). Results are shown as the mean ±S.E.M., n=5.*

5.3.4 Elucidating the role of AMPK in modulation of proliferation by diclofenac using cells from AMPKα1$^{-/-}$ mice

VSM cells were explanted from sv129 wild type and AMPKα1$^{-/-}$ mouse aortas and cultured. To confirm AMPKα1 knock out, immunoblotting for AMPKα was carried out as shown in Fig. 5.14.A. As expected, cells explanted from AMPKα1$^{-/-}$ aortas had significantly reduced levels of AMPKα expression. The effect of diclofenac (85μM and 170μM) on wild type and AMPKα1$^{-/-}$ cell proliferation was then analysed by ^{3}H thymidine incorporation (Fig. 5.14.B). In this data set, one result from the wild type and AMPKα1$^{-/-}$ was excluded as this data was >4 standard deviations from the rest of the group. Diclofenac (85μM) inhibited wild type cell proliferation by 52%, in contrast to a 6% inhibition of AMPKα1$^{-/-}$ cell proliferation (p=0.001). However, at the higher concentration of diclofenac (170μM), there were no statistically significant differences between wild type and AMPKα1$^{-/-}$ cells (82% reduction vs. 74%). The morphology of cells treated with diclofenac was studied and images are shown in Fig. 5.15. Treatment with 170μM diclofenac caused no obvious differences in the morphology of wild type cells when compared with untreated controls. However, as shown in the bottom right image of the panel in Fig. 5.15, AMPKα1$^{-/-}$ cells treated with 170μM diclofenac showed signs of stress and had begun to detach from the plate. At 85μM diclofenac, the morphology of AMPKα1$^{-/-}$ cells did not appear to differ from the untreated controls.

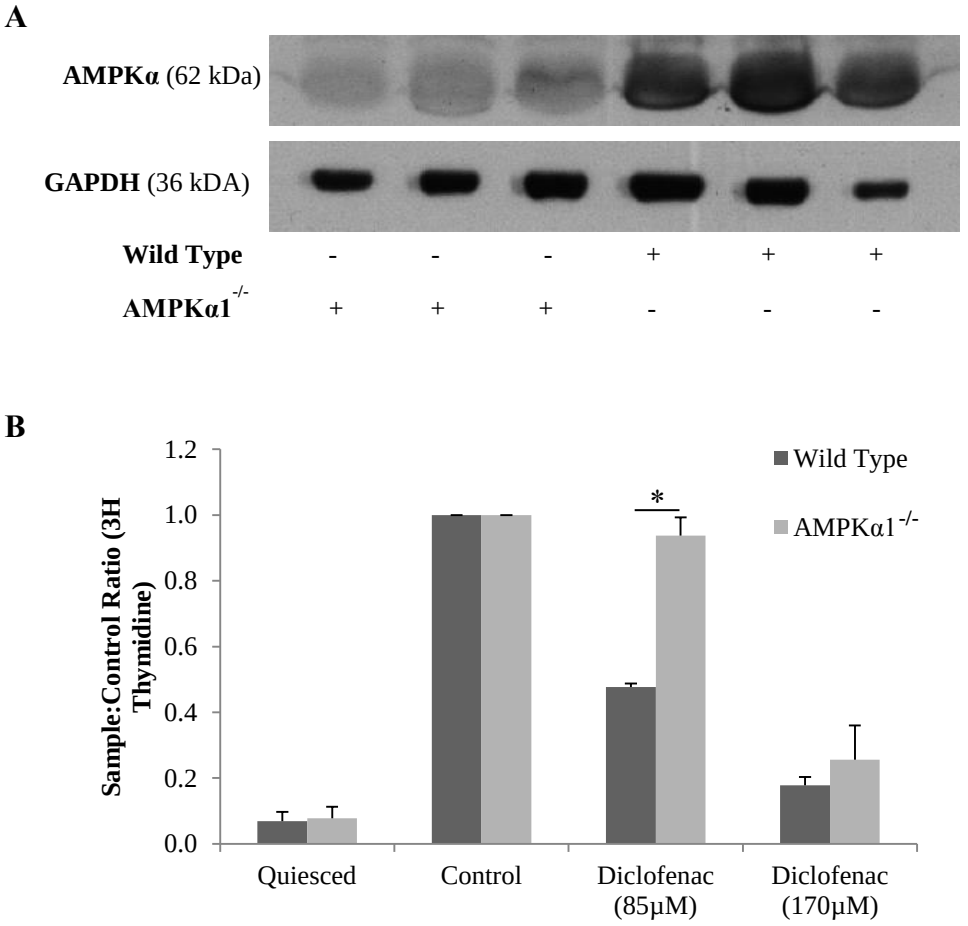

Figure 5.14. The effect of diclofenac on wild type and AMPKα1$^{-/-}$ VSM cells. ***A)*** *shows an immunoblot for basal AMPKα expression in VSM cells explanted from the aortas of AMPKα$^{-/-}$ and wild type mice (n=3).* ***B)*** *Quiesced VSM cells from both sets of mice were treated with diclofenac and stimulated for 24 hr with 10% FCS. Proliferation was measured by ^{3}H thymidine incorporation. Results are shown as the mean ±S.E.M., n=4, *=p<0.05 (unpaired T-test).*

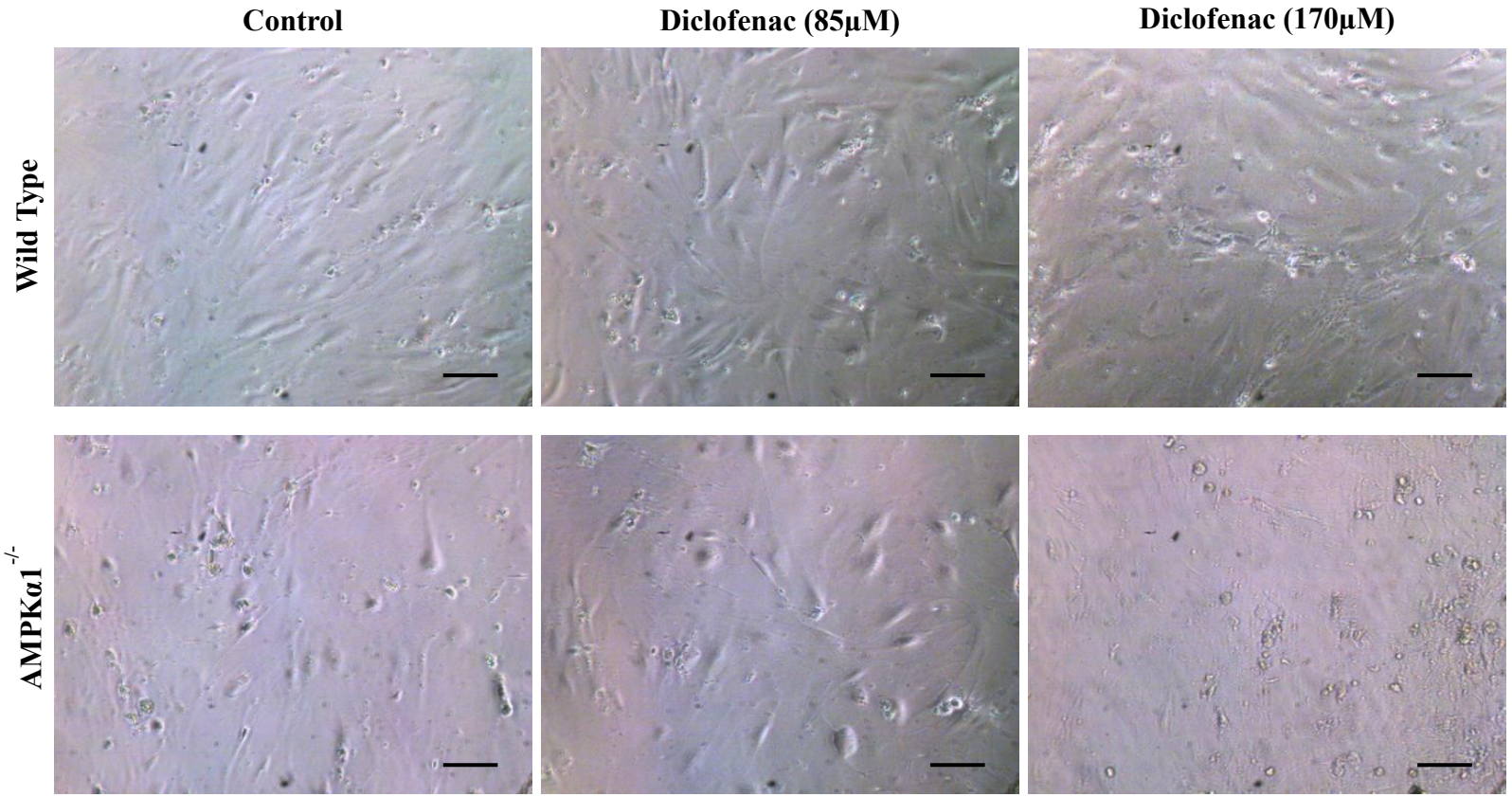

Figure 5.15. Brightfield imaging of wild type and AMPKα1$^{-/-}$ VSM cells treated with diclofenac. *Quiesced VSM cells were treated with diclofenac at 85 and 170µm for 24 hours before being stimulated for 18 hours with 10% FCS and imaged. All scale bars= 50µm.*

5.4 Discussion

5.4.1 The anti-proliferative mechanisms of diclofenac

The first finding presented in this chapter demonstrates that diclofenac mediated inhibition of proliferation is not specific to human VSM cells, with a concentration dependent decrease in rabbit VSM cell proliferation measured (Fig 5.2). The minimum concentration required for diclofenac mediated anti-proliferative activity was 42.5µM. At the highest concentration used (170µM), diclofenac reduced rabbit VSM cell proliferation by 70%. This is comparable to the 80% reduction in human VSM cell proliferation demonstrated in chapter 3, Fig. 3.16. The use of 170µM diclofenac was based on the IC_{50} value reported previously (Brooks *et al.*, 2003). In that study, the minimum inhibitory concentration of diclofenac was >100µM. However, asynchronous rat aortic VSM cells were used, which may require a higher concentration to inhibit the larger proportion of cells already proliferating when the agents are added.

The proliferative mechanisms affected by diclofenac, from MAPK activation down to cell cycle regulation, were investigated. ERK1/2 is a member of the MAPK family of proteins which is a key pathway in cell proliferation (Roux and Blenis, 2004). It is activated early in a proliferative response stimulated by a mitogen, such as the growth hormones found in FCS (Lewis *et al.*, 1998). In this study, ERK phosphorylation (activation) occurred following 15 min stimulation by 10% FCS. Diclofenac up to 170µM had no effect on the phosphorylation of ERK, suggesting that diclofenac acts later in the proliferative cascade (Fig. 5.3). In a previous study, the NSAID Indomethacin was shown to inhibit prostate cancer cell line ERK activity and proliferation (Husain *et al.*, 2001). However, limited evidence is available to support direct inhibition of ERK activation by NSAIDs. Another MAPK member, p38, was also investigated in this chapter. p38 is generally activated by stress related stimuli such as ultraviolet light, irradiation, heat shock, pro-inflammatory cytokines and certain mitogens (Obata et al., 2000). In Fig. 5.4, p38 was only detected following 15 min stimulation by FCS. Again like ERK, p38 activation was not

affected by diclofenac pre-treatment. Therefore, the point at which diclofenac acts in this signalling cascade is likely to be downstream of MAPK.

Diclofenac is known to cause arrest in the G1 phase of the cell cycle via activation of p53 leading to increased p21 (Brooks et al., 2003). The expression of cell cycle inhibitor p21 and G1 associated cyclin D1 following diclofenac treatment was assessed in this study. Three different antibodies against p21 were used; rabbit anti-p21 (Cat. No. 2947, Cell Signalling Technology), mouse anti-p21 (Cat. No. 2946, Cell Signalling Technology) and rabbit anti-p21 (Cat. No. sc-397, Santa Cruz Biotechnology Inc.). Neither of the Cell Signalling Technology antibodies detected a p21 signal. The Santa Cruz antibody detected a band at 21 kDa, as well as multiple other non-specific bands. Cell lysates were obtained from HCT116 p53 positive and negative cancer cell lines to as act as controls. p21 expression is controlled by p53, therefore a p53 negative sample will have less p21 expression. The effect of diclofenac on p21 expression was inconsistent (Fig. 5.5). Two sets of cells showed a degree of p21 increase, while the third set showed a decrease. Therefore from this data we cannot conclude that diclofenac activates p21 as reported (Brooks *et al.*, 2003). However, the effect of diclofenac on cyclin D1 expression was successfully demonstrated in Fig. 5.6. Cyclin D1 is essential for cell cycle progression, and therefore a decrease in expression causes cells to arrest in G1 phase (Morgan, 1995). Diclofenac caused a concentration dependent decrease in cyclin D1 expression. The concentrations required for this activity (42.5-170μM) were similar to those required for inhibition of overall proliferation. This indicates that diclofenac inhibits cell proliferation by reducing G1 associated cyclins, possibly via p21.

5.4.2 The role of AMPK in diclofenac mediated inhibition of proliferation

AMPK has previously been implicated in aspirin's anti-proliferative activity. For the first time, this study presents evidence which shows a relationship between diclofenac and AMPK. In Fig. 5.7, diclofenac caused a concentration dependent increase in AMPK phosphorylation from 85-170μM. In contrast to this, increasing concentrations of diclofenac caused a decrease in total AMPK expression. However,

it is likely that this decrease may be a form of negative feedback to regulate activation. Even with this decrease in total expression, significant phosphorylation of AMPK still occurred and resulted in downstream activation. To demonstrate this progression through the AMPK pathway, phosphorylation of downstream protein ACC was also analysed. ACC is directly phosphorylated by AMPK to regulate the metabolism of fatty acids within the cell (Park *et al.,* 2002), but it is not thought to be involved in the regulation of cell cycle. Diclofenac caused a significant, concentration dependent increase in ACC phosphorylation. The response generated was greater than that seen for AMPK activation, with an increase in phosphorylation occurring from 20μM. This pattern has been reported for aspirin and nifedipine, both of which activate AMPK causing an amplified ACC activation (Sung and Choi, 2012, 2011). Again, the active concentrations of diclofenac in these experiments closely correlate with those needed for anti-proliferative activity.

A number of approaches were taken to block AMPK in order to assess the impact on diclofenac activity. Firstly, a pharmacological approach was taken using the AMPK antagonist compound C, as well as the AMPK agonist A-769662. Compound C treatment inhibited basal phosphorylation of both AMPK and ACC (Fig. 5.8). Treatment with the agonist A-769662 failed to increase AMPK expression; however it caused a significant 11.3 fold increase in phosphorylation of ACC compared to untreated cells. A-769662 binds directly with AMPK to cause phosphorylation (Göransson *et al.,* 2007), leading to phosphorylation of ACC (Park *et al.,* 2002). Therefore, the A-769662 stimulated increase in ACC activation was via AMPK. This is another example of an amplified downstream response as seen in Fig. 5.7 with diclofenac treatment. Next, these agents were applied to diclofenac treated cells. Compound C significantly inhibited diclofenac mediated AMPK activation, as well as downstream activation of ACC (Fig. 5.9). Thus demonstrating the ability of 10μM compound C to inhibit diclofenac stimulated AMPK activity. The combination of diclofenac and A-769662 resulted in reduced AMPK activation, but did not decrease ACC phosphorylation compared to diclofenac only treatment. This down regulation of AMPK may represent a negative feedback mechanism stimulated by a high concentration of diclofenac and A-769662.

According to our hypothesis, AMPK inhibition should reduce diclofenac's anti-proliferative activity. Therefore, following the demonstration of compound C's ability to inhibit diclofenac stimulated AMPK, the effect of compound C and A-769662 on diclofenac's anti-proliferative activity was assessed (Fig. 5.10). In contrast to what was expected, diclofenac + compound C treatment caused further inhibition of proliferation, and compound C alone reduced proliferation to baseline levels. This result suggests that inhibition of AMPK inhibits proliferation, contrary to what is known (Motoshima *et al.,* 2006). However, it was more likely that compound C was either having a cytotoxic effect, or acting via a different pathway. The viability of cells was not affected by compound C treatment, demonstrated by trypan blue (Fig. 5.11.A). Therefore the effect of compound C on ERK, a key mediator in cell proliferation, was investigated (Fig. 5.11.B). Compound C significantly inhibited FCS mediated ERK phosphorylation, unlike diclofenac which had no effect (Fig.5.3). Therefore it appears compound C has AMPK independent anti-proliferative activity via inhibition of ERK activation. Despite compound C being used in several studies to antagonise activity downstream of AMPK (Sung & Choi 2011; Liang *et al.,* 2008; Sung & Choi 2012), non-specific activity has been reported (Peyton *et al.,* 2011). In this study Peyton and colleagues demonstrated a compound C concentration dependent decrease in VSM cell proliferation and migration. This response was not mimicked by siRNA silencing of AMPK or transfection with a dominant negative AMPK mutant by adenovirus. Therefore, due to the non-specific activity of compound C, this was not an effective model to test our hypothesis. The agonist A-769662 had no effect on cell proliferation either on its own, or in combination with diclofenac (Fig. 5.10). In other cell types A-769662 has been shown to inhibit cell proliferation (Zhou *et al.,* 2009), but the only studies demonstrating A-769662 in VSM cell proliferation are *in vivo* (Stone *et al.,* 2013). The concentration of A-769662 used in this study was 30μM, which is comparable to other studies (Cool *et al.,* 2006). However, concentrations of up to 300μM have been used (Göransson *et al.,* 2007). Therefore, a higher concentration of this agent may have more of an impact on AMPK activity without affecting cell viability.

Due to the non-specificity of compound C for AMPK, siRNA repression of AMPKα1/2 was investigated. As there were no commercially available siRNA complexes targeted to rabbit AMPK, siRNA targeting human AMPK was used. Both AMPKα1/2 are expressed in VSM cells, however α1 is thought to be the main catalytically active subunit (Rubin *et al.*, 2005). siRNA transfection was successful, and resulted in decreased AMPKα1/2 expression (Fig. 5.12). However, scrambled control siRNA also reduced AMPK expression, though not to the same extent as the targeted siRNA. This may be an artefact of the transfection process. Other studies have used this AMPK siRNA complex successfully (Sung and Choi, 2012, 2011), although these groups were able to use species-specific siRNA on rat VSM cells. Fig. 5.13 details the levels of AMPK repression and its effect on diclofenac activity for each set of cells used. The level of AMPK repression was inconsistent; the highest repression was 97.8% compared to only 38.9% in another set of cells. In the set of cells where AMPK was almost completely repressed, the diclofenac response was reduced by half. Overall, the mean AMPK repression was 68.4% which resulted in an 8.7% mean reduction in diclofenac activity. These results suggest that diclofenac's anti-proliferative activity is partially mediated by AMPK, although the inconsistency in AMPK repression means this system cannot be used to robustly test the hypothesis.

The final experimental model used in this chapter utilised VSM cells cultured from AMPKα1$^{-/-}$ and wild type mouse aortas. Cell proliferation of wild type VSM cells was inhibited by 52% using 85μM diclofenac, whereas AMPKα1$^{-/-}$ cell proliferation was only reduced by 6% (Fig. 5.14.B). For the first time, this experiment demonstrates that AMPKα1 is required for inhibition of cell proliferation by diclofenac at 85μM, and therefore confirms the role of AMPK in this activity. A diclofenac mediated anti-proliferative effect was observed with 170μM diclofenac in wild type cells; however this was not the case for the AMPKα1$^{-/-}$. Instead, the reduction in ^{3}H thymidine incorporation observed at this concentration in the AMPKα1$^{-/-}$ cells is likely due to reduced cell viability. This assumption is based on the morphology of diclofenac treated cells shown in Fig. 5.15. Wild type cell morphology does not appear to change with diclofenac treatment. However in the

AMPKα1$^{-/-}$ cells, diclofenac at 170μM appeared to cause cell stress, with some cells detaching from the bottom of the wells. The appearance of these cells is similar to reported cytokine and H_2O_2 induced VSM cell death (Geng *et al*., 1996). This change in morphology was not present in AMPKα1$^{-/-}$ cells treated with diclofenac at 85μM, where no anti-proliferative effect was seen. Therefore it appears that the lack of AMPKα1 in knock out cells makes them more susceptible to cell stress and death when treated with 170μM diclofenac, causing reduced ^{3}H thymidine incorporation. Further viability assays could be carried out to confirm the level of diclofenac mediated cell death in AMPKα1$^{-/-}$ cells.

The first clinically used drug which was shown to have AMPK activity was metformin (Zhou *et al.*, 2001). Metformin is used to treat type 2 diabetes as it lowers blood sugar levels without stimulating insulin secretion, as well as having a beneficial effect on circulating lipids linked to increased cardiovascular risk (Stumvoll *et al.*, 1995). Unexpectedly, it was shown that diabetic patients taking metformin had significantly reduced risk of developing cancer (Evans et al., 2005; Libby et al., 2009), which is believed to be via AMPK activation (Hadad *et al.*, 2012). Like diclofenac, metformin may have a positive effect on AVF stenosis. As a large proportion of renal failure patients are diabetics and may be receiving metformin, a retrospective study should be carried out analysing the correlation between metformin use and AVF patency.

5.5 Conclusion

Similar to effects observed in human VSM cells, diclofenac reduced FCS stimulated rabbit and mouse VSM cell proliferation in a concentration dependent manner. In rabbit cells, diclofenac had no effect on FCS stimulated ERK and p38 phosphorylation, indicating that it was acting downstream of these pathways. Data presented in this chapter highlighted the fact that diclofenac caused a concentration dependent decrease in cyclin D1, which would arrest the cells in G1 phase of the cell cycle. Importantly, and for the first time, data presented in this study provided evidence that diclofenac also caused a concentration dependent increase in AMPK

phosphorylation, as well as activation of downstream ACC. The diclofenac concentrations required for inhibition of cell proliferation closely correlate with those required for AMPK activation and reduction in cyclin D1 (42.5-170μM). This, along with previously reported diclofenac activity, suggests that AMPK activation is key to diclofenac mediated inhibition of proliferation (Brooks *et al.*, 2003). In the current study, attempts were made to block AMPK using the agent compound C. However this was not successful due to non-specific activity of compound C which affected ERK phosphorylation. siRNA repression of AMPK resulted in inconsistent silencing of AMPKα1/2, and therefore could not be used to reliably validate the role of AMPK in diclofenac mediated activity. A final approach using murine wild type and AMPKα1$^{-/-}$ VSM cells successfully demonstrated that diclofenac mediated inhibition of proliferation was reliant on AMPKα1. Thus the primary conclusion of this study is that diclofenac reduces VSM proliferation by activating AMPK and reducing the cell cycle protein cyclin D1.

Chapter 6

General Discussion

6.1 Summary and discussion of main experimental findings

The objectives of this thesis which are set out in chapter 1 were to investigate the inflammatory and proliferative characteristics of human arteriovenous fistula stenosis and the role of TLR-4. Secondary to this was identification of a therapy which targets the downstream mechanisms of TLR-4 activation using cells derived from human failed AVF. In addition, development of a pre-clinical *in vivo* model of AVF remodelling to investigate the contribution of cannulation injury with a therapeutic intervention identified on the human VSM cells. Finally elucidation of the mechanism of action of a therapy shown to be effective in the *in vivo* model.

Chapter 3 of this thesis involved the study of failed human AVF and characterisation of the morphology of AVF stenosis. This data demonstrates that vascular access stenosis involves the accumulation of immune and vascular smooth muscle type cells within the neointima, along with deposition and restructuring of extracellular matrix. The inflammatory characteristics of AVF stenosis were demonstrated by histological and proteomic analysis. Within stenotic AVF there was a significant increase in infiltration of inflammatory mast cells. Proteomic analysis of systemic inflammatory proteins in patients with stenosed AVF vs. functional AVF suggests that MCP-1 may play a role during stenosis. Up regulation of MCP-1 during AVF failure has been shown in previous *in vivo* studies (Juncos *et al.*, 2011), and haemodialysis patients are known to have increased MCP-1 expression vs. healthy individuals (Papayianni *et al.*, 2002). The data presented in chapter 3 demonstrates for the first time that an increase in MCP-1 expression is associated with AVF stenosis in humans.

The role of TLR-4 in AVF stenosis was also investigated in chapter 3. Activation of the TLR-4 pathway results in an inflammatory and proliferative response (Han *et al.*, 1994; Boyer and Lemichez, 2004; Han, 2006; Landström, 2010). Therefore, it was hypothesised that this mechanism would contribute to AVF stenosis. In the past, the limited data which was available suggested that TLR-4 was increased in AVF stenosis, however this was based on a qualitative study which did not quantify the increase in TLR-4 expression (de Graaf *et al.*, 2006). In chapter 3, TLR-4 expression in healthy vein vs. stenosed AVF was quantified. For the first time it was shown that

TLR-4 expression within stenotic AVF was increased by almost three fold; thus implicating TLR-4 in the pathogenesis of AVF stenosis.

Also in chapter 3, the proliferative characteristics of cells derived from healthy vein and stenosed AVF was characterised. Prior to this it was shown that VSM cells within the neointima of stenosed human arteriovenous fistulae had a significantly higher rate of proliferation compared to non-stenosed controls, analysed by expression of PCNA. On comparison of both sets of explanted cells, it was shown for the first time that VSM cells derived from stenosed AVF had a significantly higher capacity to proliferate compared to cells derived from healthy vein. Cell cycle analyses of these explants revealed a greater percentage of cells in G2/M phase within stenotic derived VSM cells, indicating a greater level of cell proliferation; however this was not statistically significant. This data demonstrates the hyper-proliferative phenotype of VSM cells within stenosed AVF, which was retained following explantation and cell culture. Therefore, the phenotype of these cells and their clinical relevance make them a good model for the study of AVF stenosis.

The role of TLR-4 in the proliferative phenotype of VSM cells was also demonstrated in chapter 3. Firstly, the ability of the archetypal TLR4 ligand LPS to prime and stimulate VSM cells towards a greater proliferative capacity was demonstrated. To date, there remains only one study which has demonstrated that activation of TLR-4 can lead to increased proliferation of VSM cells *in vitro* (Lin *et al.*, 2007). Therefore, this observation within this thesis adds to the limited evidence which is currently available. When activation of the TLR-4 pathway was investigated in stenosed AVF vs. healthy VSM cells, basal activation (phosphorylation) of IRAK-4 was increased in the stenosed AVF cells. This observation, as well as the increased expression of TLR-4 within stenosed AVF further implicates TLR-4 in vascular access failure.

The lack of reliable pharmacological TLR-4 inhibitors makes the study of this pathway difficult. The antagonist OxPAPC was shown in chapter 3 to have TLR-4 non-specific activity (Fig. 3.14). OxPAPC is reported to inhibit the binding of LPS

(Erridge *et al.*, 2008), which is currently the main mechanism of other experimental compounds which inhibit TLR-4, such as LPS-RS (Coats *et al.*, 2013) and neutralising antibodies. An alternative to pharmacological agents is the use of gene manipulation to cause repression of TLR-4. Adenovirus transfection of a dominant negative TLR-4 has been successfully used to demonstrate the role of TLR-4 in the generation of an inflammatory VSM cell phenotype (Yang *et al.*, 2005b). Yang and colleagues also demonstrated that VSM cells from TLR4 signalling-deficient mice (C3H/HeJ) had an impaired LPS induced inflammatory response and ERK activation compared to wild types. The advantage of an adenoviral approach is that it can be used in non-murine *in vivo* models, such as the rabbit model described in chapter 4 of this thesis. Delivery of genes by adenovirus during balloon catheter injury in rabbits has been shown to result in site specific transfection of arterial vascular smooth muscle and endothelial cells, while avoiding adenovirus delivery to remote organs such as the liver (Steg *et al.*, 1994).

The final observation reported in chapter 3 was the ability of diclofenac to inhibit FCS stimulated human VSM cell proliferation. While this observation has been made previously in rat aortic smooth muscle cells (Brooks *et al.*, 2003), this is the first report of diclofenac mediated anti-proliferative activity on human VSM cells. Also, for the first time it has been shown that diclofenac has the ability to inhibit LPS stimulated VSM cell proliferation (Fig. 3.16). Therefore, diclofenac has the potential to block TLR-4 mediated inflammation (via inhibition of COX-2) and proliferation.

Chapter 4 of this thesis presents a novel *in vivo* model of AVF remodelling which has been developed in the rabbit. Maturation of this femoral AVF was successfully demonstrated by a significant increase in blood flow measured by ultrasound and vein wall thickness measured histologically. The main observation demonstrated using this model was that cannulation injury significantly contributes to AVF remodelling, shown for the first time. Animals receiving puncture injury three times a week exhibited a significantly increased level of adverse remodelling (Fig. 4.7); highlighting cannulation as a central event which should be targeted therapeutically. Using this model in an intervention study, it was demonstrated that twice daily

topical application of diclofenac (1mg/cm^2) significantly reduced injury driven remodelling. This is the first report of topical NSAID use in AVF remodelling, and demonstrates the ability of diclofenac to reduce inflammation and proliferation which is driven by cannulation injury, most likely downstream of TLR-4 activation.

The concentration of diclofenac which was achieved at the AVF site, approximately 4mm below the surface of the skin, was not assessed in this thesis. Using the results from a human study of topical diclofenac absorption and the concentration of diclofenac applied in this rabbit model, it can be estimated that the concentration achieved at the rabbit AVF after 30 min at a depth of 4mm would be 400-500µM (Müller *et al.*, 1997). The results from another study of diclofenac absorption in the rat indicate an estimated local concentration of 200-300µM would be achieved at the rabbit AVF following 2 hr of absorption using the dose applied in the rabbit study (Singh and Roberts, 1994). In the *in vitro* studies presented in this thesis, the minimum inhibitory concentration of diclofenac was 42.5µM; with a 71% inhibition achieved using 170µM (Fig. 5.2). Therefore, the concentration of diclofenac which is required to inhibit proliferation of VSM cells *in vitro* (42.5µM) should be achievable locally at the rabbit AVF site, and would also result in inhibition of COX-2 (Piazza *et al.*, 2010). During this study, animals receiving topical diclofenac had an Elizabethan collar fitted to avoid interference via oral dosing during animal grooming.

Topical diclofenac is currently used as a topical analgesic for muscle pain. Therefore, diclofenac could potentially reduce the pain associated with venepuncture of the AVF. Currently, patients are given topical lidocaine/prilocaine cream (EMLA) for analgesia during cannulation (Çelik *et al.*, 2011). Therefore, topical diclofenac has the potential not only to increase AVF patency, but to also to relieve venepuncture associated pain. However, recently some concerns have been raised over the safety of diclofenac use. It has emerged that oral diclofenac should not be used in patients with a serious underlying heart condition due to a small increased risk of heart attack and stroke (Wise, 2013). This risk was highlight by meta-analysis revealing that the arterial thrombotic risk associated with oral diclofenac

was similar to selective COX-2 inhibitors which are already contraindicated for use in these patients. This risk is not associated with topical use of diclofenac and so this preparation is still safe for use in most patients.

In order to explore the potential regulation of proliferation downstream of cannulation injury and TLR-4, the anti-proliferative properties of diclofenac were investigated in chapter 5 of this thesis. Diclofenac has well established anti-inflammatory activity via the inhibition of COX. This has not been assessed further in this study as it has been extensively reported (Vane, 1971; Cryer and Feldman, 1998). Fig. 6.1 details what has been elucidated of diclofenac's anti-proliferative mechanism in chapter 5, together with what has been reported previously. As shown, diclofenac has no effect on MAPK (ERK and p38) following stimulation of VSM cells. Instead, diclofenac caused phosphorylation of AMPK, which has been shown by others to increase p53 and p21 expression (Jones *et al.*, 2005). This leads to an overall reduction in cyclin D1 expression causing a G1 phase cell cycle arrest, which in turn inhibits VSM cell proliferation. In Fig. 5.14.B the use of VSM cells from AMPK$\alpha 1^{-/-}$ vs. wild type mice demonstrated that diclofenac mediated inhibition of proliferation is dependent on the presence of AMPKα1. Therefore for the first time data presented in this thesis demonstrates that AMPK plays an essential role in diclofenac mediated activity. What remains to be investigated is the mechanism through which diclofenac activates AMPK. Salicylate, a metabolite of aspirin, has been shown to bind directly to AMPK causing allosteric activation and inhibition of dephosphorylation at the activating phosphorylation site, threonine-172 (Hawley *et al.*, 2012). It is therefore likely that diclofenac may also act in this manner, which could be investigated in a similar way using a cell free assay measuring AMPK activity. If diclofenac had no AMPK activity on its own, but instead caused an increase in activity when added with ATP/ADP, then this would suggest diclofenac activates AMPK in an allosteric manner similar to salicylate. If diclofenac pre-incubation antagonised A-769662 activity, it would suggest that, like salicylate and A-769662, diclofenac binds to the AMPKβ subunit. However, there are a number of upstream mechanisms which can lead to AMPK activation by which diclofenac could also be working. The most established event is a reduction in the ATP:AMP

ratio, usually signalling an energy deficit within the cell (Hardie and Carling, 1997). The anti-diabetic drug metformin activates AMPK through this mechanism via inhibition of mitochondrial respiration (Owen *et al.*, 2000). More recent evidence analysing metformin activity suggests that activation of AMPK is mediated by the upstream liver kinase B1 (LKB1) (Xie *et al.*, 2008). As well as LKB1, other upstream kinases that are known to directly phosphorylate AMPK include; calmodulin dependent protein kinase kinase β (CaMKKβ) which activates AMPK in response to elevated intracellular Ca2+ concentrations (Hawley *et al.*, 2005), and TGF-β activated kinase 1 (Tak1) (Momcilovic *et al.*, 2006). In the future, experiments to ascertain the mechanism through which diclofenac activates AMPK should include the assessment of the ATP:AMP ratio in treated cells. Also, the effect of blocking LKB1, CaMKKβ and TAK1 on diclofenac activity should be assessed. Full elucidation of diclofenac mediated activity is essential if this therapy is to gain approval for use in haemodialysis patients. Therefore, further studies should be undertaken to confirm the importance of AMPK and how it is activated by diclofenac, as well as the exact inflammatory mechanisms which are antagonised by this treatment. Further studies should also be undertaken to determine the concentration of diclofenac which is achieved at the AVF in humans.

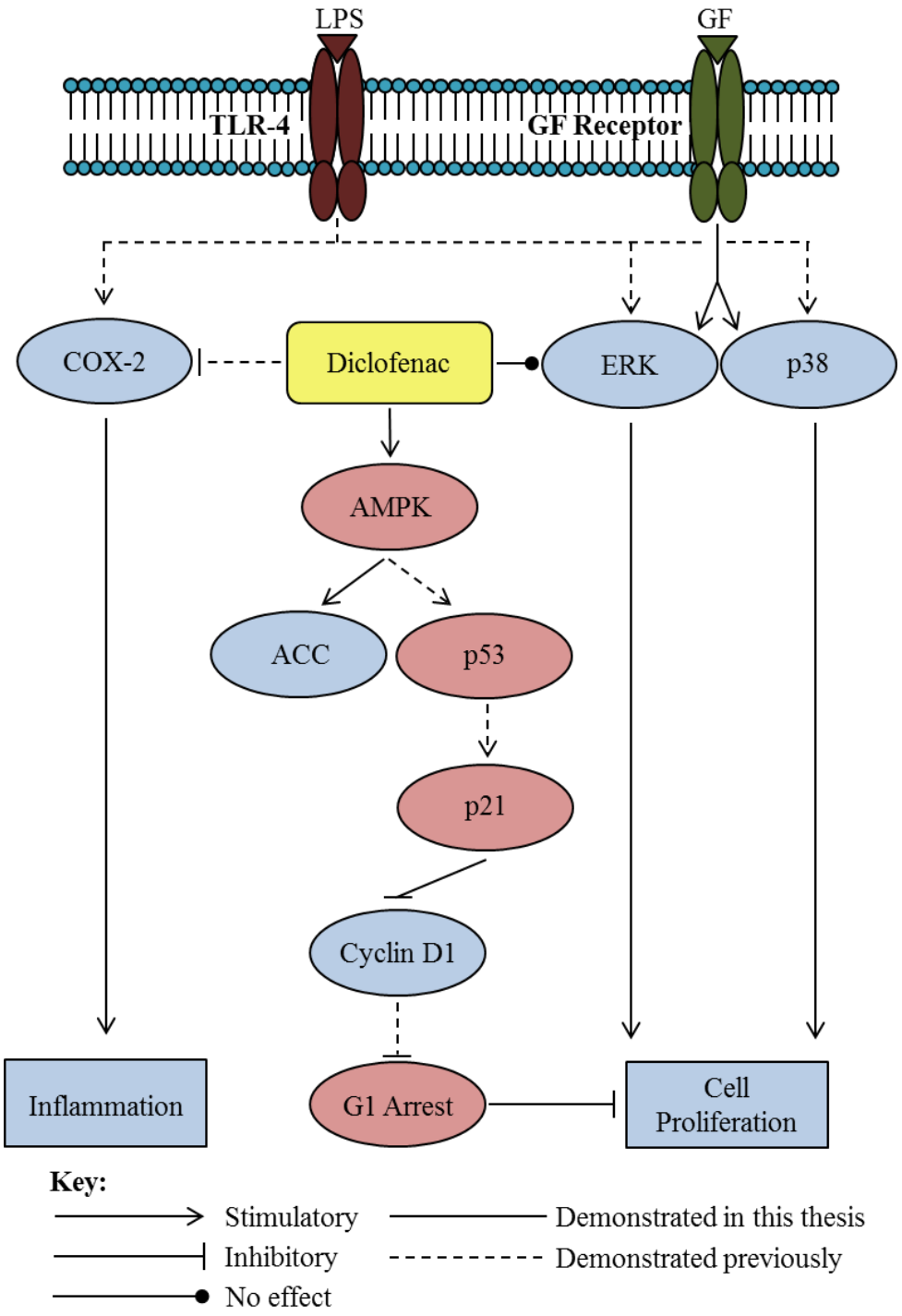

Figure 6.1. Pharmacology of diclofenac. *Inhibition of VSM cell proliferation by diclofenac is mediated by AMPK, and has no effect on MAPK activation. This leads to activation of p53 and p21 (Jones et al., 2005) causing a reduction in cyclin D1 expression leading to G1 arrest (Brooks et al., 2003; Igata et al., 2005). GF=growth factor.*

6.2 General conclusion

The pathophysiology of AVF failure involves a significant inflammatory and proliferative response which leads to vascular stenosis and therefore reduced blood flow through the AVF. TLR-4 is upregulated during stenosis and results in activation of inflammatory and proliferative mechanisms. Specifically TLR-4 has the capacity to prime VSM cells towards a greater proliferative response. Further *in vivo* studies are needed to assess the effect of blocking TLR-4 during AVF stenosis. As there are currently no clinically available TLR-4 antagonists, targeting the resulting downstream inflammation and proliferation with an agent such as diclofenac may prove therapeutically beneficial. The *in vivo* model developed in this study has highlighted for the first time that cannulation injury drives adverse AVF remodelling. Prophylactic application of topical diclofenac greatly reduced this adverse response. The evidence generated in this study demonstrates that diclofenac has the potential to inhibit VSM cell proliferation via the activation of AMPK leading to cell cycle arrest, as well as reduce inflammation via inhibition of COX-2 as previously reported (Brideau *et al.*, 1996; Rao *et al.*, 2008). Further studies should be carried out to confirm which inflammatory pathways are effected by diclofenac treatment in AVF remodelling, and also to explore the mechanism by which diclofenac activates AMPK.

Chapter 7

References

Aas, A.T., Tønnessen, T.I., Brun, A., Salford, L.G., 1995. Growth inhibition of rat glioma cells in vitro and in vivo by aspirin. J. Neurooncol. 24, 171–80.

Akira, S., Takeda, K., 2004. Toll-like receptor signalling. Nat. Rev. Immunol. 4, 499–511.

Ansell, D., Feehally, J., Fogarty, D., Inward, C., Tomson, C.R.V., Warwick, G., A. Williams, 2010. UK Renal Registry 2009 12th Annual Report of the Renal Association. Nephron. Clin. Pract. 115.

Asea, A., Rehli, M., Kabingu, E., Boch, J.A., Bare, O., Auron, P.E., Stevenson, M.A., Calderwood, S.K., 2002. Novel signal transduction pathway utilized by extracellular HSP70: role of toll-like receptor (TLR) 2 and TLR4. J. Biol. Chem. 277, 15028–34.

Asif, A., Roy-Chaudhury, P., Beathard, G.A., 2006. Early arteriovenous fistula failure: a logical proposal for when and how to intervene. Clin. J. Am. Soc. Nephrol. 1, 332–9.

Azevedo, L.C., Pedro, M.A., Souza, L.C., de Souza, H.P., Janiszewski, M., da Luz, P.L., Laurindo, F.R., 2000. Oxidative stress as a signaling mechanism of the vascular response to injury: the redox hypothesis of restenosis. Cardiovasc. Res. 47, 436–45.

Baboolal, K., McEwan, P., Sondhi, S., Spiewanowski, P., Wechowski, J., Wilson, K., 2008. The cost of renal dialysis in a UK setting--a multicentre study. Nephrol. Dial. Transplant 23, 1982–9.

Beathard, G., First, F., 2003. Hemodialysis arteriovenous fistulas. The End Stage Network of Texas, retrieved Oct. 2011 from www.esrdnetwork.org.

Besarab, A., Work, J., 2006. KDOQI Clinical Practice Guidelines for Vascular Access. Am. J. Kidney Dis. 48(Suppl 1), 176–273.

Bock, J.M., Menon, S.G., Goswami, P.C., Sinclair, L.L., Bedford, N.S., Domann, F.E., Trask, D.K., 2007. Relative Non-Steroidal Anti-inflammatory Drug (NSAID) Antiproliferative Activity is Mediated Through p21-Induced G1 Arrest and E2F Inhibition. Mol. Carcinog. 46, 857–864.

Boulton, T.G., Cobb, M.H., 1991. Identification of multiple extracellular signal-regulated kinases (ERKs) with antipeptide antibodies. Cell Regul. 2, 357–71.

Bourcier, T., 1997. The Nuclear Factor kappa -B Signaling Pathway Participates in Dysregulation of Vascular Smooth Muscle Cells in Vitro and in Human Atherosclerosis. J. Biol. Chem. 272, 15817–15824.

Boyer, L., Lemichez, E., 2004. Targeting of host-cell ubiquitin and ubiquitin-like pathways by bacterial factors. Nat. Rev. Micro. 2, 779–788.

Brand, K., Page, S., Rogler, G., Bartsch, A., Brandl, R., Knuechel, R., Page, M., Kaltschmidt, C., Baeuerle, P.A., Neumeier, D., 1996. Activated transcription factor nuclear factor-kappa B is present in the atherosclerotic lesion. J. Clin. Invest. 97, 1715–22.

Brater, D.C., 2002. Renal effects of cyclooxygyenase-2-selective inhibitors. J. Pain Symptom Manage. 23, 15–20.

Brescia, M.J., Cimino, J.E., Appel, K., Hurwich, B.J., 1966. Chronic Hemodialysis Using Venipuncture and a Surgically Created Arteriovenous Fistula. N. Engl. J. Med. 275, 1089–1092.

Brideau, C., Kargman, S., Liu, S., Dallob, A.L., Ehrich, E.W., Rodger, I.W., Chan, C.C., 1996. A human whole blood assay for clinical evaluation of biochemical efficacy of cyclooxygenase inhibitors. Inflamm. Res. 45, 68–74.

Brody, J., Pickering, N., Capuzzi, D., Fink, G., Can, C., Gomez, F., 1992. Interleukin-1 alpha as a factor in occlusive vascular disease. Am. J. Clin. Pathol. 97, 8–13.

Brooks, G., Yu, X.-M., Wang, Y., Crabbe, M.J.C., Shattock, M.J., Harper, J. V, 2003. Non-steroidal anti-inflammatory drugs (NSAIDs) inhibit vascular smooth muscle cell proliferation via differential effects on the cell cycle. J. Pharm. Pharmacol. 55, 519–26.

Burger, H., Kluchert, B., Kootstra, G., 1995. Survival of arteriovenous fistulas and shunts for haemodialysis. Eur. J. Surg. 161, 327–34.

Caplice, N.M., Wang, S., Tracz, M., Croatt, A.J., Grande, J.P., Katusic, Z.S., Nath, K.A., 2007. Neoangiogenesis and the presence of progenitor cells in the venous limb of an arteriovenous fistula in the rat. Am. J. Physiol. - Ren. Physiol. 293, 470–475.

Castier, Y., Lehoux, S., Hu, Y., Foteinos, G., Fonteinos, G., Tedgui, A., Xu, Q., 2006. Characterization of neointima lesions associated with arteriovenous fistulas in a mouse model. Kidney Int. 70, 315–20.

Çelik, G., Özbek, O., Yılmaz, M., Duman, I., Özbek, S., Apiliogullari, S., 2011. Vapocoolant spray vs lidocaine/prilocaine cream for reducing the pain of venipuncture in hemodialysis patients: a randomized, placebo-controlled, crossover study. Int. J. Med. Sci. 8, 623–7.

Chang, L., Karin, M., 2001. Mammalian MAP kinase signalling cascades. Nature 410, 37–40.

Charron, T., Nili, N., Strauss, B.H., 2006. The cell cycle: a critical therapeutic target to prevent vascular proliferative disease. Can. J. Cardiol. 22 Suppl B, 41B–55B.

Chu, Y., Jiang, Y., Zhang, J., 2010. The role of p38 mitogen-activated protein kinase in interleukin-6 induction by lipopolysaccharide in vascular smooth muscle cells. Zhongguo Wei Zhong Bing Ji Jiu Yi Xue 22, 291–4.

Clark, T.W.I., Hirsch, D.A., Jindal, K.J., Veugelers, P.J., LeBlanc, J., 2002. Outcome and Prognostic Factors of Restenosis after Percutaneous Treatment of Native Hemodialysis Fistulas. J. Vasc. Interv. Radiol. 13, 51–59.

Coats, P., Kennedy, S., Pyne, S., Wainwright, C.L., Wadsworth, R.M., 2008. Inhibition of non-Ras protein farnesylation reduces in-stent restenosis. Atherosclerosis 197, 515–23.

Coats, S.R., Pham, T.T., Bainbridge, B.W., Reife, R.A., Darveau, R.P., 2013. MD-2 mediates the ability of tetra-acylated and penta-acylated lipopolysaccharides to antagonize Escherichia coli lipopolysaccharide at the TLR4 signaling complex. J Immunol 175, 4490–4498.

Collaboration, A.T., 2002. Collaborative meta-analysis of randomised trials of antiplatelet therapy for prevention of death, myocardial infarction, and stroke in high risk patients. BMJ 324, 71–86.

Cool, B., Zinker, B., Chiou, W., Kifle, L., Cao, N., Perham, M., Dickinson, R., Adler, A., Gagne, G., Iyengar, R., Zhao, G., Marsh, K., Kym, P., Jung, P., Camp, H.S., Frevert, E., 2006. Identification and characterization of a small molecule AMPK activator that treats key components of type 2 diabetes and the metabolic syndrome. Cell Metab. 3, 403–16.

Corpataux, J.-M., Haesler, E., Silacci, P., Ris, H.B., Hayoz, D., 2002. Low-pressure environment and remodelling of the forearm vein in Brescia-Cimino haemodialysis access. Nephrol. Dial. Transplant 17, 1057–62.

Croatt, A.J., Grande, J.P., Hernandez, M.C., Ackerman, A.W., Katusic, Z.S., Nath, K.A., 2010. Characterization of a model of an arteriovenous fistula in the rat: the effect of L-NAME. Am. J. Pathol. 176, 2530–41.

Cross, K., El-Sanadiki, M., Murray, J., Mikat, E., McCann, R., Hagen, P., 1998. Mast cell infiltration: a possible mechanism for vein graft vasospasm. Surgery. 104, 171–7.

Crute, B.E., 1998. Functional Domains of the alpha 1 Catalytic Subunit of the AMP-activated Protein Kinase. J. Biol. Chem. 273, 35347–35354.

Cryer, B., Feldman, M., 1998. Cyclooxygenase-1 and cyclooxygenase-2 selectivity of widely used nonsteroidal anti-inflammatory drugs. Am. J. Med. 9343, 413–421.

Davis, R.J., 2000. Signal transduction by the JNK group of MAP kinases. Cell 103, 239–52.

Day, R.O., Graham, G.G., Bieri, D., Brown, M., Cairns, D., Harris, G., Hounsell, J., Platt-Hepworth, S., Reeve, R., Sambrook, P.N., 1989. Concentration-response relationships for salicylate-induced ototoxicity in normal volunteers. Br. J. Clin. Pharmacol. 28, 695–702.

De Graaf, R., Dammers, R., Vainas, T., Hoeks, A.P.G., Tordoir, J., 2003. Detection of cell-cycle regulators in failed arteriovenous fistulas for haemodialysis. Nephrol. Dial. Transplant. 18, 814–818.

De Graaf, R., Kloppenburg, G., Kitslaar, P.J.H.M., Bruggeman, C.A., Stassen, F., 2006. Human heat shock protein 60 stimulates vascular smooth muscle cell proliferation through Toll-like receptors 2 and 4. Microbes Infect. 8, 1859–65.

Derynck, R., Zhang, Y., Feng, X.H., 1998. Smads: transcriptional activators of TGF-beta responses. Cell 95, 737–40.

Dixon, B.S., Beck, G.J., Vazquez, M.A., Greenberg, A., Delmez, J.A., Allon, M., Dember, L.M., Himmelfarb, J., Gassman, J.J., Greene, T., Radeva, M.K., Davidson, I.J., Ikizler, T.A., Braden, G.L., Fenves, A.Z., Kaufman, J.S., Cotton, J.R., Martin, K.J., McNeil, J.W., Rahman, A., Lawson, J.H., Whiting, J.F., Hu, B., Meyers, C.M., Kusek, J.W., Feldman, H.I., 2009. Effect of dipyridamole plus aspirin on hemodialysis graft patency. N. Engl. J. Med. 360, 2191–201.

Dong, Q., Lin, C., Shang, H., Wu, W., Chen, F., Ji, X., Liu, Y., Zhang, J., Mao, T., 2010. Modified Approach to Construct a Vascularized Coral Bone in Rabbit Using an Arteriovenous Loop. J reconstr Microsurg 26, 95–102.

Eddy, A., Falk, R., Sibley, R., Hostetter, T., 2013. Subtotal nephrectomy in the rabbit: a model of chronic hypercalcemia, nephrolithiasis, and obstructive nephropathy. Reactions 182, 11–12.

Englesbe, M.J., Davies, M.G., Hawkins, S.M., Hsieh, P.C.H., Daum, G., Kenagy, R.D., Clowes, A.W., 2004. Arterial injury repair in nonhuman primates-the role of PDGF receptor-beta. J. Surg. Res. 119, 80–4.

Erridge, C., Kennedy, S., Spickett, C.M., Webb, D.J., 2008. Oxidized phospholipid inhibition of toll-like receptor (TLR) signaling is restricted to TLR2 and TLR4: roles for CD14, LPS-binding protein, and MD2 as targets for specificity of inhibition. J. Biol. Chem. 283, 24748–59.

Evans, J., Donnelly, L., Emslie-Smith, A., Alessi, D., Morris, A., 2005. Metformin and reduced risk of cancer in diabetic patients. Brittish Med. J. 330, 1304–5.

Factor, B., Sapk, J.N.K., Upstream, A., Muzio, B.M., Natoli, G., Saccani, S., Levrero, M., Mantovani, A., 1998. The Human Toll Signaling Pathway : Divergence of Nuclear Necrosis Factor Receptor – associated Factor 6 (TRAF6). J. Exp. Med. 187, 1–5.

Faries, P.L., Marin, M.L., Veith, F.J., Ramirez, J.A., Suggs, W.D., Parsons, R.E., Sanchez, L.A., Lyon, R.T., 1996. Immunolocalization and temporal distribution of cytokine expression during the development of vein graft intimal hyperplasia in an experimental model. J. Vasc. Surg. Off. Publ. Soc. Vasc. Surg. [and] Int. Soc. Cardiovasc. Surgery, North Am. Chapter 24, 463–71.

Fatigati, V., Murphy, A., 1984. Actin and Tropomyosin Variants in Smooth Muscles.

Field, M., MacNamara, K., Bailey, G., Jaipersad, A., Morgan, R.H., Pherwani, A.D., 2008. Primary patency rates of AV fistulas and the effect of patient variables. J. Vasc. Access 9, 45–50.

Fillinger, M.F., Reinitz, E.R., Schwartz, R.A., Resetarits, D.E., Paskanik, A.M., Bruch, D., Bredenberg, C.E., 1990. Graft geometry and venous intimal-medial hyperplasia in arteriovenous loop grafts. J. Vasc. Surg. 11, 556–566.

Fingerle, J., Au, Y.P., Clowes, a. W., Reidy, M. a., 1990. Intimal lesion formation in rat carotid arteries after endothelial denudation in absence of medial injury. Arterioscler. Thromb. Vasc. Biol. 10, 1082–1087.

Gabbiani, G., Schmidt, E., Wintert, S., Chaponnier, C., Chastonay, C.D.E., Vandekerckhovet, J., Weberf, K., Franket, W.W., 1981. Vascular smooth muscle cells differ from other smooth muscle cells : Predominance of vimentin filaments and a specific a-type actin. Proc. Natl. Acad. Sci. U.S.A. 78, 298–302.

Geng, Y.-J., Wu, Q., Muszynski, M., Hansson, G.K., Libby, P., 1996. Apoptosis of Vascular Smooth Muscle Cells Induced by In Vitro Stimulation With Interferon-γ, Tumor Necrosis Factor–α, and Interleukin-1β. Arterioscler. Thromb. Vasc. Biol. 16 , 19–27.

Ghosh, S., May, M.J., Kopp, E.B., 1998. NF-κB AND REL PROTEINS: Evolutionarily Conserved Mediators of Immune Responses. Annu. Rev. Immunol. 16, 225–260.

Göransson, O., McBride, A., Hawley, S.A., Ross, F.A., Shpiro, N., Foretz, M., Viollet, B., Hardie, D.G., Sakamoto, K., 2007. Mechanism of action of A-769662, a valuable tool for activation of AMP-activated protein kinase. J. Biol. Chem. 282, 32549–60.

Gordon, D., Reidy, M.A., Benditt, E.P., Schwartz, S.M., 1990. Cell proliferation in human coronary arteries. Proc. Natl. Acad. Sci. 87, 4600–4604.

Greenhill, N.S., Stehbens, W.E., 1987. Scanning Electron Microscopic Investigation of the Afferent Arteries of Experimental Femoral Arteriovenous Fistulae in Rabbits. Pathology 19, 22–27.

Greig, F.H., Kennedy, S., Spickett, C.M., 2012. Physiological effects of oxidized phospholipids and their cellular signaling mechanisms in inflammation. Free Radic. Biol. Med. 52, 266–80.

Hadad, S., Dowling, R., Chang, M., Done, S., Purdie, C., Jordan, L., Dewar, J., Goodwin, P., Stambolic, V., Thompson, A., 2012. Evidence for the anti-cancer action of metformin mediated via tumor AMPK, Akt and Ki67, in a preoperative window of opportunity trial. Cancer Res. 72, (Meeting Abstract Supplement) 24.

Han, J., 2006. MyD88 beyond Toll. Nat. Immunol. 7, 370–371.

Han, J., Lee, J.D., Bibbs, L., R.J. Ulevitch, 1994. A MAP kinase targeted by endotoxin and hyperosmolarity in mammalian cells. Sci. 265, 808–811.

Hannon, G.J., Beach, D., 1994. p15INK4B is a potential effector of TGF-beta-induced cell cycle arrest. Nature 371, 257–261.

Hardie, D., Carling, D., Carlson, M., 1998. The AMP-activated/SNF1 protein kinase subfamily: metabolic sensors of the eukaryotic cell? Annu. Rev. Biochem. 67, 821–55.

Hardie, D.G., Carling, D., 1997. The AMP-activated protein kinase--fuel gauge of the mammalian cell? Eur. J. Biochem. 246, 259–73.

Harper, J.W., Adami, G.R., Wei, N., Keyomarsi, K., Elledge, S.J., 1993. The p21 Cdk-Interacting Protein Cipl Is a Potent Inhibitor of G l Cyclin-Dependent Kinases. Cell 75, 805–816.

Hasegawa, T., Elder, S.J., Bragg-Gresham, J.L., Pisoni, R.L., Yamazaki, S., Akizawa, T., Jadoul, M., Hugh, R.C., Port, F.K., Fukuhara, S., 2008. Consistent

Aspirin Use Associated with Improved Arteriovenous Fistula Survival among Incident Hemodialysis Patients in the Dialysis Outcomes and Practice Patterns Study. Clin. J. Am. Soc. Nephrol. 3, 1373–1378.

Hawley, S.A., Fullerton, M.D., Ross, F.A., Schertzer, J.D., Chevtzoff, C., Walker, K.J., Peggie, M.W., Zibrova, D., Green, K.A., Mustard, K.J., Kemp, B.E., Sakamoto, K., Steinberg, G.R., Hardie, D.G., 2012. The ancient drug salicylate directly activates AMP-activated protein kinase. Sci. 336, 918–22.

Hawley, S.A., Pan, D.A., Mustard, K.J., Ross, L., Bain, J., Edelman, A.M., Frenguelli, B.G., Hardie, D.G., 2005. Calmodulin-dependent protein kinase kinase-β is an alternative upstream kinase for AMP-activated protein kinase. Cell Metab. 2, 9–19.

Hayashi, K., Naiki, T., 2009. Adaptation and remodeling of vascular wall; biomechanical response to hypertension. J. Mech. Behav. Biomed. Mater. 2, 3–19.

He, C., Charoenkul, V., Kahn, T., Langhoff, E., Uribarri, J., Sedlacek, M., 2002. Impact of the surgeon on the prevalence of arteriovenous fistulas. ASAIO J. 48, 39–40.

Heo, S.-K., Yun, H.-J., Noh, E.-K., Park, W.-H., Park, S.-D., 2008. LPS induces inflammatory responses in human aortic vascular smooth muscle cells via Toll-like receptor 4 expression and nitric oxide production. Immunol. Lett. 120, 57–64.

Hochleitner, B.W., Hochleitner, E.O., Obrist, P., Eberl, T., Amberger, A., Xu, Q., Margreiter, R., Wick, G., 2000a. Fluid shear stress induces heat shock protein 60 expression in endothelial cells in vitro and in vivo. Arterioscler. Thromb. Vasc. Biol. 20, 617–23.

Hochleitner, B.W., Hochleitner, E.O., Obrist, P., Eberl, T., Amberger, A., Xu, Q., Margreiter, R., Wick, G., 2000. Fluid shear stress induces heat shock protein 60

expression in endothelial cells in vitro and in vivo. Arterioscler. Thromb. Vasc. Biol. 20, 617–23.

Hong, T.-J., Ban, J.-E., Choi, K.-H., Son, Y.-H., Kim, S.-M., Eo, S.-K., Park, H.-J., Rhim, B.-Y., Kim, K., 2009. TLR-4 agonistic lipopolysaccharide upregulates interleukin-8 at the transcriptional and post-translational level in vascular smooth muscle cells. Vascul. Pharmacol. 50, 34–9.

Hsiao, J.-F., Chou, H.-H., Hsu, L.-A., Wu, L.-S., Yang, C.-W., Hsu, T.-S., Chang, C.-J., 2010. Vascular changes at the puncture segments of arteriovenous fistula for hemodialysis access. J. Vasc. Surg. 52, 669–73.

Hughes, A.L., Piontkivska, H., 2008. Functional diversification of the toll-like receptor gene family. Immunogenetics 60, 249–256.

Hunter, T., 1997. Oncoprotein networks. Cell 88, 333–346.

Husain, S.S., Szabo, I.L., Pai, R., Soreghan, B., Jones, M.K., Tarnawski, A.S., 2001. MAPK (ERK2) kinase--a key target for NSAIDs-induced inhibition of gastric cancer cell proliferation and growth. Life Sci. 69, 3045–54.

Igata, M., Motoshima, H., Tsuruzoe, K., Kojima, K., Matsumura, T., Kondo, T., Taguchi, T., Nakamaru, K., Yano, M., Kukidome, D., Matsumoto, K., Toyonaga, T., Asano, T., Nishikawa, T., Araki, E., 2005. Adenosine monophosphate-activated protein kinase suppresses vascular smooth muscle cell proliferation through the inhibition of cell cycle progression. Circ. Res. 97, 837–44.

Jacob, T., Ascher, E., Alapat, D., Olevskaia, Y., Hingorani, A., 2005. Activation of P38MAPK Signaling Cascade in a VSMC Injury Model: Role of P38MAPK Inhibitors in Limiting VSMC Proliferation. Eur. J. Vasc. Endovasc. Surg.

Jiang, W., Bhagat, L., Yu1, D., Kandimalla, E., Agrawal, S., 2009. IMO-3100, an Antagonist of Toll-Like Receptors 7 and 9, Modulates Gene Expression and

Regulatory Networks Induced by Ligands. J. Immunol. 182, (Meeting Abstract Supplement) 48.25.

Jin, D., Ueda, H., Takai, S., Okamoto, Y., Muramatsu, M., Sakaguchi, M., Shibahara, N., Katsuoka, Y., Miyazaki, M., 2005. Effect of chymase inhibition on the arteriovenous fistula stenosis in dogs. J. Am. Soc. Nephrol. 16, 1024–34.

Johnson, G.L., Lapadat, R., 2002. Mitogen-Activated Protein Kinase Pathways Mediated by ERK, JNK, and p38 Protein Kinases. Sci. 298 , 1911–1912.

Jones, G.T., Stehbens, W.E., 1995. Ultrastructure of the afferent arteries of experimental femoral arteriovenous fistulae in rabbits. Pathology 27, 333–338.

Jones, R.G., Plas, D.R., Kubek, S., Buzzai, M., Mu, J., Xu, Y., Birnbaum, M.J., Thompson, C.B., 2005. AMP-activated protein kinase induces a p53-dependent metabolic checkpoint. Mol. Cell 18, 283–93.

Juncos, J.P., Grande, J.P., Kang, L., Ackerman, A.W., Croatt, A.J., Katusic, Z.S., Nath, K.A., 2011. MCP-1 contributes to arteriovenous fistula failure. J. Am. Soc. Nephrol. 22, 43–8.

Kanellis, J., Kang, D.-H., 2005. Uric acid as a mediator of endothelial dysfunction, inflammation, and vascular disease. Semin. Nephrol. 25, 39–42.

Kargman, S., Charleson, S., Cartwright, M., Frank, J., Riendeau, D., Mancini, J., Evans, J., O'Neill, G., 1996. Characterization of Prostaglandin G/H Synthase 1 and 2 in rat, dog, monkey, and human gastrointestinal tracts. Gastroenterology 111, 445–54.

Karin, M., 1995. The regulation of AP-1 activity by mitogen-activated protein kinases. J. Biol. Chem. 270, 16483–16486.

Karin, M., Ben-Neriah, Y., 2000. Phosphorylation Meets Ubiquitination: The Control of NF-κB Activity. Annu. Rev. Immunol. 18, 621–663.

Karper, J.C., de Vries, M.R., van den Brand, B.T., Hoefer, I.E., Fischer, J.W., Jukema, J.W., Niessen, H.W.M., Quax, P.H.A., 2011. Toll-like receptor 4 is involved in human and mouse vein graft remodeling, and local gene silencing reduces vein graft disease in hypercholesterolemic APOE*3Leiden mice. Arterioscler. Thromb. Vasc. Biol. 31, 1033–40.

Katsanos, K., Karnabatidis, D., 2012. Paclitaxel-coated balloon angioplasty vs. plain balloon dilation for the treatment of failing dialysis access: 6-month interim results from a prospective randomized controlled trial. J. Endovasc. Ther. 19, 263-72.

Kaufman, J.S., O'Connor, T.Z., Zhang, J.H., Cronin, R.E., Fiore, L.D., Ganz, M.B., Goldfarb, D.S., Peduzzi, P.N., Thrombosis, for the V.A.C.S.G. on H.A.G., 2003. Randomized Controlled Trial of Clopidogrel plus Aspirin to Prevent Hemodialysis Access Graft Thrombosis. J. Am. Soc. Nephrol. 14, 2313–2321.

Kelly, B., Melhem, M., Zhang, J., Kasting, G., Li, J., Krishnamoorthy, M., Heffelfinger, S., Rudich, S., Desai, P., Roy-Chaudhury, P., 2006. Perivascular paclitaxel wraps block arteriovenous graft stenosis in a pig model. Nephrol. Dial. Transplant 21, 2425–31.

Kiechl, S., Egger, G., Mayr, M., Wiedermann, C.J., Bonora, E., Oberhollenzer, F., Muggeo, M., Xu, Q., Wick, G., Poewe, W., Willeit, J., 2001. Chronic Infections and the Risk of Carotid Atherosclerosis : Prospective Results From a Large Population Study. Circulation 103, 1064–1070.

Konner, K., 2003. The Arteriovenous Fistula. J. Am. Soc. Nephrol. 14, 1669–1680.

Konner, Klaus, 2003. The initial creation of native arteriovenous fistulas: surgical aspects and their impact on the practice of nephrology. Semin. Dial. 16, 291–8.

Kopp, E., Ghosh, S., 1994. Inhibition of NF-kappa B by sodium salicylate and aspirin. Sci. 265 , 956–959.

Kopp, E.B., Medzhitov, R., 1999. The Toll-receptor family and control of innate immunity. Curr. Opin. Immunol. 11, 13–8.

Krönung, G., 1984. Plastic deformation of Cimino fistula by repeated puncture. Dial. Transplant. 13, 635–638.

Kujubu, D., Fletcher, B., Varnum, B., 1991. TIS10, a phorbol ester tumor promoter-inducible mRNA from Swiss 3T3 cells, encodes a novel prostaglandin synthase/cyclooxygenase homologue. J. Biol. Chem. 266, 12866–72.

Landström, M., 2010. The TAK1–TRAF6 signalling pathway. Int. J. Biochem. Cell Biol. 42, 585–589.

Langer, S., Kokozidou, M., Heiss, C., Kranz, J., Kessler, T., Paulus, N., Krüger, T., Jacobs, M.J., Lente, C., Koeppel, T.A., 2010. Chronic kidney disease aggravates arteriovenous fistula damage in rats. Kidney Int. 78, 1312–21.

Lawrence, M.C., Jivan, A., Shao, C., Duan, L., Goad, D., Zaganjor, E., Osborne, J., McGlynn, K., Stippec, S., Earnest, S., Chen, W., Cobb, M.H., 2008. The roles of MAPKs in disease. Cell Res. 18, 436–42.

Lee, T., Roy-Chaudhury, P., 2009. Advances and New Frontiers in the Pathophysiology of Venous Neointimal Hyperplasia and Dialysis Access Stenosis. Adv. Chronic Kidney Dis. 16, 329–338.

Leone, G., DeGregori, J., Sears, R., Jakoi, L., Nevins, J., 1997. Myc and Ras collaborate in inducing accumulation of active cyclin E/Cdk2 and E2F. Nature 387, 422–6.

Lewis, T., Shapiro, P., Ahn, N., 1998. Signal transduction through MAP kinase cascades. Adv. Cancer Res. 74, 49–139.

Liang, K.-W., Yin, S.-C., Ting, C.-T., Lin, S.-J., Hsueh, C.-M., Chen, C.-Y., Hsu, S.-L., 2008. Berberine inhibits platelet-derived growth factor-induced growth and

migration partly through an AMPK-dependent pathway in vascular smooth muscle cells. Eur. J. Pharmacol. 590, 343–54.

Libby, G., Donnelly, L.A., Donnan, P.T., Alessi, D.R., Morris, A.D., Josie, M.M.E., 2009. New Users of Metformin Are at Low Risk of Incident Cancer. Diabetes Care 32, 1620–5.

Lin, F.-Y., Chen, Y.-H., Chen, Y.-L., Wu, T.-C., Li, C.-Y., Chen, J.-W., Lin, S.-J., 2007. Ginkgo biloba extract inhibits endotoxin-induced human aortic smooth muscle cell proliferation via suppression of toll-like receptor 4 expression and NADPH oxidase activation. J. Agric. Food Chem. 55, 1977–84.

Lin, F.-Y., Chen, Y.-H., Tasi, J.-S., Chen, J.-W., Yang, T.-L., Wang, H.-J., Li, C.-Y., Chen, Y.-L., Lin, S.-J., 2006. Endotoxin induces toll-like receptor 4 expression in vascular smooth muscle cells via NADPH oxidase activation and mitogen-activated protein kinase signaling pathways. Arterioscler. Thromb. Vasc. Biol. 26, 2630–7.

Lipari, G., Tessitore, N., Poli, A., Bedogna, V., Impedovo, A., Lupo, A., Baggio, E., 2007. Outcomes of surgical revision of stenosed and thrombosed forearm arteriovenous fistulae for haemodialysis. Nephrol. Dial. Transplant 22, 2605–12.

Liu, B., Li, L., Gao, M., Wang, Y., Yu, J., 2008. Microinflammation is involved in the dysfunction of arteriovenous fistula in patients with maintenance hemodialysis. Chin. Med. J. (Engl). 121, 2157–61.

Lobo, J.C., Stockler-Pinto, M.B., da Nóbrega, A.C.L., Carraro-Eduardo, J.C., Mafra, D., 2013. Is there association between uric acid and inflammation in hemodialysis patients? Ren. Fail. 35, 361–6.

Lok, C.E., Allon, M., Moist, L., Oliver, M.J., Shah, H., Zimmerman, D., 2006. Risk equation determining unsuccessful cannulation events and failure to maturation in arteriovenous fistulas (REDUCE FTM I). J. Am. Soc. Nephrol. 17, 3204–12.

Macrophages, H.A., Monocytes, B., Hempel, S.L., Monick, M.M., Hunninghake, G.W., 1994. Macrophages Monocytes 93, 391–396.

Madri, J.A., Bell, L., Marx, M., Merwin, J.R., Basson, C., Prinz, C., 1991. Effects of soluble factors and extracellular matrix components on vascular cell behavior in vitro and in vivo: models of de-endothelialization and repair. J. Cell. Biochem. 45, 123–30.

Marra, D.E., Liao, J.K., 2001. Salicylates and Vascular Smooth Muscle Cell Proliferation: Molecular Mechanisms for Cell Cycle Arrest. Trends Cardiovasc. Med. 11, 339–344.

Marrone, D., Pertosa, G., Simone, S., Loverre, A., Capobianco, C., Cifarelli, M., Memoli, B., Schena, F.P., Grandaliano, G., 2007. Local activation of interleukin 6 signaling is associated with arteriovenous fistula stenosis in hemodialysis patients. Am. J. Kidney Dis. 49, 664–73.

Martin, G., Stockfleth, E., 2013. Diclofenac sodium 3% gel for the management of actinic keratosis: 10+ years of cumulative evidence of efficacy and safety. Reactions 180, 15–16.

Massagué, J., 2000. How cells read TGF-β signals. Nat. Rev. Mol. cell Biol. 1, 169–78.

Melhem, M., Kelly, B., Zhang, J., Kasting, G., Li, J., 2006. Development of a Local Perivascular Paclitaxel Delivery System for Hemodialysis Vascular Access Dysfunction: Polymer Preparation and in vitroActivity. Blood Purif. 24, 289–98.

Milburn, J.A., Ford, I., Cassar, K., Fluck, N., Brittenden, J., 2012. Platelet activation, coagulation activation and C-reactive protein in simultaneous samples from the vascular access and peripheral veins of haemodialysis patients. Int. J. Lab. Hematol. 34, 52–8.

Milburn, J.A., Ford, I., Mutch, N.J., Fluck, N., Brittenden, J., 2013. Thrombin-anti-thrombin levels and patency of arterio-venous fistula in patients undergoing haemodialysis compared to healthy volunteers: a prospective analysis. PLoS One 8, e67799.

Mitchell, J.A., Akarasereenont, P., Thiemermann, C., Flower, R.J., Vane, J.R., 1994. Selectivity of nonsteroidal antiinflammatory drugs as inhibitors of constitutive and inducible cyclooxygenase. Proc. Natl. Acad. Sci. U.S.A. 90, 11693–11697.

Mitra, A.K., Gangahar, D.M., Agrawal, D.K., 2006. Cellular, molecular and immunological mechanisms in the pathophysiology of vein graft intimal hyperplasia. Immunol. Cell Biol. 84, 115–24.

Miyake, T., Aoki, M., Shiraya, S., Tanemoto, K., Ogihara, T., Kaneda, Y., Morishita, R., 2006. Inhibitory effects of NFkappaB decoy oligodeoxynucleotides on neointimal hyperplasia in a rabbit vein graft model. J. Mol. Cell. Cardiol. 41, 431–40.

Momcilovic, M., Hong, S.-P., Carlson, M., 2006. Mammalian TAK1 activates Snf1 protein kinase in yeast and phosphorylates AMP-activated protein kinase in vitro. J. Biol. Chem. 281, 25336–43.

Monos, E., 1980. Does hemodynamic adaptation take place in the vein grafted into an artery? Pfligers Arch. 384, 177– 182.

Montero Vega, M.T., de Andrés Martín, A., 2009. The significance of toll-like receptors in human diseases. Allergol. Immunopathol. (Madr). 37, 252–63.

Morgan, D., 1995. Principles of CDK regulation. Nature 374, 131–4.

Motoshima, H., Goldstein, B.J., Igata, M., Araki, E., 2006. AMPK and cell proliferation--AMPK as a therapeutic target for atherosclerosis and cancer. J. Physiol. 574, 63–71.

Müller, M., Mascher, H., Kikuta, C., Schäfer, S., Brunner, M., Dorner, G., Eichler, H.G., 1997. Diclofenac concentrations in defined tissue layers after topical administration. Clin. Pharmacol. Ther. 62, 293–9.

Muñoz, E., Valero, R.A., Quintana, A., Hoth, M., Núñez, L., Villalobos, C., 2011. Nonsteroidal anti-inflammatory drugs inhibit vascular smooth muscle cell proliferation by enabling the Ca2+-dependent inactivation of calcium release-activated calcium/orai channels normally prevented by mitochondria. J. Biol. Chem. 286, 16186–96.

Nelson, C., 2013. Diclofenac gel in the treatment of actinic keratoses. Reactions 179, 14–16.

Nguyen-Khoa, T., Massy, Z.A., De Bandt, J.P., Kebede, M., Salama, L., Lambrey, G., Witko-Sarsat, V., Drüeke, T.B., Lacour, B., Thévenin, M., 2001. Oxidative stress and haemodialysis: role of inflammation and duration of dialysis treatment. Nephrol. Dial. Transplant 16, 335–40.

Ni, J., Waldman, A., Khachigian, L.M., 2010. c-Jun regulates shear- and injury-inducible Egr-1 expression, vein graft stenosis after autologous end-to-side transplantation in rabbits, and intimal hyperplasia in human saphenous veins. J. Biol. Chem. 285, 4038–48.

Nielsen, T.G., Hesse, B., Boehme, M.W., Schroeder, T. V, 2001. Intraoperative endothelial damage is associated with increased risk of stenoses in infrainguinal vein grafts. Eur. J. Vasc. Endovasc. Surg. 21, 513–9.

Nurse, P., 1994. Ordering S phase and M phase in the cell cycle. Cell 79, 547–550.

Obata, T., Brown, G.E., Yaffe, M.B., 2000. MAP kinase pathways activated by stress: The p38 MAPK pathway. Crit. Care Med. 28, 67-77.

Onai, Z., 1998. MEKK1/JNK signaling stabilizes and activates p53. Proc. Natl. Acad. Sci. U.S.A. 95, 10541–10546.

Ott, S.J., El Mokhtari, N.E., Musfeldt, M., Hellmig, S., Freitag, S., Rehman, A., Kühbacher, T., Nikolaus, S., Namsolleck, P., Blaut, M., Hampe, J., Sahly, H., Reinecke, A., Haake, N., Günther, R., Krüger, D., Lins, M., Herrmann, G., Fölsch, U.R., Simon, R., Schreiber, S., 2006. Detection of Diverse Bacterial Signatures in Atherosclerotic Lesions of Patients With Coronary Heart Disease Circ. 113 , 929–937.

Owen, M., DORAN, E., Halestrap, A., 2000. Evidence that metformin exerts its anti-diabetic effects through inhibition of complex 1 of the mitochondrial respiratory chain. Biochem. J 614, 607–614.

Owens, G.K., Thompson, M.M., 1986. Developmental Changes in Isoactin Expression in Rat Aortic Smooth Muscle Cells in Vivo. J. Biol. Chem. 261, 13373-80

Papayianni, A., Alexopoulos, E., Giamalis, P., Gionanlis, L., Belechri, A.-M., Koukoudis, P., Memmos, D., 2002. Circulating levels of ICAM-1, VCAM-1, and MCP-1 are increased in haemodialysis patients: association with inflammation, dyslipidaemia, and vascular events. Nephrol. Dial. Transplant 17, 435–41.

Park, S.H., Gammon, S.R., Knippers, J.D., Paulsen, S.R., Rubink, D.S., Winder, W.W., 2002. Phosphorylation-activity relationships of AMPK and acetyl-CoA carboxylase in muscle. J. Appl. Physiol. 92, 2475–82.

Petti, C., Vegetti, C., Molla, A., Bersani, I., Cleris, L., Mustard, K.J., Formelli, F., Hardie, G.D., Sensi, M., Anichini, A., 2012. AMPK activators inhibit the proliferation of human melanomas bearing the activated MAPK pathway. Melanoma Res. 22, 341-50.

Peyton, K., Yu, Y., Yates, B., Shebib, A., 2011. Compound C inhibits vascular smooth muscle cell proliferation and migration in an AMP-activated protein kinase-independent fashion. J. Pharmacol. Exp. Ther. 338, 476–484.

Phuchareon, J., Tokuhisa, T., 1995. Deregulated c-Fos/AP-1 modulates expression of the cyclin and the cdk gene in splenic B cells stimulated with lipopolysaccharide. Cancer Lett. 92, 203–208.

Piazza, G. a., Keeton, A.B., Tinsley, H.N., Whitt, J.D., Gary, B.D., Mathew, B., Singh, R., Grizzle, W.E., Reynolds, R.C., 2010. NSAIDs: Old Drugs Reveal New Anticancer Targets. Pharmaceuticals 3, 1652–1667.

Picard, C., Casanova, J.-L., Puel, A., 2011. Infectious diseases in patients with IRAK-4, MyD88, NEMO, or IκBα deficiency. Clin. Microbiol. Rev.

Polyak, K., Kato, J.Y., Solomon, M.J., Sherr, C.J., Massague, J., Roberts, J.M., Koff, A., 1994. p27Kip1, a cyclin-Cdk inhibitor, links transforming growth factor-beta and contact inhibition to cell cycle arrest. Genes Dev. 8, 9–22.

Puchtler, H., Waldrop, F.S., Valentine, L.S., 1973. Polarization Microscopic Studies of Connective Tissue Stained with Picro-Sirius Red FBA. Beitr. Pathol. 150, 174–187.

Qian, M., Niu, L., Wang, Y., Jiang, B., Jin, Q., Jiang, C., Zheng, H., 2010. Measurement of flow velocity fields in small vessel-mimic phantoms and vessels of small animals using micro ultrasonic particle image velocimetry (micro-EPIV). Phys. Med. Biol. 55, 6069–88.

Quinton, W., Dillard, D., Scribner, B.H., 2004. Cannulation of Blood Vessels for Prolonged Hemodialysis. Hemodialysis International 8, 6–9 .

Rao, P.N.P., Knaus, E.E., Road, T.P., Jolla, L., 2008. Evolution of Nonsteroidal Anti-Inflammatory Cyclooxygenase (COX) Inhibition and Beyond. J. Pharm. Pharm. Sci. 11, 81–110.

Rayner, H.C., Besarab, A., Brown, W.W., Disney, A., Saito, A., Pisoni, R.L., 2004. Vascular access results from the Dialysis Outcomes and Practice Patterns Study

(DOPPS): Performance against Kidney Disease Outcomes Quality Initiative (K/DOQI) Clinical Practice Guidelines. Am. J. Kidney Dis. 44, 22–26.

Rekhter, M., Nicholls, S., Ferguson, M., Gordon, D., 1993. Cell proliferation in human arteriovenous fistulas used for hemodialysis. Arterioscler. Thromb. Vasc. Biol. 13, 609–617.

Rensen, S.S.M., Doevendans, P. A.F.M., van Eys, G.J.J.M., 2007. Regulation and characteristics of vascular smooth muscle cell phenotypic diversity. Neth. Heart J. 15, 100–8.

Reynisdottir, I., Polyak, K., Iavarone, A., Massague, J., 1995. Kip/Cip and Ink4 Cdk inhibitors cooperate to induce cell cycle arrest in response to TGF-beta. Genes Dev. 9, 1831–1845.

Ricard, J., Maingourd, Y., Lamara, S.A., Postel, J.P., Sevestre, H., Canarelli, J.P., Harichaux, P., 1992. Surcharge volumétrique cardiaque chez le lapin en croissance par fistule artério-veineuse chronique Evaluation d'un modèle original. Arch. Physiol. Biochem. 100, 13–18.

Robbin, M., Chamberlain, N., Lockhart, M., Gallichio, M., Young, C., Deierhoi, M., Allon, M., 2002. Hemodialysis arteriovenous fistula maturity: US evaluation. Radiology 225, 59–64.

Roderick, P., Nicholson, T., Armitage, A., Mehta, R., Mullee, M., Gerard, K., Drey, N., Feest, T., Greenwood, R., Lamping, D., J. Townsend J., 2005. An evaluation of the costs, effectiveness and quality of renal replacement therapy provision in renal satellite units in England and Wales. Heal. Technol Assess. 9, 1–178.

Ross, R., 1993. The pathogenesis of atherosclerosis: a perspective for the 1990s. Nature 362, 801–809.

Roux, P.P., Blenis, J., 2004. ERK and p38 MAPK-Activated Protein Kinases : a Family of Protein Kinases with Diverse Biological Functions. Society 68, 320–344.

Rowinsky, E.K., 1997. The development and clinical utility of the taxane class of antimicrotubule chemotherapy agents. Annu. Rev. Med. 48, 353–374.

Roy-Chaudhury, P., Spergel, L.M., Besarab, A., Asif, A., Ravani, P., 2007. Biology of arteriovenous fistula failure. J. Nephrol. 20, 150–63.

Roy-Chaudhury, P., Wang, Y., Krishnamoorthy, M., Zhang, J., Banerjee, R., Munda, R., Heffelfinger, S., Arend, L., 2009. Cellular phenotypes in human stenotic lesions from haemodialysis vascular access. Nephrol. Dial. Transplant 24, 2786–91.

Rubin, L.J., Magliola, L., Feng, X., Jones, A.W., Hale, C.C., 2005. Metabolic activation of AMP kinase in vascular smooth muscle. J. Appl. Physiol. 98, 296–306.

Sato, S., Sanjo, H., Takeda, K., Ninomiya-Tsuji, J., Yamamoto, M., Kawai, T., Matsumoto, K., Takeuchi, O., Akira, S., 2005. Essential function for the kinase TAK1 in innate and adaptive immune responses. Nat. Immunol. 6, 1087–95.

Saunders, P.C., Pintucci, G., Bizekis, C.S., Sharony, R., Hyman, K.M., Saponara, F., Baumann, F.G., Grossi, E.A., Colvin, S.B., Mignatti, P., Galloway, A.C., 2004. Vein graft arterialization causes differential activation of mitogen-activated protein kinases. J. Thorac. Cardiovasc. Surg. 127, 1276–84.

Schepers, A., Eefting, D., Bonta, P.I., Grimbergen, J.M., Vries, M.R. de, Weel, V. van, Vries, C.J. de, Egashira, K., Quax, P.H.A., Bockel, J.H. van, 2006. Anti-MCP-1 Gene Therapy Inhibits Vascular Smooth Muscle Cells Proliferation and Attenuates Vein Graft Thickening Both In Vitro and In Vivo. Arterioscler. Thromb. Vasc. Biol. 26, 2063–2069.

Schouten, W.E.M., Grooteman, M.P.C., Houte, A. Van, Schoorl, M., Limbeek, J. Van, Nube, M.J., 2000. Effects of dialyser and dialysate on the acute phase reaction in clinical bicarbonate dialysis. Nephrol. Dial. Transplant. 15, 379–384.

Senkaya, I., Aytac, I., Ercan, A., 2003. The graft selection for haemodialysis. Vasa 32, 209–13.

Shahbazian, H., Zand Moghadam, A., Ehsanpour, A., Khazaali, M., 2009. Changes in plasma concentrations of hypoxanthine and uric acid before and after hemodialysis. Iran. J. Kidney Dis. 3, 151–5.

Shaw, C., Pruthi, R., Pitcher, D., Fogarty, D., 2013. UK Renal Registry 15th annual report: Chapter 2 UK RRT prevalence in 2011: national and centre-specific analyses. Nephron. Clin. Pract. 123 Suppl , 29–54.

Sherr, C.J., 1994. G1 phase progression: Cycling on cue. Cell 79, 551–555.

Sherr, C.J., Roberts, J.M., 1995. Inhibitors of mammalian G1 cyclin-dependent kinases. Genes Dev. 9, 1149–1163.

Sherwood, L., 2003. Human Physiology: From Cells to Systems, 5th ed. Brooks Cole.

Shi, Y., O'Brien, J.E., Mannion, J.D., Morrison, R.C., Chung, W., Fard, A., Zalewski, A., 1997. Remodeling of Autologous Saphenous Vein Grafts : The Role of Perivascular Myofibroblasts. Circ. 95 , 2684–2693.

Singh, J.P., Rothfuss, K.J., Wiernicki, T.R., Lacefield, W.B., Kurtz, L., Brown, R.F., Brune, K.A., Bailey, D., Dubé, G.P., 1994. Dipyridamole directly inhibits vascular smooth muscle cell proliferation in vitro and in vivo: Implications in the treatment of restenosis after angioplasty. J. Am. Coll. Cardiol. 23, 665–671.

Singh, P., Roberts, M., 1994. Skin permeability and local tissue concentrations of nonsteroidal anti-inflammatory drugs after topical application. J. Pharmacol. Exp. Ther. 268, 144–151.

Skalli, O., Schürch, W., Seemayer, T., 1989. Myofibroblasts from diverse pathologic settings are heterogeneous in their content of actin isoforms and intermediate filament proteins. Lab. Invest. 60, 275–85.

Skartsis, N., Manning, E., Wei, Y., Velazquez, O.C., Liu, Z.-J., Goldschmidt-Clermont, P.J., Salman, L.H., Asif, A., Vazquez-Padron, R.I., 2011. Origin of neointimal cells in arteriovenous fistulae: bone marrow, artery, or the vein itself? Semin. Dial. 24, 242–8.

Son, Y., Jeong, Y., Lee, K., Choi, K., Kim, S., Rhim, B., Kim, K., 2008. Roles of MAPK and NF-kB in Interleukin-6 Induction by Lipopolysaccharide in Vascular Smooth Muscle Cells. J. Cardiovasc. Pharmacol. 51, 71–77.

Son, Y.-H., Jeong, Y.-T., Lee, K.-A., Choi, K.-H., Kim, S.-M., Rhim, B.-Y., Kim, K., 2008. Roles of MAPK and NF-[kappa]B in Interleukin-6 Induction by Lipopolysaccharide in Vascular Smooth Muscle Cells. J. Cardiovasc. Pharmacol. 51, 71-7.

Steg, P.G., Feldman, L.J., Scoazec, J., 1994. Arterial Gene Transfer to Rabbit Endothelial and Smooth Muscle Cells Using Percutaneous Delivery of an Adenoviral Vector. Circulation. 90, 1648–1656.

Stone, J.D., Narine, A., Shaver, P.R., Fox, J.C., Vuncannon, J.R., Tulis, D.A., 2013. AMP-activated protein kinase inhibits vascular smooth muscle cell proliferation and migration and vascular remodeling following injury. Am. J. Physiol. Heart Circ. Physiol. 304, H369–81.

Stuard, S., Belcaro, G., Dugall, M., 2010. Patency of arteriovenous fistula for dialysis improbe with topical spraygel heparin. Panminerva Med. 52, 33–6.

Stumvoll, M., Nurjhan, N., Perriello, G., Dailey, G., Gerich, J.E., 1995. Metabolic effects of metformin in non-insulin-dependent diabetes mellitus. N. Engl. J. Med. 333, 550–4.

Sun, H., Frassetto, L., Benet, L.Z., 2006. Effects of renal failure on drug transport and metabolism. Pharmacol. Ther. 109, 1–11.

Sun, J., Huang, X., Shi, D., 2005. Colour Doppler ultrosonography in traumatic femoral aneurysm and arteriovenous fistulae in rabbits. Zhongguo Chaosheng Yixue Zazhi 21, 884–886.

Sun, Y., Connors, K.E., Yang, D.-Q., 2007. AICAR induces phosphorylation of AMPK in an ATM-dependent, LKB1-independent manner. Mol. Cell. Biochem. 306, 239–45.

Sung, J.Y., Choi, H.C., 2011. Aspirin-induced AMP-activated protein kinase activation regulates the proliferation of vascular smooth muscle cells from spontaneously hypertensive rats. Biochem. Biophys. Res. Commun. 408, 312–7.

Sung, J.Y., Choi, H.C., 2012. Nifedipine inhibits vascular smooth muscle cell proliferation and reactive oxygen species production through AMP-activated protein kinase signaling pathway. Vascul. Pharmacol. 56, 1–8.

Tanner, F.C., Boehm, M., Akyurek, L.M., San, H., Yang, Z.-Y., Tashiro, J., Nabel, G.J., Nabel, E.G., 2000. Differential Effects of the Cyclin-Dependent Kinase Inhibitors p27Kip1, p21Cip1, and p16Ink4 on Vascular Smooth Muscle Cell Proliferation. Circulation 101, 2022–2025.

Tarry, W.C., Makhoul, R.G., 1994. L-arginine improves endothelium-dependent vasorelaxation and reduces intimal hyperplasia after balloon angioplasty. Arterioscler. Thromb. Vasc. Biol. 14, 938–943.

Tedgui, a., Mallat, Z., 2001. Anti-Inflammatory Mechanisms in the Vascular Wall. Circ. Res. 88, 877–887.

Tegeder, I., Pfeilschifter, J., Geisslinger, G., 2001. Cyclooxygenase-independent actions of cyclooxygenase inhibitors. FASEB J. 15, 2057–72.

Tessitore, N., 2003. A Prospective Controlled Trial on Effect of Percutaneous Transluminal Angioplasty on Functioning Arteriovenous Fistulae Survival. J. Am. Soc. Nephrol. 14, 1623–1627.

Thibodeau, G.A., K.T. Patton, K.T., 2003. Anatomy & Physiology, 5th ed. St. Louis, Mosby.

Thomson, P.C., Stirling, C.M., Geddes, C.C., Morris, S.T., Mactier, R.A., 2007. Vascular access in haemodialysis patients: a modifiable risk factor for bacteraemia and death. QJM 100, 415–22.

Thun, M.J., Namboodiri, M.M., Calle, E.E., Flanders, W.D., Heath, C.W., 1993. Aspirin Use and Risk of Fatal Cancer Aspirin Use and Risk of Fatal Cancer. Cancer Res. 15, 1322–1327.

Topper, J.N., Cai, J., Falb, D., Gimbrone, M.A., 1996. Identification of vascular endothelial genes differentially responsive to fluid mechanical stimuli: cyclooxygenase-2, manganese superoxide dismutase, and endothelial cell nitric oxide synthase are selectively up-regulated by steady laminar shear stress. Proc. Natl. Acad. Sci. U.S.A. 93, 10417–22.

Van Loon, M.M., Goovaerts, T., Kessels, A.G.H., van der Sande, F.M., Tordoir, J.H.M., 2010. Buttonhole needling of haemodialysis arteriovenous fistulae results in less complications and interventions compared to the rope-ladder technique. Nephrol. Dial. Transplant 25, 225–30.

Van Tricht, I., De Wachter, D., Tordoir, J., Verdonck, P., 2005. Hemodynamics and Complications Encountered with Arteriovenous Fistulas and Grafts as Vascular Access for Hemodialysis: A Review. Ann. Biomed. Eng. 33, 1142–1157.

Vane, J., 1971. Inhibition of prostaglandin synthesis as a mechanism of action for aspirin-like drugs. Nature 231, 232–235.

Verhallen, A.M., Kooistra, M.P., van Jaarsveld, B.C., 2007. Cannulating in haemodialysis: rope-ladder or buttonhole technique? Nephrol. Dial. Transplant 22, 2601–4.

Wang, T.H., Wang, H.S., Soong, Y.K., 2000. Paclitaxel-induced cell death: where the cell cycle and apoptosis come together. Cancer 88, 2619–28.

Wasse, H., Rivera, A.A., Huang, R., Martinson, D.E., Long, Q., McKinnon, W., Naqvi, N., Husain, A., 2011. Increased plasma chymase concentration and mast cell chymase expression in venous neointimal lesions of patients with CKD and ESRD. Semin. Dial. 24, 688–93.

Weksler, B.B., Pett, S.B., Alonso, D., Richter, R.C., Stelzer, P., Subramanian, V., Tack-Goldman, K., Gay, W.A., 1983. Differential Inhibition by Aspirin of Vascular and Platelet Prostaglandin Synthesis in Atherosclerotic Patients. N. Engl. J. Med. 308, 800–805.

Weston, C.R., Davis, R.J., 2007. The JNK signal transduction pathway. Curr. Opin. Cell Biol. 19, 142–9.

Widmaier, E.P., Raff, H., Strang, K.T., 2007. Vander's Human Physiology: The Mechanisms of Body Function, 11TH ed. McGraw-Hill Science.

Williams, K.J., Tabas, I., 1995. The Response-to-Retention Hypothesis of Early Atherogenesis. Arterioscler. Thromb. Vasc. Biol. 15 , 551–561.

Wise, J., 2013. Diclofenac shouldn't be prescribed to people with heart problems, drug agency says. BMJ 347,f4285.

Xie, Z., Dong, Y., Scholz, R., Neumann, D., Zou, M.-H., 2008. Phosphorylation of LKB1 at serine 428 by protein kinase C-zeta is required for metformin-enhanced activation of the AMP-activated protein kinase in endothelial cells. Circulation 117, 952–62.

Xu, Q., 2002. Role of Heat Shock Proteins in Atherosclerosis. Arterioscler. Thromb. Vasc. Biol. 22, 1547–1559.

Yang, X., Coriolan, D., Murthy, V., 2005. Proinflammatory phenotype of vascular smooth muscle cells: role of efficient Toll-like receptor 4 signaling. Am. J. Physiol. Heart Circ. Physiol. 289, 1069–1076.

Yang, X., Coriolan, D., Murthy, V., Schultz, K., Golenbock, D.T., Beasley, D., 2005. Proinflammatory phenotype of vascular smooth muscle cells: role of efficient Toll-like receptor 4 signaling. Am. J. Physiol. Heart Circ. Physiol. 289, 1069–76.

Yang, Z.Y., Simari, R.D., Perkins, N.D., San, H., Gordon, D., Nabel, G.J., Nabel, E.G., 1996. Role of the p21 cyclin-dependent kinase inhibitor in limiting intimal cell proliferation in response to arterial injury. Proc. Natl. Acad. Sci. U.S.A. 93, 7905–10.

Young, E.W., Dykstra, D.M., Goodkin, D.A., Mapes, D.L., Wolfe, R.A., Held, P.J., 2002. Hemodialysis vascular access preferences and outcomes in the Dialysis Outcomes and Practice Patterns Study (DOPPS). Kidney Int. 61, 2266–71.

Zarember, K.A., Godowski, P.J., 2002. Tissue Expression of Human Toll-Like Receptors and Differential Regulation of Toll-Like Receptor mRNAs in Leukocytes in Response to Microbes, Their Products, and Cytokines. J. Immunol. 168, 554–561.

Zhang, X., Morham, S., 1999. Malignant transformation and antineoplastic actions of nonsteroidal antiinflammatory drugs (NSAIDs) on cyclooxygenase-null embryo fibroblasts. J. Exp. Med. 190, 451–59.

Zhou, G., Myers, R., Li, Y., Chen, Y., Shen, X., Fenyk-melody, J., Wu, M., Ventre, J., Doebber, T., Fujii, N., Musi, N., Hirshman, M.F., Goodyear, L.J., Moller, D.E., 2001. Role of AMP-activated protein kinase in mechanism of metformin action. J. Clin. Invest. 108, 1167–1174.

Zhou, Y., Wang, D., Zhu, Q., Gao, X., Yang, S., Xu, A., Wu, D., 2009. Inhibitory effects of A-769662, a novel activator of AMP-activated protein kinase, on 3T3-L1 adipogenesis. Biol. Pharm. Bull. 32, 993–8.

Zhuplatov, S.B., Masaki, T., Blumenthal, D.K., Cheung, A.K., 2006. Mechanism of dipyridamole's action in inhibition of venous and arterial smooth muscle cell proliferation. Basic Clin. Pharmacol. Toxicol. 99, 431–9.

Zou, Y., Qi, Y., Roztocil, E., Nicholl, S.M., Davies, M.G., 2007. Patterns of kinase activation induced by injury in the murine femoral artery. J. Surg. Res. 142, 332–40.

Rabbit Arteriovenous Fistula Model and Identification of a Therapeutic Agent to Increase Fistula Patency

MacAskill, M.[1], Wadsworth, R.M.[1], Aitken, E.[2], Kingsmore, D.[2] & Coats, P.[1]

1. Strathclyde Institute of Pharmacy & Biomedical Sciences, University of Strathclyde, Glasgow, UK.
2. Renal Unit, Western Infirmary, Glasgow, UK.

Introduction

An arteriovenous fistula (AVF) is a vein graft which is typically created to permit vascular access allowing haemodialysis in renal failure patients (Fig. 1). AVF is considered the best option in clinical practice; however is associated with significant failure rate, with as little as 50% remaining patent at 6 months (Field *et al.*, 2008). Failure of these grafts is largely due to vascular smooth muscle cell (VSMC) de- differentiation and hyper-proliferation, leading to the development of neointima which invades the lumen causing stenosis and impaired blood flow (Lee and Roy-Chaudhury, 2009). Inflammation is known to play a key role in the development of vascular stenosis; although the exact mechanisms and triggers are not fully known.

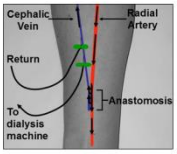

Figure 1. *shows the direction of blood flow following the creation of an AVF.*

Our study of failed human AVF within the lab has so far given insight into the role of inflammation, the changes undergone in VSMC and potential therapeutic agents. The next stage of our study was to take these observations and apply them *in vivo*.

Aims:

1) Develop an *in vivo* model of AVF stenosis in a rabbit
2) Investigate the contribution of cannulation injury in vascular remodelling
3) Identify a potential therapy to prevent AVF stenosis

AVF Creation

Rabbits were given a pre-med of hypnorm (0.3 mls Kg^{-1}) 30 minutes prior to surgery. During surgery body temperature, respirations and heart rate were observed and recorded. Based on respiration and heart rate, the isoflurane dose was adjusted between 1- 1.5% (Oxygen 1L min^{-1}, Nitrous oxide 1L min^{-1}). Subcutaneous Rimadyl (4mg Kg^{-1}) was also given at the time of surgery for analgesia. The anastomosis was then created as shown in figure 2.

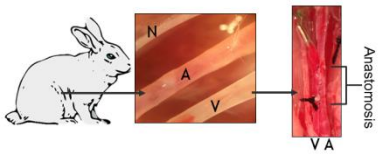

Figure 2. *The hind limb of a rabbit was chosen for the creation of an AVF. The neurovascular bundle was separated into femoral artery (A), vein (V) and nerve (N). A side to side anastomosis was created using 10-0 polyamide suture, followed by ligation of the distal vein.*

Maturation Period (Days 1-28)

For 28 days post AVF creation, maturation of the venous segment was monitored using colour doppler ultrasound to confirm arterial flow though the venous segment (Fig. 3.A and 3.B). The velocity of blood passing through the vessels was measured by pulsed wave ultrasound. There was a significant increase in venous velocity over the 28 day period, which is associated with vessel maturation (Fig. 3.E).

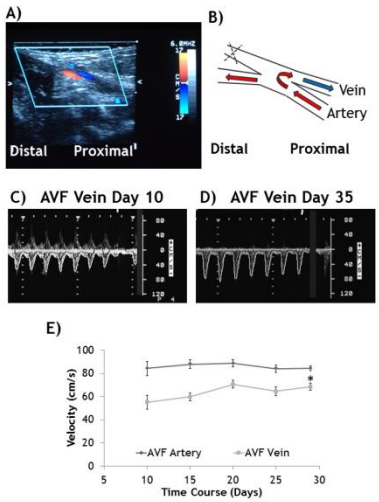

Figure 3. *Ultrasound of rabbit femoral AVF. **A)** Image showing arterial flow (Red) crossing through the anastomosis and flowing back towards the body (Blue). **B)** AVF blood flow schematic. **C)** Example of velocity waveform 10 days post AVF creation. **D)** Example of velocity waveform 35 days post AVF creation. **E)** Mean velocity of blood passing through the artery and vein over 29 days (±S.E.M., n=19, *= p<0.05 paired t-test for day 10 vs. 29).*

Experimental Period (Days 29-56)

Following maturation period, the animals were randomly split into three groups:

AVF-

Control group which receives no injury or drug treatment.

AVF + Injury-

To receive cannulation injury to the AVF three times a week, analogous to haemodialysis procedure.

AVF + Injury + Diclofenac-

To receive cannulation injury to the AVF three times a week, as well as topical diclofenac (125mg/cm^2) twice a day, 5 days a week.

Experimental Period (Days 29-56)

56 days post AVF creation the vessels were perfusion fixed in situ, wax processed and stained with H&E. Vein wall width was measured to determine the degree of injury dependent remodelling and effect of topical drug intervention (Fig. 4). The vein wall width was significantly increased in the AVF vs. contralateral control. Animals which received cannulation injury had a significantly increased vein wall width compared to the non injured group. Finally, vein wall width in the injured + diclofenac group was significantly reduced compared to the injured.

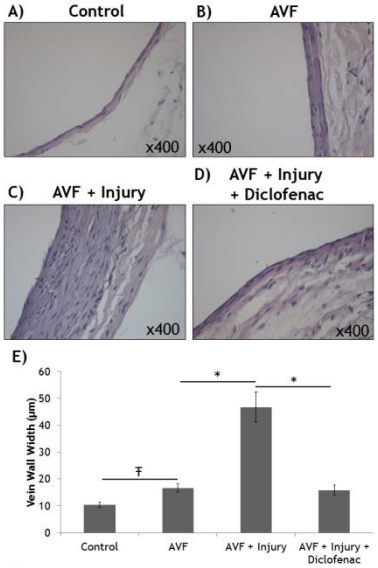

Figure 4. *shows examples from **A)** Control unoperated, **B)** AVF, **C)** AVF + Injury and **D)** AVF + Injury + Diclofenac groups. **E)** shows the mean vein wall width for each group, ± S.E.M., n=6-7, ∓= p<0.05 unpaired t-test for unoperated contralateral control vs. non injured AVF, *= p<0.05 one way ANOVA for non injured vs. injured & injured vs. injured + Diclofenac.*

Conclusions

- For the first time, cannulation injury has been shown to significantly contribute to AVF remodelling *in vivo*.
- Topical diclofenac appears to reduce injury driven remodelling within AVF.

Therefore, topical diclofenac could be used as a prophylactic treatment to reduce vascular stenosis in AVF.

References

Field, M. *et al.* (2008). *J. Vasc. Access* **9**, 45-50.

Lee, T. & Roy-Chaudhury, P. (2009). *Adv. Chronic Kidney Dis.* **16**, 329-338.

Acknowledgements

This work was funded by: BBSRC

Travel Grants: SIPBS and the Physiological Society

Correspondence: paul.coats@strath.ac.uk

PRINTED BY:

Development of a rabbit arteriovenous fistula model

MacAskill, M.[1], Wadsworth, R.M.[1], Kingsmore, D.[2] & Coats, P.[1]

1. Strathclyde Institute of Pharmacy & Biomedical Sciences, University of Strathclyde, Glasgow.
2. Renal Unit, Western Infirmary, Glasgow.

Introduction

An arteriovenous fistula (AVF) is a vein graft which is created to permit access to the bloodstream allowing haemodialysis to be performed in renal failure patients (Fig. 1). An AVF is considered the best option in clinical practice; however a significant failure rate is reported, with as little as 50% remaining patent at 6 months (Field *et al.*, 2008). Failure of these grafts is largely due to vascular smooth muscle cell (VSMC) hyper-proliferation, leading to the development of neointima which invades the lumen causing stenosis and impaired blood flow (Lee and Roy-Chaudhury, 2009). Inflammation is known to play a key role in the development of vascular stenosis; although the exact mechanisms and triggers are not fully known.

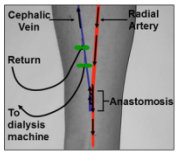

Figure 1. *This figure shows the direction of blood flow following the creation of an AVF.*

The study of failed human AVF within the lab has so far given insight into the role of inflammation, the changes undergone in VSMC and potential therapeutic agents. The next stage of this study is to take these observations and apply them *in vivo*.

Aims:

1) Develop an *in vivo* model of AVF stenosis in a rabbit
2) Investigate the contribution of cannulation injury in vascular remodelling
3) Identify a potential therapy to prevent AVF stenosis

AVF Creation

Rabbits were given a pre-med of hypnorm (0.3 mls Kg^{-1}) 30 minutes prior to surgery. During surgery body temperature, respirations and heart rate were observed and recorded. Based on respiration and heart rate, the isoflurane dose was adjusted between 1- 1.5% (Oxygen 1L min^{-1}, Nitrous oxide 1L min^{-1}). Subcutaneous Rimadyl (4mg Kg^{-1}) was also given at the time of surgery for analgesia. The anastomosis was then created as shown in figure 2.

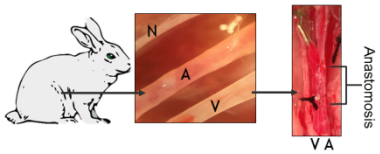

Figure 2. *The hind limb of a rabbit was chosen for the creation of an AVF. The neurovascular bundle was separated into femoral artery (A), vein (V) and nerve (N). A side to side anastomosis was created using 10-0 polyamide suture, followed by ligation of the distal vein.*

Monitoring of AVF maturation

For 28 days post AVF creation, maturation of the venous segment was monitored using colour doppler ultrasound to confirm arterial flow though the venous segment (Fig. 3.A and 3.B). The velocity of blood passing through the vessels was measured by pulsed wave ultrasound. There was a significant increase in venous velocity over the 28 day period, which is associated with vessel maturation (Fig. 3.C).

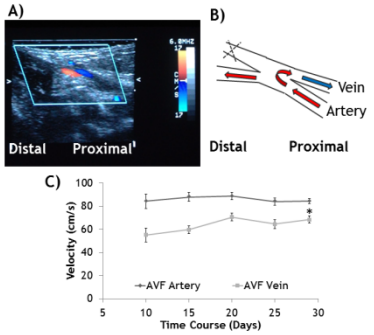

Figure 3. *Ultrasound of rabbit femoral AVF. **A)** Image showing arterial flow (Red) crossing through the anastomosis and flowing back towards the body (Blue). **B)** AVF blood flow schematic. **C)** Mean velocity of blood passing through the artery and vein over 29 days (±S.E.M., n=19, *= p<0.05 paired t-test for day 10 vs. 29).*

Maturation Period (Days 1-28)

28 days post AVF creation, the vessels were perfusion fixed in situ at 90 mmHg and processed in paraffin for histology. H & E staining was used to visualise remodelling of the vessels. The proximal vein underwent a maturation response, with the medial layer increasing from 2 to 7 smooth muscle cells thick.

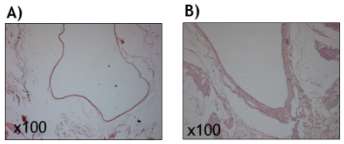

Figure 4. *A) Contralateral control vein with a medial layer ~1-2 VSMC thick. B) Thickening of the proximal vein with a medial layer 7 VSMC thick.*

Experimental Period (Days 29-56)

Following the initial maturation period, the animals were randomly split into three groups:

Non Injured-

Control group which receives no injury or drug treatment.

Injured-

To receive cannulation injury to the AVF three times a week, analogous to haemodialysis procedure.

Injured + Diclofenac-

To receive cannulation injury to the AVF three times a week, as well as topical diclofenac ($125mg/cm^2$) twice a day, 5 days a week.

Experimental Period (Days 29-56)

56 days post AVF creation, the vessels were perfusion fixed in situ and processed as described. Vein wall width was measured to determine the degree of injury dependent remodelling and effect of topical drug intervention (Fig. 5). The vein wall width was significantly increased in the AVF vs. contralateral control. Animals which received cannulation injury had a significantly increased vein wall width compared to the non injured group. Finally, vein wall width in the injured + diclofenac group was significantly reduced compared to the injured.

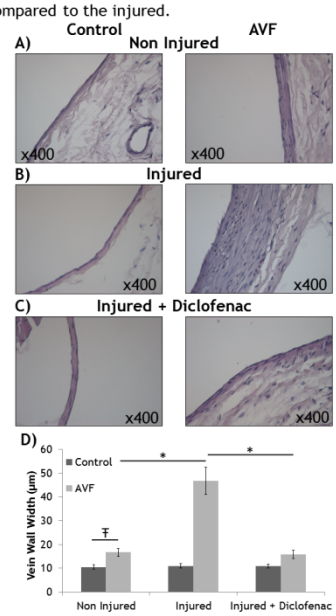

Figure 5. *This figure shows control and AVF examples from **A)** Non Injured, **B)** Injured and **C)** Injured + Diclofenac groups. **D)** shows the mean vein wall width for each group, ±S.E.M., n=6-7, ŦŦ= p<0.05 unpaired t-test for contralateral control vs. non injured AVF, *= p<0.05 one way ANOVA for non injured vs. injured & injured vs. injured + Diclofenac.*

Conclusions

- For the first time, cannulation injury has been shown to significantly contribute to AVF remodelling *in vivo*.
- Topical diclofenac appears to reduce injury driven remodelling within AVF.

Therefore, topical diclofenac could be used as a prophylactic treatment to reduce vascular stenosis in AVF.

References

Field, M. *et al.* (2008). *J. Vasc. Access* **9**, 45-50.

Lee, T. & Roy-Chaudhury, P. (2009). *Adv. Chronic Kidney Dis.* **16**, 329-338.

Acknowledgements

This work was funded by:

BBSRC bioscience for the future

University of Strathclyde Science

Vascular access failure in haemodialysis patients

MacAskill, M.[1], Wu, J.[1], Wadsworth, R.M.[1], Kingsmore, D.[2] & Coats, P.[1]

1. Strathclyde Institute of Pharmacy & Biomedical Sciences, University of Strathclyde, Glasgow.
2. Renal Unit, Western Infirmary, Glasgow.

University of Strathclyde Science

Introduction

An arteriovenous fistula (AVF) is a surgical procedure where an artery is joined to a vein to permit access to the bloodstream, allowing haemodialysis in renal failure patients. An AVF is the favoured option in clinical practice. However ~ 50% of AVFs occlude at 6 months rendering them unusable for haemodialysis. Stenotic (occlusive) failure of the AVF is largely due to vascular smooth muscle cell (VSMC) proliferation which occludes the blood vessel lumen. Inflammation is also known to play a key role in the development of vascular proliferative occlusion; although the exact mechanisms and triggers are as yet not fully known.

The aims of this study are to:

- Evaluate the morphology of AVF failure
- Study vascular smooth muscle cells grown from healthy and stenosed veins
- Investigate the inflammatory processes

Micrograph of healthy and stenosed veins

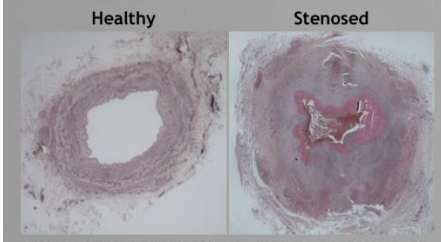

The occlusion of the lumen in the stenosed vein requires the patient to have a surgical procedure to repair or create a new AVF.

Growth of cells from human veins in cell culture

VSMCs grown from healthy and stenosed veins stained with α-SMA (Green).

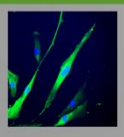

Stenosed vein cells proliferate faster than healthy cells

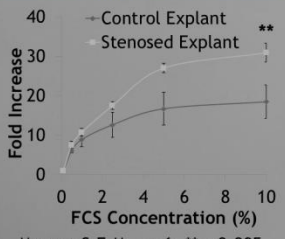

Mean ± S.E.M., n=6, **=<0.005

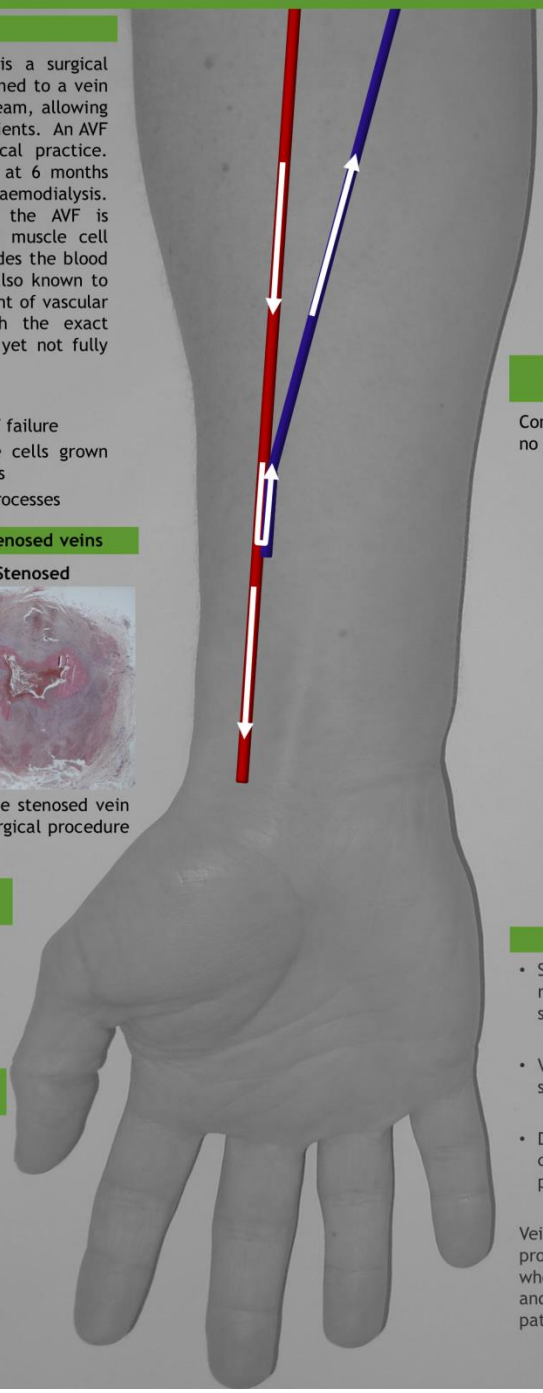

Increased movement of immune cells from the blood into stenotic vein

Mast cells were stained using toluidine blue (circled) and quantified in healthy and stenosed veins.

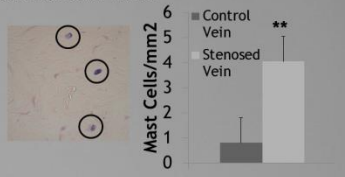

Mean ± S.E.M., n=9,7, **=<0.005

Inflammatory profile of patients with stenosis

Comparison of blood taken from patients with no stenosis vs. patients with stenosis.

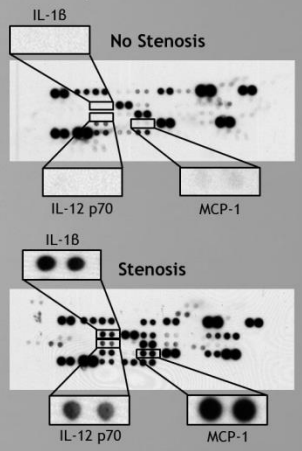

Conclusions

- Significant venous hypertrophic remodelling occurs within stenosed AVF sections
- VSMCs derived from stenotic vein have a significantly higher rate of proliferation
- During stenosis there is an increase in mast cells within the vein and pro-inflammatory proteins in the blood

Vein graft stenosis involves an inflammatory process and we are now investigating whether a combination of anti-proliferative and anti-inflammatory therapies will help patients with vascular access problems.

BBSRC Bioscience for the future

Arteriovenous fistula failure: vascular smooth muscle cell proliferation and inflammation

MacAskill, M.[1], Wu, J.[1], Wadsworth, R.M.[1], Kingsmore, D.[2] & Coats, P.[1]

1. Strathclyde Institute of Pharmacy & Biomedical Sciences, University of Strathclyde, Glasgow.
2. Renal Unit, Western Infirmary, Glasgow.

University of Strathclyde Glasgow

Introduction

An arteriovenous fistula (AVF) is a vein graft which is created to permit access to the bloodstream allowing haemodialysis to be performed in renal failure patients. An AVF is considered the best option in clinical practice; however a significant failure rate is still reported, with as little as 50% remaining patent at 6 months (Field *et al.*, 2008). Failure of these grafts is largely due to vascular smooth muscle cell (VSMC) hyper-proliferation, leading to the development of neointima which invades the lumen causing stenosis and impaired blood flow (Lee and Roy-Chaudhury, 2009). Inflammation is known to play a key role in the development of vascular stenosis; although the exact mechanisms and triggers are not fully known.

Aims:

1) Evaluate the changes in VSMC present within human failed AVF vs. non-stenosed controls
2) Investigate the inflammatory processes
3) Evaluate potential therapies to offset stenosis

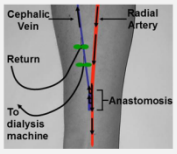

Figure 1. This figure shows the direction of blood flow following the creation of an AVF

Materials and methods

Stenosed cephalic vein was obtained with prior consent from patients undergoing arteriovenous fistula creation or revision. Long saphenous vein (LSV) was obtained from patients undergoing lower limb bypass surgery. Following tissue isolation, the specimens were transported on ice and;

1. Cultured in growth medium (1:1 Waymouths:Ham's F12, 1% Pen. Strep., 15 % FCS) for several weeks to allow spontaneous explantation of VSMC.
2. Fixed in 4% paraformaldehyde, wax embedded and cut at 4µm for histological examination.

Serum samples were obtained from patients undergoing dialysis, which were immediately aliquoted and frozen.

Hypertrophic remodeling and VSMC proliferation in vivo

Significant hypertrophic remodelling was seen in the stenosed venous sections of failed AVF. Within this, a 9.5 fold increase in the % of cells expressing proliferating cell nuclear antigen (PCNA) was observed.

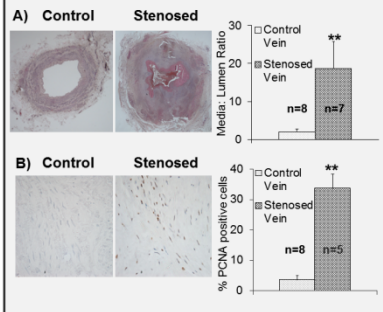

Figure 2. A) Haematoxylin and eosin stain shows the structure of the vessels (**=p<0.005 paired T test). **B)** PCNA expression (brown) was measured by immunohistochemistry (IHC) (**=p<0.005 , paired T test).

Immune cell infiltration and adhesion molecule expression

Within the failed AVF vein sections, a significant 5 fold increase in the number of mast cells within the vein were observed vs. controls. The presence of lymphocytes moving from the blood, into the neointima was also evident. Endothelial vascular cell adhesion molecule-1 (VCAM-1) expression appears reduced in the stenotic sections, with a higher expression present in the media.

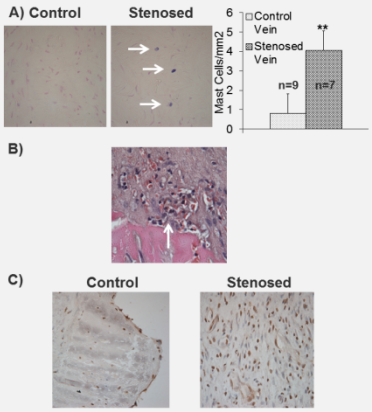

Figure 3. A) Toluidine blue staining for mast cells (**= p <0.005, paired T test). **B)** H & E staining of vein sections show the infiltration of lymphocytes. **C)** VCAM-1 expression (brown) was analysed by immunohistochemistry.

Enhanced proliferation of stenotic VSMC explants in vitro

When the proliferation rates of VSMC stimulated with foetal calf serum (FCS) were compared, explants derived from stenotic segments had an increased proliferative capacity compared to control explants. FACs analysis of cell cycle shows a trend towards a greater number of stenosed VSMC in the G2/M stages.

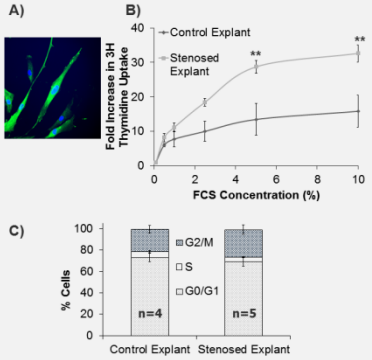

Figure 4. A) VSMC explants derived from vein specimens are positive for α-SMA (green), and display the classic 'hill and valley' growth morphology. **B)** Cell proliferation was measured by ^{3}H thymidine incorporation (Mean ± S.E.M., n=4, **= p<0.005 one-way Anova with Tukey). **C)** The cell cycle of the explants was measured by FACS using propidium iodide

Anti-proliferative activity of diclofenac

Diclofenac, a non steroidal anti-inflammatory agent, significantly reduces VSMC proliferation at 175 µM in both healthy and stenosed explants. Inclusion/exclusion of fluorescent dyes were used to determine cell viability.

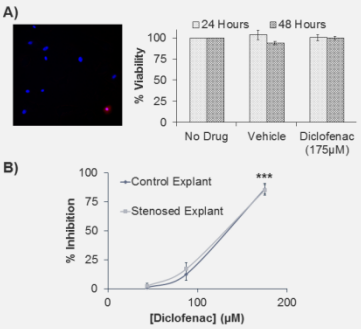

Figure 5. A) Cells were grown on glass coverslips, and viability assayed by inclusion of hoechst 33342 (blue, live cell) or propidium iodide (Red, dead cell). **B)** ^{3}H thymidine used to determine proliferation (Mean ± S.E.M., Control n=4,Stenosed n=6, ***= p<0.0005 one-way Anova with Tukey).

Conclusions

- There is a significant venous hypertrophic remodelling in stenosed AVF sections.
- Venous remodelling can be largely attributed to vascular smooth muscle cell proliferation, as well as accumulation of inflammatory cell infiltrates.
- In VSMC studies we have demonstrated that cells derived from stenosed AVF have an increased capacity to proliferate.
- Diclofenac may have the potential to be used to offset stenosis clinically.

These results demonstrate changes undergone in VSMC proliferation of failed AVF. Further work is required to elucidate VSMC hypertrophic mechanisms and the influencing role of the immune system. Moreover, additional work is required to assess the potential of diclofenac to offset stenosis.

References

Field, M. *et al.* (2008). *J. Vasc. Access* **9**, 45-50.

Lee, T. & Roy-Chaudhury, P. (2009). *Adv. Chronic Kidney Dis.* **16**, 329-338.

Acknowledgements

This work was funded by:

BBSRC bioscience for the future

Email: mark.macaskill@strath.ac.uk